INFORMATION TO USERS

RATE CONSTANTS AND MECHANISMS FOR REACTIONS OF CARBENES AND CATIONS FROM OXADIAZOLINES AND OTHER PRECURSORS

By

John Paul Pezacki, B.Sc.

A Thesis

Submitted to the School of Graduate Studies

in Partial Fulfillment of the Requirements

For the Degree

Doctor of Philosophy

McMaster University

CARBENES AND CATIONS FROM OXADIAZOLINE PRECURSORS

DOCTOR OF PHILOSOPHY (1998)   McMASTER UNIVERSITY

(CHEMISTRY)   Hamilton, Ontario

TITLE: RATE CONSTANTS AND MECHANISMS FOR

REACTIONS OF CARBENES AND CATIONS FROM

OXADIAZOLINES AND OTHER PRECURSORS

AUTHOR: John Paul Pezacki, B.Sc. (University of Toronto)

SUPERVISOR: Professor John Warkentin

NUMBER OF PAGES :   xxii, 288.

Abstract

The doctorate work presented is in the area of physical organic chemistry and has involved the study of reactive intermediates. Various oxadiazolines (**A**) have been prepared as photochemical and thermal precursors for the study of dialkoxycarbenes (**C**), dialkylcarbenes (**D**), as well as alkanediazonium ions (**E**), and carbocations (**F**) derived from them.
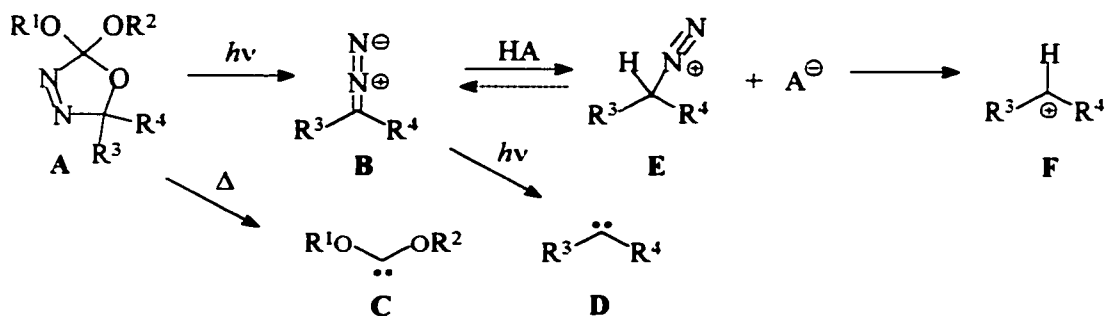
Intramolecular rearrangement reactions were studied in several dialkylcarbenes, and in the excited states of their precursors using both steady-state and laser flash photolytic techniques. Rate constants for both intra- and intermolecular reactions of dialkylcarbenes were determined.

Alkanediazonium ions (**E**), the conjugate acids of diazoalkanes (**B**), have been implicated in the carcinogenicity and mutagenicity of N-alkyl-N-nitroso compounds. Work described within has involved exploratory photochemistry of oxadiazoline precursors in acidic media. Rate constants of proton transfer reactions to diazoalkanes, generated from oxadiazoline precursors, were determined and the sensitivity of these reactions towards acid strength have been evaluated. Methodology for estimating lifetimes and determining the reactivity of alkanediazonium ions and dialkylcarbenium ions using laser flash photolytic techniques has been developed using novel probe reactions. Conclusions about

how these reactive intermediates alkylate DNA (which leads to the development of cancer) have been drawn.

Preparation of the oxadiazoline precursor to methoxytriphenylsiloxycarbene (C, R^1 = CH_3, R^2 = $SiPh_3$) was accomplished. The 1,2-silicon migration from oxygen to carbon as well as the competitive extrusion of CO in methoxytriphenylsiloxycarbene were studied.

The reactivity of dimethoxycarbene (C, R^1, R^2 = CH_3) toward polychlorinated olefins was also studied. Products of S_N2' displacement of chlorine as well as additions to carbonyl moieties were discovered, the structures of these products were elucidated using a variety of spectroscopic techniques as well as x-ray crystallography in some cases, and mechanisms for their formation proposed.

Acknowledgments

It is very difficult to express the profound impact that a few very special people have had on my carreer as a scientist and on my growth as an individual. Professor John Warkentin appears at the top of the list not simply because he has been my supervisor, but because he is an extraordinary person. It is his mentorship, guidance, unparalleled patience, and constant unwavering faith in my abilities which has allowed me to accomplish goals which I thought were beyond my capabilities when I began the journey that has culminated in this thesis. I have enjoyed many useful and productive conversations with the members of my Ph.D. committee. I am grateful to Professor Leigh and McGlinchey for always taking the time to talk with me.

A significant portion of the research contained within this thesis was performed at the Steacie Institute for Molecular Sciences which is a part of the National Research Council of Canada (NRC). I spent ~ 7 months there as a visiting scientist under the supervision of Dr. Janusz Lusztyk. This experience was incredible and I am truly grateful to Janusz for giving me the opportunity, for his time, and for many useful discussions. I would also like to acknowledge Drs. Linda Johnston, Brian Wagner, Paul Wood, and Deepak Shukla for advice regarding LFP experiments, Dr. Dan Wayner and Professor Keith Ingold for their encouragement, and Darren Snelgrove for providing a roof over my head and for taking care of me in scientific and other endeavors during my stay in Ottawa. I am grateful to all at the NRC for their friendship and help.

Many thanks to Professor Tim Gadosy (Concordia University) for performing *ab initio* calculations for some of the reactions contained within this thesis. Tim and I met at the

I would like to acknowledge my mother for her constant love, support, and generosity to me and to my family. Many thanks to her and Edzia for looking after my son so that I could finish this thesis in a reasonable amount of time. I would like to thank my Dad for always pushing me to be the best I could be (to be a doctor). Finally, I would like to express my deepest gratitude to my wonderful wife Natalie and son Aidan for all their love and patience during the course of the last several months.

This thesis is dedicated to the memory of my step-father, Dr. Edmund Cary West, who is sorely missed. It is also dedicated to my son, Aidan, who brings joy to my life every day without exception.

Table of Contents.

Contents   Page

List of Figures.

photolysis (SS) of 6-trifluoromethyl-3,4-diaza-2,2-dimethoxy-1-oxa[4.3]spirodec-3-ene (**II-1j**) in benzene-d_6.

acetonitrile at 20 °C.

List of Tables.

conjugate acids.

Chapter 1.

Introduction.

This thesis describes work which is in the area of physical organic chemistry. Specifically, the work has involved studies of reactive intermediates including carbenes, carbocations, and alkanediazonium ions (N_2 co-ordinated carbocations). The reactive intermediates were generated primarily by thermal or photochemical decomposition of oxadiazolines, however other precursors were utilized as well. Some of the studies are based solely on products of chemical reactions involving the reactive intermediates, while others have involved kinetic measurements. Most of the kinetic measurements were made with photochemical precursors utilizing a technique called laser flash photolysis. This thesis is divided into two major sections; one section involves the chemistry of carbene intermediates and the other that of alkanediazonium ions and carbocations derived from them. The section on carbene chemistry comprises the majority of the thesis. Consequently, this introduction reviews the appropriate background literature pertaining to carbene chemistry. The review is limited to background literature that will, hopefully, give context to the research presented. A smaller review of alkanediazonium ion chemistry appears at the beginning of the appropriate chapter.

Reactive intermediates referred to as "carbenes"[a] contain divalent carbon atoms.[1] The reactivity of carbenes is greatly affected by substitution. Substituents affect the ground state electronic configuration[2], the migratory aptitudes of groups adjacent to the carbene center,[3] and also determine

the electrophilic or nucleophilic character of the carbene.[4] This thesis encompasses a variety of carbenes of different structure and electrophilicity. The carbenes studied range from highly reactive voracious dialkyl and alkylchlorocarbenes, which are strongly electrophilic, to those which are more persistent and unreactive such as alkoxy and dialkoxycarbenes containing π-donor substituents. Both intra- and intermolecular reactivities of carbenes have been studied and these processes are addressed in the introduction.

I.1. Electronic Structure of Carbenes

Carbenes are neutral species that are dicoordinate at the carbene carbon and have six electrons in their valence shell. Four of these electrons are involved in σ-bonding with the substituents directly attached to the carbene carbon and two are non-bonding in nature. In principle, there are many electronic configurations which a carbene can adopt, however, only the ground state (lowest energy electronic configuration) and other higher electronic configurations which are sufficiently similar in energy to that of the ground state will lead to chemical reactions and will be responsible for chemical reactivity. Without going into too much detail, carbenes in general have two low-lying electronic states responsible for chemical reactions. They are termed the singlet and triplet states. These names reflect the relative spins (quantum spin number) of the non-bonding electrons. Both of these states are approximately sp^2 hybridized, the singlet state has both non-bonding electrons paired (opposite spin) in a σ orbital which is in the plane defined by the carbene carbon and the two substituents directly attached (R and R' below) to it, whereas the triplet state has the non-bonding electrons unpaired and with the same spin with one electron located in the σ orbital and the other in a p orbital (sometimes

---

[a] The term "carbene" was invented by Doering, Winstein, and Woodward in the back of a Chicago taxi cab (Doering, W. V.; Knox, L. H. *J. Am. Chem. Soc.* 1956, *78*, 4947.).

referred to as π^*) which is perpendicular to the plane defined by the carbene carbon and the substituents directly attached. The singlet and triplet states of carbenes are illustrated below.

Triplet Carbene
(T_1)

Singlet Carbene
(S_0)
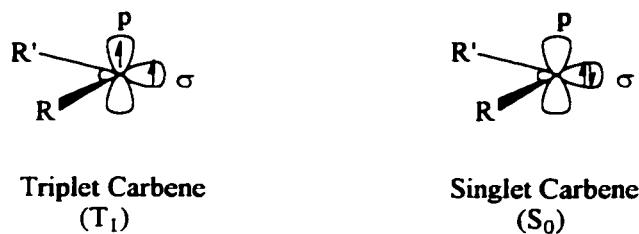
The energy difference between the singlet and the triplet states, denoted $\Delta E_{ST} = E_T - E_S$, is governed primarily by the energy difference between the σ and p orbitals and the energy required to overcome the electron-electron repulsions between two paired electrons in the same orbital.[2] These ground state electronic configurations play an important role in determining carbene reactivity considering that triplet carbenes behave as free radicals whereas singlet carbenes undergo electrophilic or nucleophilic chemistry. The significance of the magnitudes of the barriers to interconversion of the singlet and triplet states (intersystem crossing or ISC) is discussed in a following section.

1.2. Substituent Effects on the Electronic Structure of Carbenes

Methylene (1), the parent carbene, is known to be a ground state triplet with a bond angle of ~135° whereas singlet methylene (ΔE_{ST} ~ -9 kcal/mol) has a bond angle of ~102°.[5] A consequence of the differences in the preferred bond angles in singlet and triplet carbenes is that carbene carbons located within small rings, can have singlet ground states simply as a result of bond angle restrictions.[6] Replacing one or both of the hydrogens in methylene with phenyl or naphthyl substituents yields carbenes which are also ground state triplets as evidenced by low temperature electron paramagnetic resonance (EPR) spectroscopy.[7] This is attributed to the electron withdrawing nature of those

substituents. Substitution can also dramatically affect the kinetic stability of carbene intermediates. Shattering preconceptions regarding carbenes exclusively as virulent highly reactive intermediates, Arduengo and co-workers have reported the isolation and characterization of stable singlet carbenes (mostly diamino), whereas Tomioka and co-workers have successfully prepared a persistent triplet carbene **2** below.[8]

2
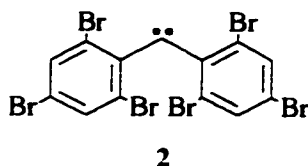
It is generally accepted that π-donating substituents, such as heteroatoms, are the most effective at stabilizing the singlet state.[9] π-Donating groups stabilize the singlet state of a carbene by widening the energy difference between the sp^2 hybridized σ orbital and the p orbital. π-Acceptor groups stabilize the triplet state, particularly when their geometry is fixed so that the π orbital overlaps with the singly occupied p orbital of the triplet carbene. However, if the π-acceptor can adopt a conformation such that its p orbital is in plane then it will also stabilize the singlet state *via* a two electron interaction involving the singlet σ and the acceptor π* orbital.[2d] Inductive effects also govern whether a carbene will have a singlet or a triplet ground state. In general, electronegative substituents stabilize the singlet state, whereas electropositive substituents stabilize the triplet state.[10] Recent computations also suggest that singlet triplet energy gaps can be influenced by solvent polarity with the singlet states of carbenes and isoelectronic nitrenium ions being favored in polar solvents.[11] In addition to affecting singlet triplet energy gaps, the relative π-donating ability of the substituent influences the electrophilicity or nucleophilicity of the carbene.
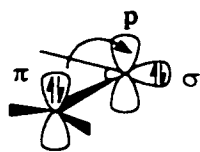
Interaction of π donor
with carbene p orbital.
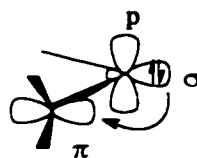
Interaction of in-plane π
acceptor with carbene σ
orbital.

Carbenes with alkyl or halogen subtituents on the carbene carbon are electrophilic in character and can have either a singlet or a triplet ground state. Halogen substituents can act as π-donors as well as σ-withdrawers. Replacing one of the hydrogens in methylene with fluorine for example gives a ΔE_{ST} ~ 15 kcal/mol (F(H)C:), whereas replacing both with fluorine raises ΔE_{ST} to ~ 56 kcal/mol (F_2C:, **3**).[12] Replacing the hydrogens in methylene with alkyl groups such as methyl groups has a less dramatic effect on the singlet-triplet energy gap as exemplified by dimethylcarbene (**4**) which has a computed ΔE_{ST} of ~ 2 kcal/mol (Me_2C:).[13] In contrast, carbenes such as oxycarbenes, which bear one or two π-donor substituents are nucleophilic in character,[14] and an example is dimethoxycarbene (**5**) illustrated below. The latter is stabilized by conjugative donation by the lone pairs on oxygen to the formally vacant p orbital at the carbene carbon.[4,15] As a result, dimethoxycarbene has dipolar character, acts as a nucleophile, and is a ground state singlet with a computed singlet-triplet energy gap of ΔE_{ST} ~ 76 kcal/mol.[15] Similarly, diaminocarbenes such as imidazol-2-ylidene (**6**) are also ground state singlets and are nucleophilic in character. The computed singlet-triplet energy gap for imidazol-2-ylidene is ΔE_{ST} ~ 79 kcal/mol.[16]

$$H \diagdown \diagup H$$
$$\cdot\cdot$$

1

Electrophilic Carbene,
Ground State Triplet,
$\Delta E_{ST} \sim -9$ kcal / mol

$$Me \diagdown \diagup Me$$
$$\cdot\cdot$$

4

Electrophilic Carbene,
Ground State Singlet,
$\Delta E_{ST} \sim 2$ kcal / mol

$$F \diagdown \diagup F$$
$$\cdot\cdot$$

3

Electrophilic Carbene,
Ground State Singlet,
$\Delta E_{ST} \sim 56$ kcal / mol

$$MeO \diagdown \diagup OMe \quad \longleftrightarrow \quad MeO \diagdown \diagup \overset{\oplus}{O}Me$$
$$\cdot\cdot \qquad\qquad\qquad\qquad \ominus$$

5

Nucleophilic Carbene,
Ground State Singlet,
$\Delta E_{ST} \sim 76$ kcal / mol

$$H\text{-}N \diagup\diagdown N\text{-}H$$
$$\cdot\cdot$$

6

Nucleophilic Carbene,
Ground State Singlet,
$\Delta E_{ST} \sim 79$ kcal / mol
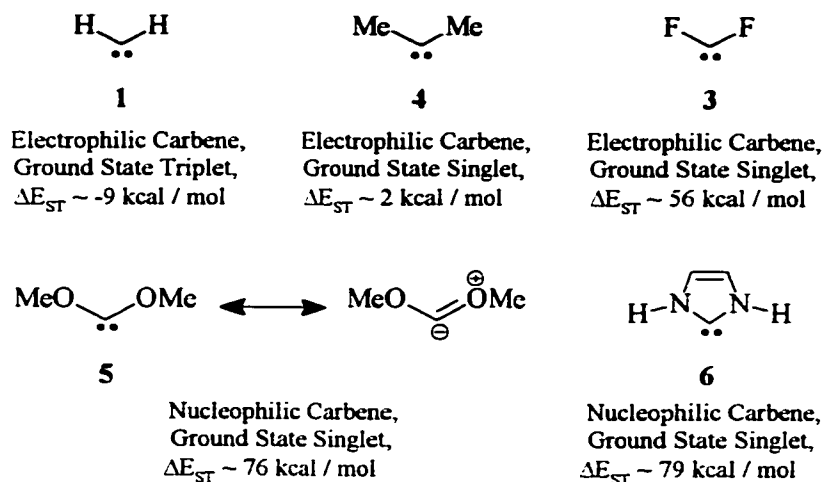
1.3. Substituent Effects on Reactivity

Substituents attached directly to carbenes play an important role in determining the ground state multiplicity, stability, geometry, and the general reactivity of these intermediates. In general, carbenes are thought of as electron deficient species because they have only six electrons in their valence shells. Rapid intramolecular migrations and insertion reactions as well as intermolecular insertions and cycloadditions are typical reactions which increase the valence shell electron count from six to eight. Reactions which lead to an octet around the former carbene carbon can occur through either the singlet or the triplet manifold and these reactions can proceed *via* step-wise or concerted mechanisms. However, these reactions do not necessarily require a carbene to act as an electrophile. For instance, cyclopropanation can occur from the singlet state of a carbene by a concerted [1+2]cycloaddition onto a double bond, or through dipolar intermediates with either negative or positive charge located at the former carbene carbon atom (Scheme 1). Non-synchronous concerted cyclopropanation reactions may also have partial charge build-up at the former carbene carbon as well. The pathways to products and the nature of the transition states to product formation necessarily depend on the substituents attached to the carbene carbon as well as the innate properties of the carbene trap.

Scheme 1.
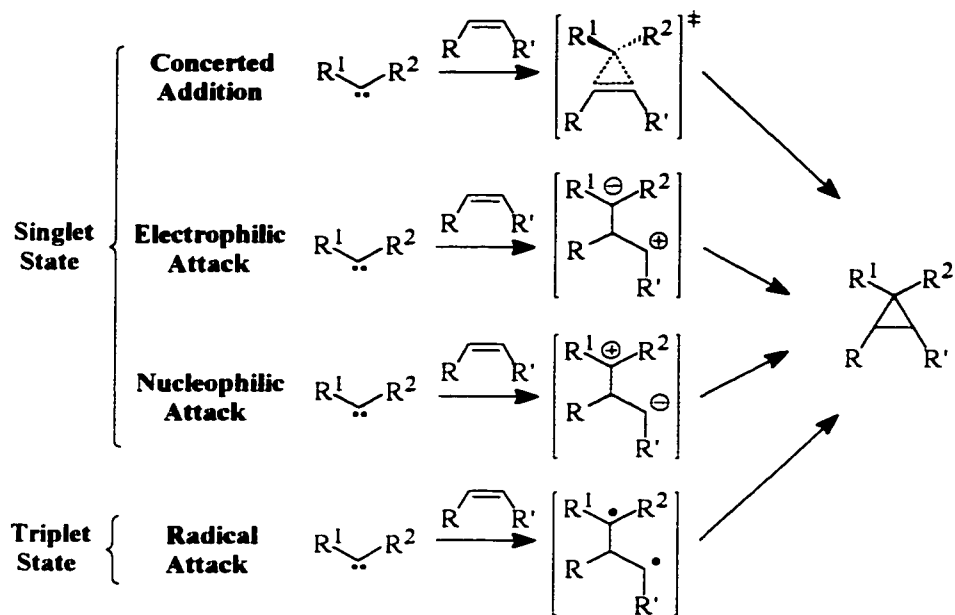
For example, diphenyl and diarylcarbenes have been shown to insert into the OH bonds of alcohols from the singlet state by a proton transfer mechanism, by direct observation of the resulting carbocationic intermediates by LFP, eq 1.[17]

(1)
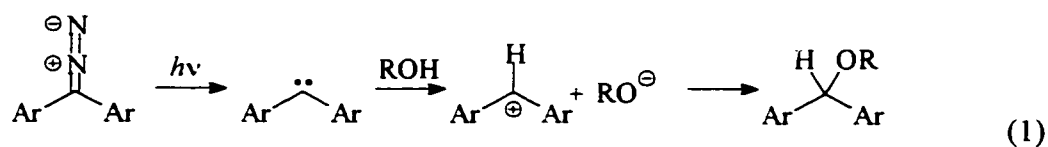
The proton transfer mechanism involves the attack of the σ lone pair of electrons onto the acidic (and electrophilic) hydrogen atom of the alcohol. The carbenes, in each case, act as Brönsted bases. On the other hand, singlet diphenylcarbene reacts with the basic (and nucleophilic) nitrogen in pyridine to form a pyridinium ylide, eq 2.[18] This reaction involves the attack of the lone pair of electrons of the pyridine nitrogen atom onto the empty p orbital of the carbene. Diphenylcarbene, in this case, acts as an electrophile.
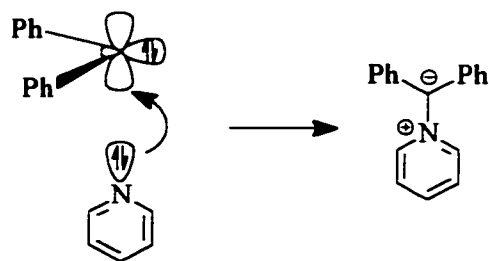
(2)

Whether a carbene will react *via* the singlet or the triplet state manifold depends on the rate constants for intersystem crossing (ISC) between the two electronic states which is reflected by computed ΔE_{ST} values and by the relative magnitudes of the rate constants for reactions from these states. For example, dimethylcarbene and dialkylcarbenes in general, which have small ΔE_{ST} values and large rate constants for ISC, can undergo 1,2-hydrogen (1,2-H) migration from the singlet state as well as react with O_2 from the triplet state (eq 3).[19]
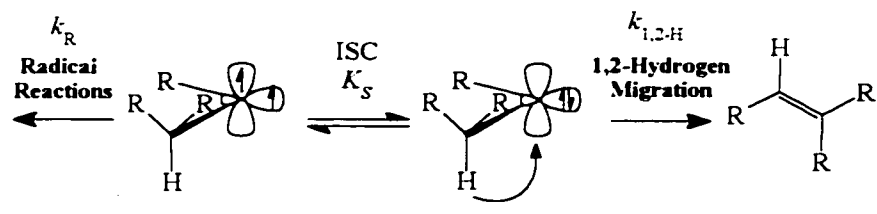
(3)

For cases in which (ISC) is rapid compared to product forming steps, the product ratio is determined entirely by the relative transition state energies for formation of products and the singlet/triplet populations are irrelevant, according to the Curtin-Hammett principle.[20] Triplet reactions generally have higher barriers than singlet reactions unless the reactant (e.g. O_2) is prone to radical chemistry. On the other hand, when the barriers for ISC are large as in the case for the conversion of singlet dimethoxycarbene to the triplet state ($\Delta E_{ST} \sim 76$ kcal/mol) then the relative populations of singlets and triplets become dominant in determining product distributions. Since the singlet state of

dimethoxycarbene is strongly favored and highly populated under most reaction conditions, its chemistry is predominantly or exclusively that of the singlet state.

1.3.1. Singlet Carbene Electrophilicity

As stated earlier, singlet carbenes may behave as electrophiles or nucleophiles depending on their inherent characteristics as well as those of the co-reactant. Moss and co-workers have established an empirical correlation relating the relative reactivities of carbenes of different structure towards olefins. These relative reactivities are the basis of Moss' carbene selectivity index m_{CXY}.[4, 14a, 14b, 21] Values for m_{CXY} are defined by the slopes of plots of logarithms of relative rate constants for the reactions of a given carbene :CXY with a standard set of electron rich olefins vs. the logarithms of the relative rate constants for reaction of :CCl$_2$ (reference carbene) with the same standard set of olefins, according to the linear free energy relationship in eq 4. Me$_2$C=CH$_2$ is the reference olefin and rate constants for the reaction of a given carbene with this olefin define k_o in eq 4. The rate constants k_i are those for the reactions with the standard set of olefins Me$_2$C=CMe$_2$, Me$_2$C=CHMe, cis-MeHC=CHMe, trans-MeHC=CHMe, and Me$_2$C=CH$_2$.

$$\log\left(k_i \, / \, k_o\right)_{CXY} \; = \; m_{CXY} \cdot \log\left(k_i \, / \, k_o\right)_{CCl_2} \tag{4}$$

Values for m_{CXY} can also be predicted using σ_R^- and σ_I which relate the degree of resonance interactions and the inductive effects between a substituent and the carbene carbon to the carbene's reactivity. The expression which relates σ_R^- and σ_I to m_{CXY} is in eq 5.[14, 21b]

$$m_{CXY} \; = \; -1.10\sum_{X,Y}\sigma_R^- \; + \; 0.53\sum_{X,Y}\sigma_I \; - \; 0.31 \tag{5}$$

Magnitudes of m_{CXY} also reflect the relative electrophilicities of carbenes. In general, values of $m_{CXY} < 1.5$ represent electrophilic carbenes, whereas values of $m_{CXY} > 2.2$ represent nucleophilic carbenes and those in between represent ambiphiles which can show parabolic selectivity patterns towards olefinic traps.[14] However, caution should be taken with such terms since any carbene has the potential for acting as either an electrophile or a nucleophile. For example, tight ion pairs have been implicated in OH insertion reactions by highly electrophilic 2-bicyclo[2.1.1]hexylidene, suggesting a proton transfer mechanism.[22]

Frontier molecular orbital theory can be used to predict and explain singlet carbene reactivities, particularly for reactions with olefins.[14, 23] Carbene electrophilicity in a cyclopropanation reaction depends on whether the electrophilic orbital interaction (**E**, Figure 1) or the nucleophilic orbital interaction (**N**, Figure 1) is dominant in the transition state.

Figure 1.

LUMO (p)   LUMO (π^*)

HOMO (π)   HOMO (σ)

E   **N**
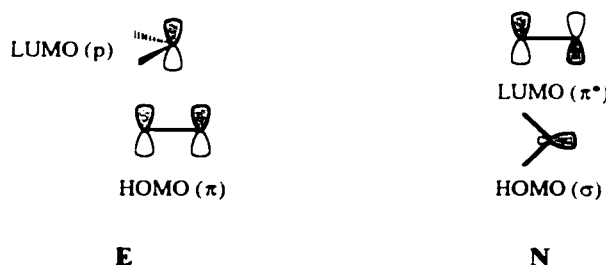
The electrophilic orbital interaction will dominate when the energy difference between the carbene LUMO and the alkene HOMO ($\Delta\varepsilon_E$) is smaller than that between the carbene HOMO and the alkene LUMO ($\Delta\varepsilon_N$). Differential orbital energies $\Delta\varepsilon_E$ and $\Delta\varepsilon_N$ can be evaluated using computational chemistry and conclusions regarding carbene philicities have been drawn.[14]

1.4. Precursors to Carbenes

A brief overview of some common methods for the generation of carbene intermediates is presented in this section. Although most of the thesis material deals with the generation of carbenes

from oxadiazolines, much of the background literature cited involves other precursors. Oxadiazolines, as thermal and photochemical presursors to carbenes, are included in a separate subsection.

1.4.1. Diazo Compounds.

Diazo compounds and diazirines are by far the most common precursors to carbenes. Diazo compounds contain cumulated C=N=N functionality and lose molecular nitrogen thermally or photochemically to yield carbene intermediates (eq 6). [1, 24]

$$
\begin{array}{c}
\ominus N \\
\oplus N \\
R^1 \diagdown R^2
\end{array}
\xrightarrow{h\nu \text{ or } \Delta}
R^1 \diagdown\!\!\ddot{\,}\!\!\diagup R^2 \;+\; N_2
\tag{6}
$$
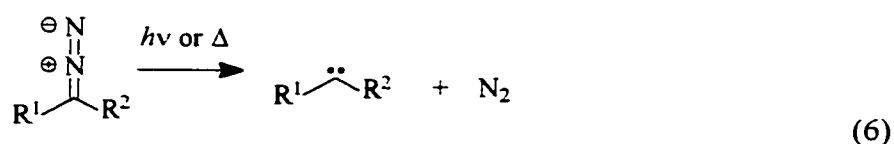
Bamford-Stevens Reactions.

There are many methods for generating diazo compounds.[25] The most common methods are the thermal and photochemical Bamford-Stevens reactions.[24, 25] These reactions involve the heat or light induced elimination of arenesulfinates from salts of arenesulfonylhydrazones which yield intermediate diazo compounds (eq 7). These compounds then lose molecular nitrogen either thermally or photochemically.

$$
\underset{R^1 \diagdown R^2}{\overset{\overset{\textstyle NHSO_2Ar}{|}}{\underset{N}{\|}}}
\xrightarrow[\text{(1 eq.)}]{\overset{\text{NaH or}}{RLi}}
\underset{R^1 \diagdown R^2}{\overset{\overset{\textstyle \ominus}{\underset{N}{NSO_2Ar}}}{\|}}
\xrightarrow[-ArSO_2^-]{h\nu \text{ or } \Delta}
\underset{R^1 \diagdown R^2}{\overset{\ominus N}{\underset{\oplus N}{\|}}}
\tag{7}
$$
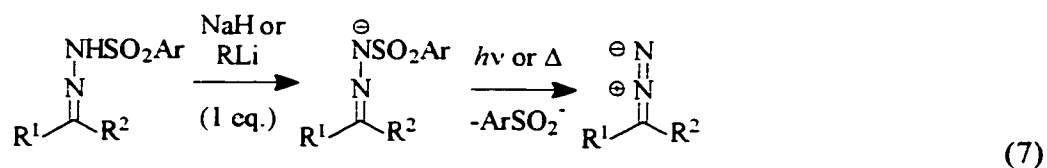
Dehydrogenation of hydrazones.

Another common method for preparing diazo compounds is the dehydrogenation of hydrazones as in eq 8.[24] Such methods are usually restricted to the preparation of more stable and isolable diazo compounds such as diaryldiazomethanes.[26]

NH₂ Dehydrogenation ⊖N⩵⊕N

Typical dehydrogenating agents:

HgO, Ag_2O, MnO_2, $Pb(OAc)_4$

(8)
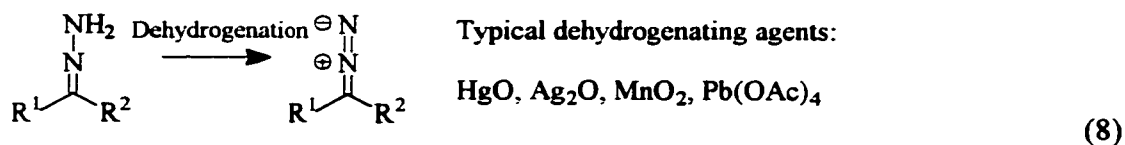
Aziridinylimines.

Aziridinylimines have emerged as a convenient neutral thermal and photochemical source of diazo compounds recently (eq 9).[27]

hv or Δ

-RCH=CHR'

(9)
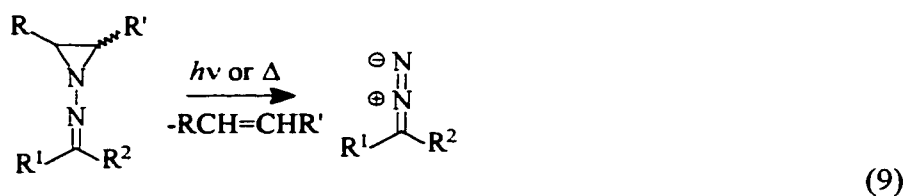
Common methods for preparing such precursors include: 1) oxidative addition of N-aminophthalimide to alkenes followed by hydrazinolysis which yields 1-amino-2,3-dialkylaziridines[28] which can be converted to aziridinylimines by condensation with ketones as in eq 10; or

PbOAc₄
CH₂Cl₂

H₂NNH₂·
H₂O

(10)
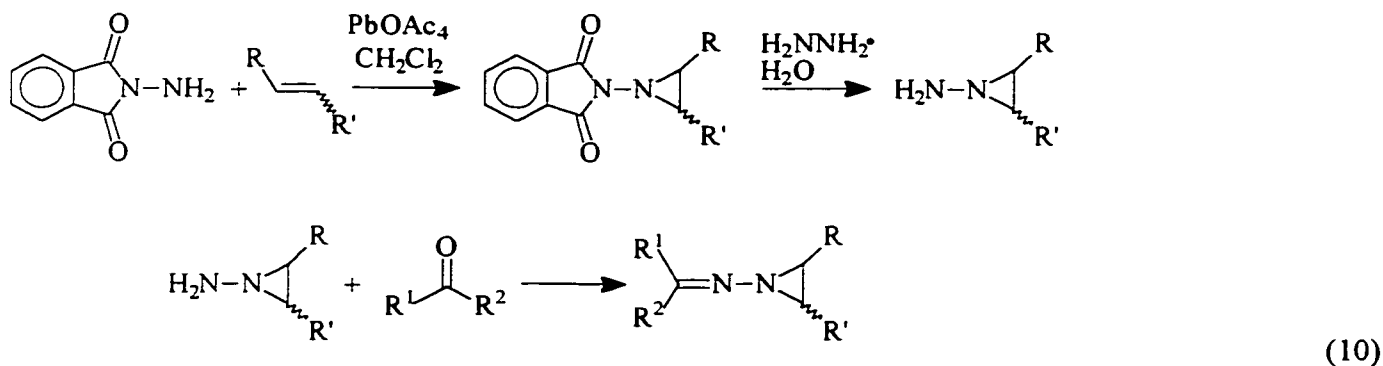
2) hydrazinolysis of 1-phenyl-ethan-1,2-diol dimesylate (eq 11), followed by neutralization and condensation with the appropriate ketone.

$$\text{Ph} \overset{\text{OMs}}{\underset{\text{OMs}}{\bigwedge}} \quad \xrightarrow[\text{2) HOAc}]{\substack{\text{1) H}_2\text{NNH}_2\text{·} \\ \text{H}_2\text{O}}} \quad \text{Ph} \overset{}{\bigtriangleup} \text{N}-\overset{\oplus}{\text{NH}}_3 \ \overset{\ominus}{\text{OAc}}$$

(11)
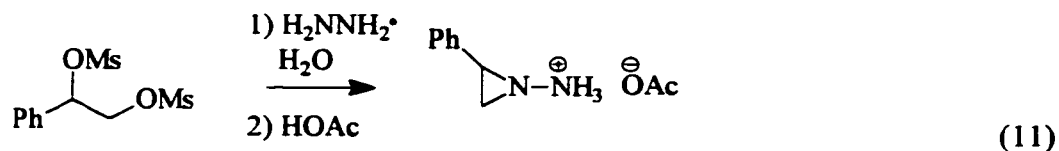
Oxadiazolines are also convenient neutral photochemical precursors to diazo compounds. These precursors are discussed in a following section.

1.4.2. Diazirines.

Diazirines (eq 12) are the most common nitrogenous thermal and photochemical precursors to carbenes used in reactivity studies and in LFP studies.[29]

$$\text{R} \overset{\text{N}=\text{N}}{\underset{\text{R'}}{\bigtriangleup}} \quad \xrightarrow{h\nu \text{ or } \Delta} \quad \text{R}^1\overset{\cdot\cdot}{\diagup}\text{R}^2 \ + \ \text{N}_2$$

(12)
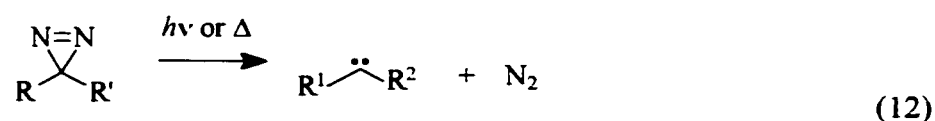
Diazirines are usually prepared by Graham hypohalite oxidations of amidines, which yield alkylhalodiazirines (eq 13),[29, 30] or alternative methods such as that in equation 14.[29c] Alkylhalodiazirines can be further converted to alkoxyalkyldiazirines by the diazirine exchange method (eq 15).[31]

$$\text{R} \overset{\text{NH}}{\underset{\text{NH}_2}{\bigparallel}} \quad \xrightarrow{\text{NaOX}} \quad \text{R} \overset{\text{N}=\text{N}}{\underset{\text{X}}{\bigtriangleup}}$$

(13)

$$\text{R} \overset{\text{O}}{\underset{\text{R'}}{\bigparallel}} \quad \xrightarrow[\text{2) I}_2]{\substack{\text{1) NH}_3, \\ \text{NH}_2\text{OSO}_3\text{H}}} \quad \text{R} \overset{\text{N}=\text{N}}{\underset{\text{R'}}{\bigtriangleup}}$$

(14)

$$\text{R} \overset{\text{N}=\text{N}}{\underset{\text{X}}{\bigtriangleup}} \quad \xrightarrow{\text{R'O}^-\text{Na}^-} \quad \text{R} \overset{\text{N}=\text{N}}{\underset{\text{OR'}}{\bigtriangleup}}$$

(15)
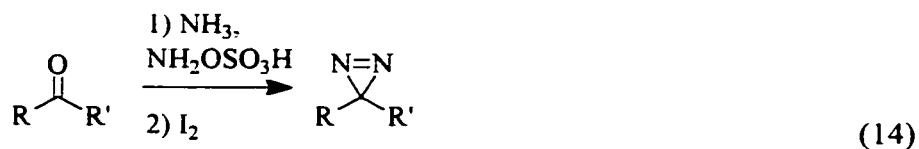
1.4.3. Cycloreversion Reactions.

Cycloreversion reactions, the reverse of cycloaddition reactions, are established methods for generating carbenes either thermally or photochemically. This section deals mainly with cycloreversion reactions involving cyclopropane or norbornadiene precursors.

Cyclopropanes.

Precursors such as 11,11 disubstituted tricyclo[4.4.1.0]undeca-2,4,8-trienes (**A**), 10,10 disubstituted tricyclo[4.3.1.0]deca-2,4-dienes (**B**), and 7,7 disubstituted dibenzo[a,c]bicyclo[4.1.0]heptanes (**C**) have been used to generate different halocarbenes photochemically (preparative and LFP studies).[32]
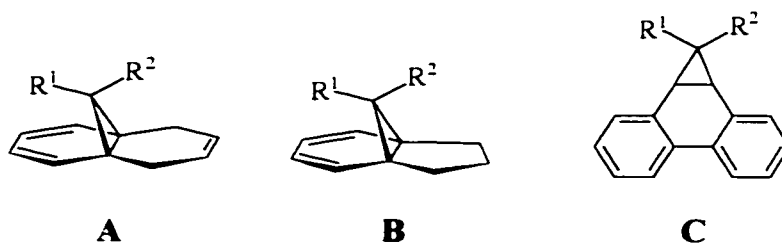
Cyclopropylmethylcarbene has also been generated by photochemical cycloreversion of 11-cyclopropyl-11-methyl-tricyclo[4.4.1.0]undeca-2,4,8-trienes (eq 16).[33]
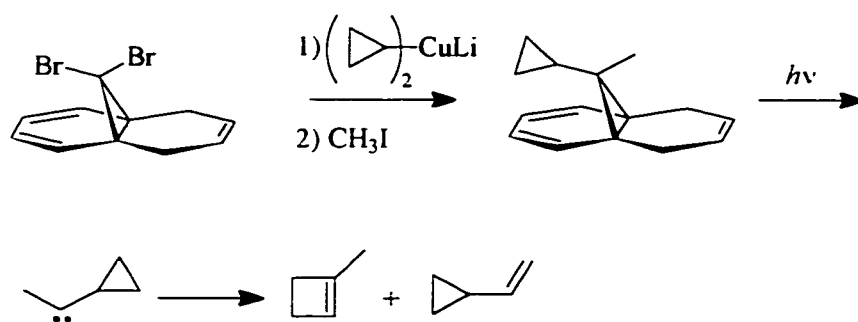
(16)

Intramolecular rearrangements of *trans*-2-*tert*-butyl-cyclopropylcarbene have also been studied from photolysis of its corresponding tricyclo[4.4.1.0]undeca-2,4,8-triene precursor (eq 17) as well as the corresponding diazirine precursor.[34]

$$(17)$$
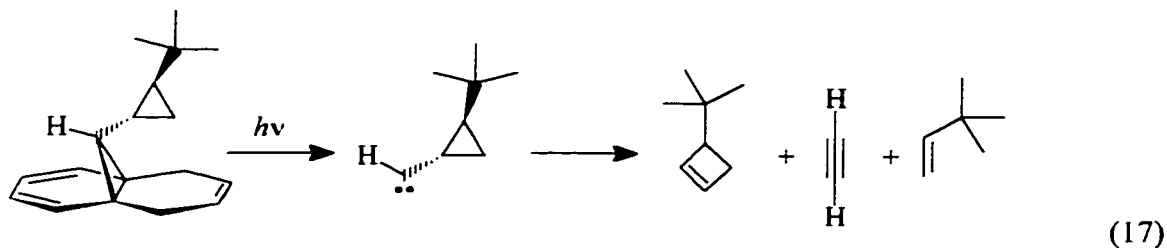
One major benefit of using non-nitrogenous precursors such as **A, B,** or **C** is that excited state migrations which mimic carbene rearrangements, which have been implicated in the photochemistry of diazirine[35] and diazo precursors,[36] may often be avoided as is the case when benzylchlorocarbene is generated from a phenanthrene precursor (eq 18).[37]

$$(18)$$
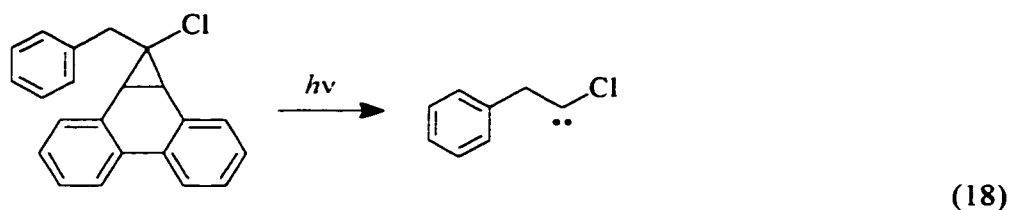
However, Huang and Platz have shown that these precursors can also give rise to carbene products *via* non-carbene pathways.[34] Tetramethylethylene trapping experiments in photolyses of the tricyclo[4.4.1.0]undeca-2,4,8-triene precursor in Scheme 2 revealed a non-trappable source of 3-*tert*-butyl-cyclobutene and a diradical was implicated as the source (Scheme 2).

Scheme 2.
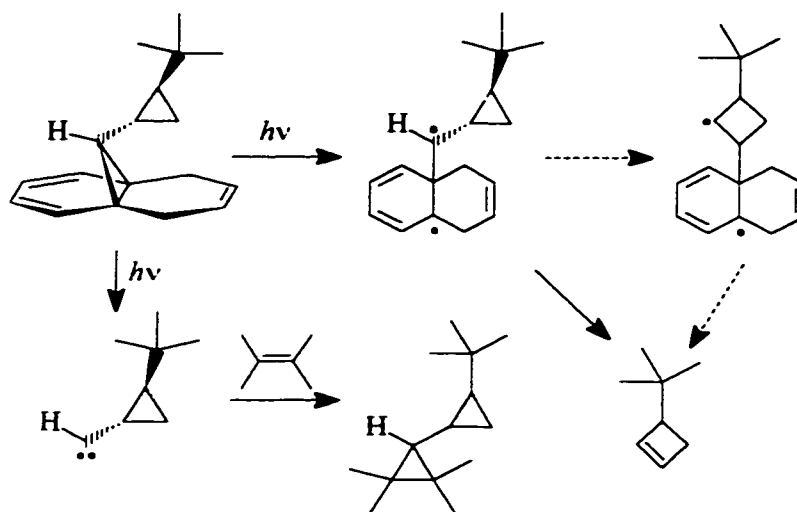
Cycloreversion reactions of cyclopropane derivatives have also been used for the generation of more nucleophilic carbenes. Hexamethoxycyclopropane has been shown to undergo thermal cycloreversion to yield tetramethoxyethylene and dimethoxycarbene (eq 19).[38]

(19)
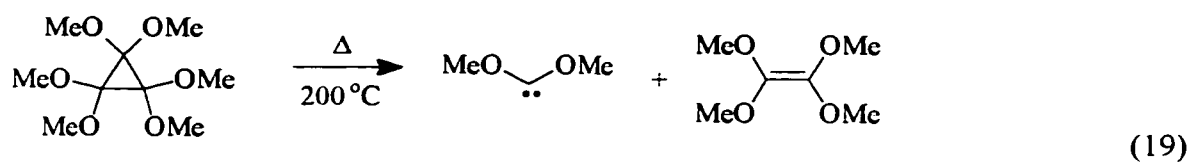
Geminal diaminocyclopropanes also undergo thermal fragmentation to give diaminocarbenes[39] under somewhat harsher conditions than those required for cycloreversion from hexamethoxycyclopropane (eq 20).

(20)
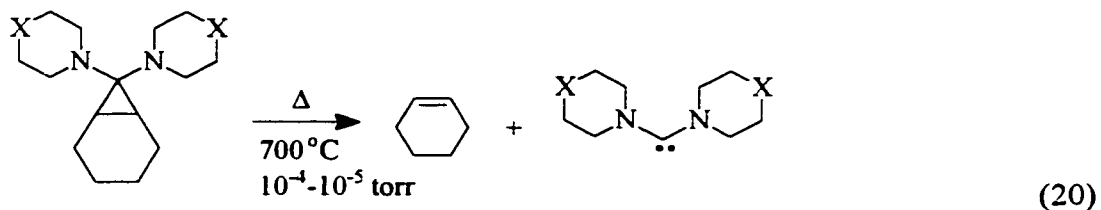
Other Cycloreversion Reactions.

Dimethoxycarbene has also been generated in cycloreversion reactions of norbornadienone ketals (eqs 21 and 22), as well as from the dimethyl ketal of tropone (eq 23), all of which generate aromatic compounds as co-products.[40]

(21)

(22)

(23)
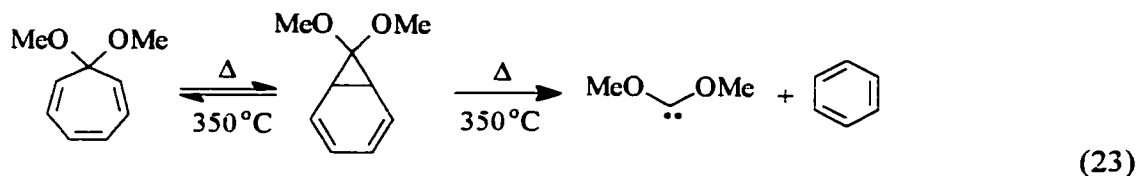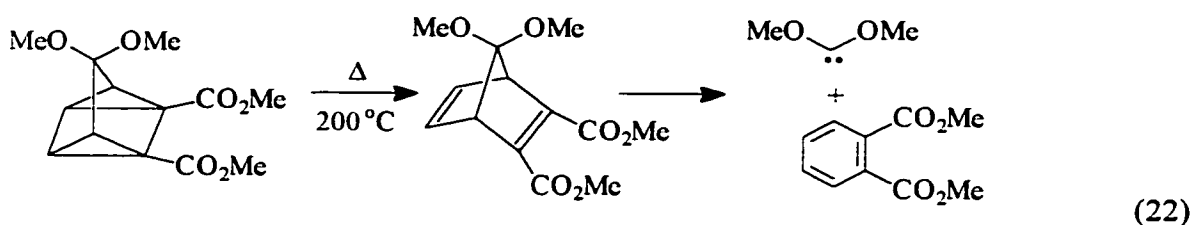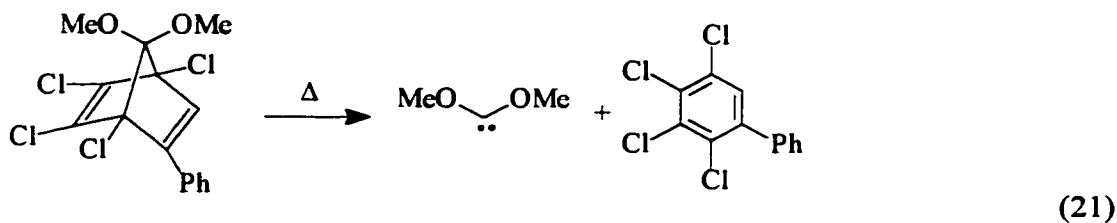
I.4.4. Thermal α-Elimination.

Thermal α-elimination reactions are known to give rise to carbenes. For example, diaminocarbenes have been generated by thermally activated α-elimination of methanol, chloroform, or hydrogen cyanide.[41]

(X= OMe. CCl₃, CN)

(24)
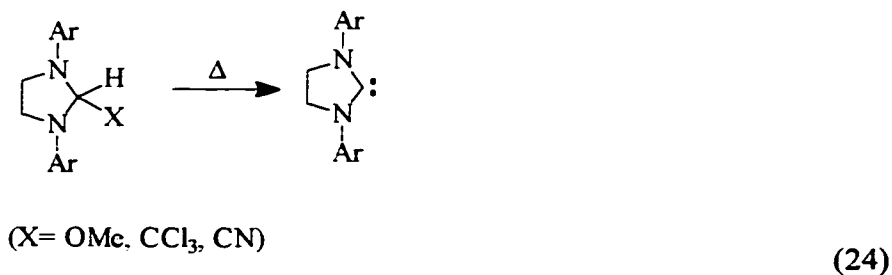
I.4.5. Oxygen or Sulfur Atom Abstraction.

Desulfurizations of thiocarbonyl compounds by P(OMe)$_3$ also yield carbene intermediates and such reactions from 5-membered ring thiocarbonates are part of the Corey-Winter reaction,[42] eq 25. The analogous deoxygenation of ketones by P(OMe)$_3$ can also give rise to carbenes as in eq 26.[43]

$$(25)$$

$$(26)$$
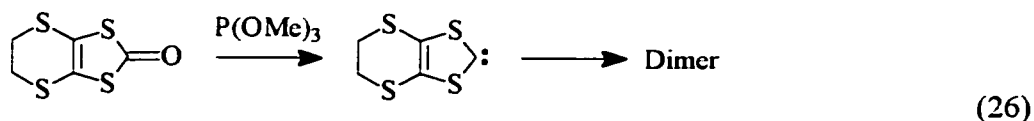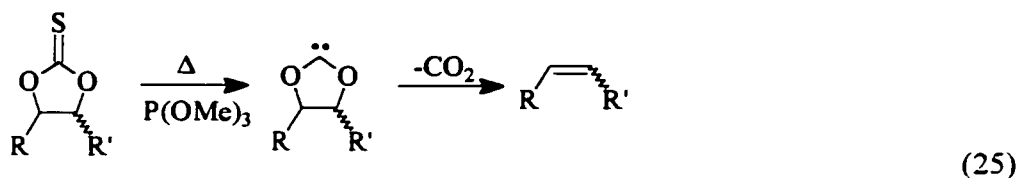
I.4.6. Deprotonation of Stable Cations.

Many nucleophilic nitrogen substituted carbenes have been generated by deprotonation of conjugate acid iminium ions. Examples include the C-2 deprotonation of imidazolinium salts[44] (eq 27) and of thiazolium salts[45] including thiamin [46] (vitamin B$_1$, eq 28).

$$(27)$$

thiamin   **C$_2$-ylide of thiamin**   **C$_2$-ylidene of thiamin**

$$(28)$$
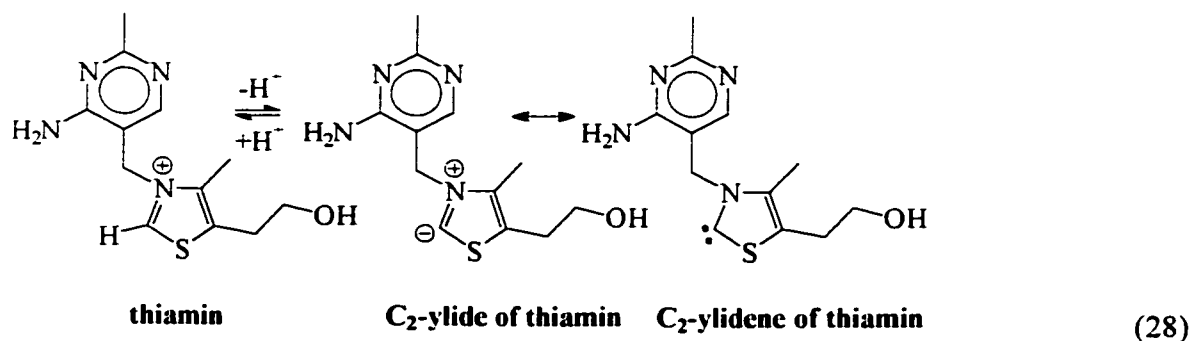
I.4.7. Brook Rearrangements.

Reactions which involve the migration of a silicon atom from carbon to oxygen are commonly referred to as "Brook rearrangements". These reactions are named after Professor Adrian Brook

(University of Toronto) for his pioneering work in the area. Both photochemical and thermal

decompositions of acylsilanes are known to give rise to α-siloxy carbenes (eq 29).[47]

$$R' \underset{O}{\overset{\qquad}{\parallel}} SiR_3 \quad \underset{\Delta\ or\ h\nu}{\rightleftharpoons} \quad R' \overset{OSiR_3}{\underset{\bullet}{\diagup}}$$

(29)
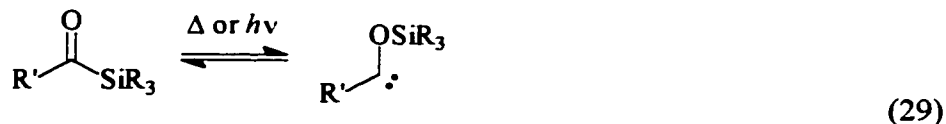
Some of the first silicon substituted carbene intermediates were generated by the photochemical

decomposition of acylsilanes leading to α-siloxy carbenes.[48] The siloxy carbene 10 (Scheme 3) derived

from the acyl silane 7 has been shown to undergo nucleophilic addition to carbonyl compounds to

yield epoxides of type 13. Carbene 10 also was shown to add to electron deficient alkenes such as

diethyl fumarate or maleate to yield cyclopropanes 14. The cyclopropanes (14) where shown to arise

from both the singlet and triplet states of carbene 10. In the absence of added traps carbene 10 inserts

into the Si-C bond of its precursor to give product 11 and undergoes dimerization to give 12.[48]

Scheme 3.
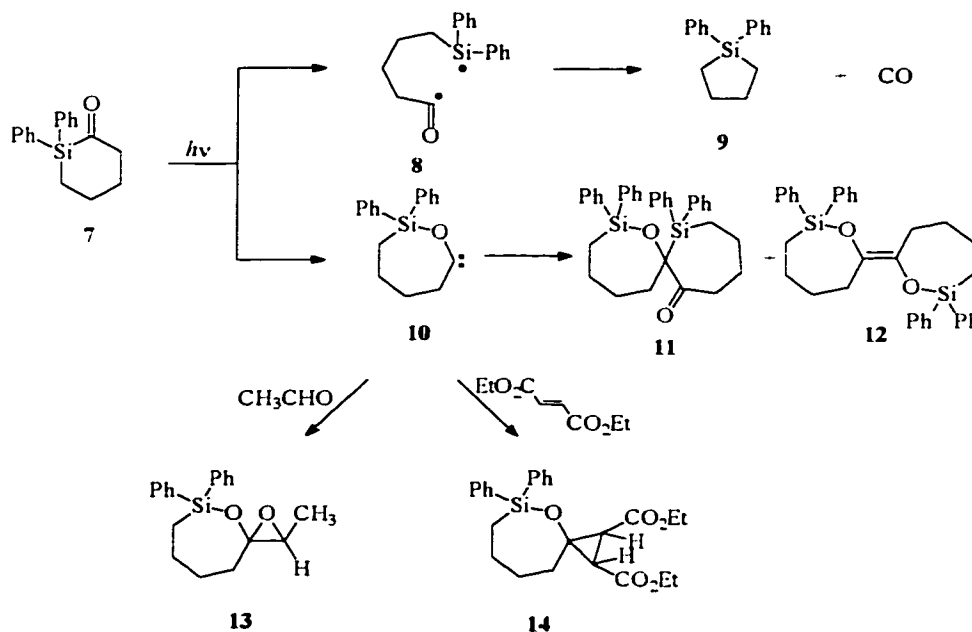
1.4.8. Oxadiazolines.

As stated earlier, nearly all of the chemistry described in this thesis pertains to reactive intermediates generated thermally and photochemically from oxadiazoline precursors. The types of oxadiazoline precursors used are 2-alkoxy-2,5,5-trialkyl-, 2,2-dialkoxy-5,5-dialkyl-, and 2-alkoxy-5,5-dialkyl-2-siloxy-Δ^3-1,3,4-oxadiazolines. Typically, oxadiazolines of this ilk are prepared by oxidative cyclizations of the corresponding hydrazones with lead tetraacetate (Pb(OAc)$_4$) in the presence of alcohols[49] (Scheme 4, upper pathway). Alternatively, hypervalent iodine oxidants such as iodobenzene diacetate may be used to prepare oxadiazolines.[50] However, such methods do not allow for the incorporation of hydroxylic or other moieties which are susceptible to oxidation (phenols for example). This problem can be circumvented by first preparing 2-acetoxy-Δ^3-1,3,4-oxadiazolines, followed by acid catalyzed exchange of the acetoxy substituent with the appropriate substrate (Scheme 4, lower pathway).[51]

Scheme 4.
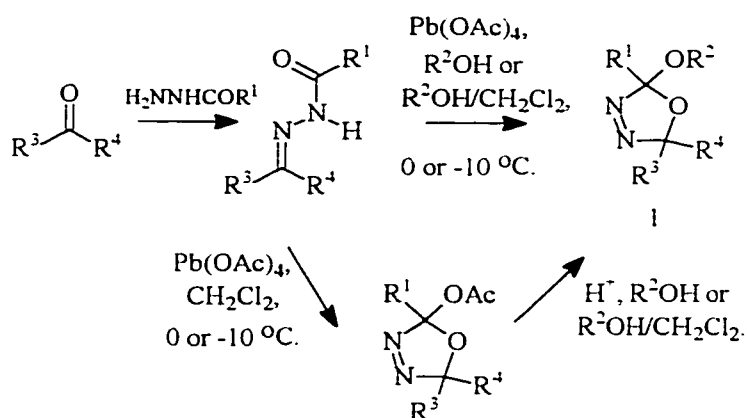
Thermal Chemistry of Oxadiazolines.

In 1992, Warkentin and coworkers first reported the thermal generation of dimethoxycarbene from 2,2-dimethoxy-5,5-dimethyl-Δ^3-1,3,4-oxadiazoline (15, eq 30) as well as other dialkoxycarbenes from their corresponding oxadiazoline precursors.[52]

(30)
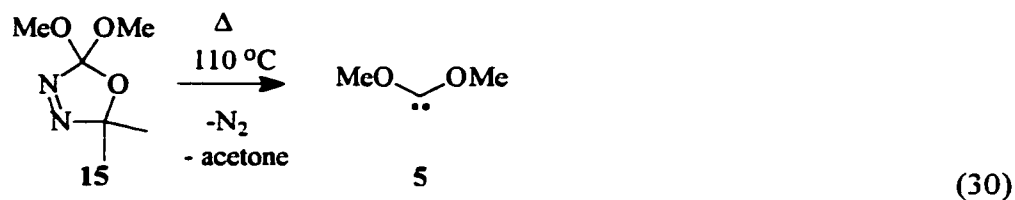
Since then precursor **15** has been extensively exploited as a convenient thermal precursor to dimethoxycarbene (**5**), [53] and other Δ^3-1,3,4-oxadiazolines which contain one or two heteroatoms at the 2 position have become established thermal precursors of dialkoxy-, alkoxy(amino)-, and alkoxy(thioalkoxy)carbene intermediates, [54, 55] as well as β-lactam-4-ylidenes (eq 31). [56]

(31)
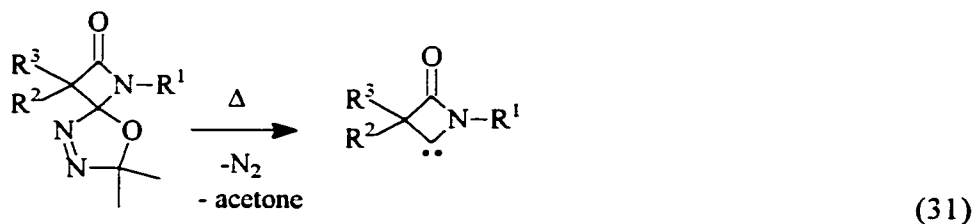
These oxadiazolines are thought to decompose thermally *via* 1,3-dipolar cycloreversions which liberate carbonyl ylides and the innocuous N_2 as a co-product (Scheme 5).

Scheme 5.
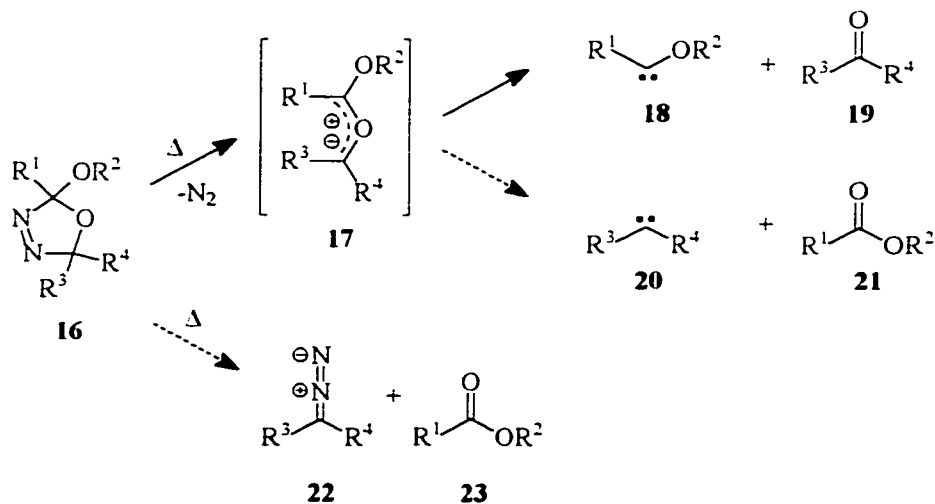
Carbonyl ylides 17 (R^1 = OR, NR$_2$, or SR, and R^3=R^4=Me) usually cleave selectively to give the

diheteroatom substituted carbene and a ketone (generally acetone, R^3=R^4=CH$_3$, upper pathway in

Scheme 5). Attempted trapping of carbonyl ylides derived from thermolysis of oxadiazolines with two

heteroatoms attached at the 2-position have for the most part been fruitless presumably because of

their short lifetimes in solution which leads one to question their existence altogether in the

thermolysis of such oxadiazolines. However, in the case of 2-alkyl-2-alkoxy-Δ^3-1,3,4-oxadiazolines,

where both alkoxy(alkyl)carbenes and dialkylcarbenes are formed competitively (upper and middle

pathways in Scheme 5), analogous carbonyl ylides have been trapped with methanol, CCl$_4$, and with

dipolarophiles such as dimethyl acetylenedicarboxylate. Comparatively, if analogous carbonyl ylides

with two heteroatoms attached are formed from the corresponding oxadiazoline, they must fragment

more rapidly and more selectively. Such innate characteristics preclude intermolecular carbonyl ylide

chemistry from such precursors, but make them good precursors for diheteroatom substituted

carbenes since carbonyl ylides (in general) do not complicate analyses or reduce yields of carbene

derived products. While 2,2-dimethoxy-5,5-dimethyl-Δ^3-1,3,4-oxadiazoline yields dimethoxycarbene,

N$_2$, and acetone exclusively upon thermolysis, other 2,2-diheteroatom substituted oxadiazolines,[57]

most notably spirocyclic 2-alkoxy-2-amino-Δ^3-1,3,4-oxadiazolines,[58] have shown the incursion of

minor products from competitive thermal cleavage of carbonyl ylides to yield dialkylcarbenes (Scheme

5, middle pathway) and from competitive thermal cleavage of oxadiazolines to yield diazoalkanes

(Scheme 5, lower pathway).

Photochemistry of Oxadiazolines.

Studies have shown that alkoxy substituted Δ^3-1,3,4-oxadiazolines, when irradiated directly (300

nm),[59, 60] efficiently generate dialkyldiazo compounds which were inferred from their characteristic IR

stretch ~2020 cm⁻¹, formation of azines, and by trapping with dipolarophiles. For example, the

photolysis of **24** in benzene with 300 nm light was shown to produce 2-diazopropane which was

found to undergo [3+2]cycloaddition with N-phenylmaleimide to yield compounds **26** and **27** in ~1:1

ratio (eq 32). Product **27** was thought to occur by loss of N_2 from **26**.[59] Photosensitization of **24** with

benzophenone as the triplet sensitizer also produces diazopropane and methyl acetate.[61]

$$(32)$$
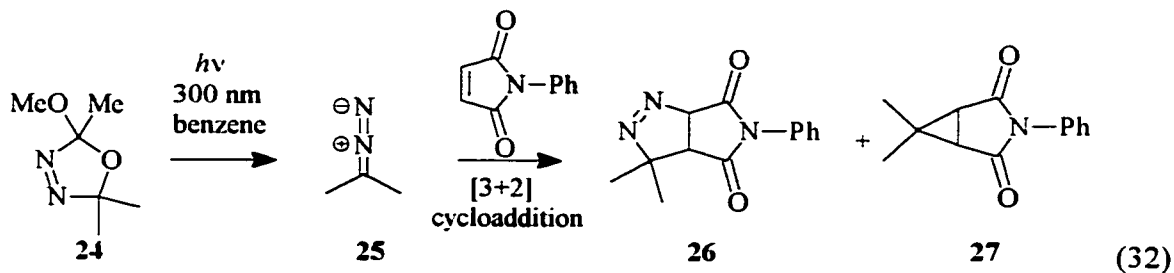
The photochemical decompositions of alkoxy-trialkyl-Δ^3-1,3,4-oxadiazolines are thought to

involve initial α-scission of the excited state to form the more stable diradical intermediate which

subsequently undergoes β-scission selectively to give a diazoalkane and an ester in nearly quantitative

yield. The β-scission leading to these products (Scheme 6, path (a)) must be significantly faster than

the loss of N_2 (Scheme 6, path (b)). The triplet diazenyl diradical intermediate can give products either

directly via β-scission or after efficient intersystem crossing (ISC) to the singlet diradical species

which then undergoes β-scission. Efficient ISC from the triplet to the singlet may result from oxygen

atom-enhanced spin orbit coupling.[62] Also, for the case when R^1=cyclopropyl, it has been observed

that cyclopropylcarbinyl rearrangement products are not formed, suggesting that the free radical clock

$(k_r > 10^8 \text{ s}^{-1})^{a \ 63}$ is too slow to compete with β-scission (a).

---

[a] Rate constants for rearrangements of alkoxy substituted cyclopropylcarbinyl radicals are not known but are expected to be smaller than those for *secondary* cyclopropylcarbinyl radicals which rearrange with rate constants of ~ 10^8 s⁻¹ at room temperature.[64]

Scheme 6. Photochemical Decomposition of Δ^3-1,3,4-Oxadiazolines.
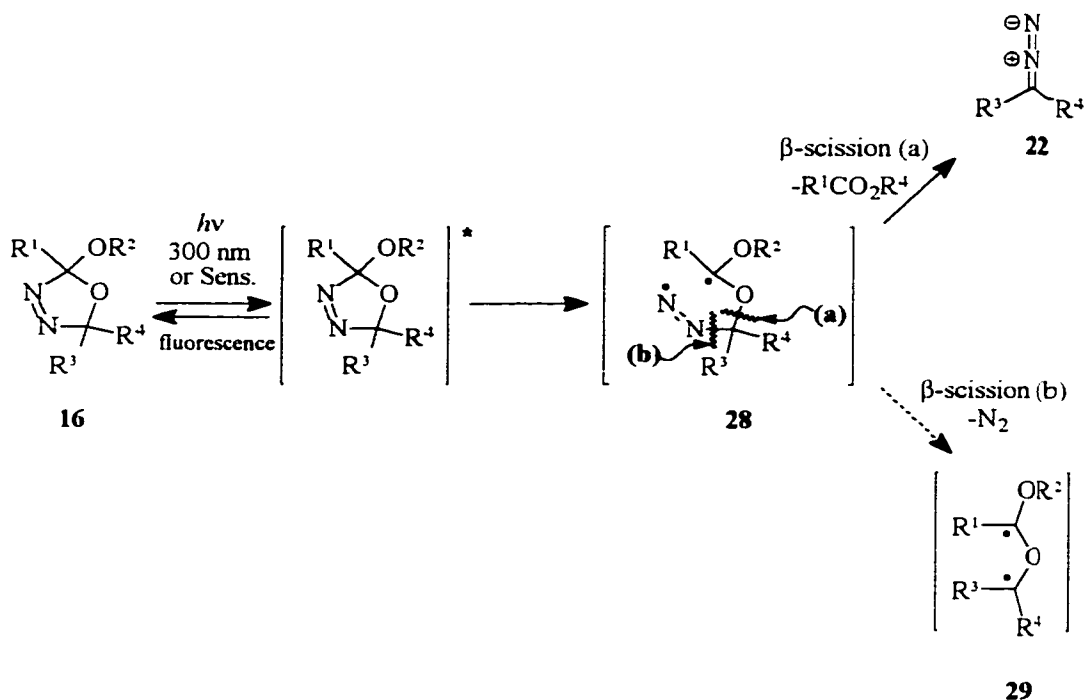
Selective formation of diazoalkanes from photolysis of oxadiazolines is contrary to the photochemistry of all carbon analogues, azoalkanes (30), which eliminate molecular nitrogen preferentially in both thermal and photochemical reactions leading to the formation of diradical intermediates (eq 33).[64]

$$(33)$$
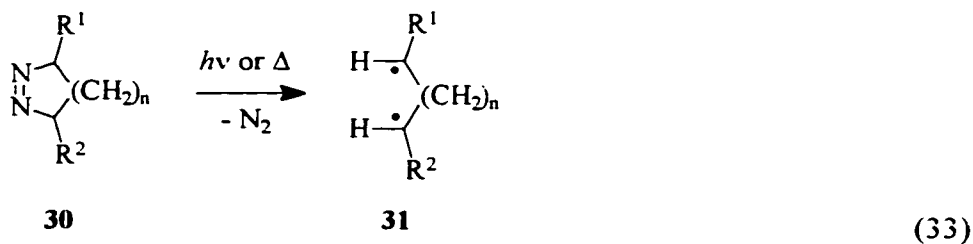
1.5. Measuring Rate Constants for Carbene Reactions.

Relative rate constants, based on ratios of products derived from competing pathways (preferably only two), give important insight about the preferences (or lack of preferences) a particular

intermediate may have towards different substrates. Such insights may allow for the logical altering of reaction conditions for preparative scale syntheses with maximal yields. In order to determine the absolute rate constants for individual processes from product studies the absolute rate constant for at least one "clock" reaction, which can be used to determine those for other reactions by competition kinetics, is required. Absolute rate constants for first order or pseudo-first order reactions are usually measured by monitoring the decays of starting materials or growths of products according to simple exponential growth/decay functions. However measuring such rate constants for carbenes, using conventional spectroscopic methods such as UV, IR, or NMR methods for monitoring signals associated with either the carbene or its reaction product(s), is difficult or impossible because most known carbenes are not stable enough to be isolated prior to kinetic measurements and because most reactions involving carbenes are too fast for such techniques. A technique which circumvents such problems, and which has become a standard tool for the study of reactive intermediates in general, is laser flash photolysis (LFP).

1.5.1. Laser Flash Photolysis

The technique of laser flash photolysis involves the photochemical generation of a reactive intermediate from a suitable photochemical precursor using a short-pulse-width monochromatic laser beam, directed from the laser source through the sample using a series of mirrors. A second monitoring beam is also directed through the sample and through a monochromator (either before or after the sample) and then through a photomultiplier tube (PMT) detector which transmits a signal through a digitizer to a computer for data storage and processing. Typically, the monitoring beam comes from a xenon arc lamp for UV-visible detection of transients or an infra-red (IR) diode laser for IR detection of transients. Both types of detection were used in LFP experiments described within

this thesis[a] and simplified schematic diagrams of both LFP setups which were used at the National

Research Council of Canada's Steacie Institute for Molecular Sciences (NRCC-SIMS) are in Figures

2 and 3.

Figure 2.

Figure 3.

---
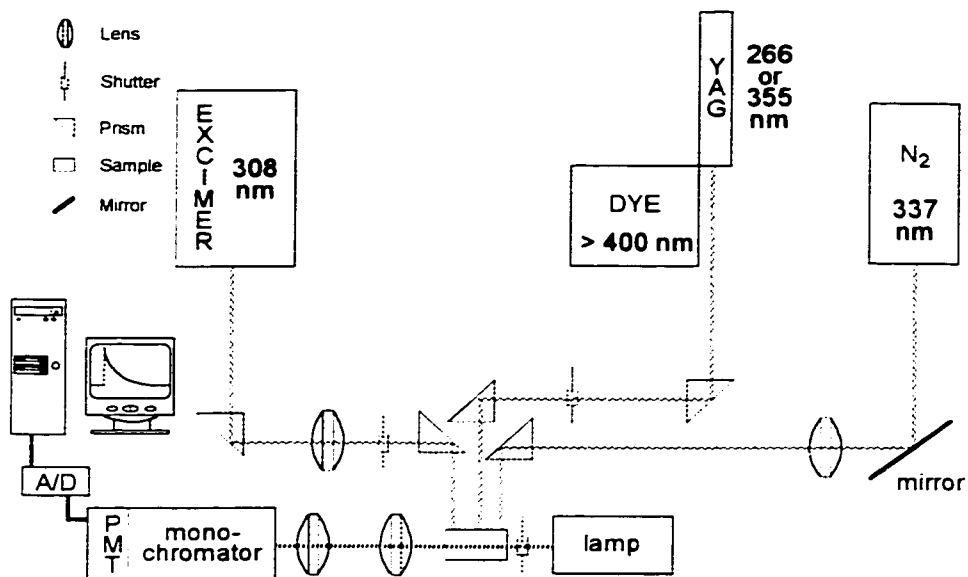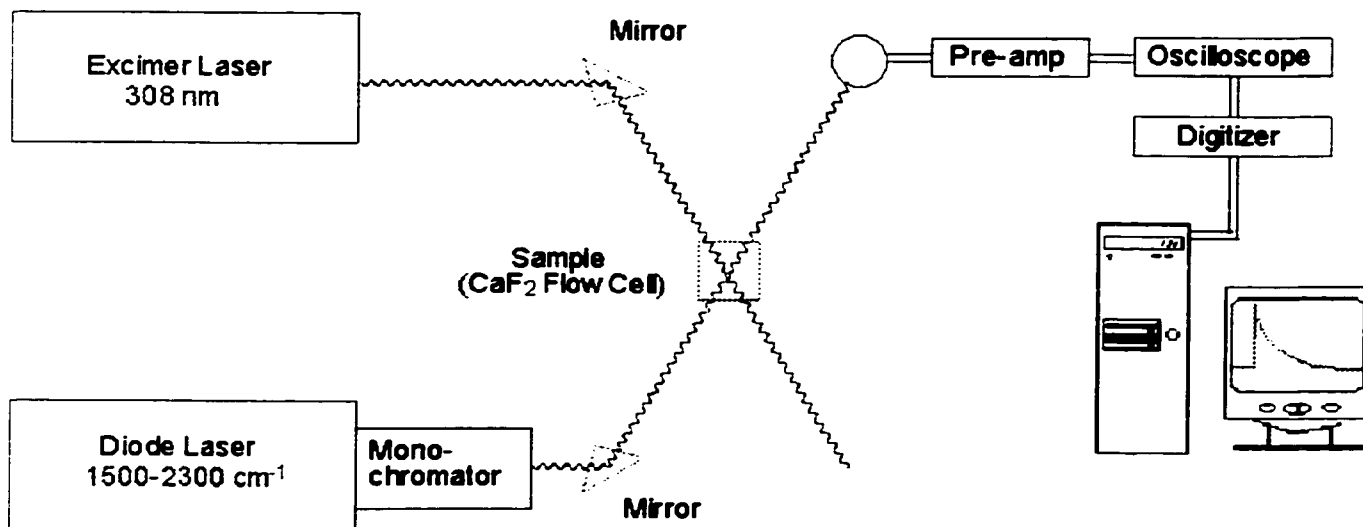
[a] The author spent ~ 7 months at NRCC-SIMS performing the LFP experiments described within this thesis.

I.5.1.a. Direct Detection of Transient Carbenes

Using LFP techniques, it is possible to measure the time-resolved UV or IR spectra at short time intervals following a laser pulse which generates a transient carbene. Such time-resolved spectra can correspond to singlet or triplet carbenes generated in the laser pulse. The decays of such transient signals then give rate constants, k_{obs}, which are equal to the sum of all rate constants for the disappearance of a particular carbene (eq 34). In eq 34, k_o is the sum of all uni- and bimolecular rate constants for the disappearance of the carbene in the absence of added carbene trap and k_{trap} are the bimolecular rate constants for intermolecular trapping of a carbene. Rate constants k_{trap} can be obtained as the slopes of plots of observed rate constants k_{obs} as a function of trap concentration.

$$k_{obs} = k_o + \sum k_{trap} \cdot [\text{trap}] \qquad (34)$$

Examples include the direct observation of triplet diphenylcarbene (**DPC:**),[65] fluorenylidene (**FL:**),[66] and singlet phenylchlorocarbene (**PCC:**).[67]

DPC: ᴧ **FL:** **PCC:**
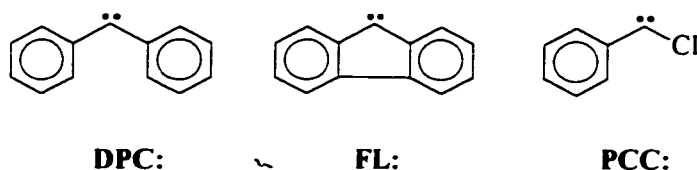
However, problems associated with overlap of signals associated with precursors, carbenes, and traps often prevent direct kinetic measurements based on carbene decays and in such cases kinetic measurements based on product signals which are well resolved from other signals are preferable.

It is well known that electrophilic singlet carbenes interact with lone pairs of electrons of heteroatoms to form ylide intermediates, eq 35, as do electrophilic transition metal carbenoids.[68] Ylide-forming reactions, such as the reactions of carbenes with pyridine,

$$R^1 \overset{\cdots}{\frown} R^2 \; + \; R^3 \overset{\cdots}{\underset{}{X}} R^4 \longrightarrow \underset{R^1 \underset{\ominus}{\frown} R^2}{\overset{R^3 \overset{\oplus}{\underset{X}{}} R^4}{}}$$

(35)
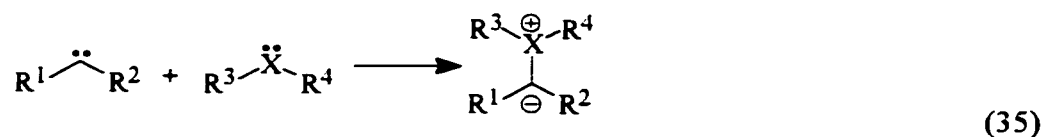
thiophene, or with nitriles, have been used extensively for determining inter- and intramolecular reactivity of carbenes that do not have absorptions in useful regions of the UV-visible spectrum.[69]

I.5.1.b. Pyridine Probe Method.

The capture of singlet carbenes by the Lewis base pyridine has become a powerful reaction for probing the reaction dynamics of inter- and intramolecular processes within those carbenes by UV-LFP (Scheme 7).

Scheme 7.
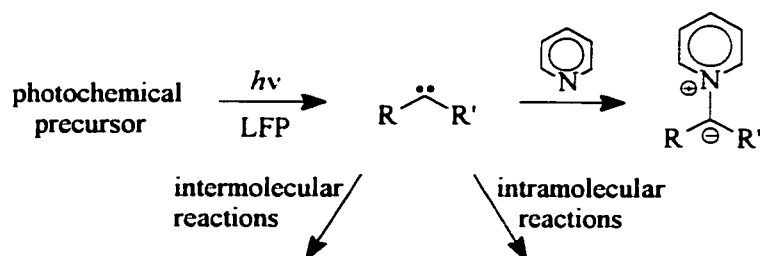
In general, the rate constant for the reaction of a particular singlet carbene with pyridine can be determined from the slope of the plot of observed rate constants for the growth of the product pyridinium ylide, k_{obs}, as a function of [pyridine] according to the linear expression in eq 36. The intercept of such a plot gives a value for k_o which is the sum of all competing uni- and bimolecular processes leading to the disappearance of the carbene. Values of k_o may represent rate constants for only one particular inter- or intramolecular pathway or a composite of many pathways. Ideally, one chooses reaction conditions such that only one or two processes compete with pyridinium ylide formation.

$$k_{obs} = k_o + k_{pyr} \text{[pyridine]} \tag{36}$$

Ylides derived from pyridine have been employed in this fashion and it has been shown that carbenes of different structure react with pyridine with rate constants ranging from 10^5 to 10^{10} M^{-1} s^{-1} (Table 1).[70] Carbenes such as oxycarbenes, which bear one or two π-donor substituents and are ambiphilic or nucleophilic in character,[14] have been shown to react with pyridine up to five orders of magnitude more slowly than electrophilic carbenes, such as those with alkyl or halogen substituents.[71,72] For example, methoxyphenylcarbene, which contains two π-donor substituents and is considered to be an ambiphilic carbene with a large degree of nucleophilic character ($m_{CXY}^{calcd} = 1.34$), reacts with pyridine with a bimolecular rate constant of $k_{pyr} = 1.2 \times 10^5$ M^{-1} s^{-1}, whereas phenylchlorocarbene, which is a more electrophilic ambiphile by comparison ($m_{CXY}^{calcd} = 0.71$),[14a, 14b, 72, 73] reacts with pyridine with a rate constant of $k_{pyr} = 7.6 \times 10^8$ M^{-1} s^{-1} in hexane at ambient temperatures.[71c]

Electrophilic carbenes such as dialkylcarbenes[74,75] ($m_{CXY} \approx 0.2$, dimethylcarbene has an $m_{CXY}^{calcd} = 0.19$), and chlorocarbene[23] ($m_{CXY}^{calcd} = 0.46$) react with pyridine with rate constants at or near the diffusion controlled limit; $k_{pyr} = 1$-8×10^9 M^{-1} s^{-1}. The relative reactivites of singlet carbenes are illustrated in Figure 4.

It is clear that the rate constants for reactions of carbenes of different structure do vary according to the relative electrophilicities of those carbenes at least qualitatively. Such differences are reflected in the relative magnitudes of carbene selectivity parameters m_{CXY}. In fact, if one plots the logarithms of the rate constants for reactions with pyridine against m_{CXY} values calculated from eq 5 then one does find a linear free energy relationship with a leveling effect (rate constants at least partially

Table 1. Rate constants for reactions of singlet carbenes with pyridine.[70]

Carbene	k_{pyr} (M^{-1} s^{-1}) in hydrocarbon solvent	k_{pyr} (M^{-1} s^{-1}) in acetonitrile solvent
MeO(Me)C:	6.6×10^5	---
CF$_3$CH$_2$O(Me)C:	1.6×10^7	6.6×10^6
CF$_3$CH$_2$O(C$_6$H$_{11}$)C:	1.0×10^6	3.4×10^5
MeO(Ph)C:	1.2×10^5	1.2×10^5
CF$_3$CH$_2$O(Ph)C:	1.8×10^6	1.4×10^6
CH$_3$CO$_2$(Ph)C:	3.5×10^7	2.0×10^7
MeO(Cl)C:	---	9.0×10^5
CF$_3$CH$_2$O(Cl)C:	---	2.8×10^7
CF$_3$CH$_2$O(PhOCH$_2$)C:	8.6×10^8	---
CH$_3$CO$_2$(PhOCH$_2$)C:	1.0×10^9	6.4×10^8
PhOCH$_2$(F)C:	1.4×10^{10}	---
PhOCH$_2$(Cl)C:	1.2×10^{10}	---
Ph(F)C:	1.5×10^9	9.5×10^8
Ph(Cl)C:	1.5×10^9	5.9×10^8
	7.6×10^8	---
	3.3×10^8	---
Ph(Br)C:	1.2×10^9	5.2×10^8

diffusion controlled) for more electrophilic carbenes, Figure 5.[a] For highly electrophilic carbenes, factors other than electrophilicity presumably govern small changes in rate constants for reaction (eg. pyridinium ylide stabilities, and changes in heavy atom bond angles and distances). The non-horizontal line in Figure 5a has a slope of -5.0 (r=0.99) whereas the analogous line in Figure 5b has a slope of -5.2 (r=0.99) when one omits the points for dimethylcarbene, chlorocarbene, and phenylfluorocarbene. However, some carbenes, most notably phenylfluorocarbene, do not follow the trend for unknown

---

[a] These interpretations and plots in Figure 5 are my own evaluation of literature data.

reasons. There is no question that rate constants for the reactions of carbenes with pyridine do

decrease for carbenes with increasing nucleophilic character, at least qualitatively.

Figure 4. Reactivities of selected singlet carbenes toward pyridine.[70, 74, 137]
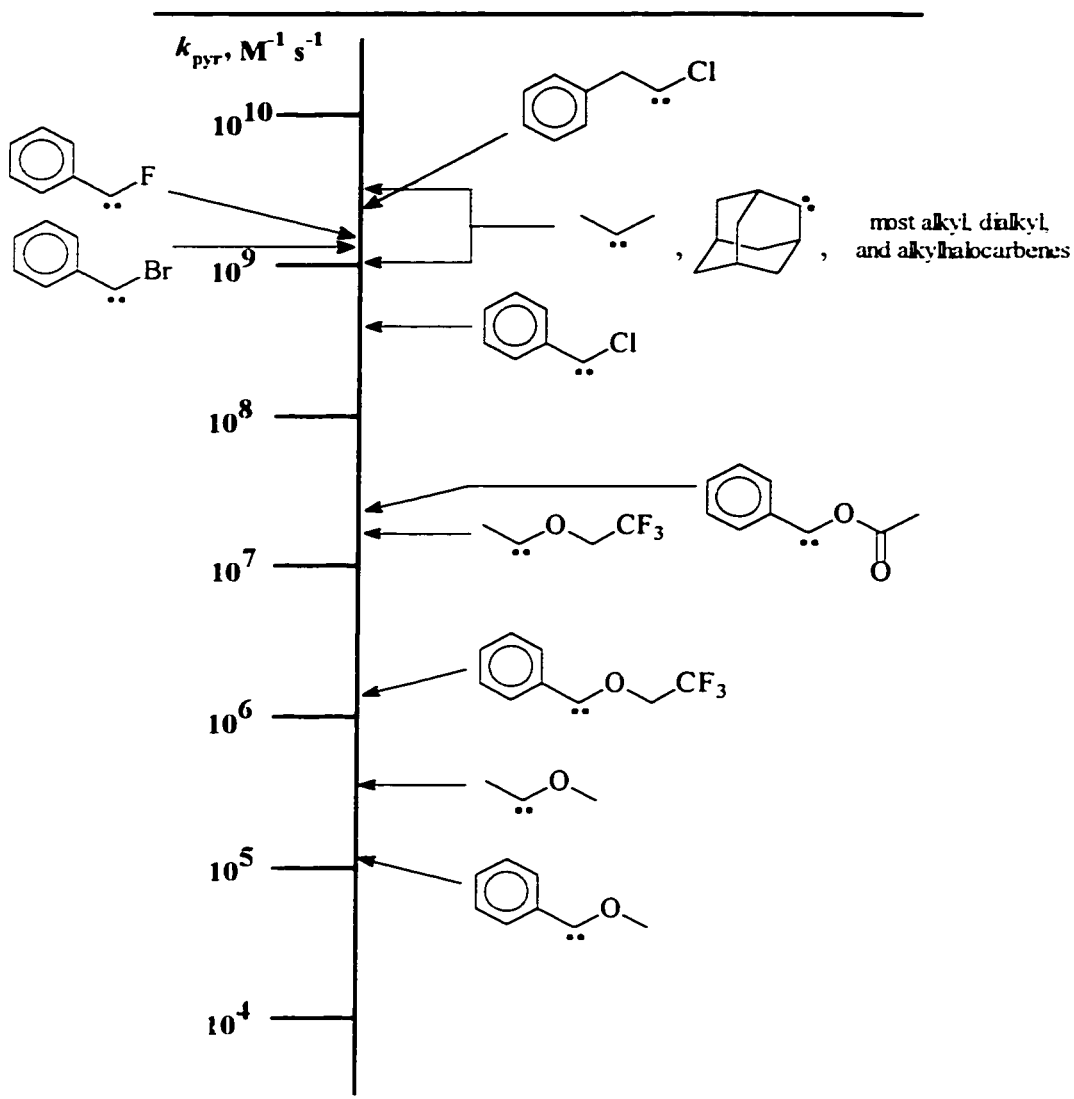
(a)

(b)
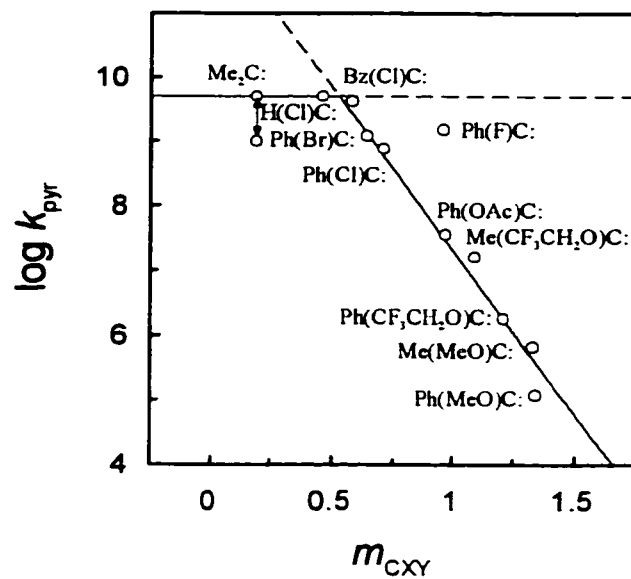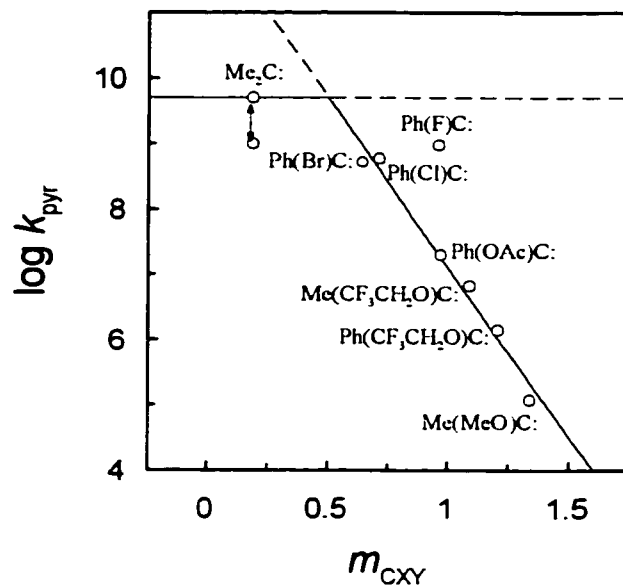
Figure 5. Plots of log k_{pyr} *vs.* m_{CXY} for reactions in (a) hydrocarbon solvent, and in (b) acetonitrile.

Intermolecular rate constants for trapping of carbene intermediates can also be determined by the pyridinium probe method taking advantage of the relation in eq 37.

$$k_{obs} = k_o + k_{pyr} \text{[pyridine]} + k_{trap} \text{[trap]} \tag{37}$$

However, in some cases intramolecular rearrangements or intermolecular reaction with solvent may be too fast (i.e. values of k_o are too large and therefore [pyridine] has to be large to compete) to allow for the direct measurement of k_{pyr}. In such instances, Stern-Volmer methods are usually used.

1.5.1.c. Stern-Volmer Kinetics.

Stern-Volmer type analyses[76] relate the yield of product of a trapping reaction as a function of trap concentration to that for the trapping reaction at infinite trap concentration, based on the competition of all other reactions of an intermediate (k_o) with the trapping reaction (k_{pyr} [pyridine] in this case) and assuming that all of the intermediate is consumed in the trapping reaction at infinite trap concentration. Such techniques have been used within this thesis. The lifetimes of carbenes (τ which equals $1/k_o$) can be determined using the Stern-Volmer relation in eq 40 by curve fitting or using its linearized reciprocal in eq 41. (assuming that the intensity of light is constant through a series of experiments)

$$\phi_{Ylide} = \phi_C \cdot \frac{k_{pyr} \text{[pyridine]}}{k_o + k_{pyr} \text{[pyridine]}} \tag{38}$$

$$A_{Ylide} = \phi_{Ylide} \cdot A^{\infty}_{Ylide} \tag{39}$$

$$A_{Ylide} = A^{\infty}_{Ylide} \cdot \frac{k_{pyr} \text{[pyridine]}}{k_o + k_{pyr} \text{[pyridine]}} = A^{\infty}_{Ylide} \cdot \frac{k_{pyr}\tau \text{[pyridine]}}{1 + k_{pyr}\tau \text{[pyridine]}} \tag{40}$$

$$\frac{1}{A_{Ylide}} = \frac{k_o}{A^{\infty}_{Ylide} \cdot \phi_C \cdot k_{pyr} \text{[pyridine]}} + \frac{1}{A^{\infty}_{Ylide} \cdot \phi_C} \tag{41}$$

Equation 40 is derived from eq 38 which relates the quantum yield for formation of the pyridinium

ylide (ϕ_{Ylide}) to the rate constants for the various competing processes where ϕ_C is the quantum yield

for carbene formation (usually assumed to be ~1) and from eq 39 which relates ϕ_{Ylide} to the amplitudes

of the absorbances of pyridinium ylides (A_{ylide}) where A_{Ylide}^{∞} is the maximum amplitude of the

absorbance possible for the pyridinium ylides at infinite trap concentration. Intercept:slope ratios from

double reciprocal plots of $1/A_{Ylide}$ vs. $1/[pyridine]$ (eq 41) yield values for $k_{pyr}\tau$ according to eq 42.

$$\frac{\text{Intercept}}{\text{Slope}} = \frac{A_{Ylide}^{\infty} \cdot \phi_C \cdot k_{pyr}}{A_{Ylide}^{\infty} \cdot \phi_C \cdot k_o} = \frac{k_{pyr}}{k_o} = k_{pyr}\tau \tag{42}$$

Stern-Volmer techniques do not require LFP, although UV absorptions of unstable pyridinium

ylides can be conveniently measured using that technique. Lifetime determinations may be made based

on product yields as a function of trap concentration as well. One only needs knowledge of the rate

constant(s) for trapping, k_{pyr} above, or reasonable estimates, to determine the lifetime of a given

carbene by Stern-Volmer techniques.[76]

Intermolecular rate constants can also be determined using Stern-Volmer methods and the linear

relation in eq 43. This can be accomplished by measuring the amplitudes of the

$$\frac{\phi_o}{\phi} = \frac{A_{Ylide}^{o}}{A_{Ylide}} = \frac{k_{trap}}{k_{pyr} [\text{pyridine}]} [\text{trap}] + 1 \tag{43}$$

absorbances of pyridinium ylides at a constant concentration of pyridine in the absence of added trap

(A_{Ylide}^{o}) and as a function of added carbene trap (A_{Ylide}). The slopes of plots of the ratios of

A_{Ylide}^{o}/A_{Ylide} vs. [trap] give values which correspond to ratios k_{trap} / k_{pyr} [pyridine], where k_{trap} is the

bimolecular rate constant for the reaction of a given carbene with the added trap. From the slopes of

such plots, with known values of k_{pyr} and [pyridine], k_{trap} may then be determined.[76]

I.6. Intramolecular Chemistry of Carbenes.

Intramolecular reactions of carbenes usually involve 1,2-migrations of atoms or groups located α

to the carbene carbon, the most common of which are 1,2-hydrogen migrations, or insertions into

remote bonds, or additions to π-bonds (Scheme 8).

Scheme 8.
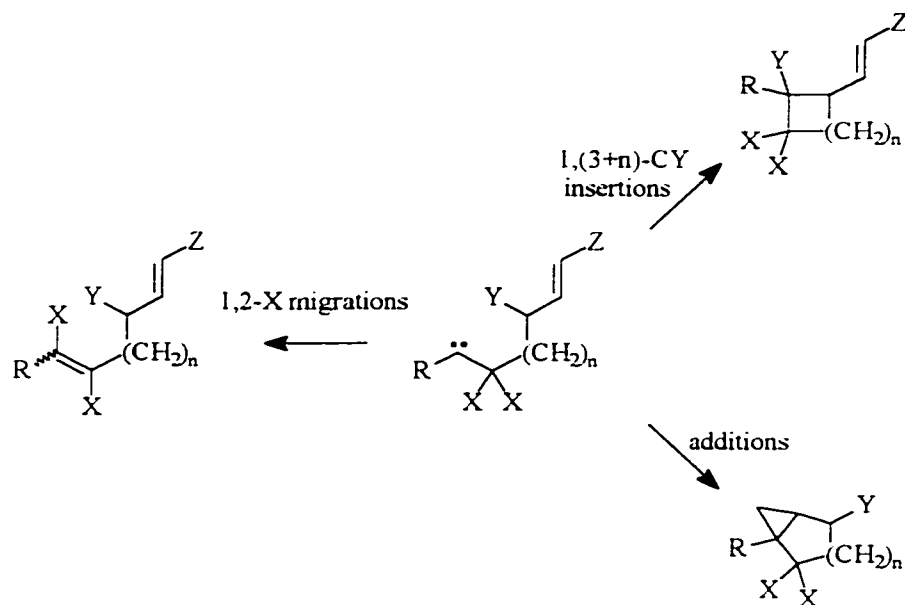
In general, intramolecular reactions tend to dominate in very reactive carbenes where the barriers

for such reactions are small, whereas more stable and less reactive carbenes tend to favor

intermolecular pathways. The research pertaining to intramolecular carbene rearrangements within

this thesis concerns mainly 1,2-hydrogen and 1,2-carbon migrations within dialkylcarbenes, and 1,2-

silicon migration within alkoxysiloxycarbenes, and those processes are highlighted in this introductory

section.

I.6.1. 1,2-Hydrogen Migration.

The intra- and intermolecular reactivities of alkyl and dialkyl carbenes have been actively studied

in recent years.[69, 77] For singlet dialkylcarbenes, 1,2-hydrogen (1,2-H) migration is well known[1,74] and

is modulated by substitution at the carbene carbon.[2a] For example, dimethylcarbene has a lifetime (τ)

of ~7 ns[4] in perfluorohexane at ambient temperature which corresponds to $k_{1,2-H} \cong 1.4 \times 10^8$ s^{-1} (eq

44), while $k_{1,2-H} = 1-3 \times 10^6$ s^{-1} in chloromethylcarbene (eq 45).[78] For bromo(methyl)carbene $k_{1,2-H} =$

5-6 $\times 10^6$ s^{-1} (eq 46),[79] and 1,2-H migration in methoxy(methyl)carbene is much slower by comparison

(eq 47).[80] Methoxy(methyl)carbene gives less than 10% methyl vinyl ether when generated in dilute

pentane solutions from either thermal or photochemical decomposition of the corresponding diazirine

precursor. Instead azine formation tends to dominate.[80]

$$k_{1,2-H} \sim 1.4 \times 10^8 \text{M}^{-1}\text{s}^{-1}$$

(44)

$$k_{1,2-H} = 1-3 \times 10^6 \text{M}^{-1}\text{s}^{-1}$$

(45)

$$k_{1,2-H} = 5-6 \times 10^6 \text{M}^{-1}\text{s}^{-1}$$

(46)

slow

(47)
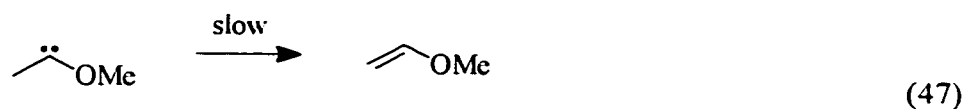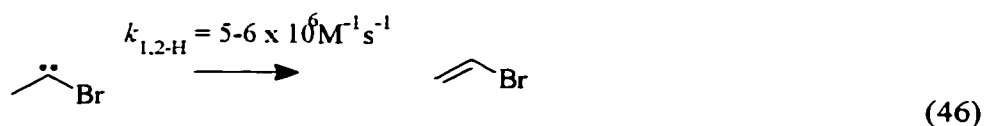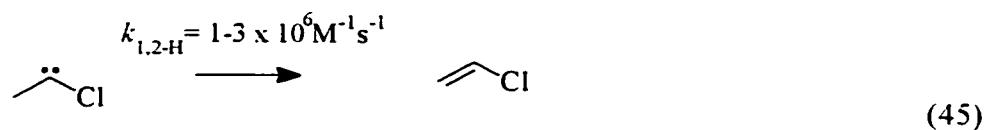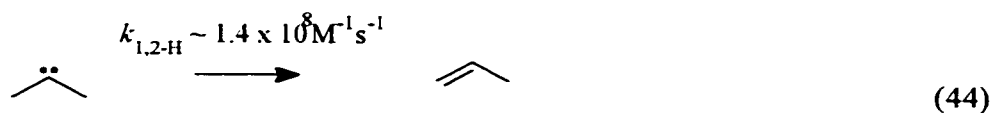
Presumably modulation of rate constants for 1,2-H migration occurs through substituent effects

on both the ground and transition state stabilities for intramolecular rearrangement. 1,2-H migration in

carbenes appears to be accelerated, in some cases, by polar solvents.[81] In other cases the formation of

π-complexes with arenes may affect the rate constants for intramolecular rearrangement.[82]

The 1,2-H migrations within alkyl and dialkylcarbenes are sometimes referred to as "hydride"

shifts. Such migrations are thought to occur in a manner similar to those within carbocations where

the hydrogen atom migrates with a pair of electrons into a vacant p-orbital on an adjacent carbon

atom. Theoretical calculations predict that 1,2-H migration in ethylidene (eq 48) proceeds with the

migrating hydrogen atom being perpendicular to the plane defined by the carbene carbon and the

atoms directly attached.[83]

(48)
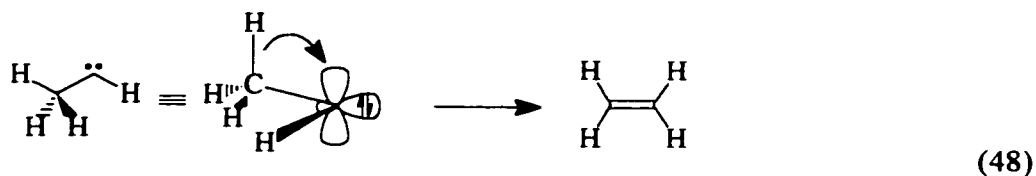
It is thought that the degree of overlap between the C-H bond orbital of the migrating hydrogen

and the virtual p-orbital of the carbene, in cases where conformational interconversion is restricted,

affects the absolute rate constant for migration.[84] Stereochemical dissection of the 1,2-H migrations of

conformationally restricted dialkylcarbenes such as cyclohexylidenes have been reported.[84, 85-88] It has

been shown that there is a 2.2:1 ratio of rate constants for 1,2-H migration from the axial and

equatorial positions in homobrexylidene (32),[84a,85] and that $k_{ax} : k_{eq} = 1.9 : 1$ for 2,2-dimethyl-4-t-

butylcyclohexylidene (33).[84a, 86]

32   33
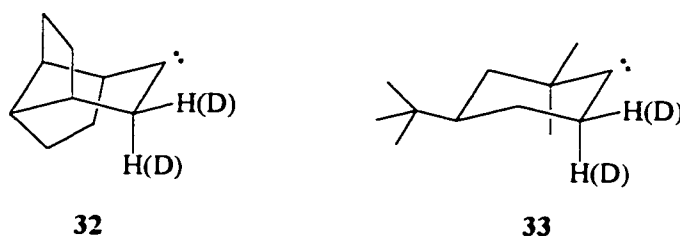
Substituents such as phenyl in 5-t-butyl-2-phenylcyclohexylidene (34)[87] or methoxy in 4-t-butyl-2-

methoxycyclohexylidene (37),[88] capable of stabilizing positive charge buildup at the α-position, have

also been shown to accelerate 1,2-H migration, leading to the preferential formation of products 35

and 38 (eqns 49 and 50). The degree to which 1,2-H migration is favored in these systems depends on

whether the substituent is in an axial or equatorial position (eqns 49 and 50). Substituent effects such

as these have been described previously as "bystander effects".[84b]

phenyl equatorial :   77.1%   21.6%
phenyl axial :   52.3%   41.3%   (49)

methoxy equatorial :   95.1%   4.70%
methoxy axial :   29.4%   58.4%   (50)
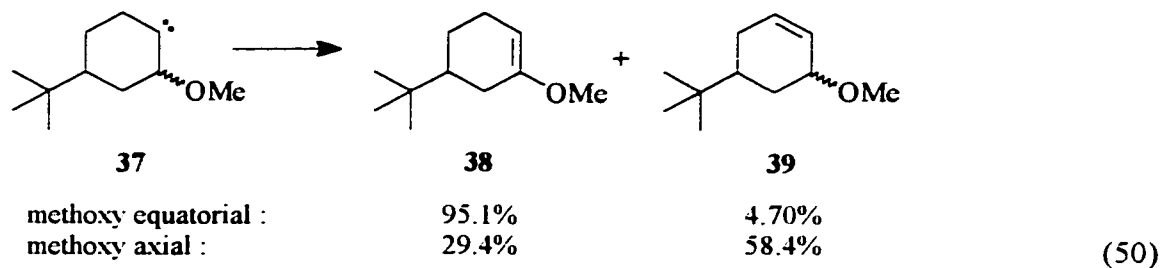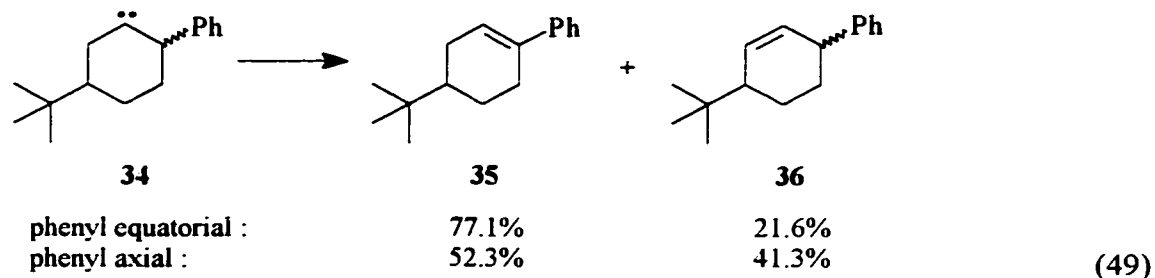
I.6.2. Bystander Effects.

Nickon has analyzed published data of 1,2-H migrations in acyclic and cyclic alkyl and dialkylcarbenes in terms of the effects of substituents located α to the carbene center (bystander groups), the inherent nature of the migrating group, and the effects of substituents directly attached to the carbene carbon (terminus group) as well as geometric effects on the relative rates of intramolecular 1,2-shifts.[84] Three factors purported to control the rate constants for 1,2-migrations are the inherent migratory aptitude of the migrating group (termed M), the assistance to migration provided by a bystander group (termed the B factor), and the efficiency with which two geminal bystander groups combine to affect migration (G factor).[84] Since many of the absolute rate constants for 1,2-migrations are not known, Nickon's analyses are restricted to carbenes of the same class and geometric structure and relative rate constants come from comparisons of competing intramolecular migratory pathways within individual carbenes. It is generally accepted that the order of migratory aptitudes of hydrogen, phenyl, and methyl is H > Ph > Me based on product studies of carbenes containing these groups attached to the same migration origin in direct competition, however, Nickon has pointed out that if one corrects for the "bystander" effect that a competing phenyl group has on

the rate constant for 1,2-H migration then one can conclude that phenyl is inherently better than hydrogen as a migrating group.[84] In terms of 1,2-hydrogen migration, substituents Ph-, Me-, Et-, allyl-, and MeO- all accelerate 1,2-H migration relative to the prototype carbene, dimethylcarbene, in the order MeO > Et > Me ~ allyl > Ph. There are conformational effects on the abilities of these groups to accelerate 1,2-H migration with "anti" transition states being favored, in general, for acyclic carbenes.[84] For cyclohexylidenes, equatorial bystanders show more of an effect than axial bystanders, in general.

anti-like conformation   syn-like conformation
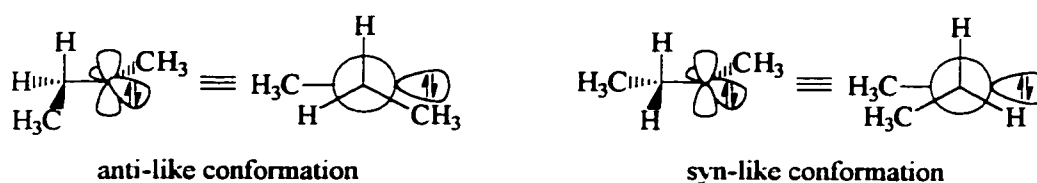
The bystander effects first proposed by Nickon have been supported by computational chemistry recently.[89] The order of relative abilities of selected substituents to accelerate 1,2-H migration was found to be Ph > Me > F > Cl > H. The computed barriers for migrations and substituent effects are summarized in Table 2.

1.6.3. 1,2-Carbon Migrations.

Intramolecular 1,2-carbon migrations are less common than 1,2-H migrations in alkyl-, dialkyl-, and alkylhalocarbenes. Ring expansion reactions of strained carbocyclic ring systems α to carbene centers have been observed and involve 1,2-carbon migrations to the carbene center. Examples include the ring expansions of cyclopropylcarbene, cyclopropylhalocarbenes (eq 51), cyclopropylmethylcarbene (eq 52), and dicyclopropylcarbene (eq 53) to cyclobutenes (eqs 51 and 52), as well as ring expansion of analogous cyclobutylcarbenes (eq 54).[35c]

Table 2. Computed Substituent Effects.[a, b]

Substituent X	carbene	reaction	Δ charge at C₂ in parent	position	ΔEₐ, kcal/mol	ΔΔG‡, kcal/mol
methyl	XCH₂(Cl)C:	H shift	+0.33	syn	4.7	5.2
			+0.33	anti	4.5	4.6
methyl		singlet Ph	+0.23	syn	1.8	2.1
		shift	+0.23	anti	1.3	1.4
methyl	XCH₂(H)C:	singlet Ph	+0.09	syn	no barrier	
		shift	+0.09	anti	0.0	-0.1
methyl		triplet Ph	+0.14	syn	2.1	2.7
		shift	+0.14	anti	2.0	2.5
Cl	XCH₂(Cl)C:	*cis*-H shift	+0.33	syn	3.0	3.4
		trans-H shift	+0.33	anti	0.6	0.5
F	XCH₂(Cl)C:	*cis*-H shift	+0.33	syn	5.3	5.8
		trans-H shift	+0.33	anti	2.5	2.8
phenyl	XCH₂(Cl)C:	H shift	+0.33	syn	3.0	3.4
			+0.33	anti	6.0	6.0
phenyl	XCH₂(Ph)C:	H shift	+0.28	syn	—	—
			+0.28	anti	—	—

[a] Taken from Keating. A. E.; Garcia-Garibay. M. A.; Houk. K. N. *J. Phys. Chem.* **1998.** *102*. 8467.

[b] Energies were calculated at the B3LYP/6-311G**//B3LYP/6-31G* level and include ZPE correction.

(51)

(52)

(53)

$$\square\kern-0.3em\raise0.5ex\hbox{$\ddot{}$}X \longrightarrow \langle\!\!\!\!\!\!\bigcirc^{X} + \diamondsuit\!\!=\!\!CHX \qquad X = Cl, Ph$$

$$(54)$$
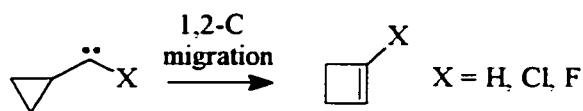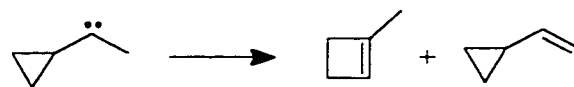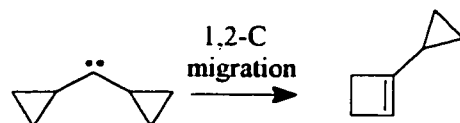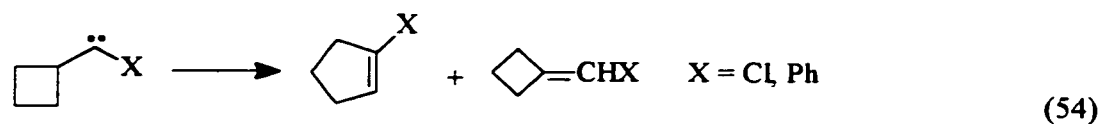
The relative migratory aptitudes of CH_2 and CMe_2 groups in unsymmetrically substituted cyclopropylcarbenes have also been investigated (eq 55).[35h] It was found that CH_2 migration is favored by 39 fold when X=Me and by 5 fold when X=Cl in eq 55.[35h] The differences in migratory abilities have been attributed to differential steric effects but could also be attributable to a buildup of negative charge at the migrating carbon in the transition states for ring expansion.

$$\text{(structure)} \longrightarrow \text{(structure)}^{X} + \text{(structure)}^{X} \qquad X = Me, Cl$$

-CMe₂	-CH₂
migration	migration

$$(55)$$
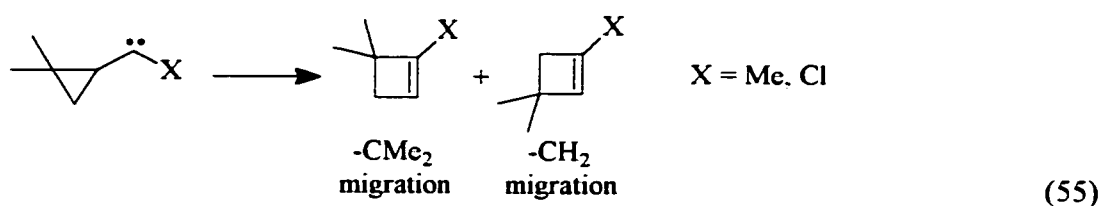
Results from the thermal decomposition of the sodium salt of cyclobutanone tosylhydrazone[90] and from the dehalogenation of halocyclobutanes[91] indicate that 1,2-C migration in cyclobutylidene is favored by ~5:1 over 1,2-H migration (eq 56). 1,2-Carbon migration is special in the case of cyclobutylidene, which rearranges through a dipolar, non-classical transition structure according to Schoeller[92] and Sulzbach, et al.[93]

$$\square\kern-0.3em\raise0.5ex\hbox{$\ddot{}$} \longrightarrow \square\!\!\!| + \triangleright\!\!=$$

$$(56)$$
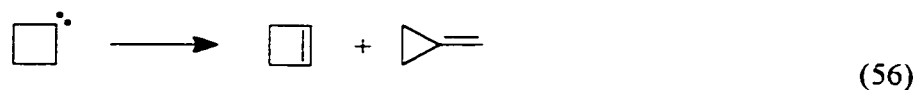
1.5.3.a. Wolff Rearrangements.

The Wolff rearrangement is a well established method for generating ketenes (**43**) by either the photochemical or thermal decomposition of α-diazoketones and α-diazoesters (**40**).[94] These rearrangements are thought to occur via acyl carbene intermediates (**41**) which, in some cases, have been trapped by pyridine in LFP experiments.[95, 96]

Scheme 9.
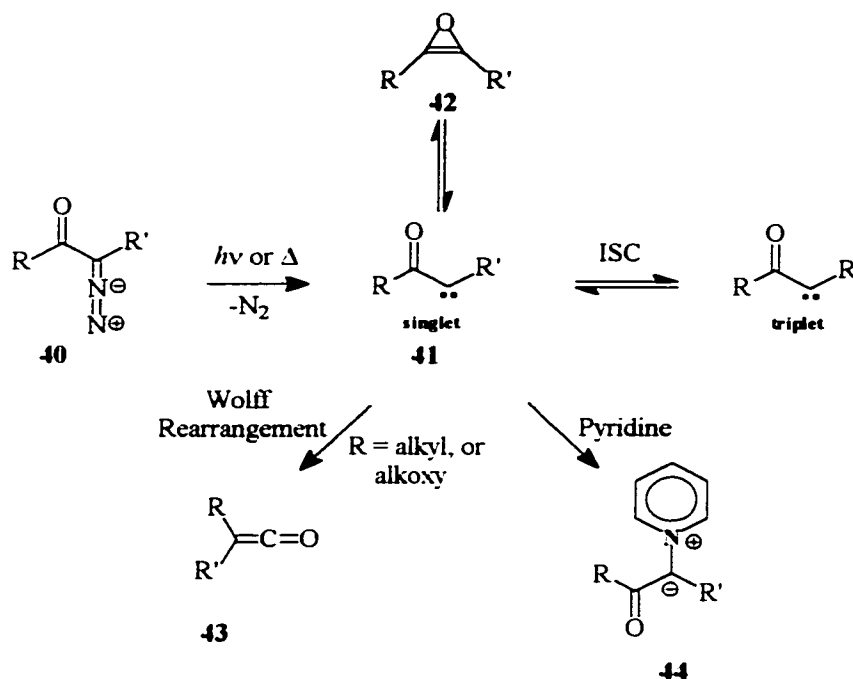
I.6.3.b. Acyl Migrations.

Formal 1,2-carbon migrations can also occur when the migration origin is an atom other than

carbon as is the case for 1,2-acyl migrations in acyloxycarbenes (eq 57).[97]
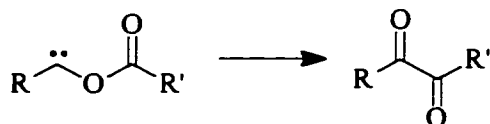
$$(57)$$

The rate constants for such migrations have been measured recently using the pyridinium ylide

method. Substituent effects on the rate constants for 1,2-acyl migration in benzoyloxycarbenes

Ph(ArCO$_2$)C: showed that electron donating groups modestly accelerate acyl migration ($\rho \sim 1$) and

those in arylacetoxycarbenes Ar(CH$_3$CO$_2$)C: showed that electron-withdrawing groups attached at the

migration terminus also mildly accelerate 1,2-acyl migrations. Both these results are consistent with a

mechanism involving acyl carbanion-like migration (Scheme 10, upper pathway) akin to that of

hydride-like 1,2-H migration in dialkylcarbenes bearing α-hydrogens. However, *ab initio* calculations

support a mechanism involving carbanion-like attack of the σ lone pair of the carbene onto the carbonyl carbon (Scheme 10, lower pathway).

Scheme 10.
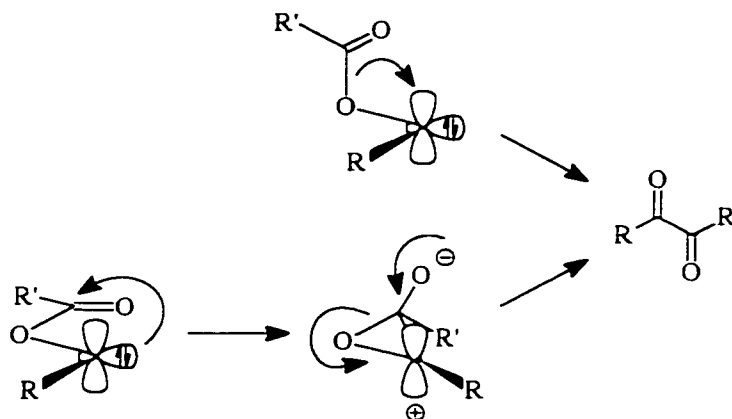
I.6.4. 1,3 C-H Insertions (1,3-H migrations).

Although not often observed, 1,3 C-H bond insertion products (cyclopropanes) are usually found from carbenes without α-hydrogens as is the case for *tert*-butylchlorocarbene.[98] They also occur in carbenes such as adamantylidene (eq 57) where 1,2-hydrogen migration is disfavored as a result of strain in the resulting bridgehead alkene product.[99, 100]

(57)
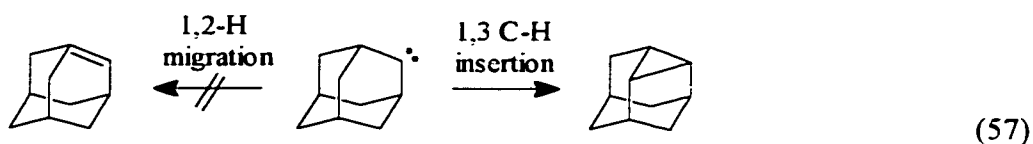
I.6.5. 1,2- and 1,n-Silicon Migrations.

In the past two decades there has been remarkable growth in the use of silicon based chemistry in organic synthesis.[101] Consequently, the effect of silicon-based reactive intermediates has been of considerable interest. In contrast to the stabilizing effects of silicon on carbocation, carbanion, and free radical intermediates, the effects of silicon on electron deficient carbenes is not well understood.

As was mentioned earlier, siloxycarbenes can be generated by photolysis or thermolysis of acylsilanes. In the absence of carbene trap these carbenes revert back to starting material *via* 1,2-silicon shifts from oxygen to carbon. The lifetimes of aryl(trimethylsiloxy)carbenes have been measured in acetonitrile and cyclohexane solvents by LFP and the corresponding rate constants for reversion to starting material were found to range between 1×10^8 - 1×10^6 s^{-1}. [102, 103]

Creary and Wang[104] have observed that the β-SiMe₃ substituted carbene **45** undergoes rearrangement to give alkenes **46** and **47** with a minor amount of product **48**, eq 58. Product **46** seemed to have arisen from a 1,2-SiMe₃ migration while **47** arose from 1,2-H migration. In the case of the analogous compound **49**, with no trimethylsilyl group present the only product obtained is the tricyclic compound **50**, eq 59. These results suggest that the TMS group in carbene **45** increases the migratory power of the exo-hydrogen in comparison to the unsubstituted compound **49**.

$$(58)$$

$$(59)$$
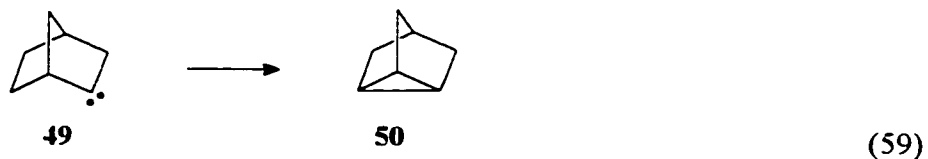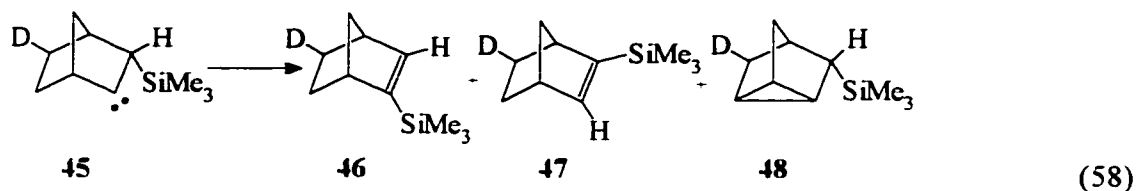
Creary and Wang have also looked at γ-trimethylsilyl substituted carbenes.[105] It was found that the TMS group still had a profound effect on product distribution even when remotely located relative to the carbenic center (see eqs 60 to 62).

$$(60)$$

$$(61)$$

$$(62)$$
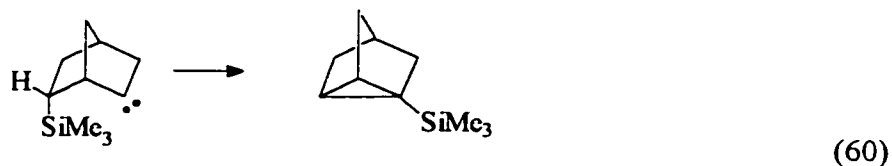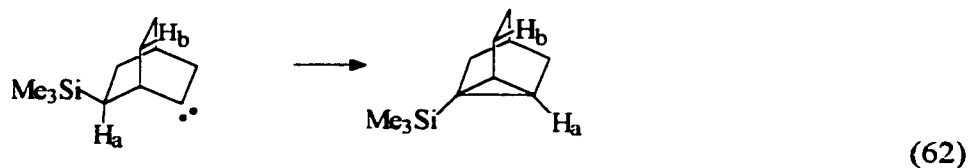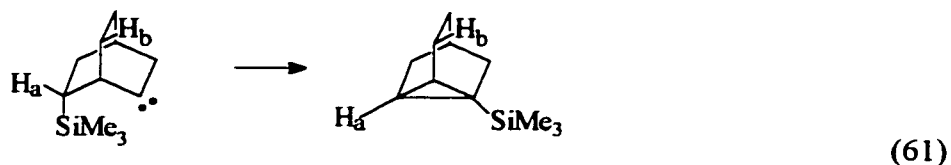
In γ-trimethylsilyl substituted carbenes, the only hydrogen migration that was observed was the 1,3 migration of the hydrogen attached to the carbon bearing the trimethylsilyl group. The presence of the trimethylsilyl group has been postulated to make the α-hydrogen "hydridic", thus increasing its' migratory aptitude to the electron deficient center relative to other hydrogens (i.e. H_b) that are equidistant to the carbene center.

The Wolff rearrangement is a well established method for generating ketenes by either the photochemical or thermal decomposition of α-diazoketones and α-diazoesters.[94] These rearrangements are thought to occur *via* acyl carbene intermediates which have been trapped by pyridine in LFP experiments.[95-96] Silyl substituted α-diazoketones and α-diazoesters undergo analogous rearrangements under photolytic conditions.[106]

The photolysis of diazo compounds **51** leads to the formation of α-silyl carbenes **52** and, depending on the acyl migrating group R', either ketene **55** or **56** is formed, Scheme 11. When R' is an alkyl group then ketene **55** is usually observed. However, the α-silyl group provides for a migratory process which is competitive with that of the Wolff rearrangement. The migration of silicon leads to the formation of silene **53**, which then undergoes a subsequent rearrangement to yield ketene **56**. Silene formation is enhanced when substituents R are phenyl or trimethylsilyl. Ketene **56** becomes

the predominant product when R'=alkoxy since the migratory ability of alkyl groups is much higher than alkoxy groups for the Wolff rearrangement.

Scheme 11.
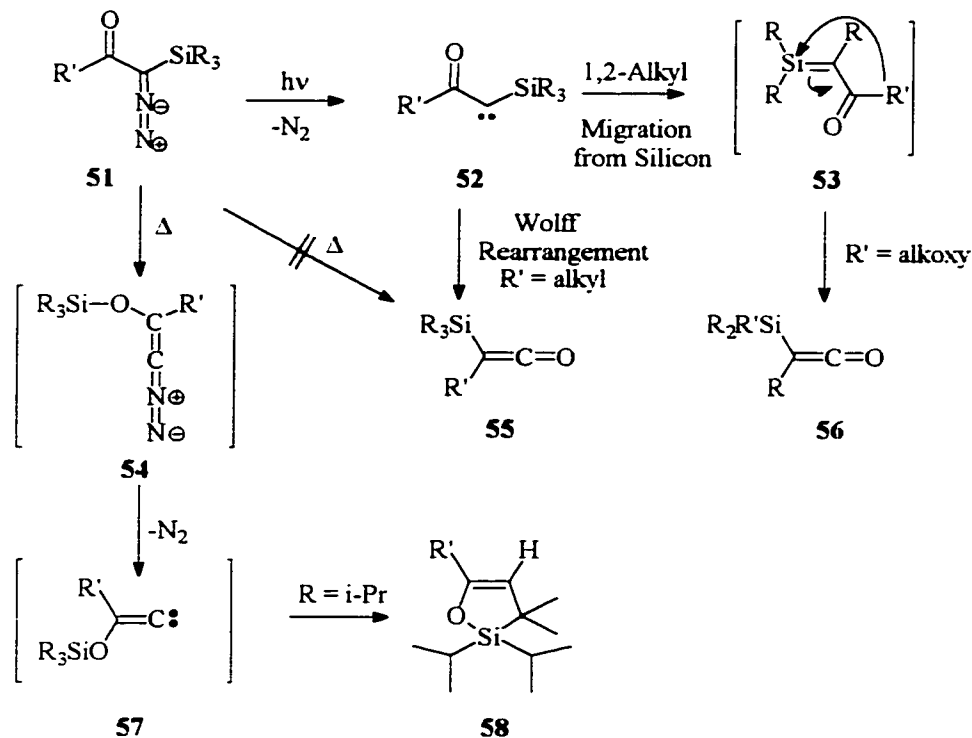
Generation of carbene **52** does not occur via thermal decomposition of diazo compounds of type **51** since a 1,3-silyl migration occurs faster than loss of nitrogen, Scheme 11. The 1,3-silyl migration leads to the intermediate **54** which then loses molecular nitrogen to form the alkylidine **57**. The alkylidine then inserts into a carbon hydrogen bond of one of the substituents on silicon to yield the cyclic silyl enol ether **58**.[107]

1.6.6. Rearrangements in Excited-states(RIES) and Carbene-olefin Complexes (COC).

Dialkylcarbenes can undergo competitive intramolecular rearrangements including 1,2-hydrogen and 1,2-carbon migrations. When this is the case, and the lifetime of the carbene is known, then rate constants for the individual processes may be evaluated based on product studies. However,

dialkylcarbenes generated from photochemical precursors, have been observed to give complex product distributions resulting from intramolecular reactions of the excited states of the precursors (RIES) which may mimic carbene reactions[35] but give product distributions which are not representative of carbene reactivity.[108] Although the RIES mechanism from diazirine photochemical precursors appears to be firmly established, alternative explanations for product distributions involving carbene-olefin complexes (COC) have also been put forth.[35m, 67b, 109] The postulate is that carbene rearrangement products are formed directly from carbene-olefin complexes. Evidence supporting the COC mechanism includes untrappable sources of carbene rearrangement products in the thermolysis of analogous precursors, results from time-resolved photoacoustic calorimetry, and non-linear plots of carbene-olefin adducts/carbene rearrangement products vs. [olefin]. However, calculations predict that such complexes are not free energy minima and collapse immediately to form cyclopropanes.[110] The debate regarding the existence and behavior of carbene-olefin complexes rages on in the literature with some groups sticking to a firm belief that these complexes partition between cycloaddition and rearrangement while others stand firmly against the COC mechanism. One example of the intervention of either excited state chemistry or COC chemistry in the formation of 1,2-hydrogen migration products comes from benzylchlorodiazirine (59).[35m, 37] When 59 is irradiated in the presence of the carbene trap tetramethylethylene (TME) yields of 1,2-hydrogen migration products 62 and 63 are not only reduced but the ratio of the two alkene products also changes (Scheme 12). Plots of 64/ (62 + 63) vs. [TME] are also curved. These results are inconsistent with alkenes 62 and 63 arising from benzylchlorocarbene (61) alone. It is possible that the RIES (Scheme 12) or the COC (Scheme 13) or both in combination contribute to the untrappable pathway to carbene rearrangement products. Although it is not known for certain that anomalies in product distributions are the result of the incursion of excited state rearrangement (Scheme 12), there is strong evidence that yields of carbenes from alkylchlorodiazirines are proportional to the α-C-H bond dissociation energies,[26a] which is

consistent with the RIES interpretation. Recent results from a non-nitrogenous phenanthrene precursor appear to exclude the COC mechanism for benzylchlorocarbene.[37]

Scheme 12. 1,2-Hydrogen Migration from the Excited State of Benzylchlorodiazirine and from Benzylchlorocarbene: The RIES Mechanism.
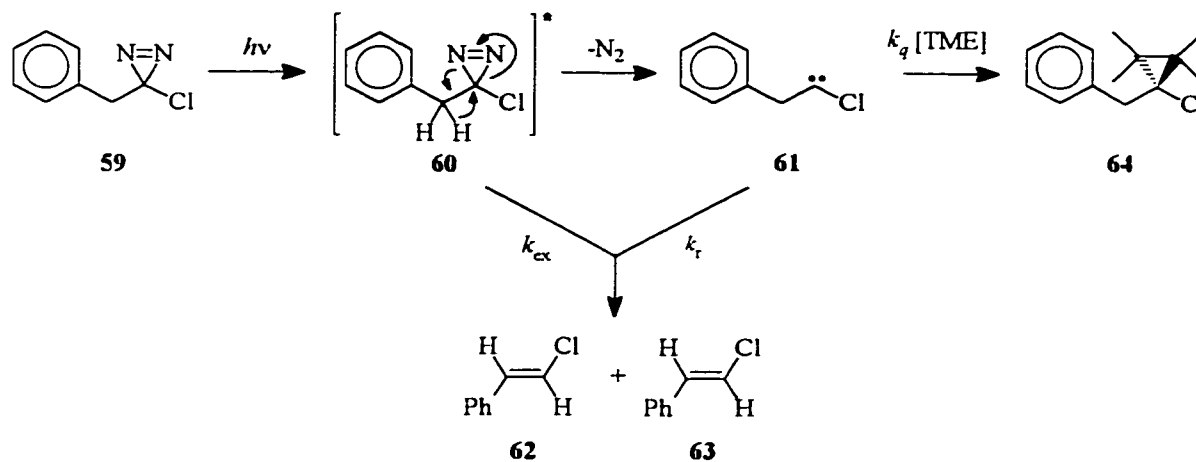
Scheme 13. The COC Mechanism for Benzylchlorocarbene.
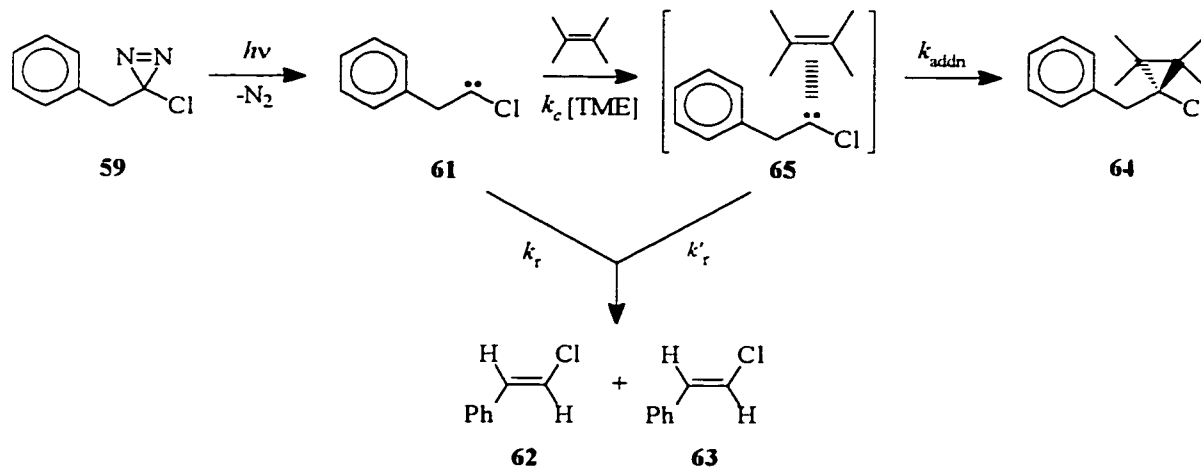
Carbene-Benzene Complexes.

Although the existence of carbene-olefin complexes is questionable, carbene-arene complexes which modulate carbene reactivity have been implicated recently.[111] Comparisons of yields of intramolecular rearrangement products and products of cycloaddition to tetramethylethylene (TME) at constant [TME] from either thermally and photochemically generated benzylchloro-, propylchloro-, and cyclopropylchlorocarbenes in isooctane, benzene, and anisole solvents indicate that intramolecular rearrangements are strongly favored in aromatic solvents. These observations have been explained in terms of transient carbene-arene π complexes which form rapidly and prevent intermolecular addition of TME to the carbenes but allow for intramolecular rearrangements within the complexes. The lifetimes were also found to be extended by as much as 100 fold in benzene as compared with those in isooctane by LFP. Carbene-benzene complexes for dichlorocarbene and methylchlorocarbene were also found to be energy minima by *ab initio* computational methods and the geometries of those minima are below.[111]

$$r_1 = r_3 = 3.48 \text{ Å}, r_2 = 3.14 \text{ Å} \qquad r_1 = 3.15 \text{ Å}, r_2 = 3.45 \text{ Å}$$
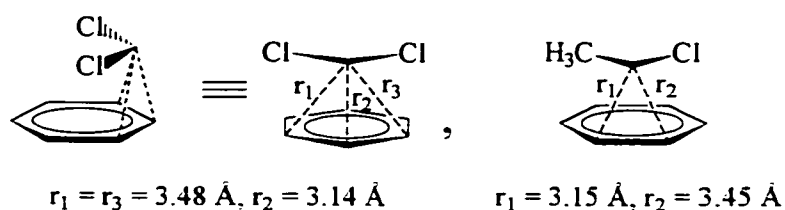
I.7. Intermolecular Reactivity of Carbenes.

Arguably the most common intermolecular reactions of carbenes are cyclopropanations. There are at least as many examples of these reactions as there are known carbenes. Cyclopropanations can occur from either the triplet or singlet states of carbenes. Evidence obtained from product studies of such reactions can implicate one or both carbene states according to Skell-Woodworth rules.[112] Reactions with heteroatoms and OH insertion reactions are also common in singlet carbenes.

I.7.1. OH Insertion Reactions.

The formal insertions of carbene intermediates into O-H bonds are well known processes and can occur by different mechanisms depending on the nature of the carbene intermediate. [113] Carbenes may insert into O-H bonds from the singlet spin state by a concerted mechanism, or by initial formation of an oxonium ylide intermediate followed by a 1,2-hydrogen shift, or by proton transfer (Scheme 14).

Scheme 14.
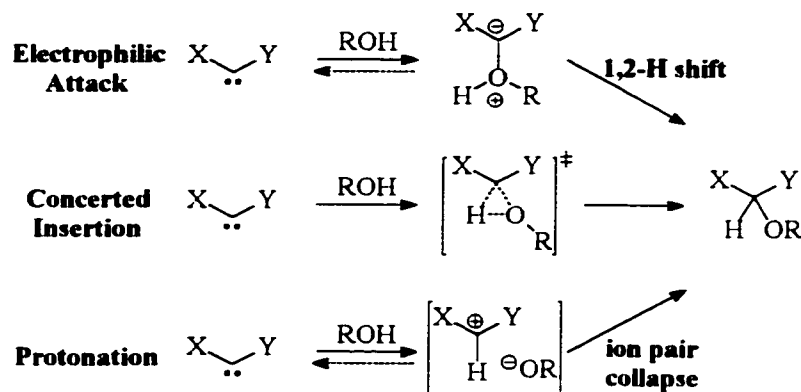
For example, tetrachlorocyclopentadienylidene is thought to undergo OH insertion with alcohols by an ylide mechanism, whereas cyclopentadienylidene and fluorenylidene are thought to undergo OH insertion *via* proton transfer or a concerted insertion or a composite, based on small slopes in Brönsted plots ($\alpha < 0.1$).[114]

The proton transfer mechanism leads to the formation of a carbocation/alkoxy anion pair which can collapse to form formal O-H insertion products. The observation of carbocationic intermediates after the photochemical generation of carbenes in solutions containing hydroxylic reactants, in laser flash photolysis (LFP) experiments, has shown that several carbenes of different structure undergo O-H insertion into alcohols *via* this mechanism. Mentioned earlier, diphenyl and diarylcarbenes have been shown to insert into the OH bonds of alcohols by a proton transfer mechanism, by direct observation of the resulting carbocationic intermediates by LFP, eq 1.

In other cases, proton transfers to carbenes have been implied based on product distributions. An example is the trapping of cycloheptatrienylidene with deuterated alcohols, which leads to mixtures of products with deuterium and the alkoxy substituent located at different positions in the cycloheptatriene products (eq 63).[115] Deuterium scrambling implicates a mechanism involving initial proton transfer to the carbene center which leads to the formation of the aromatic tropylium cation and an alkoxide ion. Ion pair collapse occurs at any of the tropylium ion's ring carbons, which results in a mixture of products. Benzotropylium cations have also been implicated in reactions of benzannulated cycloheptatrienylidenes with alcohols. [116]

$$(63)$$
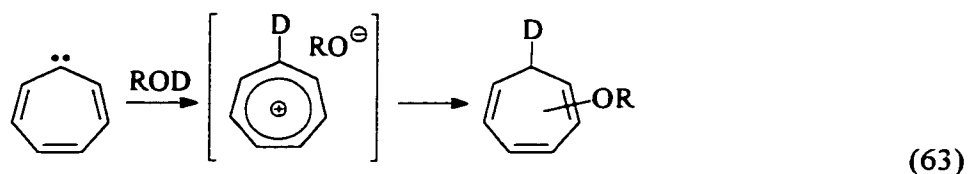
In general, the stepwise mechanism for O-H insertion of carbenes into hydroxyl groups involving initial proton transfer to the carbene carbon is favoured when the conjugate acid of the carbene is a relatively stable and persistent carbocationic intermediate. For carbenes whose conjugate acids are highly unstable species, a concerted mechanism is *enforced* by the lack of a significant lifetime of the resulting carbocation/alkoxy anion pair in solution. However, predicting which mechanistic pathway in Scheme 14 will dominate for a given carbene is difficult since more *electrophilic* carbenes may also attack at oxygen, even when proton transfer leads to the formation of stable carbocationic intermediates.

I.7.2. Reactions with Heteroatoms

I.7.2.a. Ylides.

Reactions of singlet carbenes with substrates containing heteroatoms usually lead to heteroatom-carbene ylides as is the case for pyridine and in some cases nitriles. Carbenes such as methylene have

also been observed to react with oxetane *via* competitive C-H insertion, ring expansion, and ring

cleavage reactions (eq 64), the latter two processes are thought to arise from oxetane ylides.[117]

$$ (64) $$
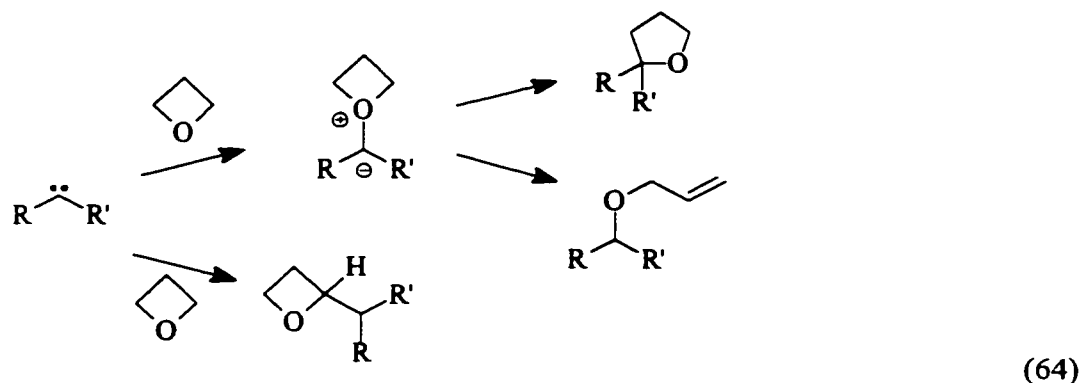
Another example is the reaction of phenylchlorocarbene with 3-ethyl-1-azabicyclo[1.1.0]butane

which occurs with a rate constant of $k = 3.2 \times 10^8$ M^{-1} s^{-1} in pentane at room temperature.[118] The

reaction presumably proceeds through an amonium ylide which cleaves to give the phenylchloroimine

in eq 65.

$$ (65) $$
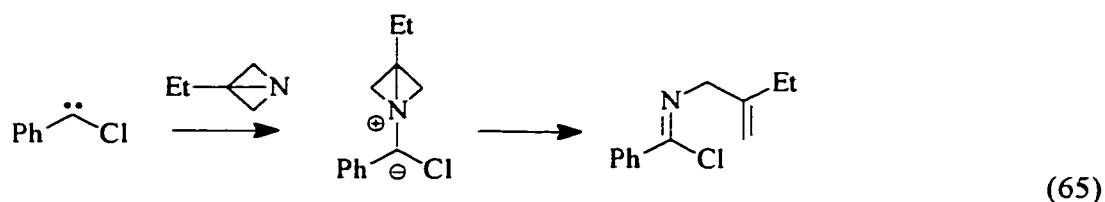
It has been reported that the reaction of dichlorocarbene with allylsulfides leads to the formation of

sulfonium ylides which subsequently undergo [2,3] sigmatropic rearrangements, Eq. 66.[119]

$$ (66) $$
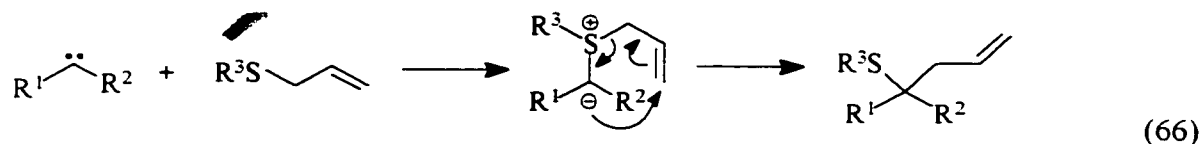
Other [2,3] sigmatropic rearrangements of sulfonium and oxonium ylides result from the reactions

of carbenes and carbenoids with allyl sulfides and allyl ethers in inter- and intramolecular reactions.[120]

Despite the many interesting variations to these reactions reported in the literature, only one report

exists on the kinetics of ylide formation for reactions of carbenes with allylsulfides and kinetics of the subsequent [2,3] sigmatropic rearrangements from these ylides.[121] Moss and co-workers found that ylides derived from the reactions of phenylchlorocarbene and phenylfluorocarbene with three allylsulfides were detectable in LFP experiments, and that sigmatropic rearrangements from these ylides occured with rate constants smaller than those for ylide formation. It was suggested, based on kinetic data, that anion stabilizing groups (F vs. Cl) on the carbene carbon slowed rates of sigmatropic rearrangement in the sulfonium ylide intermediates.

Carbenes can also react with carbonyl compounds at oxygen to form carbonyl ylides. For example, spin equilibrated fluorenylidene (FL:), generated from 9-diazofluorene, is known to react with various carbonyl compounds, including acetone ($k = 1 \times 10^7$ M^{-1} s^{-1}), to form carbonyl ylides (eq 67) and rate constants for these processes have been measured by LFP.[122]

(67)
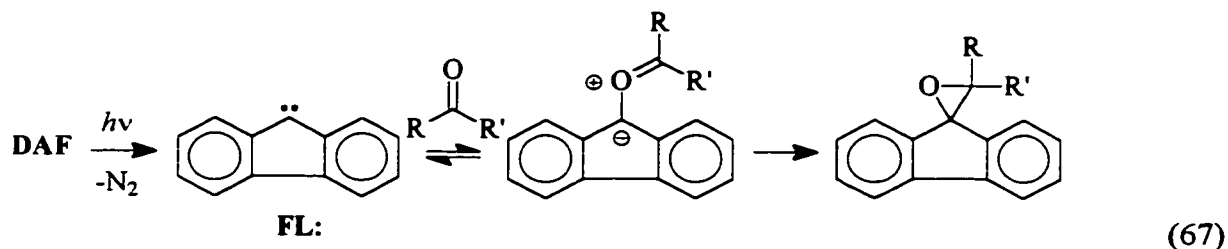
I.7.2.b. Heteroatom Transfers.

Electrophilic singlet carbenes are capable of abstracting oxygen, nitrogen, and sulfur atoms by mechanisms involving the formation of ylide intermediates (or ylide-like transition states), followed by heteroatom transfer. Some examples include heteroatom abstraction from CO_2,[123] N-oxides,[124] PF_3O,[125] epoxides,[126] aziridines,[127] thiiranes,[128] and carbonyl compounds.[129] Shields and Schuster have shown that oxygen atom abstraction from epoxides by singlet fluorenylidene (FL:) occurs stereospecifically (eq 68).[126a]

$$\text{DAF} \xrightarrow[-N_2]{hv} \text{FL:} \longrightarrow$$

(68)
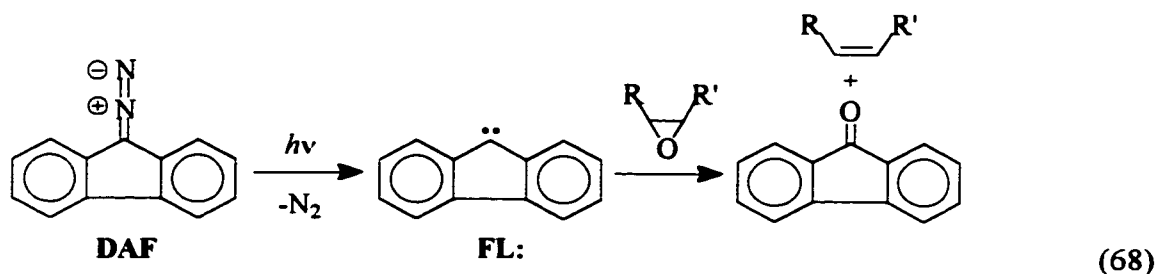
Reaction of carboethoxycarbene with styrene oxide leads to deoxygenation products as well as a diastereomeric mixture of oxetanes,[126c] presumably resulting from the intramolecular rearrangement of an oxonium ylide intermediate. Carboethoxycarbene has also been shown to abstract the sulfur atom from cyclohexene sulfide without similar intramolecular rearrangement.[128]

This introduction contains only a limited survey of carbene chemistry about which volumes have been, and continue to be, written. It is hoped that the material presented will provide adequate background for the following chapters. This author recommends that readers look to the references cited, particularly those which review the literature, for more details.

Chapter 2.

Laser Flash and Steady State Photolysis Studies of Intra- and Intermolecular Reactions of Carbenes.

II. General Introduction.

The first two sections of this chapter contain results and discussion regarding 1,2-hydrogen and 1,2-carbon shifts in dialkyl- and cycloalkylcarbenes generated photochemically from oxadiazoline precursors. Rate constants for these processes have been determined by LFP using the pyridinium probe method and products of reactions produced by steady state (SS) photolysis have been identified.[a] Dialkyl- and cycloalkylcarbenes have been generated by 308 nm LFP of the corresponding oxadiazoline precursors as well as by dual wavelength (250 + 300 nm) photolysis. LFP (308 nm) experiments with UV and IR detection of transients demonstrated that both diazoalkanes (II-2) and dialkylcarbenes (II-3) are formed from irradiations of oxadiazoline precursors (II-1), and in some cases alkoxyalkylcarbenes (II-5) are also formed in minor amounts (Scheme II-1). While SS photolyses (300 nm) have shown that the primary photoproducts are diazoalkanes which are typically formed in 95 - 99 % yield, two colour SS photolyses (250 + 300 nm) lead to efficient generation of dialkylcarbenes in steady state experiments.

---

[a] Some of this work was done in collaboration with Professor Platz's Group at the Ohio State University. Some of those results are presented within because they complement the material presented and are pertinent to discussions. However, results which were not obtained by the author are clearly marked and the origins clearly stated. Results which are not marked in such a manner belong to the author and were obtained by him at McMaster or at the National Research Council of Canada's Steacie Institute for Molecular Sciences.

Scheme II-1.
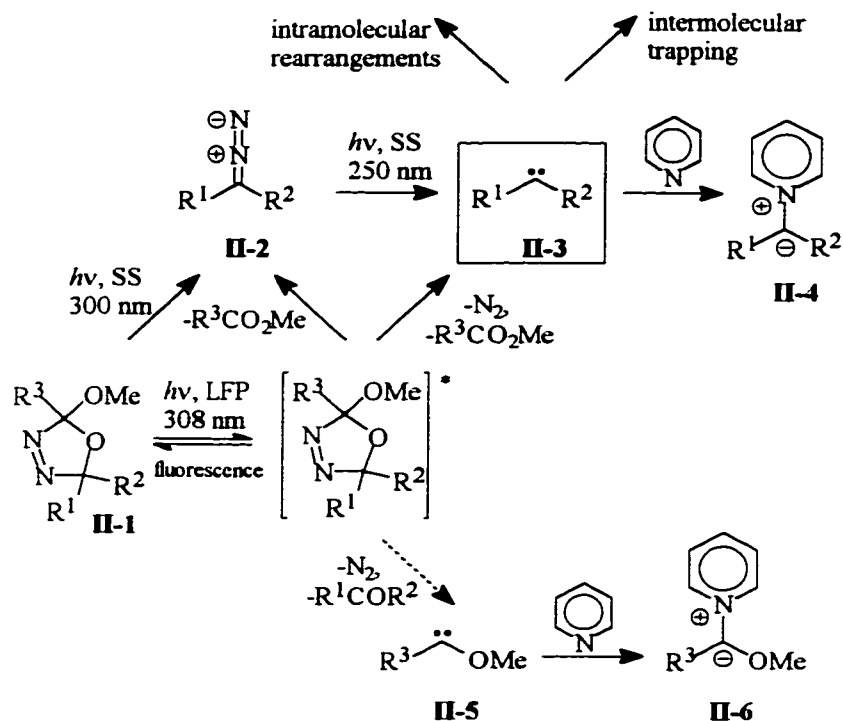
Scheme II-2.
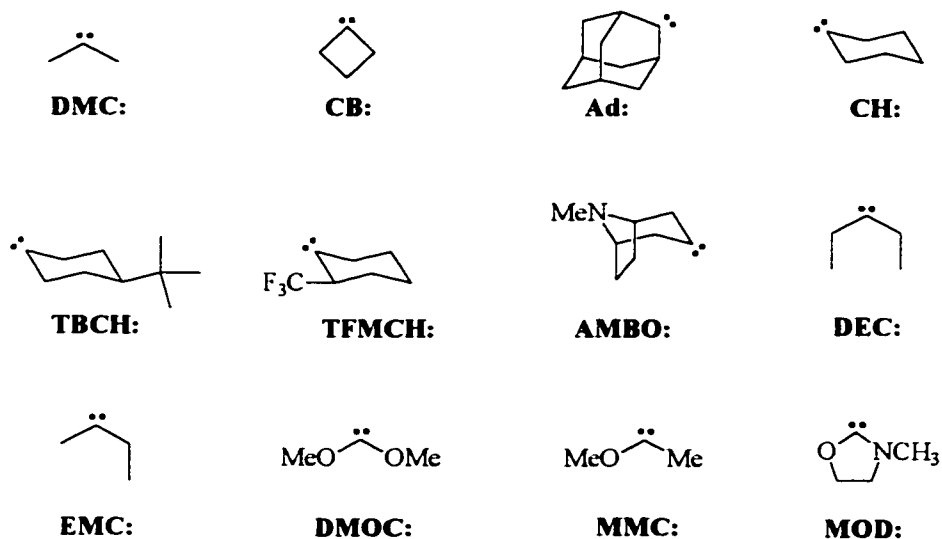
In some cases more than one type of oxadiazoline precursor was used to generate the same dialkylcarbene. In order to avoid confusion with the numbering, acronyms have been given to the dialkylcarbenes studied *via* the oxadiazoline route. For the reader's convenience, they are placed

alongside the corresponding structures in Scheme 2 in the order in which they appear in the following text.

The last section of this chapter concerns intermolecular oxygen and sulfur atom transfer reactions from oxiranes and thiiranes to carbenes of different structure generated from oxadiazolines, diazirines and diazo compounds.

Chapter 2. Section 1. Subsection 1.

Dimethylcarbene.

II.1. Background.

Dimethylcarbene (**DMC:**) has been generated photochemically and thermally from 3,3-dimethyldiazirine (**II-7**). Its lifetimes in various solvents have been measured by LFP using the pyridinium probe method (Scheme II-3 and Table II-1). Dimethylcarbene (**DMC:**) is now believed to have a singlet ground state, with ΔE_{ST} calculated to be ~1.6 kcal mol^{-1},[13] and intersystem crossing (ISC) is competitive with 1,2-hydrogen migration as evidenced by trapping of the triplet state by O_2 in LFP studies.[74]

DMC: also inserts into solvents such as $CHCl_3$ and shows a solvent deuterium kinetic isotope effect of $k_{SH} / k_{SD} = 1.1.$[74] Fully deuterated **DMC:** is ~3.2 times longer lived in pentane indicating a substantial primary kinetic isotope effect on 1,2-H migration. Trapping of **DMC:** by neat methanol gives only ~50% of the OH insertion product and the inefficient trapping has been attributed to rearrangement in the excited state (RIES) of 3,3-dimethyldiazirine.[74]

Platz and coworkers have also performed LFP studies on 2-methoxy-2,5,5-trimethyl- Δ^3-1,3,4-oxadiazoline (**II-1a**) and it was found that dimethylcarbene, which was captured using pyridine, was
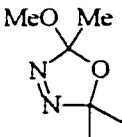
generated from 308 nm LFP of this precursor. The similarity of transient spectra for the pyridinium

ylide of dimethylcarbene and lifetimes of dimethylcarbene from an oxadiazoline and a diazirine were

established by LFP of **II-1a** (308 nm) and **II-7** (351 nm).

Scheme II-3.
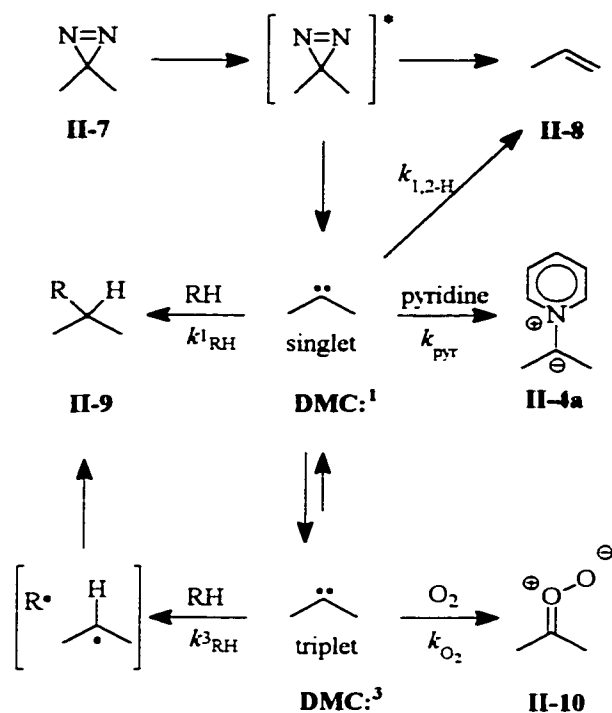
Photolysis of **II-1a** also showed a slow growth ($k_{pyr} \sim 5.5 \times 10^5$ M^{-1} s^{-1}) of a second pyridinium

ylide at higher pyridine concentrations which was assigned to the ylide derived from

methoxymethylcarbene (**II-5a**). The formation of the second ylide appeared to be a lower yielding

process.

Table II-1. Lifetimes of Dimethylcarbene deduced using the Pyridine Probe Method from a Diazirine and an Oxadiazoline.[a]

Precursor	Solvent	τ (ns)
N=N II-7	Pentane	23 - 4.6[b, c]
	CF₂ClCFCl₂	21 - 4.2[b, c]
	α,α,α-trifluorotoluene	27 - 5.4[b, c]
	CHCl₃	6.8 - 1.4[b, c]
	CDCl₃	7.3 - 1.5[b, c]
	CH₃CN	8 - 1.6[b, c]
	CD₃CN	9 - 1.8[b, c]
	C₆F₁₄	7[d]
MeO Me II-1a	Pentane	23 - 4.6[a, b]
	CF₂ClCFCl₂	21 - 4.2[a, b]

[a] Measured by Platz's Group at the Ohio State University.
[b] Assuming $k_{pyr} = (1\text{-}5) \times 10^9$ M⁻¹ s⁻¹.
[c] Taken from Modarelli, D. A.; Morgan, S.; Platz, M. S. *J. Am. Chem. Soc.* **1992**, *114*, 7034.
[d] Taken from Ford, F.; Yuzawa, T.; Platz, M. S.; Matzinger, S.; Fülscher, M. *J. Am. Chem. Soc.* **1998**, *120*, 4430.

II.1.1. Dimethylcarbene generated from Oxadiazoline precursors.

In an attempt to understand results obtained in Platz's laboratory, product studies were performed using steady state photolysis techniques. Those results are presented here. In addition, steady state and LFP experiments were performed using 2,2-dimethoxy-5,5-dimethyl-Δ³-1,3,4-oxadiazoline (II-1b).

II.1.1.a. 300 nm SS Photolysis.

Steady state photolyses (300 nm) were performed on solutions of oxadiazoline (1a) (0.1 M in benzene-d₆) in Pyrex NMR tubes and the reactions were monitored by ¹H-NMR. The growth of a signal at δ1.20 ppm, assigned to 2-diazopropane (II-2a), was observed and the starting material was completely converted after 1 hr of exposure to 300 nm light in the Rayonet chamber. Support for the assignment of the signal at δ1.20 ppm to II-2a came from a strong band in the IR spectrum of the photolysis mixture at $v_{CNN} \sim 2040$ cm⁻¹, from the pink colour of the solutions, and from a UV-visible

absorption at ~ 240 nm. The stable co-product methyl acetate was also observed (^{1}H NMR (500 MHz, C_6D_6) δ 3.27 ppm (s, 3H), and δ 1.61 ppm (s, 3H)).

The slow growth of acetone azine (**II-11**) was observed (two singlets δ 1.86 and 1.81 ppm) over time and trace amounts of propene were detected only after more than 12 hours had elapsed. No signals associated with either methoxydiazoethane or its corresponding azine were detected. The results suggest that if methoxymethylcarbene is formed in the laser experiments, then it is likely to be the result of a multiphoton process. Slow formation of acetone azine (**II-11**) with very little (<5%) propene being formed from solutions of 2-diazopropane upon standing at room temperature, even at concentrations of 10^{-3} M, suggests that a mechanism other than the reaction of dimethylcarbene with 2-diazopropane is responsible for the formation of acetone azine. If dimethylcarbene has a lifetime of ~20 ns in hydrocarbon solvent at room temperature then the rate constant for 1,2-H migration (unimolecular disappearance of the carbene) is $k_{1,2H} = 5 \times 10^7$ s^{-1}. Assuming that dimethylcarbene traps 2-diazopropane with a rate constant of 5x 10^9 M^{-1} s^{-1} then, at concentrations of 10^{-3} M diazoalkane, the product ratio should be at least 10:1 in favor of intramolecular rearrangement and not the observed >9:1 ratio of acetone azine to propene (^{1}H-NMR, sealed tube).

II-2a   DMC:

II-11

II-2a   II-2a
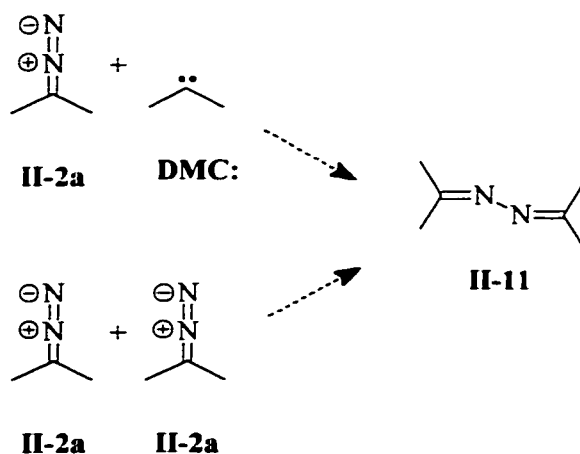
Under identical conditions, 300 nm steady state photolysis of 2,2-dimethoxy-5,5-dimethyl-Δ^3-1,3,4-oxadiazoline (**II-1b**, eq II-1) and oxadiazoline **II-1c** (eq II-2) gave similar results with 2-diazopropane being the major photoproduct formed after 300 nm irradiation (~95-99 % yield based on internal standard hexamethyldisilane) as well as co-products dimethylcarbonate and 3-methyl-2-oxazolidinone, respectively. These results are in contrast to the thermal chemistry of **II-1b** and **II-1c**[a] which yield dimethoxycarbene (**DMOC:**) and 3-methyl-2-oxazolidinylidene (**MOD:**), respectively, suggesting that oxadiazolines are not photochemical precursors to diheteroatom substituted carbenes.

(II-1)

(II-2)
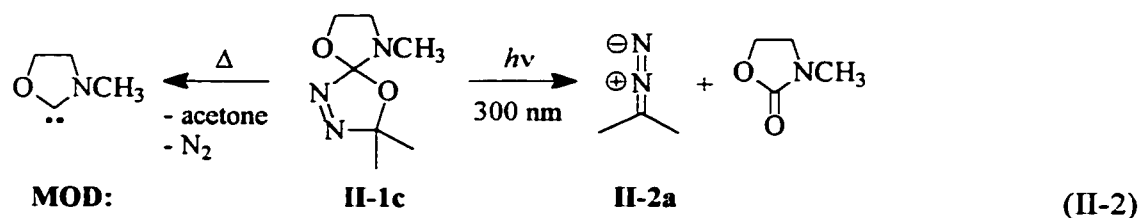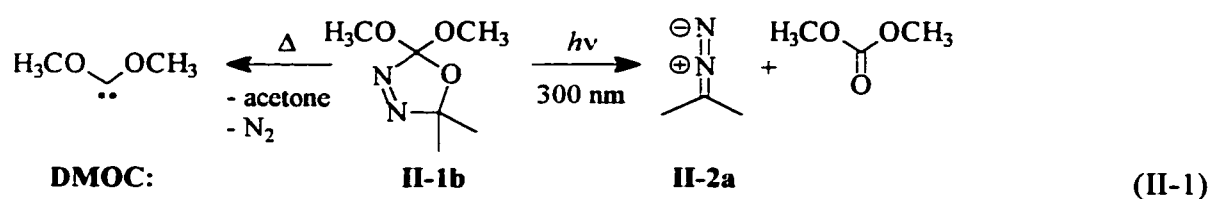
II.1.1.b. 250 and 300 nm Dual Wavelength Photolysis.

We were interested in developing a methodology for generating dimethylcarbene and, more generally, for dialkylcarbenes photochemically from oxadiazoline precursors. Since diazoalkanes are generated efficiently by 300 nm irradiations of oxadiazolines, and these diazoalkanes have UV-visible absorptions at ~250 nm (ε ~ 10000), two colour photolyses with both 250 and 300 nm light seemed to be an obvious choice. Steady state photolyses of oxadiazoline **II-1a** and **II-1b** with both 250 and 300 nm light (0.1 M in benzene-d_6) in quartz NMR tubes were therefore performed (Scheme II-4).

---

[a] This oxadiazoline was obtained from Dr. Philippe Couture.

Irradiation of **II-1a,b** with only 300 nm light again produced a signal at $\delta 1.20$ ppm, assigned to 2-diazopropane, and the starting material was fully converted after only 15 minutes with only trace amounts of propene detected. However, when these solutions were irradiated with 250 nm light significant amounts of propene (ca. 5%) were formed after 5 minutes of photolysis. After 1 hr of photolysis with 250 nm light only signals associated with methyl acetate or dimethylcarbonate, as well as propene and acetone azine were observed (propene:azine=2:1 with the initial concentration of oxadiazoline being 0.1 M). Similar results were obtained by simultaneous 250 nm and 300 nm irradiations in cyclohexane-d_{12}. GC-MS analysis of the resulting photolysis mixtures did not show any evidence for the formation of either methoxydiazoethane, or methoxy vinyl ether, or mixed azines. It is possible that some of the 2-diazopropane was photoisomerized to 3,3-dimethyldiazirine, however, there was no evidence for such a process competing with carbene formation.

Scheme II-4.
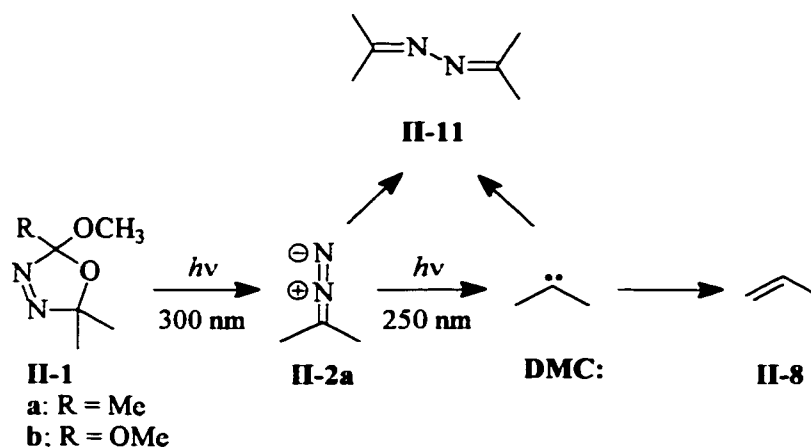
II.1.1.c. 308 nm LFP of 2,2-dimethoxy-5,5-dimethyl-Δ^3-1,3,4-oxadiazoline.

Time-resolved UV-visible spectra were collected 400 ns after 308 nm LFP of oxadiazoline **II-1b** in the absence and presence of added pyridine. In the absence of pyridine a strong persistent band with λ_{max} at approximately 250 nm was observed and assigned to 2-diazopropane with no other signals

observed (Figure II-1). In the presence of pyridine a strong persistent band with λ_{max} at approximately 360 nm was observed and was assigned to the π-$\pi^{\bullet}$ transition of the pyridinium ylide of dimethylcarbene (**DMC:**) as for oxadiazoline **II-1a**. A broad absorption in the visible region of the spectra was also observed and assigned to the n-$\pi^{\bullet}$ transition of pyridinium ylide **II-4a** (Figure II-2). A typical kinetic trace (Figure II-3) shows that the growth of this pyridinium ylide was "instantaneous" (i.e. within the response time of the instrument).
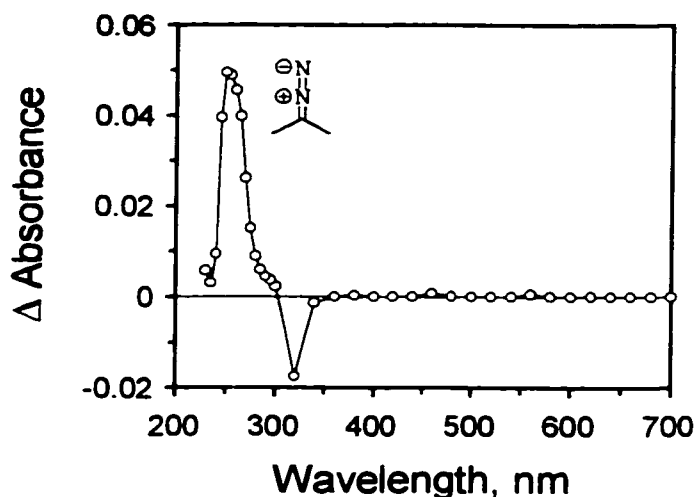
FIGURE II-1. Time-resolved UV-Vis spectrum observed 400 ns following 308-nm laser flash photolysis of 2,2-dimethoxy-5,5-dimethyl-Δ^3-1,3,4-oxadiazoline (**II-1b**) in cyclohexane at 22 °C.

A lifetime of 20 ns for the dimethylcarbene generated from precursor **II-1b** was measured using the pyridine probe method in oxygen free cyclohexane at 22 °C, which is consistent with previous reports. No other transients were observed at pyridine concentrations ranging from 0.05-5.0 M indicating that precursor **II-1b** is superior to **II-1a** which shows the incursion of a second ylide thought to be derived from methoxymethylcarbene at high pyridine concentrations. It is possible that minor amounts of dimethoxycarbene (**DMOC:**) are formed in an analogous fashion, however its reaction with pyridine is known to be too slow to be measured by LFP.[31b] Direct observation of **DMOC:** was not possible

because the absorption of 2-diazopropane dominates the region of the UV-visible spectrum where

dimethoxycarbene (**DMOC:**) is known to absorb (~ 270 nm).[31b]
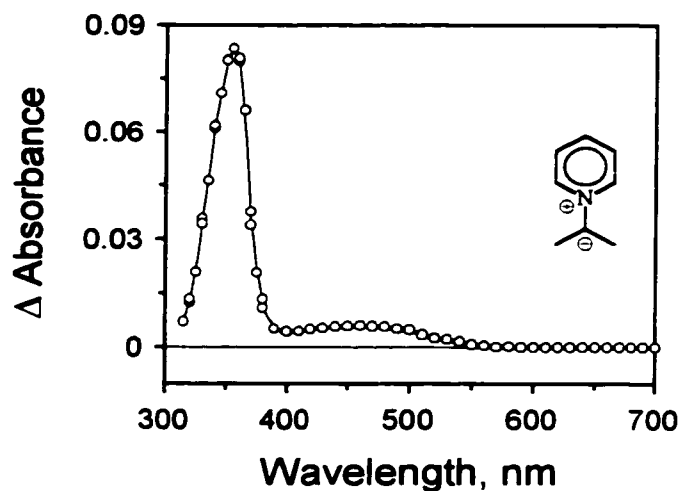
FIGURE II-2. Time-resolved UV-Vis spectrum observed 400 ns following 308-nm laser flash photolysis of 2,2-dimethoxy-5,5-dimethyl-Δ^3-1,3,4-oxadiazoline (**II-1b**) in cyclohexane containing 0.5 M pyridine at 22 °C.
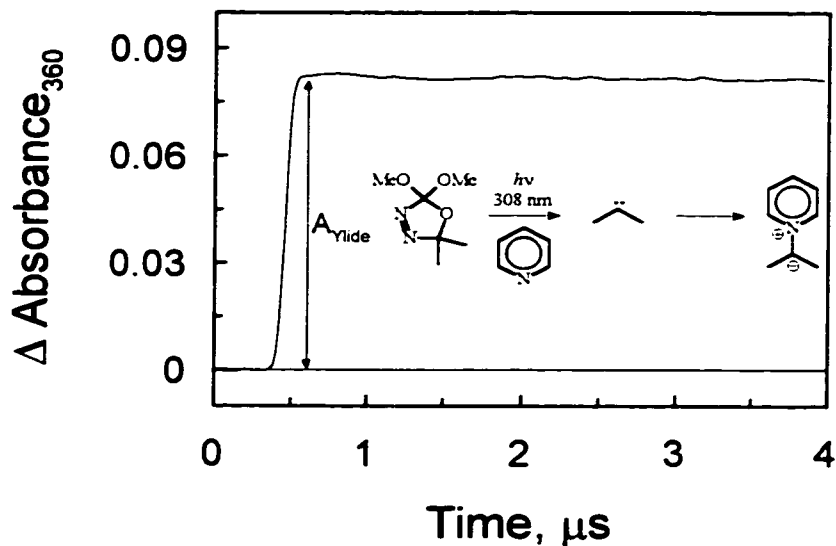
FIGURE II-3. The formation of the pyridinium ylide of dimethylcarbene produced following UV-LFP of **II-1b** in cyclohexane containing 0.5 M pyridine at 22 °C.

308 nm TRIR-LFP of **II-1b** in cyclohexane (2.3 x 10^{-2} M, continuous flow) led to the observation of two absorption bands, one centered at 2036 ± 3 cm^{-1}, assigned to the diazo band of 2-diazopropane, and the second centered at 1756 ± 3 cm^{-1}, assigned to the carbonyl band of dimethylcarbonate. In the IR region of 2100 - 1680 cm^{-1} no other absorption bands were observed (Figure II-4).
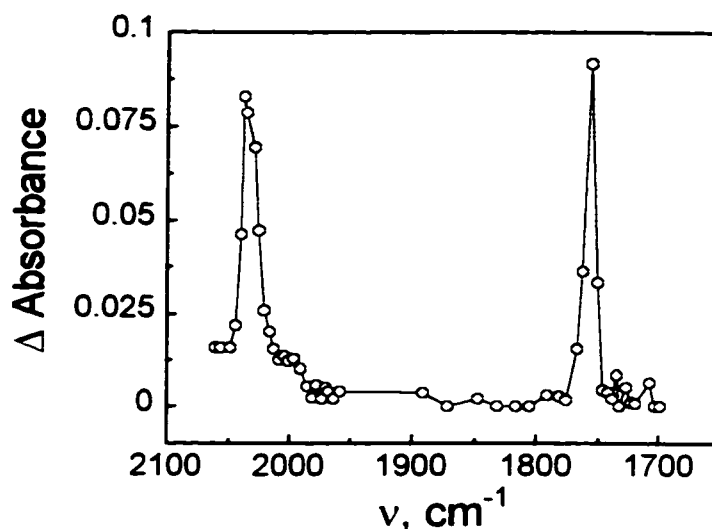
Figure II-4. Time resolved infra-red spectrum recorded 1 μs following LFP of **II-1b** in cyclohexane at ambient temperature. The signal centered at 2036 cm^{-1} is assigned to 2-diazopropane and the signal at 1756 cm^{-1} is assigned to dimethylcarbonate.

In order to test whether carbene formation in the 308 nm LFP of **II-1b** occurs *via* a multiphoton process, solutions of precursor **II-1b** in cyclohexane and in cyclohexane containing 0.5 M pyridine were irradiated (308 nm LFP) over a range of laser energies. Changes in the intensities of absorbance were monitored at λ = 250 nm for 2-diazopropane, and at λ = 360 nm for the pyridine ylide of dimethylcarbene. Surprisingly, the linear correlation of the laser energy *vs.* Δ absorbance for the pyridinium ylide of dimethylcarbene (Figure II-5) seems to suggest that carbene formation is monophotonic. The downward curvature in the plot of laser energy *vs.* Δ absorbance for 2-diazopropane suggests a saturation of a monophotonic process.
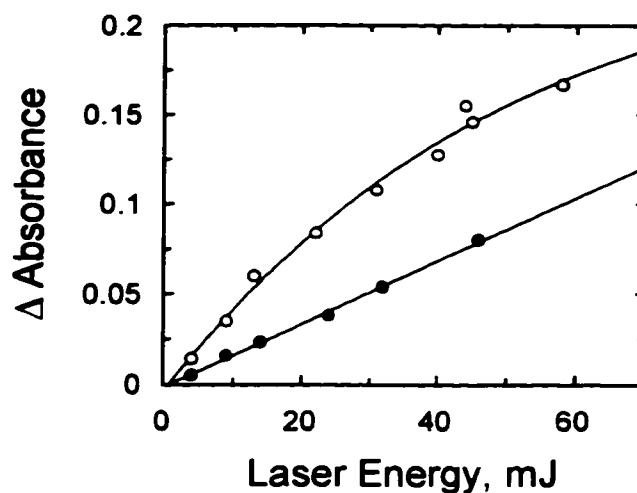
FIGURE II-5. Laser energy *vs.* the change in maximum absorbance plot, measured after 308-nm laser flash photolysis of **II-1b** in cyclohexane and in cyclohexane containing 0.5 M pyridine, for 2-diazopropane at 250 nm (○), and for the pyridinium ylide of dimethylcarbene at 360 nm (●).

Chapter 2. Section 2.

Cycloalkylidenes.

II.2. 1,2-H and 1,2-C Migrations in Cycloalkylidenes.

With the ultimate goal being to gain insight into the effects of orbital alignment on the absolute rate constants for 1,2-H migration, we have investigated cycloalkylidenes, from oxadiazoline precursors, where the orbital alignments of α-hydrogens are necessarily restricted by ring geometries. The following sections contain new results concerning the lifetimes and rate constants for 1,2-H migrations within cyclobutylidene, adamantylidene, cyclohexylidene, and substituted cyclohexylidenes. For cyclobutylidene, 1,2-C migration is competitive with 1,2-H migration.

Subsection 1. Cyclobutylidene

II.2.1. 1,2-H and 1,2-C Migration in Cyclobutylidene.

Cyclobutylidene (**CB:**) has been studied previously from thermal decomposition of cyclobutanone tosylhydrazone salt[90] and by dehalogenation of chlorocyclobutane[91] and it was observed that 1,2-C migration, which gives methylenecyclopropane (**II-14**), is favoured by ~5:1 over 1,2-H migration, which gives cyclobutene (**II-13**).[6] The intramolecular reactivity of the analogous 3-oxacyclobutylidene, however, is dominated by 1,2-H and not 1,2-C migration (eq II-3).[130]

$$(II\text{-}3)$$
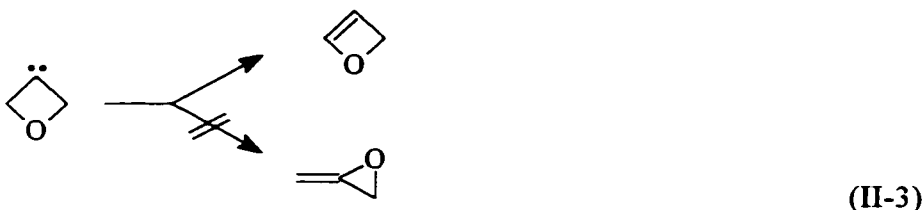
With the intent of gaining insight into the preferences for intramolecular reactivity within cyclobutylidene (**CB:**), we prepared 3,4-diaza-2-methoxy-2-methyl-1-oxa[4.3]spirooct-3-ene (**II-1d**) and 3,4-diaza-2,2-dimethoxy-1-oxa[4.3]spirooct-3-ene (**II-1e**). Platz and co-workers have found that the LFP (308 nm) of **II-1d** in the presence of pyridine gives an intense spectrum of the pyridinium ylide of **II-4d** (eq II-4). Analysis of the data[77c,131] from different pyridine concentrations in different solvent systems gave the lifetimes (τ) for cyclobutylidene (**CB:**) which are summarized in Table II-2. Stern-Volmer (LFP) experiments[77c] reveal that carbene **CB:** reacts with TME and pyridine with the same rate constant within experimental error. As τ is identical in C_6H_{12} and C_6D_{12} (Table II-2), it has been concluded that the lifetime of **CB:** in alkane solvent is controlled by intramolecular processes and that $k_{1,2\text{-}H} + k_{1,2\text{-}C} = 0.5 - 2.5 \times 10^8 \text{ s}^{-1}$ in cyclohexane and in $CF_2ClCFCl_2$ at ambient temperature.[36]

$$(\text{II-4})$$
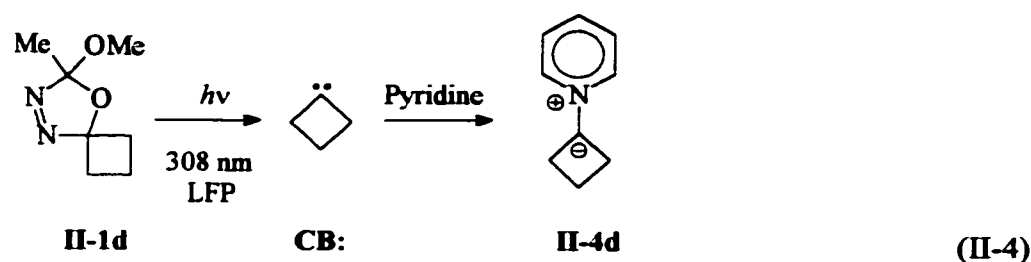
Table II-2. Lifetimes of Cyclobutylidene deduced using the Pyridine Probe Method from an Oxadiazoline Precursor.[a]

Solvent	τ (ns)[b]
$CF_2ClCFCl_2$	4-20 ns
CH_3CN	0.4-2 ns
Cyclohexane	4-20 ns
Cyclohexane-d_{12}	4-20 ns

[a] Measured by Platz's Group at the Ohio State University.
[b] Assuming $k_{pyr} = (1\text{-}5) \times 10^9$ M^{-1} s^{-1}.

II.2.1.a. 308 nm LFP of 3,4-diaza-2,2-dimethoxy-1-oxa[4.3]spirooct-3-ene (II-1e).

We have found that 308 nm LFP of 3,4-diaza-2,2-dimethoxy-1-oxa[4.3]spirooct-3-ene (**II-1e**) also generates cyclobutylidene (**CB:**). Again, time-resolved UV-visible spectra were collected 400 ns after 308 nm LFP of oxadiazoline **II-1e** in the absence and presence of added pyridine. In the absence of pyridine a strong persistent band with λ_{max} at approximately 250 nm was observed and assigned to diazocyclobutane (**II-2d**) with no other signals observed. In the presence of pyridine a strong persistent band with λ_{max} at approximately 360 nm, assigned to the π-π^* transition of the pyridinium ylide of dimethylcarbene (**II-4d**), and a broad absorption in the visible region of the spectra, assigned to the n-π^* transition of pyridinium ylide **II-4d** (Figure II-6), were observed as from oxadiazoline **II-1d**.
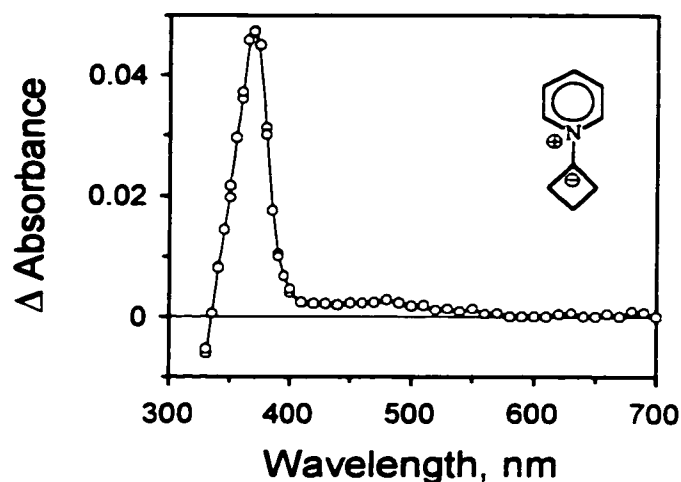
FIGURE II-6. Time-resolved UV-Vis spectrum observed 400 ns following 308-nm laser flash photolysis of of 3,4-diaza-2,2-dimethoxy-1-oxa[4.3]spirooct-3-ene (**II-1e**) in cyclohexane containing 0.5 M pyridine at 22 °C.

A lifetime of ~20 ns for the cyclobutylidene, generated from precursor **II-1e**, was measured using the pyridine probe method in oxygen free cyclohexane at 22 °C. Again, precursor **II-1e** appears to be better than **II-1d** which shows the incursion of a second ylide thought to be derived from methoxymethylcarbene at high pyridine concentrations.

II.2.1.b. 300 nm SS Photolysis.

Oxadiazoline **II-1e** was chosen as a starting material for the generation of diazocyclobutane (**II-2d**) and cyclobutylidine (**CB:**) in SS experiments rather than the monomethoxy compound because it has a much simpler ^{1}H-NMR spectrum which makes the observation of photoproducts at low conversion easier. Upon photolysis of oxadiazoline **II-1e** with 300 nm light in benzene (0.1 M) a triplet at 2.94 ppm (J = 5.3 Hz), a triplet at 2.75 ppm (J = 5.3 Hz), and a pentet at 1.49 ppm (J = 5.3 Hz) were observed and assigned to diazocyclobutane. As was the case for oxadiazoline **II-1a** and **b**, the starting material was completely converted to diazoalkane after ~1 hr of photolysis. Cyclobutanone azine **II-**

12 formed slowly and only trace amounts of methylenecyclopropane (pentet at 5.46 ppm (J = 2.1 Hz) and a triplet at 0.88 ppm (J = 2.1 Hz)) were observed after 12 hours of photolysis.

II.2.1.c. 250 and 300 nm SS Photolysis.

Steady state photolyses of oxadiazoline **II-1e** with both 250 and 300 nm light (0.1 M in benzene-d_6 and in cyclohexane-d_{12}) in quartz NMR tubes led to the growth of signals assigned to diazocyclobutane. However under these conditions significant amounts of methylenecyclopropane and cyclobutene (two singlets at 5.91 and 2.44 ppm in benzene-d_6) were formed after 30 minutes of photolysis. The methylenecyclopropane to cyclobutene ratio (5.5:1) was determined based on integrations of unobscured peaks in the vinyl region of the spectrum which did not change dramatically as a function of photolysis time. It appeared that the photolysis of diazocyclobutane was less efficient than that of 2-diazopropane. A mixture of **II-13** and **II-14** (2- 5 % yield, relative to internal standard, remainder mostly diazocyclobutane) was isolated by preparative GC and identified by ^{1}H-NMR and GC-MS. ^{1}H-NMR (C_6D_6, 200 MHz) δ: 5.46 (quintet, J = 2.1 Hz, 2H; 0.88 (t, J = 2.1 Hz, 4H) from **II-14** and δ 5.91 and 2.44 (singlets; unresolved coupling) from **II-13**. GC-MS (oven 30°C) showed a broad peak at *ca* 2 minutes retention time (before solvent) with M= 54 (C_4H_6) and a base peak of mass 39 (M-15). Yields of **II-13** and **II-14** were increased significantly over the same photolysis times when the precursor concentrations were dropped to 10^{-2} - 10^{-3} M.

II.2.1.d. Trapping of Cyclobutylidene with Tetramethylethylene.

Two color photolysis of **II-1e** in neat TME gave 4,4,5,5-tetramethyl[3.2]spirohexane (**II-15**), Scheme II-5. Diazocyclobutane is known to undergo [3+2]cycloaddition reactions with alkenes to give pyrazolines[132,133] which can subsequently lose N_2 thermally[134,135] or photochemically.[132] Therefore

precursor **II-1e** was photolyzed in neat TME with 300 nm light alone to determine whether **II-15** was the indirect result of [3+2]cycloaddition of **II-2d** to TME or the direct result of carbene trapping. The resulting mixtures, analyzed by ^{1}H-NMR and GC-MS, revealed that **II-15** was not formed with 300 nm light alone under the conditions of the SS photolyses, excluding diazocyclobutane (**II-2d**) as the source of adduct **II-15**.

Scheme II-5.

II-1d, e   **II-2d**   **II-2d***   **CB:**   **II-15**

1d: R=Me
1e: R=OMe

II-12   **II-13**   **II-14**
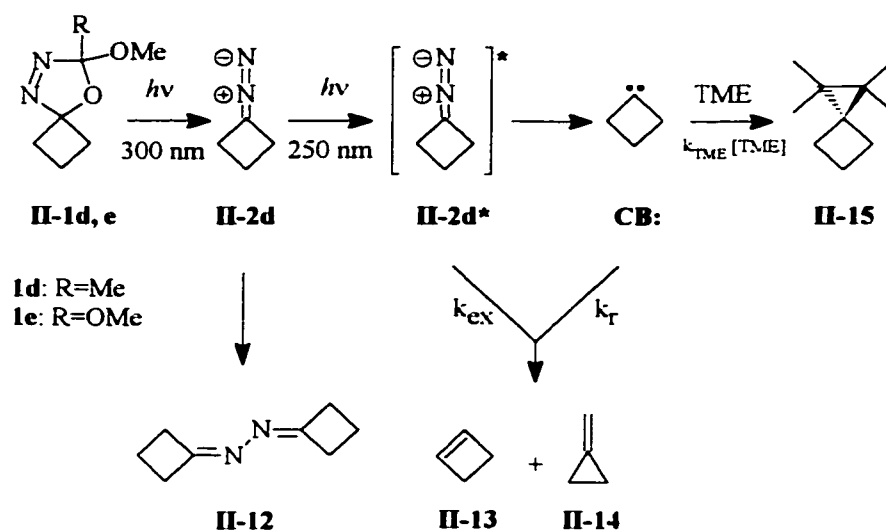
Photolyses of **II-1e** (250 and 300 nm) in cyclohexane solutions with different concentrations of TME showed that yields of **II-13** and **II-14** decreased as a function of increasing [TME] and then leveled off, indicating that part of the rearrangement reactions cannot be quenched by a carbene trap. Yields of **II-15** showed a similar saturation, at a maximum near 21% relative to **II-13** and **II-14**, with increasing [TME] (Figure II-7).
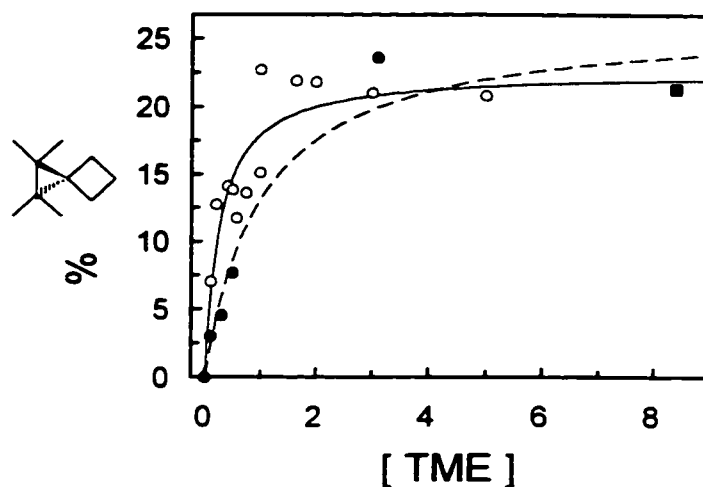
FIGURE II-7. Percent yield of **II-15** vs. TME concentration in cyclohexane-d_{12} ($\bigcirc$), in acetonitrile-d_3 ($\bullet$), and in neat TME ($\blacksquare$). Curve fitting of the data in cyclohexane solutions is shown by the solid line, and in acetonitrile solutions by the dashed line. The plot shows a leveling off at ~21% indicating that an unquenchable reaction is occurring.

Based on the observed ratio of **II-14**: **II-13** of 5.5: 1 in cyclohexane upper limits for the absolute

rate constants for 1,2-H and 1,2-C migrations in **CB:**, at ~25 °C, would be $k_{1,2\text{-}H}$ = 4 x 10^7 and $k_{1,2\text{-}C}$ =

2 x 10^8 s^{-1}. Corresponding lower limits would be $k_{1,2\text{-}H}$ = 8 x 10^6 s^{-1} and $k_{1,2\text{-}C}$ = 4 x 10^7 s^{-1}. However,

the ratio of 1,2-H and 1,2-C migrations was also observed to change as a function of [TME] (Table

II-3). The data suggest that ca 21 % of the observed products are the result of the intramolecular

rearrangement of **CB:** and that the remainder results from migrations in the excited state (**II-2d***) of

diazo precursor **II-2d**. Another interpretation would ascribe the untrappable carbene to the formation

of a carbene-olefin complex which can rearrange to **II-13** and **II-14** or collapse to form adduct,

however, it is assumed here that the observations are the result of rearrangements in the excited state

of **II-2d** (RIES). Since TME at $\geq$ 3 M captured all the **CB:**, the limiting ratio **II-13**: **II-14** reflects the

partitioning of **II-2d*** between 1,2-C and 1,2-H migration. At [TME]= 0, when the ratio reflects a

composite of excited state and carbene rearrangements, the value was ca 5.5 in cyclohexane while at

high [TME] it was 3.6. In order to change the ratio from 3.6 (excited state alone) to 5.5 (composite)

with a 21 % contribution from **CB:**, it is clear that most or all of **CB:** must rearrange to **II-14**. While

the data require that the 21% contribution from **CB:** be in the form of **II-14**, it is not possible to

exclude **II-13** formation entirely, because of experimental errors. If excited state chemistry is not

involved but cyclobutylidene (**CB:**) forms a complex with TME,[a] then the ratio **II-14**: **II-13** without

added TME represents the product distribution from the free carbene. In either case, the data suggest

that 1,2-C is highly favored. Given that the lifetime (τ) of **CB:** was measured as 4-20 ns in

cyclohexane-d_{12} (above), based[70] on $k_{pyr} = 1\text{-}5 \times 10^9 \ M^{-1} \ s^{-1}$, upper and lower limits of the absolute

rate constant for 1,2-C migration would then be $2.5 \times 10^8 \ s^{-1}$, and $5.0 \times 10^7 \ s^{-1}$, at ~25 °C,

respectively.

---

[a] Another interpretation would ascribe the untrappable carbene to the formation of a carbene-olefin complex which can rearrange to **CB** and **MC** or collapse to form adduct. See Tomioka, H.; Hayashi, N.; Izawa, Y.; Liu, M. T. H. *J. Am. Chem. Soc.* **1984**, *106*, 454 and Bonneau, R.; Liu, M. T. H.; Kim, K. C.; Goodman, J. L. *J. Am. Chem. Soc.* **1996**, *118*, 3829 and references therein.

Table II-3. Yields and Ratios of Products of Quenching of **CB:** by TME .

[TME], M	II-14 (%)	II-15 (%)	Ratio II-14: II-13
0[a]	84.7, 84.5	-	5.55, 5.37
0.1[a]	79.3	7.02	5.79
0.2[a]	73.1	12.7	5.17
0.4[a]	69.8	14.1	4.34
0.5[a]	71.7	13.8	4.95
0.57[a]	72.7	11.7	4.67
0.75[a]	71.7	13.6	4.89
1.0[a]	62.5	22.7	4.20
1.64[a]	61.3	21.9	3.67
2.0[a]	61.2	21.8	3.87
3.0[a]	61.9	21.0	3.61
5.0[a]	61.2	20.8	3.43
0[b]	85.4	-	5.87
0.1[b]	82.4	3.01	5.65
0.3[b]	80.5	4.55	5.40
0.5[b]	73.4	7.67	3.88
3.1[b]	60.1	23.6	3.69
8.4[c]	61.1	21.3	3.50

a) cyclohexane-d_{12}; b) acetonitrile-d_3; c) neat TME.

Two color photolyses of **1b** in acetonitrile gave changes in **II-14: II-13** ratios, as a function of [TME], analogous to those obtained in cyclohexane solvent. Thus, for **CB:**, solvent effects on 1,2-H and 1,2-C migrations are similar. Yields of [1+2]cycloaddition adduct **II-15** as a function of [TME] increased more rapidly in cyclohexane compared with acetonitrile solutions (Figure II-7). Double reciprocal plots[77c,131] (Figure II-8) gave the ratio intercept: slope which is equal to $k_{TME}\tau$ for quenching according to eqs II-5 to 9.

$$\phi_{II-13} = \phi_C \cdot \frac{k_{TME}[TME]}{k_o + k_{TME}[TME]}$$ (II-5)

$$(\% \text{ II} - 13) = \phi_{II-13} \cdot (\% \text{ II} - 13)^{\infty}$$ (II-6)

$$(\% \, \mathbf{II} - 13) = (\% \, \mathbf{II} - 13)^{\infty} \cdot \frac{k_{TME}[TME]}{k_o + k_{TME}[TME]}$$

$$= (\% \, \mathbf{II} - 13)^{\infty} \cdot \frac{k_{TME}\tau[TME]}{1 + k_{TME}\tau[TME]} \tag{II-7}$$

$$\frac{1}{(\% \, \mathbf{II} - 13)} = \frac{k_o}{(\% \, \mathbf{II} - 13)^{\infty} \cdot \phi_C \cdot k_{TME}[TME]} + \frac{1}{(\% \, \mathbf{II} - 13)^{\infty} \cdot \phi_C} \tag{II-8}$$

$$\frac{Intercept}{Slope} = \frac{(\% \, \mathbf{II} - 13)^{\infty} \cdot \phi_C \cdot k_{TME}}{(\% \, \mathbf{II} - 13)^{\infty} \cdot \phi_C \cdot k_o} = \frac{k_{TME}}{k_o} = k_{TME}\tau \tag{II-9}$$
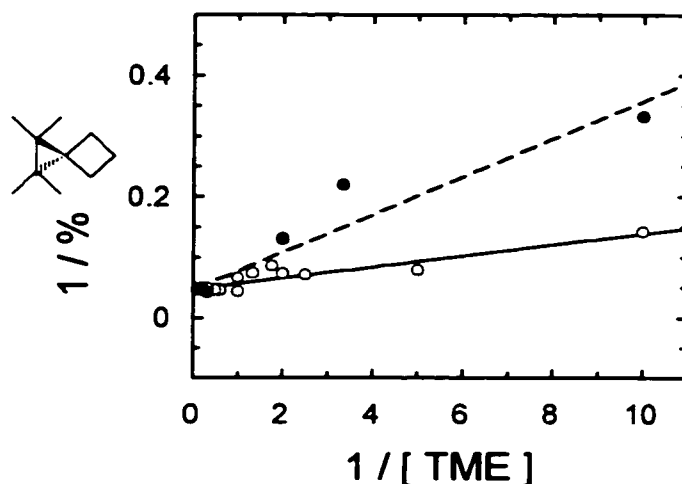
Figure II-8.[a] Double reciprocal plots for quenching of **CB:** by TME in cyclohexane-d_{12} ($\bigcirc$) and in acetonitrile-d_3 ($\bullet$). The slope: intercept ratio gives $k_q\tau$ in each solvent.

[a] Curvature in the plots of quenching data in both solvents, as a result of more than one adduct forming intermediate, could introduce additional errors in $k_q\tau$.
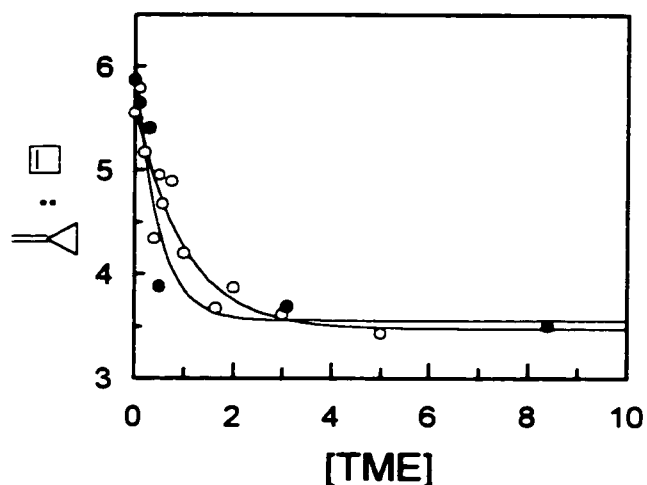
Figure II-9. The change in ratio of **II-14:II-13** as a function of [TME] in cyclohexane-d_{12} ($\bigcirc$) and in acetonitrile-d_3 (●).

For cyclohexane the ratio was 5.2 M^{-1} meaning that k_{TME} = 0.26 - 1.3 x 10^9 M^{-1} s^{-1} at ~25 °C (τ = 4-20 ns). For acetonitrile the ratio was 1.3 M^{-1} indicating that **CB:** has a much shorter lifetime in that solvent (0.3- 1 ns). Both results are consistent with the data obtained by quenching with pyridine (above). More facile 1,2-H and 1,2-C migrations in a polar solvent indicates that corresponding transition states from **CB:** are polar. 1,2-Hydrogen migration in carbenes appears to be accelerated in other cases by polar solvents.[136] 1,2-Carbon migration is special in the case of **CB:**, which rearranges through a dipolar, non-classical transition structure according to Schoeller[92] and Sulzbach, et al.[93]
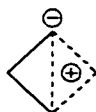
Assuming that k_{pyr} for dimethylcarbene (**DMC:**) and cyclobutylidene (**CB:**) are equal and each k_{pyr} = 1 x 10^9 M^{-1} s^{-1} , then their lifetimes are 21 and 20 ns, respectively, and $k_{1,2-H}$ = 8 x 10^6 s^{-1} for dimethylcarbene (**DMC:**) on a per hydrogen basis whereas $k_{1,2-H}$ < 2 x 10^6 s^{-1} for cyclobutylidene

(CB:) on a per hydrogen basis. Thus 1,2-hydrogen migration is at least 4 times slower (on a per

hydrogen basis) than the analogous rearrangement in dimethylcarbene where the bond angle between

the carbene p-orbital and the migrating hydrogen is not restricted and where bond angle strain does

not occur in the transition state.

| 1,2-H migration in CB: | 1,2-H migration vs. 1,2-C migration in CB: | 1,2-H migration in DMC: |
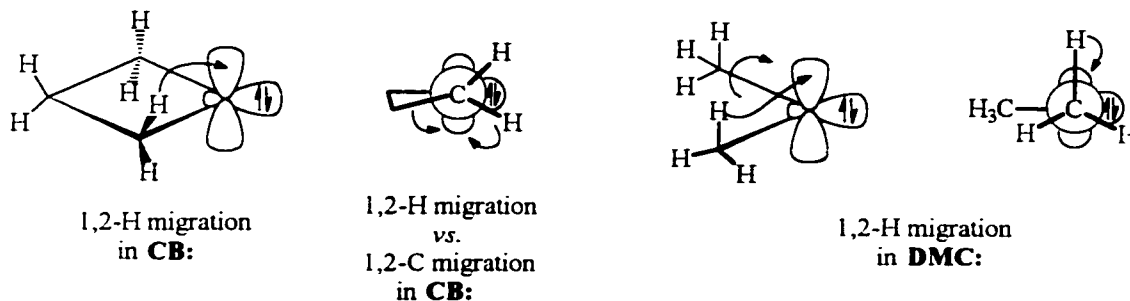
Subsection 2. Adamantylidene.

II.2.2. Adamantylidene.

As part of our investigation of cycloalkylidenes, we prepared 5',5'-dimethoxyspiro[adamantane]-

2,2'-[Δ^3-1,3,4-oxadiazoline] (**II-1f**), an oxadiazoline precursor to adamantylidene (**Ad:**).

Adamantylidene (**Ad:**) is structurally related to other cyclohexylidenes studied in a following section.

In constrast to cyclohexylidene, 1,2-H migration in **Ad:** is strongly disfavored as a result of strain in

the resulting bridgehead alkene product.[99,100] Instead, adamantylidene undergoes 1,3 C-H bond

insertion to yield dehydroadamantane (**II-17**). From LFP studies of 2-adamantane-2,3'-[3H]-diazirine

(**II-16**, eq II-10), a photochemical source of adamantylidene, a lifetime of ~ 2 μs,[99a] dependent on

diazirine precursor concentration, was determined suggesting that intramolecular rearrangement in

this carbene is slow relative to intermolecular processes.

$$\textbf{II-I6} \xrightarrow{h\nu} \textbf{Ad:} \xrightarrow{k_{pyr}} \textbf{II-4f} \tag{II-10}$$
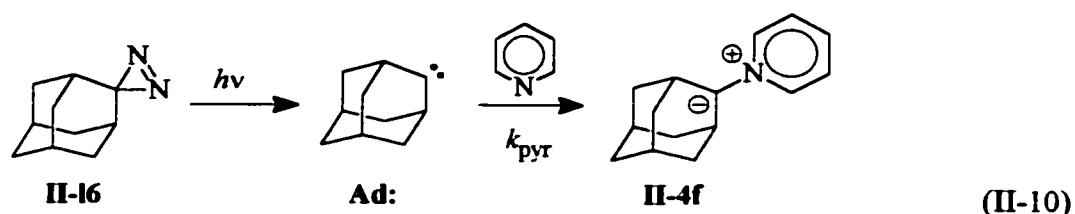
A rate constant for formation of the pyridinium ylide of adamantylidene of $k_{pyr} = 1.54 \times 10^6\ M^{-1}\ s^{-1}$ and absorption maximum at ~ 390 nm in benzene were also reported.[99a] The rate constant for the reaction of **Ad:** with pyridine appeared to be unusually small for such a highly electrophilic species. This rate constant is about 3 orders of magnitude smaller than those of other dialkylcarbenes of similar structure. As well, it was reported that diazirine fluorescence complicated the kinetic studies significantly such that confirmation of the previously reported numbers derived from an independent precursor would be beneficial. Steric effects and ground state spin multiplicity could possibly be responsible for the low reactivity of **Ad:** towards pyridine. We were interested in reproducing these rate constants from oxadiazoline **II-1f** and performing additional experiments to gain more insight into the apparently unique behaviour of adamantylidene (**Ad:**). As it turns out, the LFP results from oxadiazoline **II-1f** contained in this section were found to be incongruous with the previous report by Morgan, Jackson, and Platz.[19a] Our results, summarized in Scheme II-6, in combination with those from Bonneau, Hellrung, Liu, and Wirz (which we were unaware of when we were performing our LFP studies), led to a re-investigation of 2-adamantane-2,3'-[3H]-diazirine, a retraction of the previously published data, and the publication of updated lifetimes and rate constants for **Ad:**.[137]

Scheme II-6.
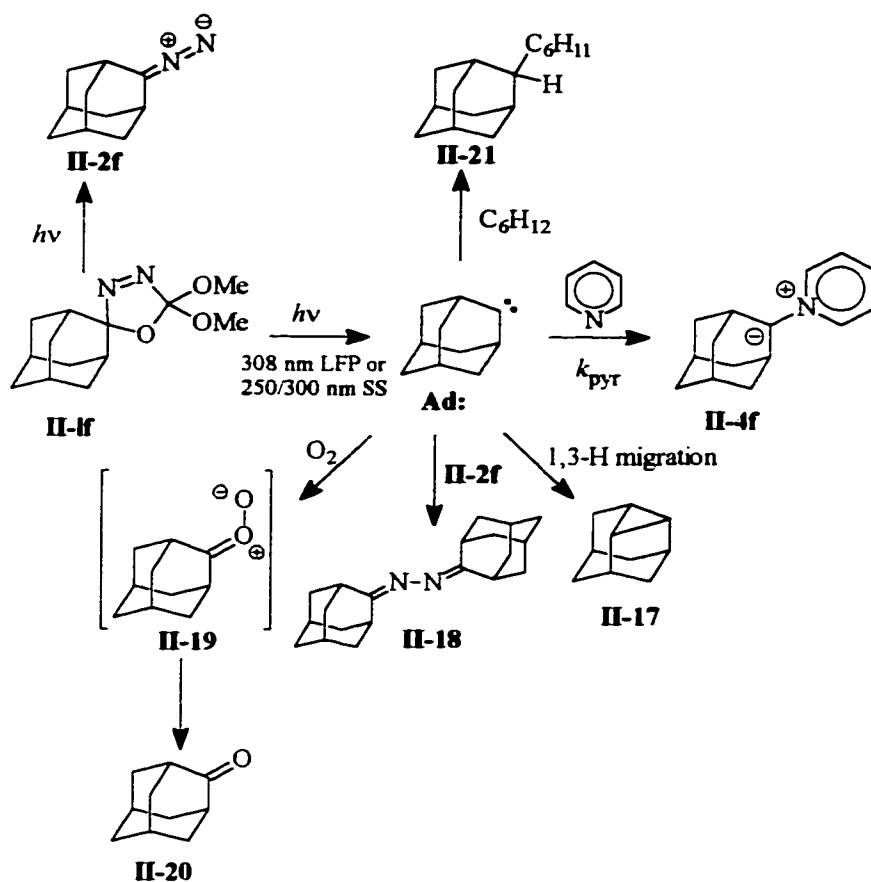
II.2.2.a. Rate Constants for Reaction of Ad: with Pyridine.

The time-resolved UV-vis spectrum acquired (220-300, and 315-700 nm) after 308 nm LFP of oxadiazoline **II-1f** in cyclohexane showed only a strong persistent band with λ_{max} ~250 nm which was assigned to diazoadamantane (**II-2f**). The time-resolved UV-vis spectrum acquired (315-700 nm) after 308 nm LFP of oxadiazoline **II-1f** in cyclohexane in the presence of 0.5 M pyridine showed a strong persistent band with λ_{max} ~380 nm, assigned to the π-π^* transition of the pyridinium ylide of adamantylidene (**Ad:**) and a broad absorption in the visible region of the spectrum that was assigned to the n-π^* transition of the pyridinium ylide of adamantylidene (Figure II-10).
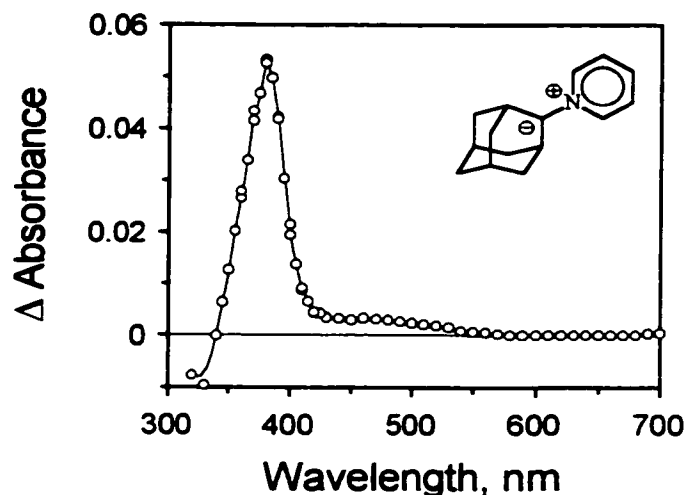
FIGURE II-10. Time-resolved UV-Vis spectrum observed 400 ns following 308-nm laser flash photolysis of **II-1f** in cyclohexane containing 0.5 M pyridine at 22 °C.

However, attempts to reproduce the reported slow kinetics for the reaction of adamantylidene[99a] with pyridine in cyclohexane by direct monitoring of the growth of the ylide absorption were unsuccessful. Rather, the ylide absorption was formed "instantaneously" (within the time resolution of our instrument) for the range of 0.005-1.0 M pyridine concentrations studied. However, it was possible to resolve the growth of the pyridinium ylide in benzene (Figure II-11).
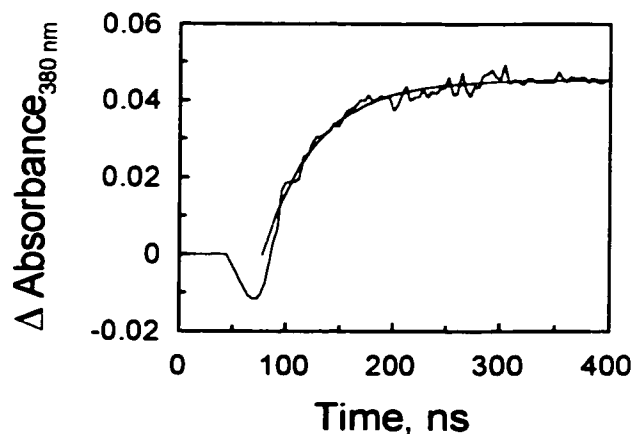
FIGURE II-11. Kinetic trace for the formation of the pyridinium ylide of adamantylidene (**Ad:**) obtained from 308 nm LFP of **II-1f** in 6 mM pyridine in benzene at 22 °C. Solid line corresponds to the least-squares fit of the data to a single exponential growth function ($k_{obs} = 2.04 \pm 0.11 \times 10^7 \text{ s}^{-1}$).

The observed rate constants for the formation of the pyridinium ylide of adamantylidene (**Ad:**) are linearly dependent on the concentration of pyridine and from the slope of the plot of pseudo-first order rate constants k_{obs} vs. [pyridine] (Figure II-12) a bimolecular rate constant for the reaction of adamantylidene (**Ad:**) with pyridine was determined to be $k_{pyr} = 2.01 \pm 0.09 \times 10^9$ M^{-1} s^{-1}. Extrapolation to [pyridine]=0 in Figure II-12 gives a value of $k_0 = 9.95 \times 10^6$ s^{-1} which corresponds to a lifetime (τ) of 101 ns for adamantylidene in benzene at 22 °C.
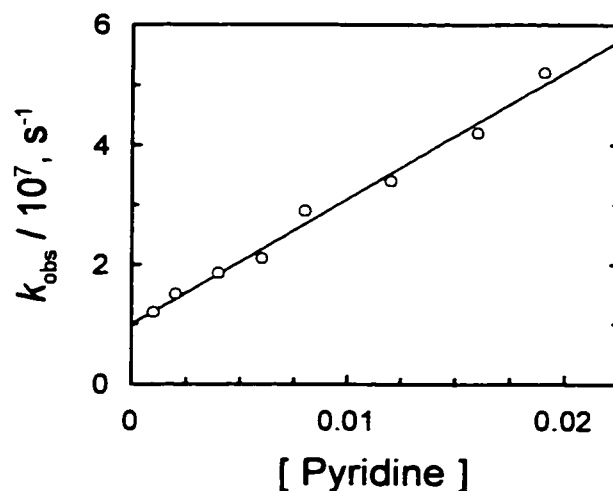
FIGURE II-12. Plot of the pseudo first order rate constants for formation of the pyridinium ylide of adamantylidene (**II-4f**) vs [pyridine] in benzene at 22 °C.

II.2.2.b. Lifetimes of Ad: in Cyclohexane and in Benzene.

The lifetimes of adamantylidene (**Ad:**) were determined in cyclohexane and benzene solvents by 308 nm LFP using Stern-Volmer methods by measuring the amplitudes of the absorbance for the pyridinium ylide **II-4f** at 380 nm (A$_{YLIDE}$) as a function of pyridine concentration. It was found that essentially all of the adamantylidene was captured by pyridine in 0.1 M pyridine in cyclohexane (Figure II-13).
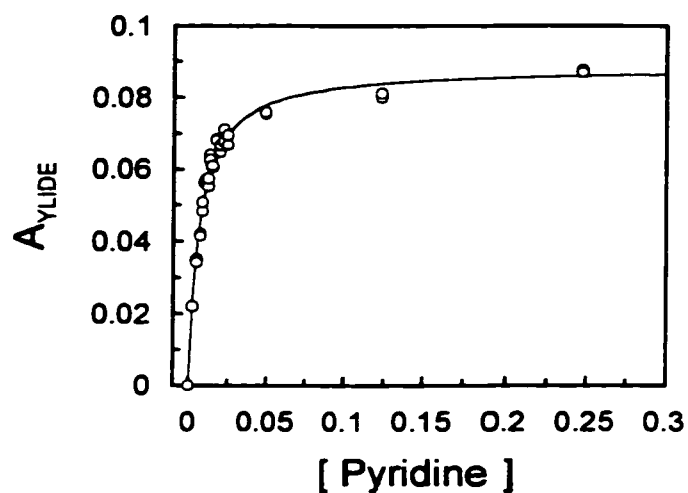
FIGURE II-13. Absorbance of the pyridinium ylide of adamantylidene vs. pyridine concentration in cyclohexane.

Double reciprocal treatment (Figure II-14) of the data gave, after analysis, a value of k_{pyr} τ of 125 M^{-1} which corresponds to a lifetime of 125-25 ns assuming k_{pyr} = (1-5) x 10^9 M^{-1} s^{-1}.
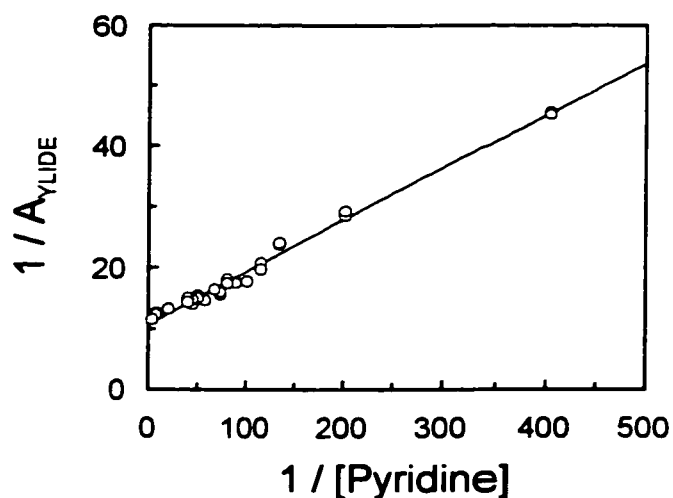
FIGURE II-14. Double reciprocal plot of 1 / Absorbance of the pyridinium ylide of adamantylidene vs. 1 / pyridine concentration in cyclohexane.

Similar Stern-Volmer quenching experiments were performed in benzene (Figure II-15) and a value for k_{pyr} τ was determined to be 200 M^{-1} which is in good agreement with that determined from

measuring the growths of the pyridinium ylide **II-4f**. The lifetime data determined from oxadiazoline

precursor **II-1f** are summarized in Table II-4.
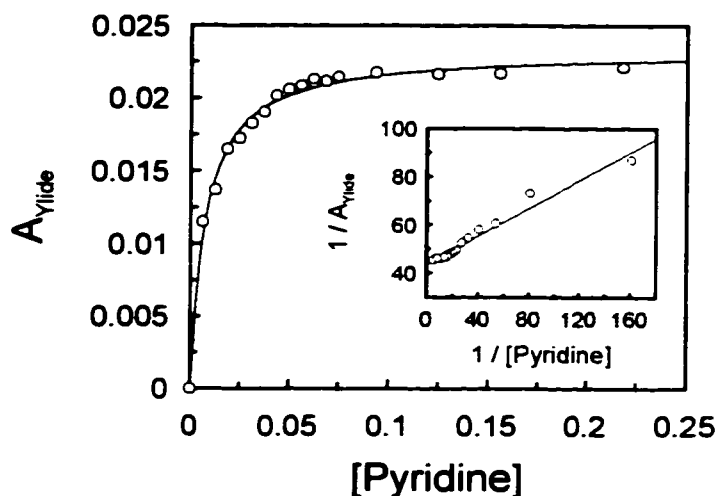
FIGURE II-15. Absorbance of the pyridinium ylide of adamantylidene *vs.* pyridine concentration in benzene. Inset shows the double reciprocal plot of 1 / Absorbance of the pyridinium ylide of adamantylidene *vs.* 1 / pyridine concentration.

Table II-4. Lifetimes of adamantylidene deduced using the pyridine probe method from oxadiazoline precursor **II-1f**.

Solvent	$k_{pyr} \tau$	τ (ns)[a]
Cyclohexane	125	125 - 25 ns
Benzene	200	200 - 40 ns
		101 ns[b]

[a] Assuming $k_{pyr} = (1-5) \times 10^9 \, M^{-1} \, s^{-1}$
[b] From the intercept of the plot in Figure II-12.

II.2.2.c. Products from Dual Wavelength SS Photolysis.

Experiments involving 300 nm SS photolysis of **II-1f** again showed that diazoadamantane (**II-2f**)

was the major product in ~ 90% yield. Minor amounts (3-4%) of adamantanone were also detected by

GC-MS analysis. Dual wavelength SS photolysis of **II-1f** (0.01 M in degassed benzene) with 250 and

300 nm light (Rayonet) did reveal approximately 22 % of dehydroadamantane (II-17) with the major

co-product being adamantanone azine (II-18) 71 %. Minor amounts of adamantanone (3-4 %) were

also detected. Other minor products were formed but were not identified. The source of

adamantanone is unknown but could be the result of an alternative fragmentation of the oxadiazoline

precursor. An identical solution which was saturated with O_2 was also photolyzed with 250 and 300

nm light showed a significant increase in the amount of adamantanone (18%). The increase in yield of

adamantanone in O_2 saturated solutions is most likely the result of the reaction of triplet

adamantylidene with molecular oxygen to form the corresponding carbonyl oxide (II-19) which

eventually gives adamantanone. This implicates a substantially populated low lying triplet state for

adamantylidene (Ad:).

Dual wavelength photolyses of II-1f in cyclohexane gave similar results. Adamantanone azine was

the major product observed in 56% yield with dehydroadamantane being formed in ~ 11 % yield (GC

analysis). In cyclohexane, however, an apparent solvent derived product (II-19) with mass m/z = 218

(by GC-MS) was also formed in ~ 13 % yield suggesting that adamantylidene undergoes an

intermolecular C-H insertion.

II.2.2.d. Conclusions.

From our results we conclude that adamantylidene (II-1f) is a short lived intermediate in benzene

and cyclohexane solvents and that it reacts with pyridine with bimolecular rate constants of similar

magnitude to those of other alkyl and dialkylcarbenes of similar structure. Substantial re-investigations

of the LFP of 2-adamantane-2,3'-[3H]-diazirine (II-16, eq II-10) have led to similar conclusions

regarding adamantylidene (Ad:) and some of the earlier work, while reproducible, was

misinterpreted.[137]

Subsection 3. Cyclohexylidenes.

II.2.3. 1,2-H Migration in Cyclohexylidene and Substituted Cyclohexylidenes.

Cyclohexylidenes have been actively studied in recent years.[84-88] Most of the studies have involved substituent effects or "bystander" effects on the relative rates for 1,2-H migration. Implications regarding the effects of orbital alignment of the C-H bond of the migrating hydrogen with that of the empty p-orbital of the adjacent carbene carbon have been made. Conformational restriction imposed by the cyclohexane ring is thought to give rise to better alignment of axial hydrogens located α to the carbene center for migration *via* a hydride shift mechanism, and to less favourable orbital alignment of equatorial α-hydrogens. In general, migrations from an axial position tend to be favoured over those from an equatorial position by as much as 2:1, although theoretical calculations have suggested that 1,2-H migration from these positions occur by a common transition state.[84b] Despite considerable literature data, based on product studies, pertaining to the relative rates for 1,2-H migrations within a variety of cyclohexylidenes, absolute rate constants for these processes are not known. It has been postulated that 1,2-H migration within cyclohexylidene and analogous progenitors are too fast to allow for intermolecular reactions to compete. For instance, attempts to observe the pyridinium ylide of cyclohexylidene from its corresponding diazirine precursor, 1,2-diazaspiro[2.5]oct-1-ene (**II-22**),[138] have failed (eq. II-11).

$$(II-11)$$
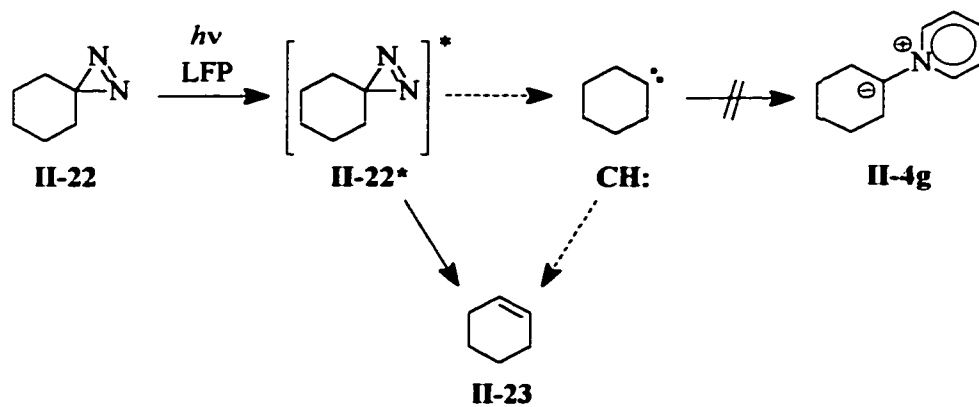
However, such suggestions had been made incorrectly regarding other simple alkyl and dialkylcarbenes. The occurrence of excited state reactions that mimic carbene reactions in terms of products, but not necessarily in terms of product ratios, has been established,[35] and it is possible that this type of excited state chemistry precludes or minimizes carbene formation from precursors such as II-22. Therefore we endeavoured to generate and trap cyclohexylidene and several substituted cyclohexylidenes using the oxadiazoline approach.

II.2.3.a. Lifetimes of Cyclohexylidene and Substituted Cyclohexylidenes.

Oxadiazolines II-1g-n were prepared for the study of absolute rate constants for 1,2-H migration in cyclohexylidene (CH:), 4-*t*-butyl-cyclohexylidene (TBCH:), 2-trifluoromethylcyclohexylidene (TFMCH:), 8-aza-8-methyl[3.2.1]oct-3-ylidene (AMBO:), diethylcarbene (DEC:), and ethylmethylcarbene (EMC:).

II-1g

II-1h: R³ = Me
II-1i: R³ = OMe

II-1j

II-1k

II-1l: R³ = Me
II-1m: R³ = OMe

II-1n

Scheme II-7.

II-24

II-25
33 % yield

H₂NNHCO₂Me
Δ, toluene, HOAc

II-1j
12 % yield

Pb(OAc)₄

MeOH,
0 °C,
5 days

II-26
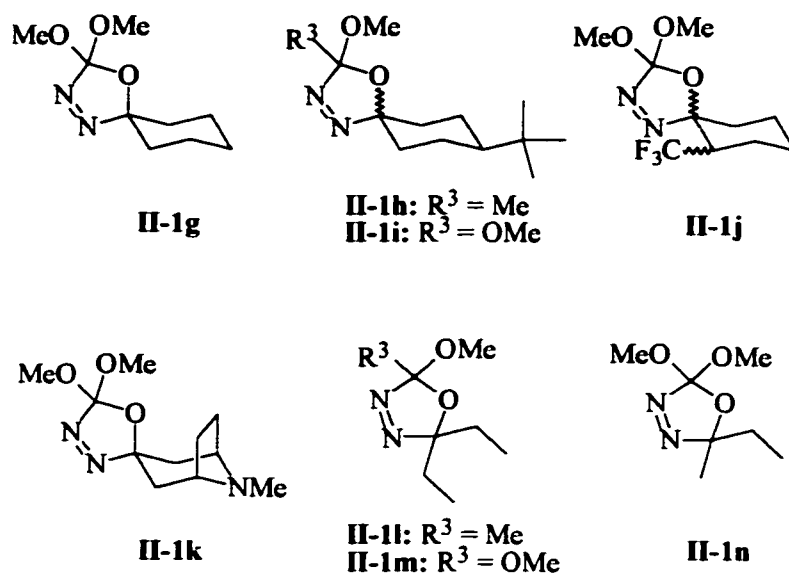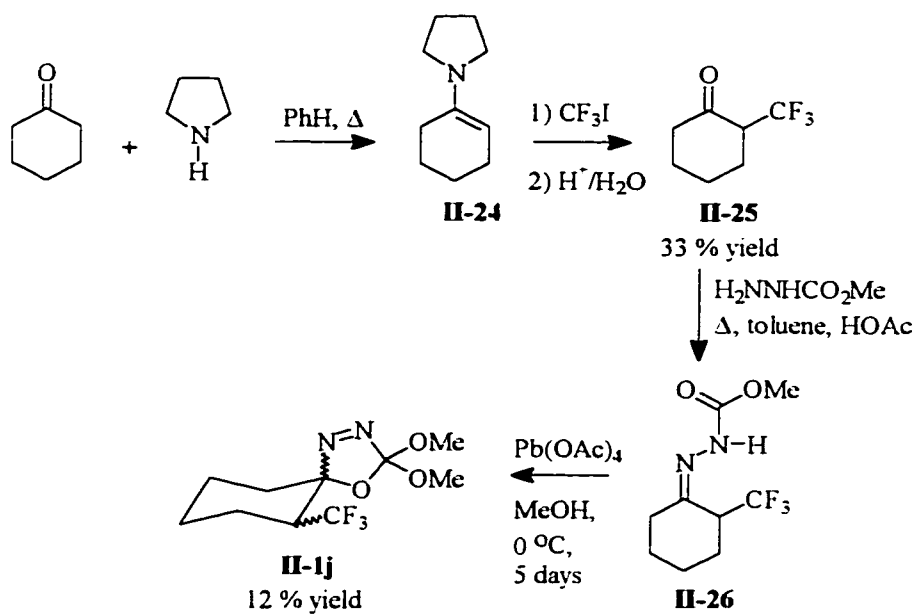
Oxadiazolines **II-1g-i**, and **k-n** were prepared by oxidative cyclization of the corresponding acyl hydrazones with lead tetraacetate as described previously.[139] Precursor **II-1j** was prepared by alkylation of the pyrrolidine enamine of cyclohexanone with CF₃I to give 2-trifluoromethylcyclohexanone(**II-25**),[140] which was converted to **II-26** and then to a mixture of diastereomeric oxadiazolines **II-1j** according to Scheme II-7.

II.2.3.a.1. Laser flash photolysis of oxadiazolines II-1g to n.

Laser flash photolysis (LFP, 308 nm) of oxadiazolines **II-1g** to **n** in the presence of pyridine[141]

gave rise to transient absorptions, all with λ_{max} ~360 nm. Examples of time resolved pyridinium ylide

spectra are given in Figure II-16. The lifetimes of **CH:**, **TBCH:**, **TFMCH:**, **AMBO:**, **DEC:**, and

EMC: were determined by Stern-Volmer analysis of the maximum amplitudes of the ylide absorptions

as a function of [pyridine], Figure II-17.
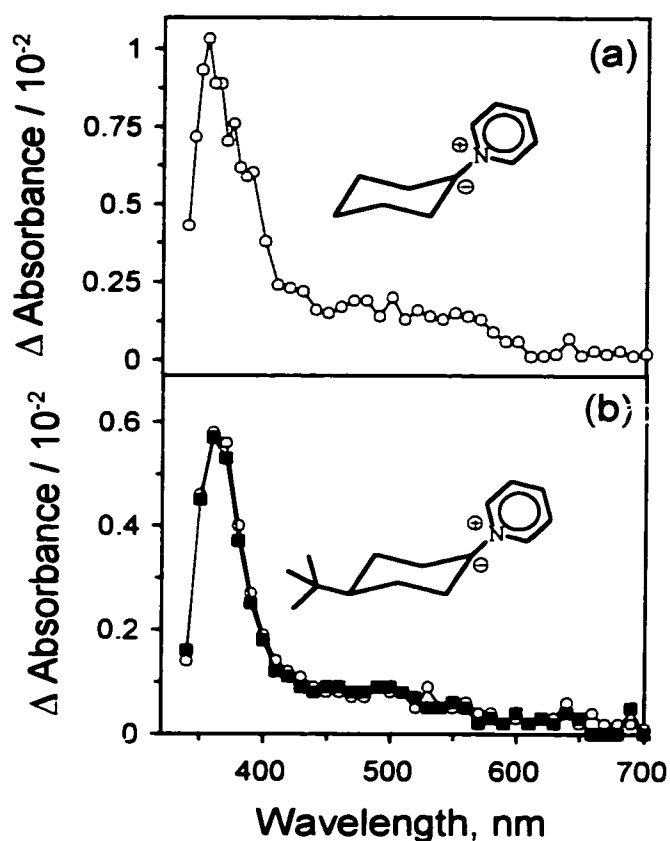
FIGURE II-16. (a) Time-resolved UV-Vis spectrum observed 380 ns after 308-nm laser flash photolysis of **II-1g** in cyclohexane containing 2.0 M pyridine at 22 °C. (b) Time-resolved UV-Vis spectrum observed following 308-nm laser flash photolysis of **II-1h** in cyclohexane containing 1.0 M pyridine at 22 °C. The data were collected at intervals of 460 ns (○) and 32.6 ms (■) after the laser pulse.
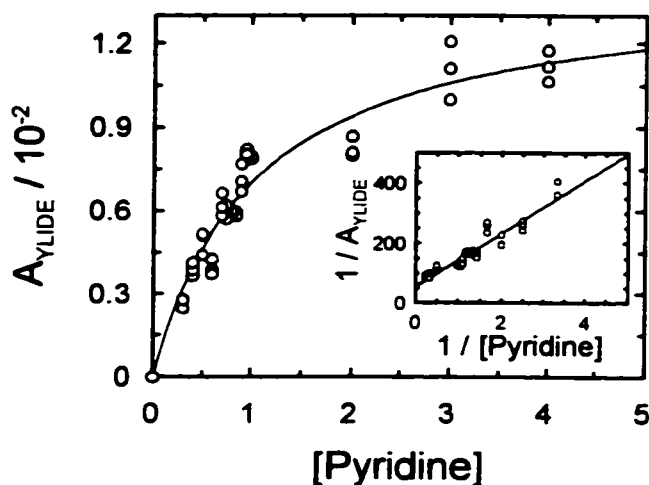
FIGURE II-17. Absorbance of the pyridinium ylide of cyclohexylidene *vs.* pyridine concentration in cyclohexane at 22 °C. Inset shows the double reciprocal plot of 1 / Absorbance of the pyridinium ylide of cyclohexylidene *vs.* 1 / pyridine concentration in cyclohexane at 22 °C.

The data were analyzed by linear least squares fitting of the curve to eq II-12, and by double reciprocal treatment of the data.[77c,131] In equation II-12, A_{YLIDE} is the amplitude of absorbance of the pyridinium ylide in the present of various amounts of added pyridine, A^{∞}_{YLIDE} is the amplitude of absorbance of the pyridinium ylide at infinite [pyridine], k_o is the sum of all the rate constants leading to the disappearance of the transient carbene, $\tau = 1/k_o$ is the lifetime of the transient carbene, and k_{pyr} is the bimolecular rate constant for the reaction of the carbene with pyridine. Fitting the data to a curve allows one to solve for the product $k_q\tau$ without using linearized model functions (i.e. double reciprocal plots).[a]

$$A_{YLIDE} = A^{\infty}_{YLIDE} \cdot \frac{k_{pyr} \text{[pyridine]}}{k_o + k_{pyr} \text{[pyridine]}} = A^{\infty}_{YLIDE} \cdot \frac{k_{pyr}\tau \text{[pyridine]}}{1 + k_{pyr}\tau \text{[pyridine]}} \qquad \text{(II-12)}$$

[a]. The major problem with the linearized functions is that they give excessive weighting to points which may be poorly defined.

The results of lifetime measurements in cyclohexane, cyclohexane-d_{12}, and in benzene are summarized in Table II-5. The lifetimes of carbenes **CH:**, **TBCH:**, **TFMCH:**, and **AMBO:** do not depend significantly on the isotope (H or D) in the cyclohexane solvent and the slightly longer lifetimes in benzene may be the result of the formation of π-complexes with these carbenes or to a slightly smaller value of k_{pyr} in benzene. Such π-complexes, arising from the reaction of other carbenes with benzene, have been implicated as the cause of extended carbene lifetimes in benzene vs. non-aromatic hydrocarbon solvents by as much as an order of magnitude.[80] Dimethylcarbene is believed to have a singlet ground state,[4] with ΔE_{ST} ~1.6 kcal mol^{-1}.[13] Adamantylidene, a better model with an angle constraint similar to that expected in cyclohexylidene, is also a singlet in the ground state, with ΔE_{ST} ~3 kcal mol^{-1}.[99, 137b] These models suggest that cyclohexylidenes are likely to have singlet ground states with low lying triplet states. In cyclohexylidenes however, 1,2-H migration dominates over triplet state chemistry, presumably because the barriers for triplet state reactions are higher.[b]

Precursors **II-1h** and **II-1l** also afforded the pyridinium ylide from methoxy(methyl)carbene in the LFP experiments. The rate factor was sufficient to permit separation of the kinetics for the fast formation of pyridinium ylides **II-4h** and **II-4l**, and the slower formation of the ylide from methoxy(methyl)carbene. Kinetic traces obtained following 308 nm LFP of **II-1h** in the presence of

---

[b]. It is most likely that vertical transitions lead to the formation of singlet carbenes ^{1}**CH:**, ^{1}**TBCH:**, ^{1}**TFMCH:**, ^{1}**AMBO:**, ^{1}**DEC:**, and ^{1}**EMC:** in photolyses of oxadiazolines **II-1g** to **n**. The rate constants for reactions proceeding through the triplet state manifold are then the products of the equilibrium constants for intersystem crossing (ISC), K_{ISC}, with the rate constants for the reactions of triplet carbenes ^{3}**CH:**, ^{3}**TBCH:**, ^{3}**TFMCH:**, ^{3}**AMBO:**, ^{3}**DEC:**, and ^{3}**EMC:**, k_t. (assuming that the pre-equilibrium approximation applies) according to the scheme below.

$$\text{II-1g-n} \xrightarrow{h\nu} {}^1(R(R')C\text{:}) \underset{}{\overset{K_{ISC}}{\rightleftharpoons}} {}^3(R(R')C\text{:}) \xrightarrow{k_t} \text{Triplet Derived Products}$$
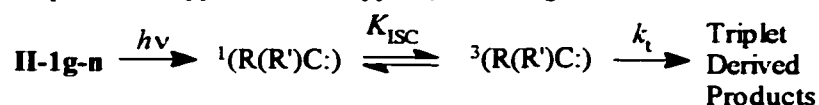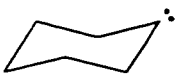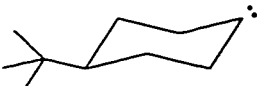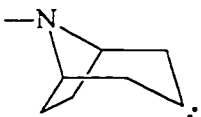
Table II-5. Lifetimes of cyclohexylidenes deduced using the pyridine ylide technique from oxadiazoline precursors.

Carbene	Solvent	τ (ns)^a double reciprocal	τ (ns)^{a,b} curvefit
(CH:)	Cyclohexane	0.7 - 0.14	(0.97 - 0.19) ± 9.2 %
	Cyclohexane-d$_{12}$	0.7 - 0.14	(1.2 - 0.24) ± 23.2 %
	Benzene	3.9 - 0.78	(3.0 - 0.60) ± 22 %
(TBCH:)	Cyclohexane	1.6 - 0.32	(0.86 - 0.17) ± 15 %
	Cyclohexane-d$_{12}$	1 - 0.2	(1.2 - 0.24) ± 26 %
	Benzene	4.9 - 0.98	(2.3 - 0.46) ± 20 %
(TFMCH:)	Cyclohexane	5.8 - 1.2	(4.9 - 0.98) ± 12 %
	Cyclohexane-d$_{12}$	5.0 - 0.99	(4.7 - 0.74) ± 11 %
(AMBO:)	Cyclohexane	6.9 - 1.4	(8.3 - 1.7) ± 9.3 %
	Cyclohexane-d$_{12}$	7.6 - 1.5	(7.9 - 0.98) ± 9.1 %
	Benzene	3.0 - 0.6	(3.1 - 0.62) ± 9.8 %
(DEC:)	CF$_2$ClCFCl$_2$	3.0 - 0.6	----
	Cyclohexane	6.0 - 1.2	
	Benzene	6.0 - 1.2	
(EMC:)	CF$_2$ClCFCl$_2$	3.0 - 0.6	----
	Cyclohexane	6.0 - 1.2	
	Benzene	6.0 - 1.2	

^{a} Assuming k_{PYR} = (1-5) x 10^9 M^{-1} s^{-1}. ^{b} Errors were from curve fitting of the data.

pyridine, observed at 360 nm, showed "instantaneous" growths which varied in amplitude as a function of pyridine concentration (A$_{ylide1}$, Figure II-18 and 20a), and a slow growth the kinetics of which also varied with pyridine concentration (A$_{ylide2}$, Figure II-18 and II-20a). For methoxy(methyl)carbene k_{pyr}= 5.5 x 10^5 M^{-1} s^{-1},[15] and this slow growth could easily be distinguished from the "instantaneous" growths of the pyridinium ylides of both 4-*tert*-butyl-cyclohexylidene

(TBCH:) and 3-pentylidene (DEC:). Linear least-squares fitting of the rate constants for formation of

the pyridinium ylide of methoxy(methyl)carbene as a function of pyridine concentration gave $k_{pyr}=$ 6.4

$\pm$ 0.9 x 10^5 $M^{-1}s^{-1}$ (Figure II-19), in reasonable agreement with the literature value.[15] LFP (308 nm) of

oxadiazoline precursors II-1i and II-1m in the presence of pyridine led to the observation of only one

pyridinium ylide in each case, assigned to II-4h and II-4l, respectively. The lifetimes of carbenes

TBCH: and DEC:, derived from Stern-Volmer analyses of data obtained from dimethoxy precursors

II-1i and m, were the same as those from monomethoxy analogs II-h and l but analyses of the data

from the dimethoxy precursors were more straightforward (Figure II-20b).
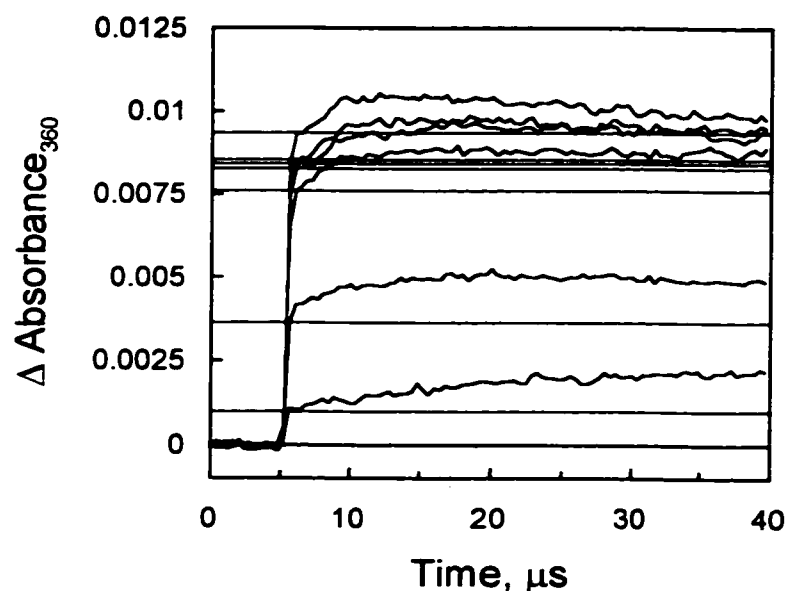
FIGURE II-18. Time-resolved UV-Vis traces observed following 308-nm laser flash photolyses of 8-*t*-butyl-3,4-diaza-2-methoxy-2-methyl-1-oxa[4.3]spirodec-3-ene (II-1h) in cyclohexane containing 0.12, 0.19, 0.25, 0.31, 0.37, 0.43, 0.5 M pyridine at 22° C.
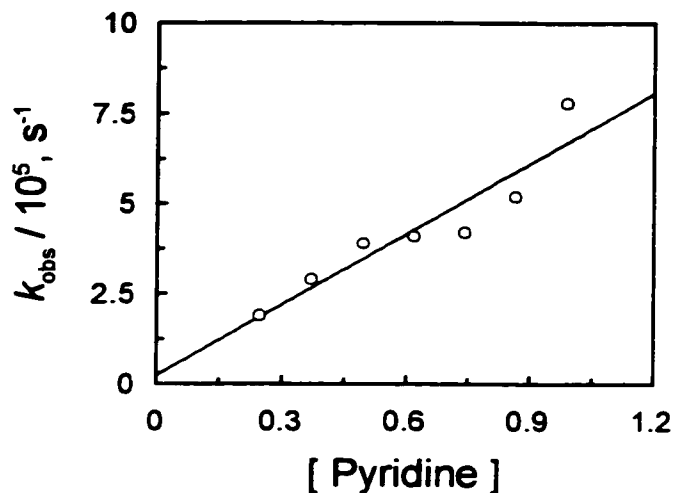
FIGURE II-19. Plot of the change in k_{obs}, for the growth of the pyridinium ylide of methylmethoxycarbene, as a function of pyridine concentration.
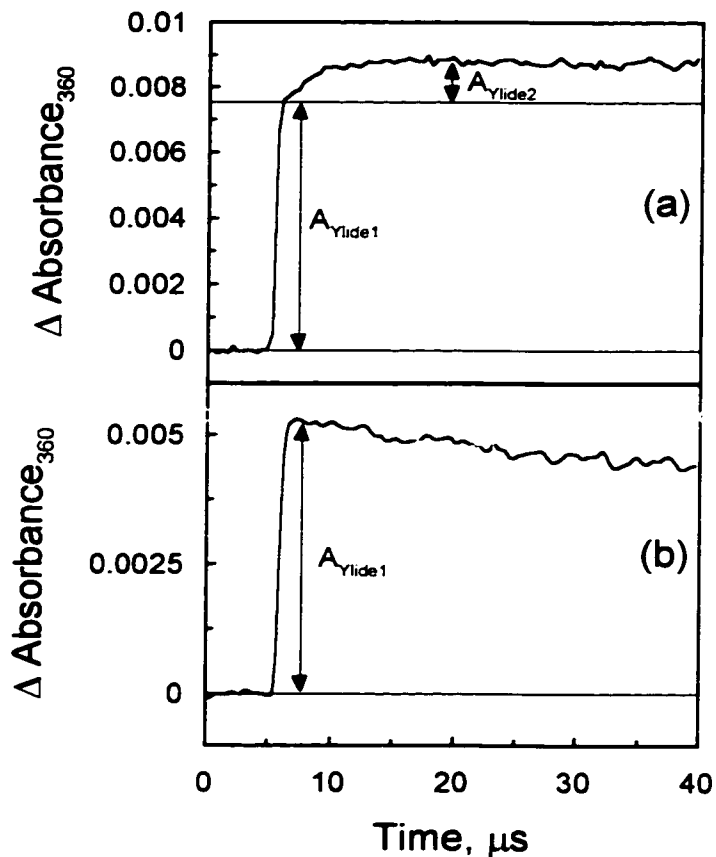
Figure II-20. *(a)* Trace obtained upon 308 nm LFP of 8-*tert*-butyl-3,4-diaza-2-methoxy-2-methyl-1-oxa[4.3]spirodec-3-ene (**II-1h**) in the presence of 0.4 M pyridine in cyclohexane at 22° C. *(b)* Trace obtained upon 308 nm LFP of 8-*tert*-butyl-3,4-diaza-2,2-dimethoxy-1-oxa[4.3]spirodec-3-ene (**II-1i**) in the presence of 0.4 M pyridine in cyclohexane at 22° C.

II.2.3.b. 1,2-H Migration in Cyclohexylidene and 4-tert-butyl-cyclohexylidene.

The lifetimes of cyclohexylidene (**CH:**) and 4-*tert*-butyl-cyclohexylidene (**TBCH:**), in both cyclohexane and benzene solutions, were the same within experimental error, indicating that the rate constant for 1,2-H migration in **TBCH:** is either not accelerated by the favorable orbital overlap which is imposed by the conformational locking of the chair conformer by the *t*-butyl substituent, as compared with the mobile **CH:**, or that carbene **CH:** undergoes migration primarily from the chair conformer (**II-27**), which is expected to be a conformation of minimum energy.

II-27   II-28
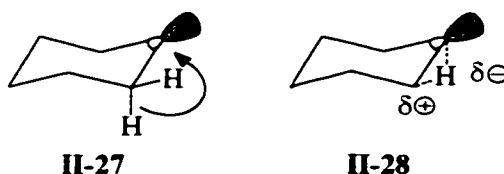
The lifetimes of carbenes **CH:**, **TBCH:**, and **AMBO:** in benzene, relative to that of dimethylcarbene, are between (~0.1 - 0.3) : 1 in spite of the fact that they should be somewhat longer-lived if statistics were dominant. Presumably the increase in rates of 1,2-H migration in the former carbenes results mainly from increased substitution at the α-carbon, which would stabilize a build-up of positive charge at that carbon in the transition state (**II-28**). This effect has been described previously as a "bystander effect".[3] Analysis of the products of photolysis of **II-1g** (hexadecane, 308 nm LFP, and 250 + 300 nm SS) by GC-MS showed that cyclohexene is the major product in both experiments. ¹H-NMR (500 MHz) analyses of the products of photolysis of **II-1g-i**, **l**, and **n** (cyclohexane-d_{12}, 250 + 300 nm SS) showed that 1,2-H migration is the major reaction pathway of carbenes **CH:**, **TBCH:**, **TFMCH:**, and **AMBO:**, **DEC:**, and **EMC:**. It is likely that excited state migrations in the diazo precursors to carbenes **CH:**, **TBCH:**, **TFMCH:**, and **AMBO:**, **DEC:**, and **EMC:** also yield the analogous alkene products derived from 1,2-H migration in the carbenes.[35,36]

Therefore the ratios of products from dual wavelength irradiations most likely represent a composite of carbene rearrangement products and excited state rearrangement products. The determination of the contributions of each process to the overall yield of products from a given carbene can be accomplished by the trapping of all (or nearly all) of the carbene with a suitable trap. When all the carbene is trapped the yields of alkene products represent the contribution of the excited state rearrangement. However, very short lifetimes of carbenes **CH:, TBCH:, TFMCH:,** and **AMBO:,** **DEC:,** and **EMC:** preclude the complete trapping of these carbenes and the accurate evaluation of the excited state *vs.* carbene rearrangements. Attempts were made to trap cyclohexylidene (**CH:**) with tetramethylethylene in dual wavelength SS experiments (eq II-13), and a product consistent with the structure of the cycloaddition product **II-29** was identified by GC-MS and by ^{1}H-NMR but the yield of this adduct was very low (~ 7 %).

(II-13)
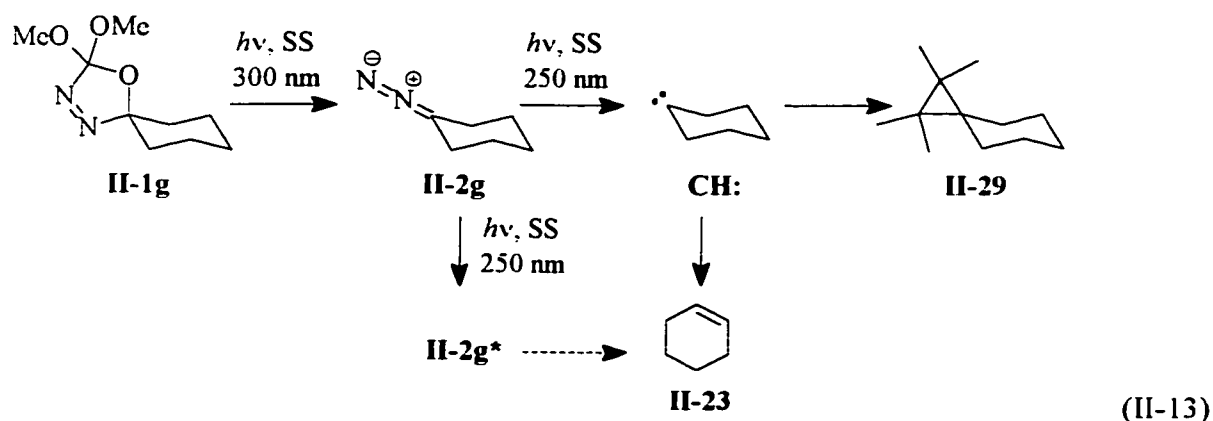
II.2.3.c. 2-Trifluoromethylcyclohexylidene. Modulation of reactivity by an α-trifluoromethyl substituent.

Previous studies of substituted cyclohexylidenes have shown that electron donating substituents at the α-position accelerate 1,2-H migration preferentially, as inferred from product ratios.[87,88] 2-Trifluoromethylcyclohexylidene (**TFMCH:**) was generated with the expectation that it might have an increased lifetime, as compared with that measured for cyclohexylidene. Photolysis (250 + 300 nm

SS) of **II-1j** in benzene and in hexadecane gave 3-trifluoromethylcyclohexene (**II-30**) and 1-trifluoromethylcyclohexene (**II-31**) in a 9.8 : 1 ratio. Both products were identified by means of ^{1}H-NMR, ^{19}F NMR, and GC-MS.[142] Although excited state rearrangement in diazoalkane **II-2j** may have contributed to the formation of products **II-30** and **II-31**, it is unlikely that hydrogen migrations in the excited state would be more selective than those in the carbene.[35, 36] Thus, the CF₃ substituent in TFMCH: directs the migration so that C6 is the favored migration origin. That result could reflect either an electronic effect or a stereochemical effect, for it is known that the orientation of the substituent at C2 of cyclohexylidenes plays a role in determining product ratios.[3] If the CF₃ group of TFMCH: were in the axial position, then migration of equatorial H from C2 would be slowed relative to migration of an axially oriented counterpart. Fortunately it was possible to assign the conformation of diazo compound **II-2j** and, by extrapolation, that of carbene **TFMCH:** as described below.

II-2j   **TFMCH:**   **II-30**   **II-31**

~9.8 : 1
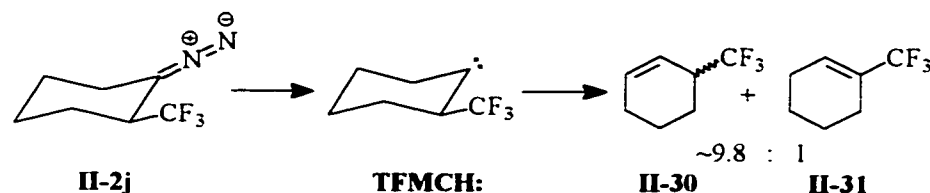
Although precursor **II-1j** was obtained as a mixture of diastereomers, diazoalkane **II-2j** was stable enough to permit its analysis by spectroscopy. The infrared spectrum recorded following the photolysis of **II-1j** in a SS experiment with 300 nm light (30 minutes) showed a diazo stretching band at 2052 cm⁻¹ corresponding to **II-2j**, as well as a broad C-F stretching band centered at 1282 cm⁻¹ (not shown), and a carbonyl band at 1756 cm⁻¹ assigned to dimethylcarbonate (Figure II-21). Only one conformer of 2-trifluoromethyldiazocyclohexane (**II-2j**) was generated by photolysis of **II-1j** in the SS experiment with 300 nm light only. The COSY spectrum (Figure II-22) of the photolysis mixture indicated that two major products were formed upon photolysis, dimethylcarbonate (^{1}H-NMR 500 MHz, C₆D₆, δ 3.38 ppm) and diazoalkane **II-2j**. Cross peaks in the COSY spectrum in Figure 6

showed that all peaks assigned to **II-2j** are correlated with each other and therefore originate from the same molecule. The coupling interactions for the $CF_3C\underline{H}$ group (δ 2.37) showed that diazoalkane **II-2j** has the CF_3-group in the equatorial position. Three coupling constants were found, one of 10.0 Hz due to coupling with the fluorine nuclei of the CF_3 group, and two (7.1 Hz and 3.3 Hz) for coupling to protons at C3. The 7.1 and 3.3 Hz values must be from axial/axial and axial/equatorial coupling, respectively, and thus C2-H and CF_3 in **II-2j**, must be axial and equatorial, respectively. Since 2-trifluoromethyldiazocyclohexane is generated initially in the SS experiment and is subsequently converted to the carbene, the product ratio (~9.8 : 1) presumably reflects reactions of the carbene with the CF_3 group in the equatorial position. Thus, migration of H from C2 is that of axially-oriented H (normally favored) and its retardation, relative to migration from C6, must reflect an electronic effect of the CF_3 group (**II-32**). This result is in accord with the view that 1,2-H migration in singlet carbenes involves a transition state in which the migrating H is hydride-like and, consequently, the migration origin is cation-like. This analysis is predicated upon the assumption that 1,2-H migration from the excited state of **II-2j** causes only minor skewing of the product distribution.
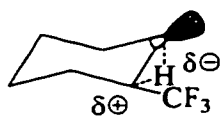
II-32
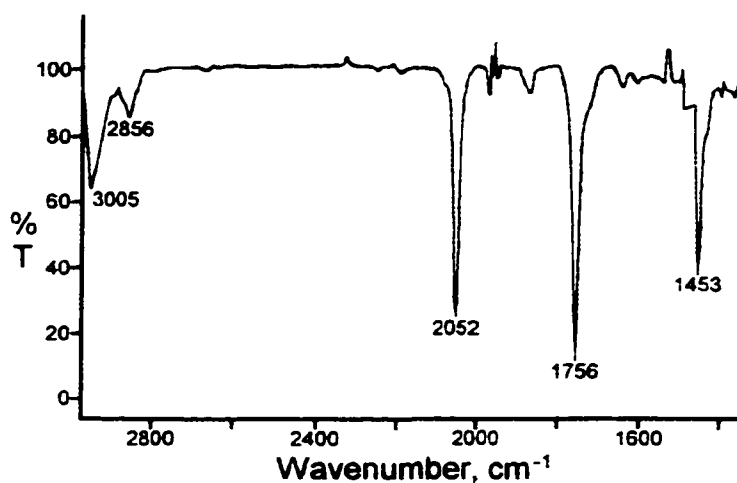
Figure II-21. Infrared spectrum recorded after steady state photolysis (30 minutes) of a 0.01 M solution of oxadiazoline **II-1j** in benzene. The absorption at 2052 cm⁻¹ is assigned to the C=N=N stretch of diazoalkane **II-2j** and the absorption at 1756 cm⁻¹ is assigned to the carbonyl stretch of the photoproduct dimethylcarbonate.
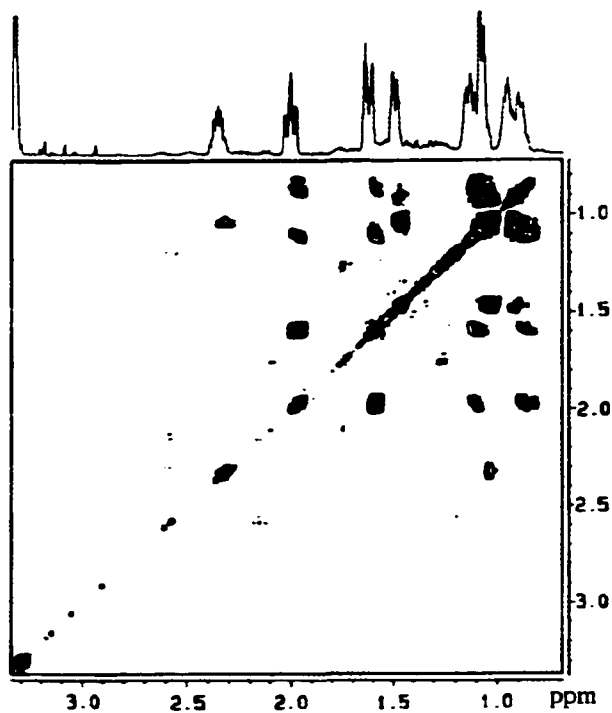
FIGURE II-22. Gradient COSY spectrum (^{1}H- ^{1}H correlated 2-D NMR spectrum) of 2-trifluoromethyldiazocyclohexane (**II-2j**) generated upon photolysis (SS) of 6-trifluoromethyl-3,4-diaza-2,2-dimethoxy-1-oxa[4.3]spirodec-3-ene (**II-1j**) in benzene-d_6.

Although the presence of the CF₃ substituent affects the distribution of products from 2-trifluorocyclohexylidene (**TFMCH:**) substantially, the lifetime of **TFMCH:** is not significantly longer than that of the parent cyclohexylidene. Carbene **TFMCH:** did not show a significant solvent kinetic isotope effect (C_6H_{12} vs. C_6D_{12}). It is therefore assumed that **TFMCH:** is a ground state singlet, and that its chemistry in solution is predominantly that of the singlet state. The lifetime of **TFMCH:** is not observably enhanced because its dominant reaction, migration from C6, is not strongly affected by the CF₃ group at C2.

II.2.3.d. Dative stabilization in 8-aza-8-methylbicyclo[3.2.1]oct-3-ylidene.

Photolysis of **II-1k** (LFP, 308 nm) in the presence of pyridine also led to the formation of a pyridinium ylide. The lifetimes of 8-aza-8-methyl[3.2.1]oct-3-ylidene (**AMBO:**) were determined as described above and are given in Table II-5. Lifetime enhancement for **AMBO:**, relative to that of cyclohexylidene, which might be anticipated from dative stabilization of the carbenic center by the neighboring amino group in a pseudo-boat conformation (**II-33**), is modest. A
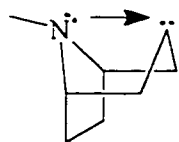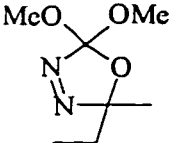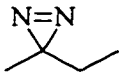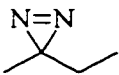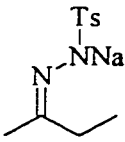
II-33

possible explanation for the increased lifetimes of **AMBO:** relative to the others is that the rate constants for reactions of **AMBO:** with pyridine in the different solvents are smaller as a result of steric hinderance.

II.2.3.e. 1,2-H Migration in Ethyl(methyl)carbene and Diethylcarbene.

From diethylcarbene (**DEC:**), three products of intramolecular rearrangement were detected, (E)-2-pentene, (Z)-2-pentene, and 1,2-dimethylcyclopropane. The ratios (E)-2-pentene: (Z)-2-pentene: 1,2-dimethylcyclopropane were ~15:10:1 (58%, 38%, 3.8%). From ethyl(methyl)carbene (**EMC:**), four products of intramolecular rearrangement were detected. They were (E)-2-butene, (Z)-2-butene,

1-butene, and methylcyclopropane which were found in ratios of 45:34:20:1, respectively. Similar ratios of products have been reported from ethyl(methyl)carbene generated from other nitrogenous precursors (Table II-6).[143] The barriers for migrations in ethylmethylcarbene leading to (E)-2-butene, (Z)-2-butene, 1-butene and methylcyclopropane have recently been computed to be 5.2, 5.9, 8.5, and 8.3 kcal/mol, respectively.[93]

Table II-6. Product distributions for the decomposition of oxadiazoline, diazirine, and tosylhydrazone precursors to ethyl(methyl)carbene (see reference 143 and references therein).

Precursor	Conditions	(structure 1)	(structure 2)	(structure 3)	(structure 4)	(structure 5)
(oxadiazoline, McO OMe)	$h\nu$	44.7	33.6	20.7	1.0	0.0
(diazirine, N=N)	$h\nu$	38.0	34.7	23.2	3.7	0.3
(diazirine, N=N)	Δ	66.6	29.5	3.3	0.5	0.0
(tosylhydrazone, Ts-NNa)	Δ	67	28	5	0.5	0.0

II.2.3.f. Azine Formation.

Steady state irradiations of oxadiazolines **II-1g** to **n** with 300 nm light led to the formation of diazoalkanes (as evidenced by the pink color of the resulting solutions and the characteristic CNN band in IR spectra) in high yield as determined spectroscopically (see Experimental). The slow thermal decomposition of these diazo compounds at room temperature led to the formation of the corresponding azines with little (0-2%) or no products of rearrangement of the

corresponding carbene intermediate even at concentrations of 10^{-3} M. This suggests that a mechanism other than the reaction of carbenes **CH:**, **TBCH:**, **TFMCH:**, and **AMBO:**, **DEC:**, and **EMC:** with their corresponding diazoalkanes **II-2g** to **n** (eq II-14) is responsible for the formation of azine products.
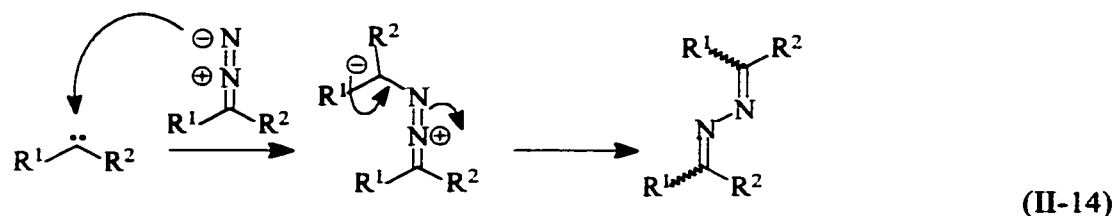
(II-14)

For example, if cyclohexylidene (**CH:**) has a lifetime of ~1 ns in a hydrocarbon solvent at room temperature then $k_{1,2-H}$ is *ca* 1 x 10^9 s^{-1}. Assuming that cyclohexylidene traps diazocyclohexane, as in eq II-14, with a rate constant of 5x 10^9 M^{-1} s^{-1} then, at concentrations of 10^{-3} M diazoalkane, intramolecular rearrangement rather than intermolecular capture of cyclohexylidene should dominate. Therefore a bimolecular reaction of diazoalkanes **II-2g** to **n**, such as that in Scheme II-8, must be responsible for the high yields of azines. Dimerization of diazo compounds has been proposed previously to explain stereoselective azine formation in the decomposition of phenyldiazomethanes.[144] The lack of azine products in dual wavelength irradiations, where dialkyl and cycloalkylcarbenes are generated photochemically, supports this conclusion.

Scheme II-8.
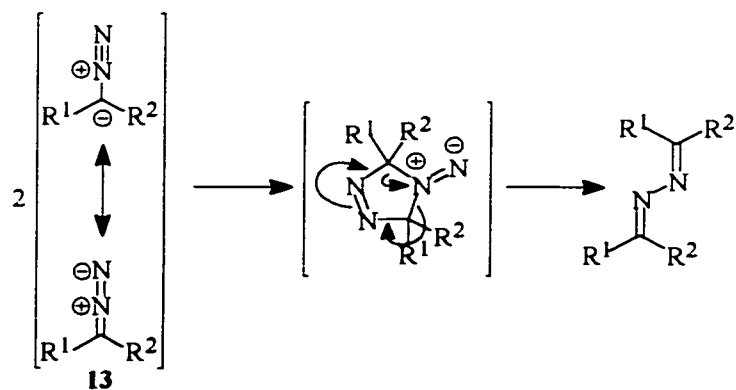
II.2.3.g. Conclusions.

Cyclohexylidenes can be generated photochemically from oxadiazolines, by laser flash photolysis (LFP). Three substituted cyclohexylidenes, and the parent, were trapped with pyridine to form the corresponding pyridinium ylides. This trapping led to the first absolute rate constants for 1,2-H migrations in cyclohexylidenes. Those rate constants show that the effects of conformational locking with a 4-*t*-butyl substituent are small and that an amino group, which could stabilize the carbene intermediate by intramolecular nucleophilic attack, does not have a large effect. The 2-trifluoromethyl substituent does decrease the rate constant for 1,2-H migration from the 2-position roughly ten fold, as indicated by the product distribution.

Diethylcarbene and ethylmethylcarbene can also be generated by means of the oxadiazoline approach. Those carbenes undergo 1,2-H migrations somewhat more slowly (*ca* 1.7 x10^8 s^{-1} *vs. ca* 1.4 x 10^9 s^{-1} for cyclohexylidene in hydrocarbon solvent, assuming that k_{pyr} = 1 x 10^9 M^{-1} s^{-1} and is invariant) but previous failures to trap cyclohexylidenes with pyridine can probably be attributed to low yields of the carbenes (e.g. from diazirines), rather than to extraordinarily fast 1,2-H migrations.

Steady state photolysis of the oxadiazolines leads to the same carbenes, *via* diazoalkane intermediates. With a suitable choice of wavelength, the diazoalkanes can be accumulated and characterized. The steady state photolysis makes it possible to characterize carbene derived products under conditions that roughly simulate LFP conditions.

Chapter 2. Section 3.

Oxygen and Sulfur Atom Transfer Reactions.

II.3. Oxygen and Sulfur Atom Transfer from Oxiranes and Thiiranes to Carbenes.

Heteroatom transfer reactions from oxiranes and thiiranes to a variety of carbenes of different structure and philicity (m_{CXY}) were studied. The heteroatom transfer chemistry of benzylchlorocarbene (**BCC:**),[145,146,147] phenylchlorocarbene (**PCC:**),[148] and methoxyphenylcarbene (**MPC:**)[14c] all of which have singlet ground states and are ambiphilic have been explored. These carbenes were generated from the photolysis of the corresponding diazirine precursors (**II-34a-c**). Oxadiazoline precursors were used to study heteroatom transfer reactions of dimethylcarbene (**DMC:**), cyclobutylidene (**CB:**), and 2-adamantylidene (**Ad:**) with oxiranes and thiiranes. LFP studies of oxadiazoline precursors by time resolved infra-red detection (TRIR) have demonstrated the formation of diazoalkanes.[60a] Dialkylcarbenes,[36] possibly formed *via* a multiphoton absorption by these precursors in the laser beam, are also generated. Diazofluorene (**DAF**) was also employed here to study the atom transfer chemistry between propylene sulfide and fluorenylidene (**FL:**). Rate constants for heteroatom transfer reactions between heteroatom donors and carbenes **BCC:**, **PCC:**, **MPC:**, **DMC:**, **CB:**, **Ad:**, and **FL:** were determined by laser flash photolysis (LFP).

In contrast to the photochemical reaction of 2,2-dimethoxy-5,5-dimethyl-Δ^3-1,3,4-oxadiazoline (**II-1b**), thermal decomposition of **II-1b** leads to the formation of dimethoxycarbene (**DMOC:**).[52,53] The latter is stabilized by conjugative donation by the lone pairs on oxygen to the formally vacant p-orbital at the carbene carbon.[4,15] As a result, dimethoxycarbene (**DMOC:**) has dipolar character and acts as a nucleophile. This conjugative donation strongly stabilizes the singlet state and the singlet/triplet energy gap has been calculated to be ~76 kcal/mol.[15] Inclusion of dimethoxycarbene in the present

study expands the range of carbene reactivities to include electrophilic, ambiphilic, and archetypal nucleophilic carbenes (m_{CXY} varying between ~0.2 to 2.22).

II.3.1. O, S Transfer to Benzylchlorocarbene.

Absolute rate constants for the reaction of benzylchlorocarbene (**BCC:**) with oxygen and sulfur atom donors were measured by means of UV-LFP and the pyridine ylide probe method (Scheme II-9). Upon irradiation of 3-benzyl-3-chlorodiazirine (**II-34a**) (355 nm, 10 ns pulse, 40 mJ) in the presence of pyridine, a long-lived (stable on the μs-ms time scale) absorption centered at λ ~370 nm, previously assigned to the pyridinium ylide **II-35a**, was observed.[145,149] It was found that the intensity of this absorption was inversely proportional to the concentration of heteroatom donor, with constant diazirine and pyridine concentrations.

Scheme II-9.

a: $R^1 = C_6H_5CH_2$, $R^2 = Cl$;
b: $R^1 = C_6H_5$, $R^2 = Cl$;
c: $R^1 = C_6H_5$, $R^2 = OMe$;

k_X Oxygen or Sulfur Atom Donor

Products of Heteroatom Loss

II-36, X = O;
II-37, X = S.

BCC: **PCC:**   **MPC:**
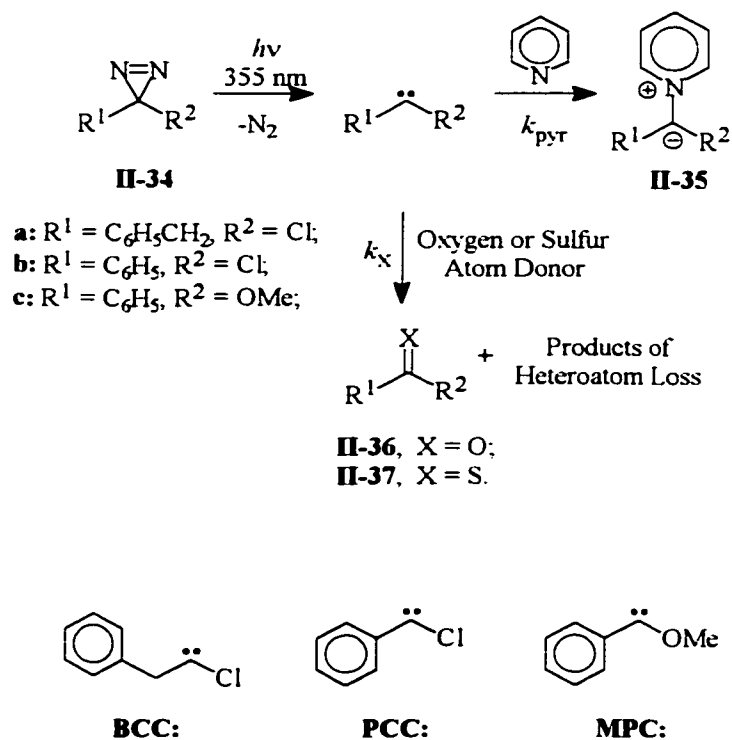
The ratios k_X / k_{pyr} [pyridine], where k_X are the bimolecular rate constants for the reactions of

benzylchlorocarbene (BCC:) with heteroatom donor traps, and k_{pyr} is the bimolecular rate constant

for the reaction of BCC: with pyridine, were determined by linear least-squares analysis of the ratio

(A°_{ylide} / A_{ylide}) vs. trap concentration, with the y-intercept defined as 1, according to the Stern-

Volmer[77c] relation in eq II-17 (derived from eqs II-15 and 17). In eq II-17, ϕ_o is the quantum yield of

pyridinium ylide formation in the absence of a second trap and ϕ is the quantum yield of pyridinium

ylide formation in the presence of trap. A°_{ylide} is the intensity of the absorbance of pyridinium ylide II-

35a in the absence of added trap, and A_{ylide} is the intensity of the absorbance of ylide II-35a in the

presence of trap. A typical plot, for the reaction of BCC: with propylene sulfide, is shown in Figure

II-23 where the slope of the line is equal to k_X / k_{pyr} [pyridine]. The values for k_X were then calculated

by using a known value for k_{pyr} of 4.2×10^9 M^{-1} s^{-1} and known concentrations of pyridine. Bimolecular

rate constants of 1.4×10^7, 1.4×10^8, 2.3×10^9, and 7.1×10^9 M^{-1} s^{-1} were determined in this manner

for the transfer of oxygen from propylene oxide, butadiene monoxide, pyridine N-oxide, and

dimethylsulfoxide (DMSO), respectively, to benzylchlorocarbene. The rate constants for transfer of

oxygen from propylene oxide and from butadiene monoxide were measured in cyclohexane solvent

whereas those for transfer from pyridine N-oxide and from DMSO were measured in acetonitrile due

to their insolubility in hydrocarbon media. A rate constant of 2.5×10^9 M^{-1} s^{-1} for the transfer of a

sulfur atom from propylene sulfide to benzylchlorocarbene was also measured in cyclohexane.

$$k_{obs} \;=\; k_o \;+\; k_{pyr} \text{[pyridine]} \;+\; k_X \text{[heteroatom donor]} \tag{II-15}$$

$$\phi = \frac{k_{pyr} \, [\text{pyridine}]}{k_{pyr} \, [\text{pyridine}] \; + \; k_X \, [\text{heteroatom donor}]} \qquad \text{(II-16)}$$

$$\frac{\phi_o}{\phi} = \frac{A^o_{ylide}}{A^o} = \frac{k_X}{k_{pyr} \, [\text{pyridine}]} \, [\text{heteroatom donor}] \; + \; 1 \qquad \text{(II-17)}$$

Alternatively, k_X can be obtained as the slope of the plot of observed rate constants of either the decay of carbene **BCC**: (monitored at 310 nm) using the kinetic expression in eq II-18, or the growth of pyridine ylide **II-34a**, vs. heteroatom donor concentration using the kinetic expression in eq II-15.

$$k_{obs} = k_o + k_X \, [\text{heteroatom donor}] \qquad \text{(II-18)}$$

Such a plot constructed from the pseudo-first order rate constants for the decay of benzylchlorocarbene vs [propylene sulfide] in cyclohexane at 22 °C (Figure II-24) yielded a value of $4 \times 10^9 \, M^{-1} \, s^{-1}$ for the reaction which is in reasonable agreement with the value of $2.5 \times 10^9 \, M^{-1} \, s^{-1}$ determined by Stern-Volmer quenching of the yield of ylide **II-35a**. Here, the latter method is more reliable because of difficulties in determining accurate pseudo-first order rate constants by measuring decays/growths, imposed by the time resolution of our instrument. [150]
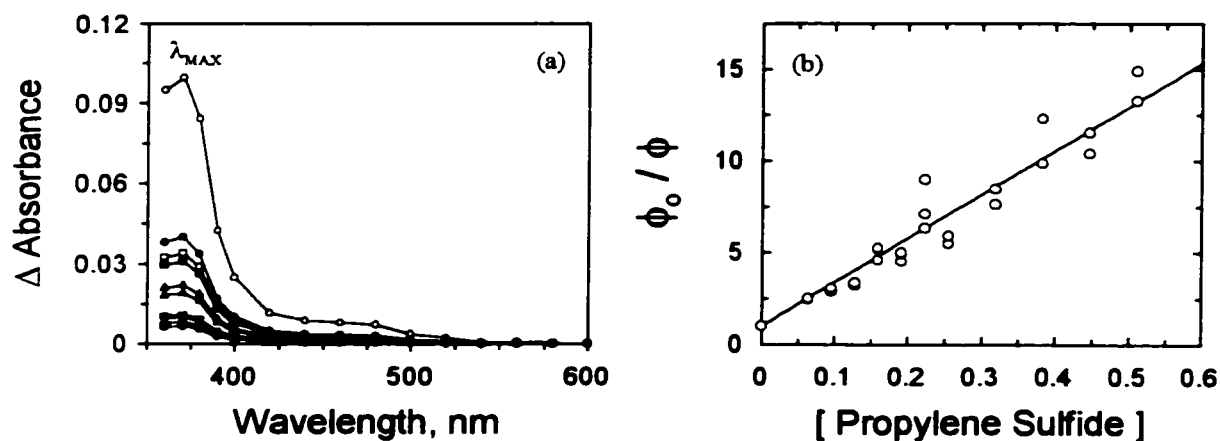
FIGURE II-23. *(a)* Time resolved UV-visible spectra of the pyridinium ylide of benzylchlorocarbene as a function of [propylene sulfide]. *(b)* Stern-Volmer quenching plot for the reaction of propylene sulfide with benzylchlorocarbene in cyclohexane at 22 °C.
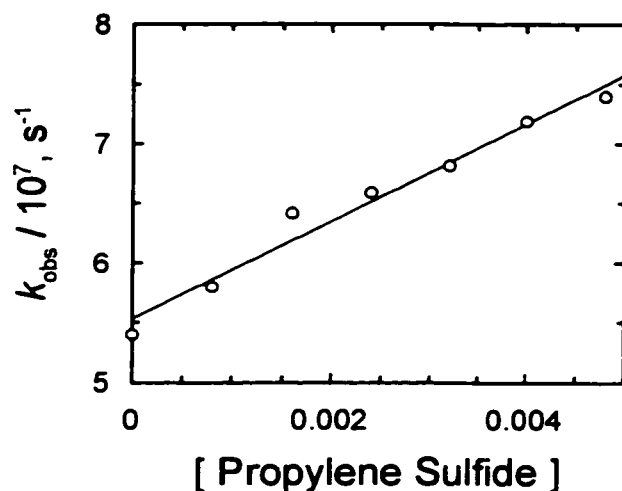
FIGURE II-24. Plot of the pseudo first order rate constants for the decay of benzylchlorocarbene vs [propylene sulfide] in cyclohexane at 22 °C.

Laser Flash Photolysis: Infra-red Detection. The formation of phenylacetylchloride was readily confirmed upon 308 nm LFP of **II-32a** (1×10^{-3} M, continuous flow, purged with N_2) in neat propylene oxide at 22 °C, by means of time-resolved infra-red detection. An absorption assigned to phenylacetyl chloride, centered at 1796 cm^{-1}, was formed within the time resolution (~ 500 ns) of the instrument, Figure II-25.
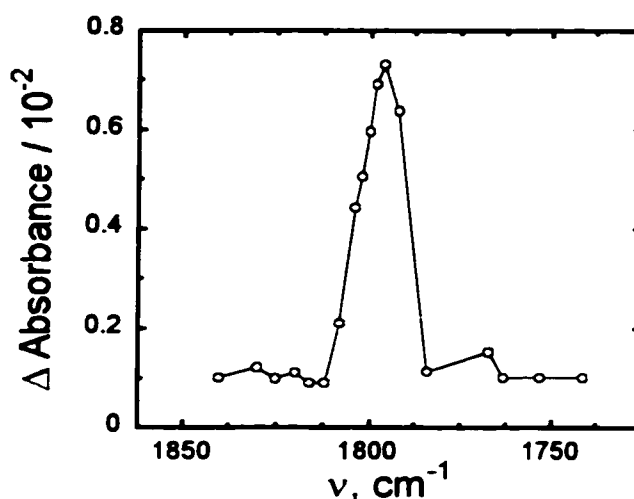
FIGURE II-25. Time resolved IR spectrum observed 500 ns after 308 nm LFP of **II-34a** in neat propylene oxide at 22 °C.

From Stern-Volmer quenching experiments it was found that the pyridinium ylide from carbene **BCC:** (and from the other carbenes and heteroatom donors studied here) reacted with the oxirane and thiirane traps with rate constants ranging from 10^3 to 10^5 $M^{-1} s^{-1}$. For example, the pyridine ylide of benzylchlorocarbene reacts with butadiene monoxide with a rate constant of 3.0×10^5 $M^{-1} s^{-1}$ (Figure II-26). Probably the pyridinium ylides react with oxiranes and thiiranes *via* a nucleophilic ring opening reaction.
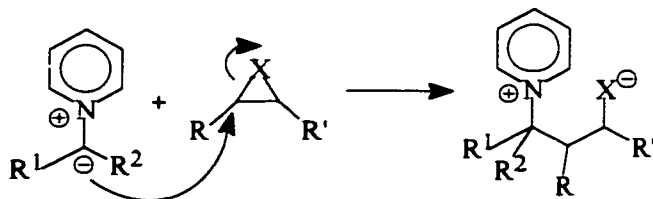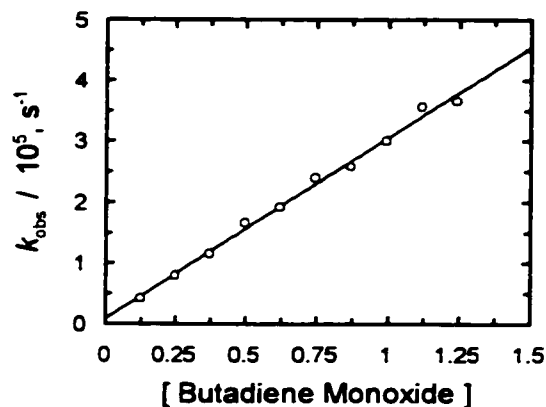
FIGURE II-26. Plot of the pseudo first order rate constants for the decay of pyridine ylide of benzylchlorocarbene *vs* [butadiene monoxide] in cyclohexane at 25 °C.

II.3.2. O, S Transfer to Phenylchlorocarbene.

LFP (355 nm, 10 ns pulse, 40 mJ) of 3-chloro-3-phenyldiazirine (**II-34b**) in cyclohexane produced a long lived transient (decays on the μs timescale) with $\lambda_{max} \sim 315$ nm which has previously been assigned to phenylchlorocarbene (**PCC:**).[38] LFP of **II-34b** in cyclohexane containing pyridine produced a transient signal associated with the pyridinium ylide of phenylchlorocarbene (**II-35b**) (stable on the ms timescale) with $\lambda_{max} \sim 480$ nm. The rate constants for reaction of phenylchlorocarbene with heteroatom donors could be measured either by the decay of the carbene signal or by Stern-Volmer quenching of the pyridinium ylide signal as described above for benzylchlorocarbene. The latter was found to be most convenient due to the relative intensities of the two signals. The bimolecular rate constant for the reaction of **PCC:** with propylene sulfide was measured in this manner and was found to be 3.6 x 10^7 M^{-1} s^{-1} which is almost 2 orders of magnitude smaller than that of the analogous reaction with benzylchlorocarbene. The rate constant for the reaction of phenylchlorocarbene with propylene oxide could only be estimated based on small changes in the decays of carbene signal and on small changes in pyridinium ylide amplitudes at high concentrations of trap.

II.3.3. O, S Transfer to Phenylmethoxycarbene.

3-Methoxy-3-phenyldiazirine (**II-34c**) was prepared by the exchange reaction of 3-bromo-3-phenyldiazirine with sodium methoxide in dimethylformamide (DMF) as described previously.[14c,151] Diazirine **II-34c** has a lifetime of 4-5 minutes at room temperature and does not survive for long periods even when stored on dry ice. Therefore this precursor was prepared just prior to use. All solutions were prepared at -10 to -30 °C and warmed to room temperature just prior to photolysis. Fresh solutions were used for each kinetic measurement. We were able to reproduce the kinetic decays for methoxyphenylcarbene (**MPC:**) monitored at λ = 290 nm and the slow growth for pyridinium ylide **II-35c** with k_{pyr} = 1.2 x 10^5 M^{-1} s^{-1}. The rate constant for the reaction between methoxyphenylcarbene (**MPC:**) and propylene sulfide was determined by monitoring the growth of pyridinium ylide at λ = 480 nm and by monitoring the decay of the carbene signal at λ = 290 nm. The kinetic runs were repeated several times and the rate constant for reaction was determined to be 7.1 x 10^4 M^{-1} s^{-1}. Attempts to measure the kinetics of oxygen atom transfer from propylene oxide to methoxyphenylcarbene (**MPC:**) were unsuccessful. The reaction was too slow even in neat propylene oxide.

II.3.4. O,S Transfer to Dimethylcarbene, Cyclobutylidene, and Adamantylidene.

Electrophilic carbenes such as dialkylcarbenes[22,74] (m_{CXY} ≈ 0.2, dimethylcarbene has an m_{CXY}^{calcd} = 0.19), and chlorocarbene[32c] (m_{CXY}^{calcd} = 0.46) react with pyridine with rate constants at or near the diffusion controlled limit; k_{pyr} = 1-8 x 10^9 M^{-1} s^{-1}. Dialkylcarbenes tend to show electrophilic singlet state chemistry, and intramolecular 1,2-hydrogen shifts are usually dominant for these intermediates. Exceptions include carbenes without α-hydrogens as exemplified by di(1-adamantylcarbene).[152] In singlet alkyl and dialkylcarbenes those shifts involve transition states in which the migrating atom is

Scheme II-10.

II-38, X = O;
II-39, X = S.

II-1b   II-1e   II-1f

DMC: CB: Ad:
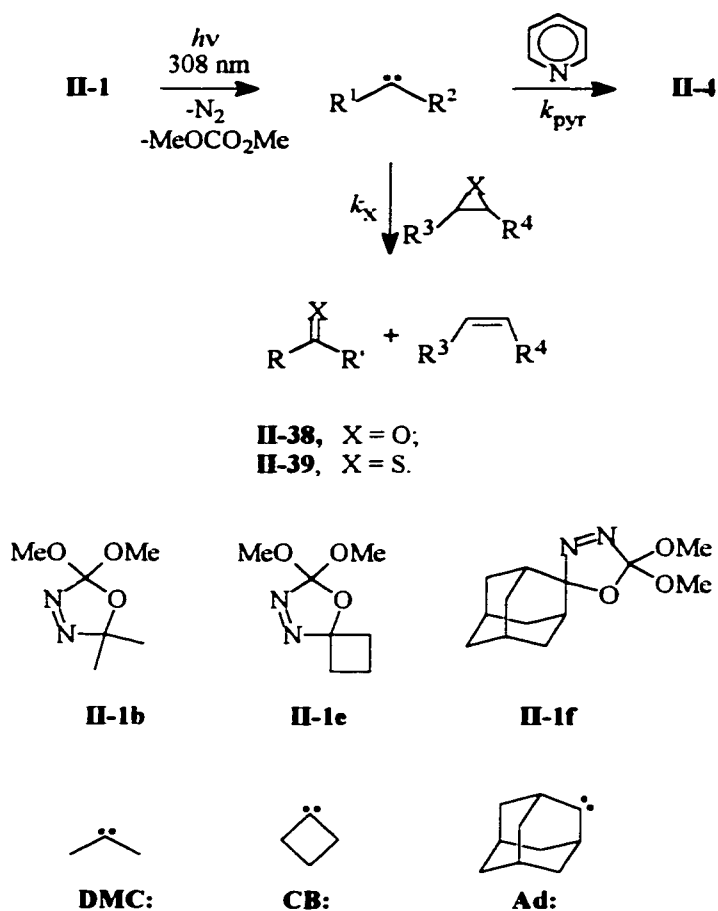
hydride-like. The electrophilic character of such carbenes is also indicated by their preference for electron-rich olefins in cyclopropanation reactions, and by their rapid reactions with substrates, such as pyridine, containing heteroatoms. The rapid (close to the diffusion controlled limit) formation of pyridine ylide intermediates from singlet dialkylcarbenes suggests that reactions of these carbenes with heteroatom donors could successfully compete with intramolecular rearrangement reactions.

The ratios k_X / k_{pyr} [pyridine] for the reactions of dimethylcarbene (**DMC:**), cyclobutylidene (**CB:**), and adamantylidene (**Ad:**) with heteroatom donors were determined by 308 nm LFP (8-10ns pulse,

40-50mJ) of the corresponding oxadiazoline precursors **II-1b**, **II-1e**, and **II-1f**, respectively, by means of the pyridine ylide method, using the Stern-Volmer treatment in the same manner as described for carbene **BCC:** (Scheme II-10). The ranges of rate constants for these reactions are summarized in Table II-7.

Laser Flash Photolysis: Infra-red Detection. A TRIR-LFP study of **II-1b** in pentane (308 nm, 2.3 x 10^{-2} M, continuous flow, purged with N$_2$) led to absorption bands at 2036 ± 3 cm^{-1}, assigned to the diazo band of 2-diazopropane, and at 1756 ± 3 cm^{-1}, assigned to the carbonyl band of dimethylcarbonate. There were no other absorption bands in the 2160 - 1690 cm^{-1} region of the IR. Formation of acetone upon 308 nm LFP of **II-1b** in 5.0 M cyclohexene oxide in pentane at 22 °C was readily confirmed by means of TRIR detection.[153] Absorptions assigned to the carbonyl band of dimethylcarbonate, centered at 1756 cm^{-1}, and to acetone, centered at 1724 cm^{-1}, were formed instantaneously (i.e. within the response time of the instrument) after 308 nm TRIR-LFP.

Analyses of oxygen and sulfur atom transfer reactions were also carried out using steady state (SS) photolytic methods. Dialkylcarbenes **DMC:**, **CB:**, and **Ad:** were generated using dual wavelength irradiations with both 250 and 300 nm light, as described previously. Adamantylidene and cyclobutylidene were generated in this manner in both neat propylene oxide and in 0.1 M propylene sulfide in hexadecane. The reaction mixtures were analyzed by GC-MS and it was found that the corresponding oxygen and sulfur atom transfer products were formed. In all reactions higher molecular weight products were also observed but they are attributed to products of direct irradiation of propylene oxide, and propylene sulfide, in the steady state experiments. Dimethylcarbene was also generated in this manner in both neat propylene oxide and in 0.1 M propylene sulfide in hexadecane, but the analysis of the products was not achieved due to the similarity between the products and
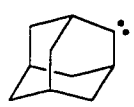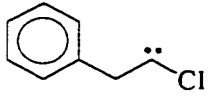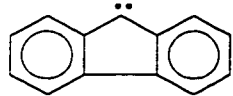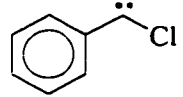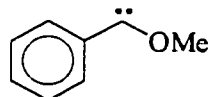
reactants. Carbenes **DMC:**, **CB:**, and **Ad:** were also generated (250 and 300 nm, SS) in the presence of neat butadiene monoxide. In most cases, the corresponding oxygen atom transfer products were observed by GC-MS. Mass spectra attributed to cyclopropanation of butadiene monoxide were also observed. In most cases it was not possible to determine the ratios of these competing pathways due to secondary photolysis products. An exception was the reaction of adamantylidene with butadiene monoxide for which a ratio of ~3:1 for oxygen transfer vs. cyclopropanation was observed (eq II-19).

(II-19)
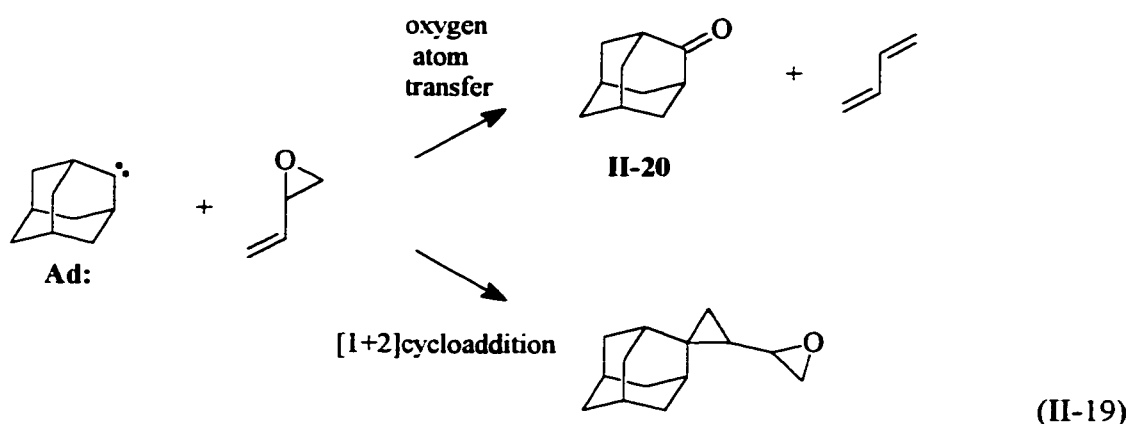
II.3.5. S Transfer to Fluorenylidene.

Rate constants for the oxygen atom transfer reactions from epoxides to spin equilibrated fluorenylidene (**FL:**) have been measured previously by Stern-Volmer quenching of the acetonitrile ylide of **FL:** in acetonitrile solutions.[126a] Upon 355 or 337 nm LFP of **DAF** in N$_2$ saturated acetonitrile three transients are observable centered at 400, 470, and 500 nm.[154] These signals are associated with ylide **II-40**, triplet fluorenylidene (^{3}**FL:**), and fluorenyl radical **II-41** (Scheme II-11).

Table II-7. Rate Constants for Quenching of Carbenes with Oxygen and Sulfur Atom Donors at 22 °C.

Carbene	Heteroatom Donor	k_X / k_{ylide}	k_X, M^{-1}s^{-1}
	Propylene Oxide	1.6×10^{-2}	$(1.6 - 8.0) \times 10^{7\,a,\,b}$
	Cyclohexene Oxide	1.5×10^{-2}	$(1.5 - 7.5) \times 10^{7\,a,\,b}$
	Butadiene Monoxide	7.6×10^{-2}	$(0.76 - 3.8) \times 10^{8\,a,\,b}$
	Propylene Sulfide	3.3	$(0.33 - 1.65) \times 10^{10\,a,\,b}$
	Propylene Oxide	3.9×10^{-2}	$(0.39 - 2.0) \times 10^{8\,a,\,b}$
	Butadiene Monoxide	6.3×10^{-2}	$(0.63 - 3.2) \times 10^{8\,a,\,b}$
	Propylene Sulfide	7.7	$(0.77 - 3.9) \times 10^{10\,a,\,b}$
	Propylene Oxide	1.9×10^{-2}	$4.9 \times 10^{7\,b,\,c}$
	Butadiene Monoxide	5.3×10^{-2}	$1.4 \times 10^{8\,b,\,c}$
	Propylene Sulfide	5.6	$1.5 \times 10^{10\,b,\,c}$
	Propylene Oxide	3.2×10^{-3}	$1.3 \times 10^{7\,b,\,d}$
	Butadiene Monoxide	3.3×10^{-2}	$1.4 \times 10^{8\,b,\,d}$
	Propylene Sulfide	6.0×10^{-1}	$2.5 \times 10^{9\,b,\,d}$
			$4 \times 10^{9\,b,\,e}$
	DMSO	5.5×10^{-1}	$2.3 \times 10^{9\,d,\,f}$
	Pyridine N-Oxide	1.7	$7.1 \times 10^{9\,d,\,f}$
	Propylene Sulfide	1.5×10^{2}	$3.2 \times 10^{8\,f,\,g}$
	cis-2-butene oxide	4.4×10^{2}	$9.2 \times 10^{8\,f,\,h}$
	trans-2-butene oxide	1.5×10^{2}	$3.2 \times 10^{8\,f,\,h}$
	Propylene Sulfide	4.8×10^{-2}	$3.6 \times 10^{7\,b,\,i}$
	Propylene Oxide	$\sim 5 \times 10^{-4}$	$\sim 4 \times 10^{5\,b,\,i}$
	Propylene Sulfide	5.9×10^{-1}	$7.1 \times 10^{4\,d,\,j}$
	Propylene Oxide	k	k

[a] Assuming $k_{pyr} = (1 - 5) \times 10^{9}$ M^{-1} s^{-1}; [b] in cyclohexane; [c] $k_{pyr} = 2.6 \times 10^{9}$ M^{-1} s^{-1}, see text; [d] $k_{pyr} = 4.2 \times 10^{9}$ M^{-1} s^{-1}, see text; [e] measured from the decays of the carbene, monitored at 310 nm; [f] in acetonitrile; [g] measured using the changes in maximum absorbance of the MeCN ylide monitored at 400 nm as a function of propylene sulfide and assuming a rate constant of $k_{MeCN} = 2.1 \times 10^{6}$ M^{-1} s^{-1}; [h] assuming $k_{MeCN} = 2.1 \times 10^{6}$ M^{-1} s^{-1}, see text; [i] $k_{pyr} = 7.6 \times 10^{8}$ M^{-1} s^{-1}; [j] $k_{pyr} = 1.2 \times 10^{5}$ M^{-1} s^{-1}; [k] Too small to measure.

Scheme II-11.
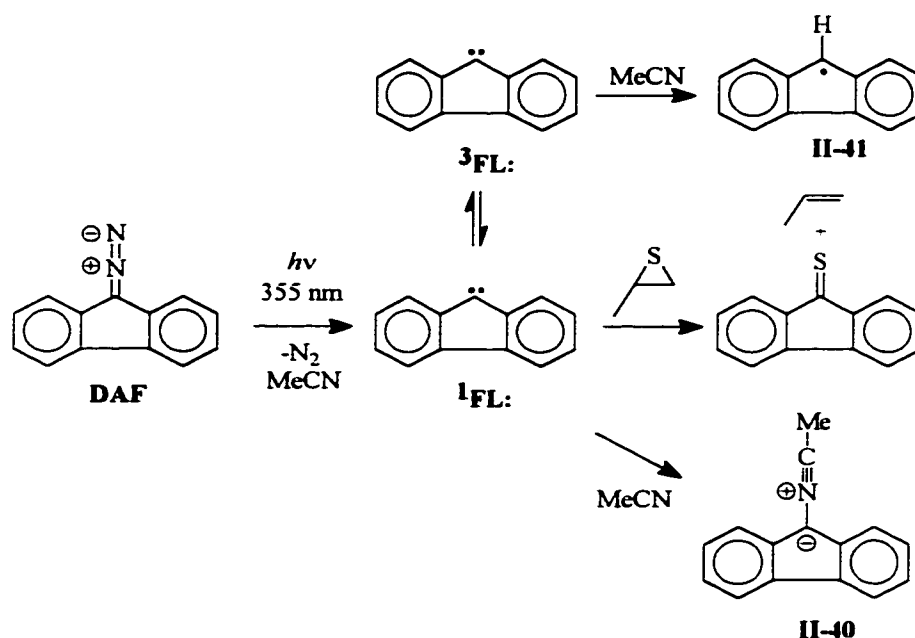
The half-life of spin equilibrated fluorenylidene in acetonitrile solution is ~17 ns which corresponds to a rate constant of 2.1×10^6 M^{-1} s^{-1},[154] which is assumed here to be the rate constant for the formation of ylide **II-40**. Using Stern-Volmer methods analogous to those used for pyridine quenching above, we have measured the rate constant for the sulfur atom transfer reaction from propylene sulfide to spin equilibrated fluorenylidene, using fresh solutions of **DAF** for each concentration of sulfide. No signals which could be attributed to either a propylene sulfide ylide of fluorenylidene, or to radical intermediates other than **II-41**, were detected in time-resolved UV-visible spectra recorded for a range of trap concentrations. The rate constant for sulfur atom transfer was determined to be 3.2×10^8 M^{-1} s^{-1}. This reaction could not be followed in cyclohexane because of the rapid formation of the fluorenyl radical by hydrogen atom abstraction from the solvent.

II.3.6. Thermal Generation of Dimethoxycarbene.

The propensity of dimethoxycarbene (**DMOC:**), generated thermally from oxadiazoline **II-1b**, to undergo O and S atom transfer reactions was also studied. Thermolyses of oxadiazoline **II-1b** (0.1 M)

in the presence of either cyclohexene oxide or propylene sulfide (0.1 M) were performed in benzene in sealed tubes (degassed) for 24 hours at 110 °C. The resulting mixtures were analyzed by ^{1}H-NMR (500 MHz) and GC-MS. Products associated with oxygen and sulfur transfer were detected in both cases. The major product was found to be tetramethoxyethylene, the dimerization product of dimethoxycarbene (Scheme II-12). For the reaction of dimethoxycarbene with cyclohexene oxide, cyclohexene and dimethyl carbonate (II-42b) were detected in ~0.9 % yields relative to internal standard p-xylene. Their GC/MS spectra were compared with those of authentic commercial samples. Neither of these products was detected in control experiments that involved heating of cyclohexene oxide in the absence of II-1b, or the thermolysis of II-1b alone. Thermal decomposition of II-1b in the presence of propylene sulfide led to the formation of propylene and dimethyl thiocarbonate (II-42a) in ~15 % yield; the major product again being tetramethoxyethylene. In both reactions unobscured alkene proton signals in the ^{1}H-NMR spectra were attributed to cyclohexene and propene respectively.

Scheme II-12.
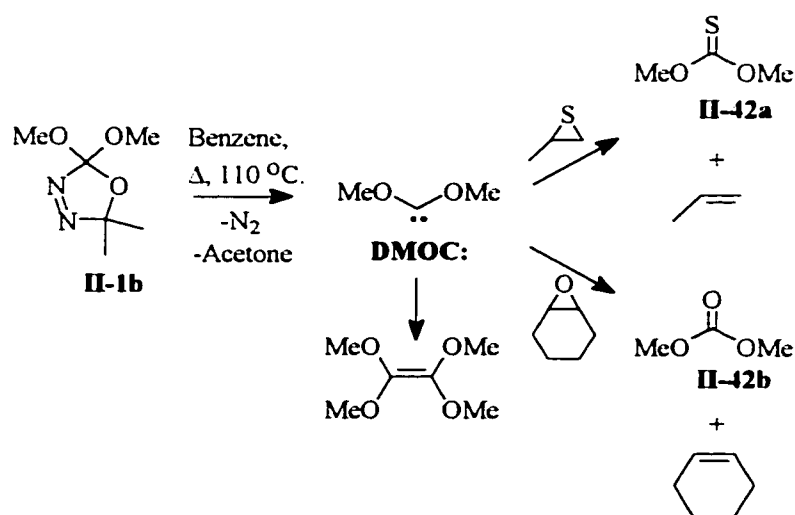
II.4.7. Mechanistic Considerations.

Bimolecular rate constants for oxygen transfer to carbenes **DMC:**, **CB:**, and **Ad:** were of the order of 10^7 - 10^8 M^{-1} s^{-1} and those for sulfur atom transfer were of the order of 10^9 - 10^{10} M^{-1} s^{-1}. These reactions are presumably those of the singlet carbenes. When (ICS) is rapid compared to product forming steps, then the product ratio is determined entirely by the relative transition state energies for formation of products and the singlet/triplet populations are irrelevant, according to the Curtin-Hammet principle.[20] Triplet reactions generally have higher barriers than singlet reactions unless the reactant (e.g. O_2) is prone to radical chemistry. Oxiranes are not good substrates for reactions with carbon-centred radicals. As far as we know there is no precedence for hydrogen atom abstraction from a ring carbon of a cyclopropyl system by a carbon centered radical. Oxiranylmethyl radicals[155] open rapidly to allyloxy radicals (in general) but show either C-C or C-O bond scission depending on substituent.[156] For the case of the reaction of a triplet carbene with epoxides, oxiranylmethyl radicals would have to be formed first by H-abstraction, from the methyl group of propene oxide for example. Carbon-centered radicals, which are good models for triplet carbenes, are poor abstractors of hydrogen from saturated carbon atoms, especially primary hydrogens. Similar arguments apply to thiiranes except for the added possibility of radical attack (S_H2) at sulfur. Tributyltin radicals have recently been shown to abstract sulfur atoms from thiiranes to yield alkene products in high yields.[157]

Cyclobutylidene chemistry is dominated by singlet state behavior as evidenced by a lack of a significant solvent deuterium isotope effect on its lifetime in solution.[36] Although it is possible that dimethylcarbene (**DMC:**), adamantylidene (**Ad:**), or fluorenylidene (**FL:**) react with oxiranes and thiiranes by hydrogen atom abstraction or S_H2 substitution at oxygen or sulfur, because all of these carbenes have low-lying and accessible triplet states, it is likely that singlet state chemistry is dominant because of the high reactivity of singlets toward heteroatom lone pairs. If triplet fluorenylidene (^{3}**FL:**)

reacted with propylene sulfide by an S_H2 substitution mechanism at sulfur we might expect to observe diradical **II-43** by LFP. The 9-chloro-9-fluorenyl radical (**II-44**, ~480 nm) is easily detectable by LFP when ^{3}**FL:** abstracts a chlorine radical from carbon tetrachloride.[154f] However, our failure to observe **II-43** may be the result of its short lifetime.

II-43   **II-44**
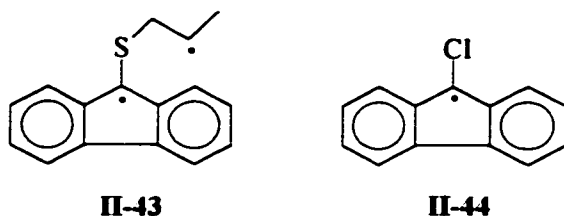
Fluorenylidene also reacts with sulfides and disulfides with rate constants ranging between 10^8 and 10^9 M^{-1} s^{-1} to produce transient sulfur ylides with λ_{max} between 350 and 450 nm.[158] The lack of any detectable intermediates in the reaction between **FL:** and propylene sulfide therefore implies a completely concerted mechanism.

The fact that bimolecular rate constants obtained for benzylchlorocarbene (**BCC:**), a known ground state singlet, with oxygen and sulfur atom donors were similar to those for **DMC:**, **CB:**, and **Ad:** is consistent with the interpretation that all the abstractions are predominantly or exclusively singlet state reactions. Thus, while the observed rate constants for oxygen and sulfur atom transfers represent the sum of all reactions of a carbene with a trap, it is reasonable to assume that they adequately represent the absolute rate constants for singlet processes. Phenylchlorocarbene (**PCC:**) and methoxyphenylcarbene (**MPC:**) are also ground state singlet carbenes and differences in their absolute reactivities are most likely due to substituent effects on the carbene carbon rather than differences in inter-system crossing (ISC) rate constants leading to triplet state chemistry. An example of the differences in reactivities of singlet phenylchlorocarbene (**PCC:**) and methoxyphenylcarbene (**MPC:**) is their propensity to undergo electrophilic attack onto the lone pair on the nitrogen atom in

pyridine to form pyridinium ylides (k_{pyr} = 7.6 x 10^8 M^{-1} s^{-1} for **PCC:** and k_{pyr} = 1.2 x 10^5 M^{-1} s^{-1} for **MPC:** in hydrocarbon solvent at ambient temperatures).[14c, 149]

Oxonium ion intermediates have been implicated during oxygen atom transfer from oxiranes to fluorenylidene, although such intermediates were not detectable *via* UV-LFP experiments. Intermediates were not observed for any of the reactions of epoxides and sulfides with carbenes **DMC:, CB:, Ad:, BCC:, PCC:, MPC:,** and **FL:,** by UV-LFP. Here, acetone and phenylacetyl chloride were formed "instantaneously" from reactions of dimethylcarbene with cyclohexene oxide and of benzylchlorocarbene with propylene oxide, as observed by 308 nm laser flash photolysis with time resolved infra-red detection (TRIR-LFP). An upper limit for the lifetimes of the cyclohexene oxide ylide of dimethylcarbene and the propylene oxide ylide of benzylchlorocarbene can therefore be placed at ~500 ns, which corresponds to the rise time of the TRIR system.

The atom transfer reactions to electrophilic carbenes are fast reactions which implies that they are exothermic. The thermodynamic driving force can be understood from the fact that while two sigma bonds are being broken, they are strained sigma bonds which are replaced by one sigma and two pi bonds. One pi bond is that of the strong carbonyl double bond. Although the LFP results did not confirm or exclude the formation of oxonium ion or sulfonium ion intermediates, other sulfur ylides from the reactions of sulfides and disulfides with **FL:** have been observed directly by LFP,[152] suggesting that the barrier, if any, for heteroatom transfer from ylide intermediates to products are small. It is possible that heteroatom transfer from oxiranes and thiiranes might occur *via* ylide-like transition states rather than through a persistent ylide intermediate which then fragments.
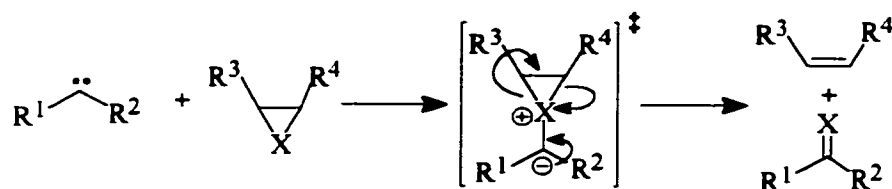
Reactions of ambiphilic and electrophilic carbenes **BCC:, DMC:, CB:**, and **Ad:** with butadiene monoxide may follow oxygen transfer and cyclopropanation pathways, as evidenced by product studies. Therefore, for the reactions of carbenes **BCC:, DMC:, CB:**, and **Ad:** with butadiene monoxide, the observed quenching rate constants represent the sum of both processes. Since oxygen transfer is favored (~3:1) over cyclopropanation, the majority of the quenching of these carbenes must occur *via* the oxygen atom transfer manifold. It is possible therefore that oxygen transfer rates are accelerated relative to those from propylene oxide as a result of increased stabilization of the transition state by the alkene substituent, and also by the additional thermodynamic stability of the butadiene product.

Frontier Molecular Orbital Theory.

Carbene selectivities have been successfully predicted using frontier molecular orbital theory.[14,23] Differential orbital energies ($\Delta\varepsilon_E$ and $\Delta\varepsilon_N$) for oxygen, sulfur, and nitrogen atom transfer reactions from ethylene oxide, ethylene sulfide, and aziridine to phenylchlorocarbene (**PCC:**), methoxyphenylcarbene (**MPC:**), dimethylcarbene (**DMC:**), cyclobutylidene (**CB:**), fluorenylidene (**FL:**), and dimethoxycarbene (**DMOC:**) were calculated at the RHF/6-31+G*//RHF/6-31+G* and the MP2/6-311+G*//MP2/6-311+G* by Professor Tim Gadosy at Concordia using Gaussian 94.[159] The nucleophilic orbital interactions, $\Delta\varepsilon_N$, (N, carbene σ with donor σ* orbital) were calculated to be either dominant for the case of reactions with ethylene oxide, or else equal to the electrophilic

interactions, $\Delta\varepsilon_E$, as is the case for ethylene sulfide and aziridine (E, carbene p orbital with heteroatom donor orbital), Figure II-27. Given the charge distribution in the ylide transition states, it is surprising that the nucleophilic orbital interactions (N) dominate for reactions with ethylene oxide. For a given carbene, the differential orbital energies are lower for sulfur than for oxygen or nitrogen which is consistent with an increase in nucleophilic character for the sulfur-containing heteroatom donors. However, the magnitudes of the differential orbital energies do not reflect the observed rate constants for the carbenes, especially on going from highly electrophilic to more nucleophilic carbenes. If one considers only carbene LUMO-heteroatom donor HOMO interactions ($\Delta\varepsilon_E$, i.e. electrophilic attack) then FMO theory would predict negligible reactivity differences between electrophilic and more nucleophilic carbenes. It is possible that smaller orbital coefficients (carbene LUMO) and favorable electrostatic interactions are responsible for the high rate constants for heteroatom transfer to electrophilic dialkylcarbenes as compared with those to nucleophilic carbenes.
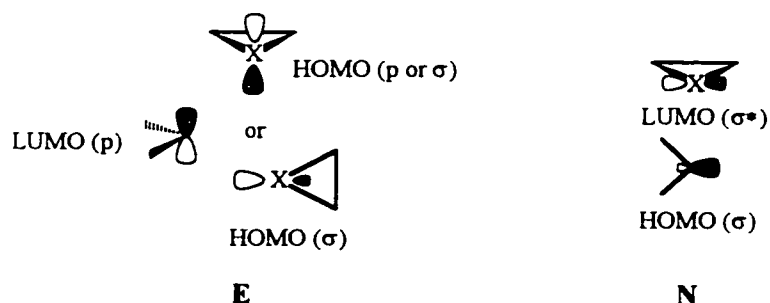
FIGURE II-27. HOMO-LUMO interactions in oxygen and sulfur abstraction reactions between carbenes and oxiranes and thiiranes.

Scheme II-12.
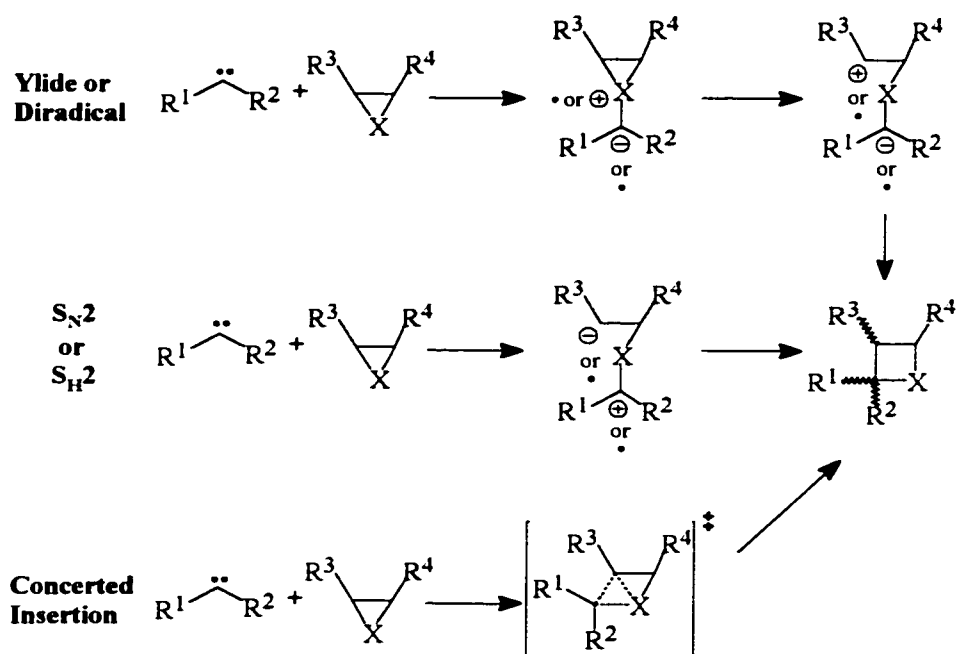
While oxetanes were not observed in the oxygen transfer reactions studied here, they have been reported previously.[126c] For the reaction of carboethoxycarbene with styrene oxide, anionic charge buildup at the carbene carbon as the ylide species is being formed is highly stabilized by the carboethoxy substituent, whereas positive charge buildup at oxygen and at one of the epoxide carbons is also stabilized by the phenyl group. Oxetane formation can occur by either a stepwise mechanism involving the formation of an oxonium ylide which then opens to give a charge separated species (Scheme II-12, upper pathway), a concerted mechanism involving selective cleavage of only one epoxide C-O bond to form a charge separated intermediate (Scheme II-12, middle pathway), or a fully concerted insertion of the carbene into the C-O bond of the epoxide (Scheme II-12, lower pathway). Given that insertion products were not observed in the reactions studied here, it is unlikely that a fully concerted mechanism is responsible for oxetane formation in the case of the reaction of

carboethoxycarbene with styrene oxide. The intermediacy of a charge separated zwitterionic intermediate *via* a selective ring opening seems more likely.

II.4.8. Carbene Philicity and Heteroatom Transfer: Linear Free Energy Relationships.

The reactivities of carbene intermediates may be predicted based on Moss' carbene selectivity scale m_{CXY}.[14, 160] Values for m_{CXY} can be determined empirically based on selectivities of carbenes towards olefins or they can be predicted using σ_R^- and σ_I which relate the degree of resonance interactions and the inductive effects between a substituent and the carbene carbon to the carbene's reactivity. The expression which relates σ_R^- and σ_I to m_{CXY} is in chapter 1, eq 5.

Values for m_{CXY} were calculated for all of the carbenes in Table II-7 using eq II-20.[14] Least-squares fitting of log k_X vs. m_{CXY}^{calcd} to the equation for a straight line, for the rate constants for sulfur atom transfer from propylene sulfide to the carbenes studied, gave a slope of -4.2, with R = 0.96. A similar slope was found for the least squares fitting of log k_X vs. m_{CXY}^{calcd} for the rate constants for oxygen atom transfer from propylene oxide, Figure II-28.

The linear free energy relationship between the barriers for heteroatom transfer and calculated m_{CXY} values indicates that the reaction is sensitive to carbene philicity and that electrophilic carbenes will undergo heteroatom transfer more readily than their nucleophilic counterparts.[82] For the reaction of dimethoxycarbene (**DMOC:**) with oxiranes and thiiranes, high yields of carbene dimer imply that the rate constants for oxygen and sulfur atom transfer are several orders of magnitude lower than those for more electrophilic carbenes. Carbene **II-5b**, considered to be an "archetypal" nucleophilic carbene, has a lifetime of ~2 ms in dilute solution at ambient temperatures with dimerization being the main pathway by which it is consumed.[31] That lifetime must depend on carbene concentration (the

reaction is bimolecular) and is expected to be shorter at 110 than at 22 °C. Nevertheless, a strong

preference for this carbene to undergo dimerization over heteroatom transfer is in keeping with small

rate constants for reaction of carbenes of similar structure with pyridine. Extrapolation of the line in

Figure II-28 gives a predicted rate constant for the reaction of dimethoxycarbene with propylene

sulfide of ~ 2.6×10^1 M^{-1} s^{-1}, a value too small to be confirmed by LFP techniques but large enough to

lead to heteroatom transfer if the steady state concentration of carbene is low enough.
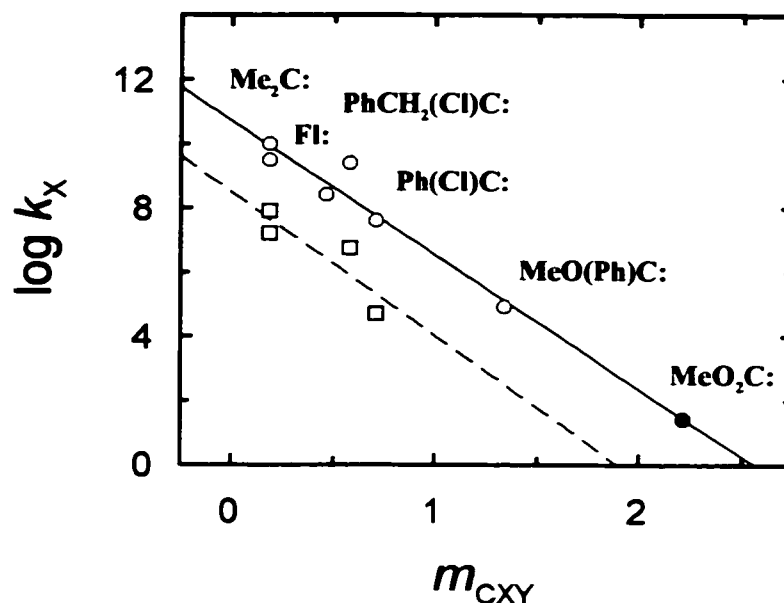
Figure II-28. Plots of log k_X vs. m_{CXY} for the abstraction of oxygen atoms from propylene oxide (open squares) and for sulfur atoms from propylene sulfide (open circles). The closed circle is an extrapolated point for the reaction of dimethoxycarbene with propylene sulfide.

Linear least-squares fitting of log k_X vs. log k_{pyr} for sulfur atom transfer from propylene sulfide gave

a straight line with slope 0.9 for sulfur atom transfer from propylene sulfide, and a slope of 0.2 for

oxygen atom transfer from propylene oxide (Figure II-29). These correlations are consistent with the

mechanistic interpretation that heteroatom transfer occurs from the singlet states of carbenes and by

electrophilic attack of the carbene carbon onto the heteroatom lone pair of the donor towards either

an ylide intermediate or a transition state that is ylide-like. Linear least-squares fitting of log k_X for

the reactions with propylene sulfide vs. log k_X for the reactions with propylene oxide gave a straight

line with a slope of 1.3 with R = 0.99 suggesting that both heteroatoms are abstracted by the same mechanism.
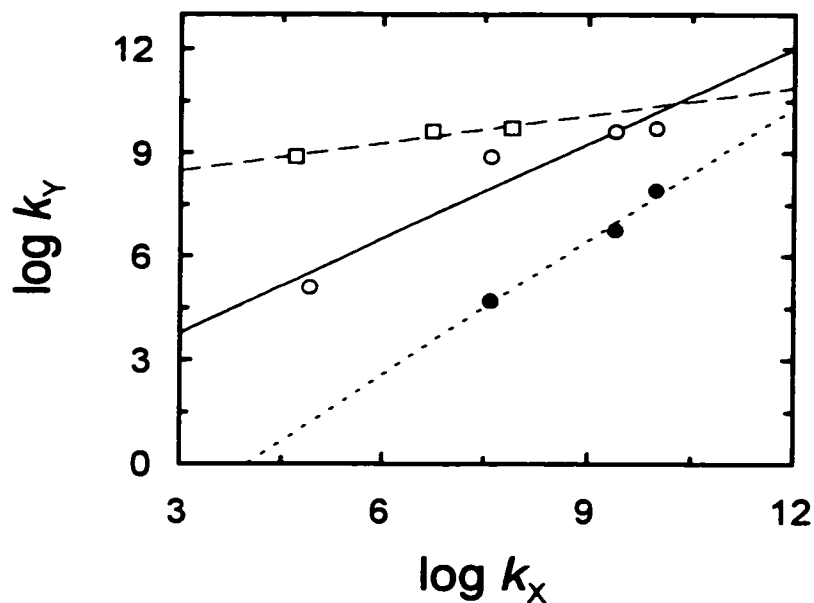
Figure II-29. Plots of log k_X vs. log k_Y. The open circles are log k_X (propylene sulfide) vs. log k_{pyr} data and the solid line represents the linear least-squares fit. Open squares are log k_X (propylene oxide) vs. log k_{pyr} data and the dashed line is the linear least-squares fit. The filled circles are log k_X (propylene sulfide) vs. log k_X (propylene oxide) data and the dotted line is the linear least-squares fit.

II.4.9. Conclusions.

Absolute rate constants for heteroatom transfer from propylene oxide and propylene sulfide to carbenes **DMC:**, **CB:**, **Ad:**, **BCC:**, **PCC:**, and **MPC:** measured here range from 10^4-10^{10} M^{-1} s^{-1} at 22 °C and appear to obey linear free energy relationships with respect to the carbene philicity parameter m_{CXY}. Electrophilic carbenes, such as singlet dimethylcarbene (**DMC:**), cyclobutylidene (**CB:**), and adamantylidene (**Ad:**) are more reactive towards heteroatom abstraction whereas ambiphilic carbenes, exemplified by phenylchlorocarbene (**PCC:**) and methoxyphenylcarbene (**MPC:**), are less reactive. Dimethoxycarbene, considered to be nucleophilic in character, is much less reactive toward propylene sulfide and cyclohexene oxide than the electrophilic/ambiphilic carbenes above. Although absolute rate constants are not known, the fact that tetramethoxyethylene was the

major product in each case (at 110 °C, [trap]= 0.1M) strongly suggests that encounters between dimethoxycarbene and those substrates do not generally result in reaction. Ylides from the reaction of carbenes with oxiranes and thiiranes were not observed by LFP methods. Benzylchlorocarbene also abstracts the oxygen atom from DMSO and from pyridine-N-oxide with rate constants exceeding 10^9 $M^{-1}s^{-1}$ at 22 °C.

Chapter 3.

Intra- and Intermolecular Reactions of Dioxycarbenes

Generated by Thermolysis of Oxadiazolines.

III. General Introduction.

This chapter describes results involving methoxytriphenylsiloxycarbene (**MSC:**) and dimethoxycarbene (**DMOC:**) generated by thermal decompositions of their corresponding oxadiazoline precursors **III-1a** and **b** according to the general scheme below (Scheme III-1).

Scheme III-1.
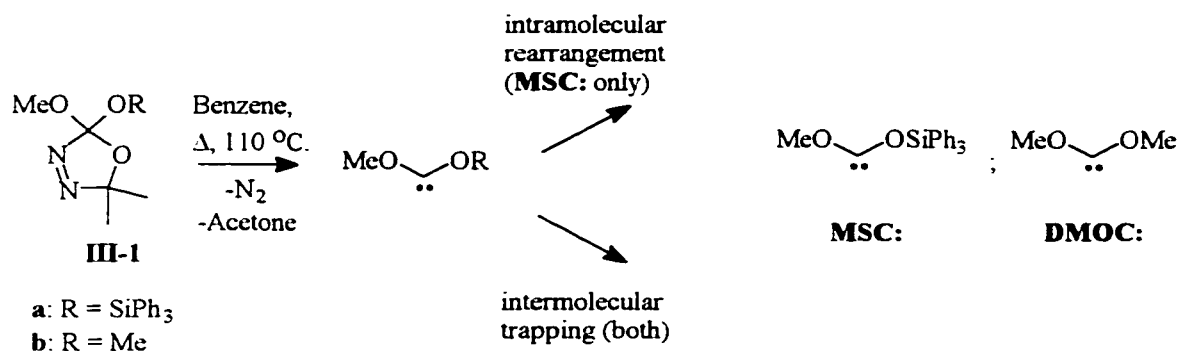
The first section of this chapter involves the study of competitive intramolecular 1,2-Si migration and decarbonylation within methoxytriphenylsiloxycarbene (**MSC:**) as well as the intermolecular trapping of **MSC:** with alcohols such as methanol. The second section details this author's contribution to a collaborative effort with J. Dunn and Professor M. J. McGlinchey involving the investigation of reactions of dimethoxycarbene (**DMOC:**) with polychlorinated olefins.

Chapter 3. Section 1.

1,2-Silicon Migration and Decarbonylation in Methoxytriphenylsiloxycarbene.

III.1. Introduction.

Photochemical or thermal "Brook rearrangements" in acylsilanes are known to give rise to siloxycarbenes.[47,48] Most, if not all, studies reported in the literature thus far have involved the generation of alkylsiloxy- or arylsiloxycarbenes. The generation of alkoxysiloxycarbenes *via* this route are, as far as this author is aware, unknown. A long time ago, Brook and co-workers did report the synthesis of silyl formates **III-3** and found that, upon heating, they extrude carbon monoxide giving silyl ethers as products by a proposed three-membered ring intermediate (eq III-1).[161] Alkoxysiloxycarbenes were not implicated in the thermal chemistry of **III-3**.

$$\left[\begin{array}{c} \overset{O}{\underset{R'}{\overset{\|}{\diagdown}}} \overset{\oplus}{O} \overset{\ominus}{\underset{R}{\overset{\diagup}{Si}}} \overset{R}{\underset{R}{\diagdown}} \end{array} \right]$$

$$\underset{R'O}{\overset{O}{\overset{\|}{\diagdown}}} SiR_3 \quad \overset{\Delta}{\longrightarrow} \quad R'OSiR_3 \; + \; CO$$

III-3 **III-4** (III-1)
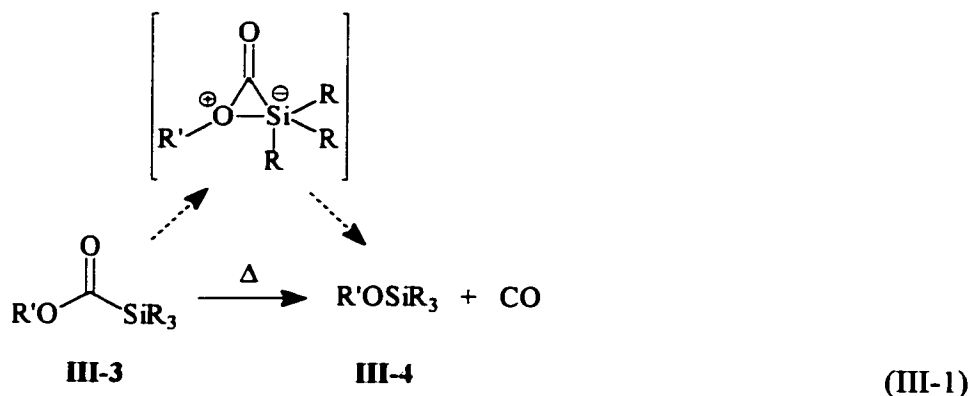
Since oxadiazolines are now an established route to dioxycarbenes, we sought to prepare alkoxysiloxycarbenes using the oxadiazoline approach to provide an alternative and complimentary method to the "Brook rearrangement" for studying such carbenes. The special properties of silyl moieties in carbene chemistry that have emerged recently,[162] including the migration of trimethylsilyl in a cyclopropylidene to the carbene site, to the exclusion of allene formation,[163] eq III-2, led us to attempt the generation of methoxytriphenylsiloxycarbene (MeO(Ph₃SiO)C:) by the oxadiazoline route.

(III-2)
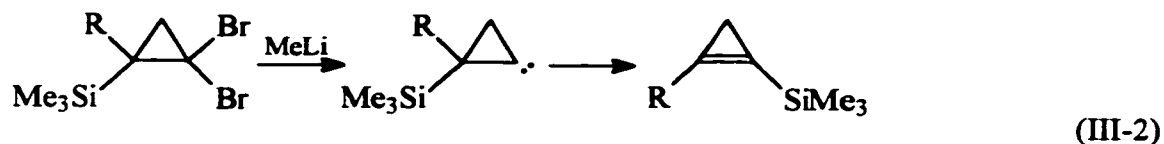
In addition, we were interested in generating alkoxysiloxycarbenes in order to study their general intermolecular reactivity. Such carbenes might be more nucleophilic than their dialkoxycarbene counterparts as a result of the electropositive nature of silicon and as a result of hyperconjugative resonance contributors such as the one illustrated below. Also, adducts of these carbenes could potentially be converted to ketones under mild conditions with fluoride ions.
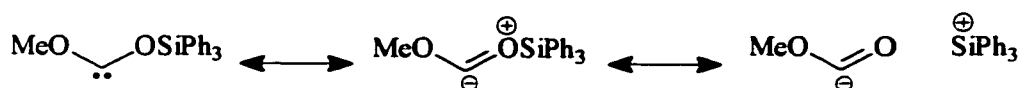
III.1.a. Preparation of 2-Methoxy-5,5-dimethyl -2-triphenylsiloxy-Δ³-1,3,4-oxadiazoline (III-1a).

2-Acetoxy-2-methoxy-5,5-dimethyl-Δ³-1,3,4-oxadiazoline (**III-1c**) was prepared by oxidative cyclization of the carbomethoxyhydrazone of acetone with lead tetraacetate according to a literature procedure (eq III-3). Treatment of **III-1c** with triphenysilanol in the presence of catalytic trifluoroacetic acid afforded 2-methoxy-5,5-dimethyl-2-triphenylsiloxy-Δ³-1,3,4-oxadiazoline (**III-1a**), *via* the oxadiazoline exchange route, in ~33 % yield (eq III-3). Oxadiazoline **III-1a** was then purified by chromatography on silica.

(III-3)
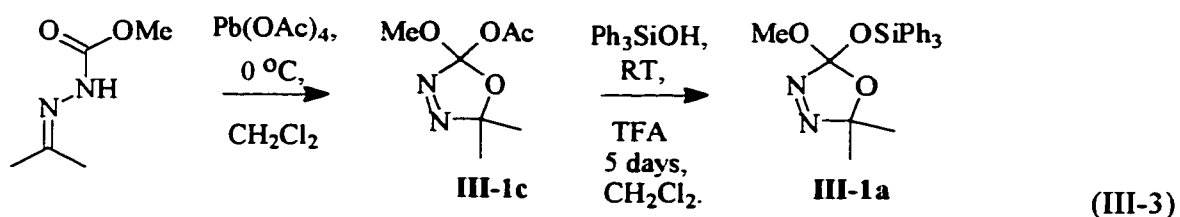
Other methods, such as that outlined in eq III-4, for preparing oxadiazoline precursors to alkoxysiloxycarbenes failed, presumably as a result of the instability of anion III-1d (eq III-4).
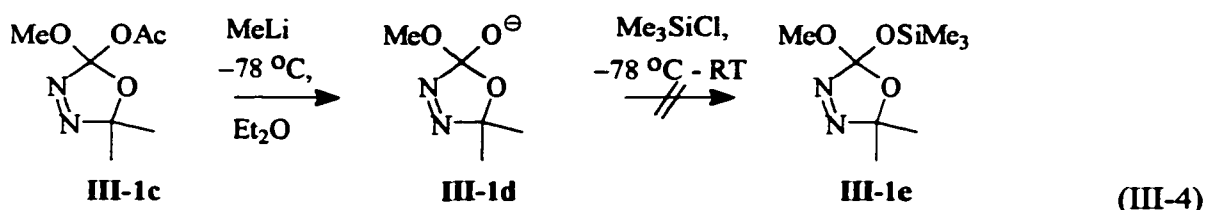
III.1.b. Thermolysis of Oxadiazoline III-1a :Generation of Methoxytriphenylsiloxycarbene (MSC:).

Oxadiazoline III-1a was heated in degassed benzene for 24 hours at 110 °C, in a sealed tube. Major products were acetone, methyl triphenylsilyl formate (III-3), and methyl triphenylsilyl ether (III-4), with III-3 : III-4 = 1 : 3 (together 90%) (eq III-5). Isolation of III-3, and heating of a solution of pure III-3 in benzene (150 °C, 24 hr., sealed tube) converted it cleanly to methyl triphenylsilyl ether (III-4), as reported in 1955 by Brook and coworkers.[161]

$$(III-5)$$
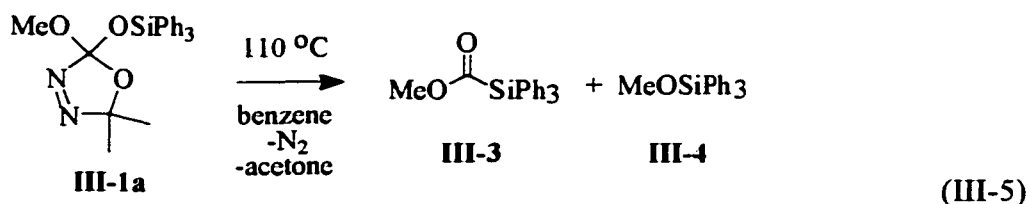
One possible interpretation of this result is that oxadiazoline III-1a undergoes cycloreversion with loss of N_2 and loss of acetone to give methoxytriphenylsiloxycarbene (MSC:) which then undergoes rapid 1,2-Si migration to give methyl triphenylsilyl formate (III-3). Formate III-3 then undergoes thermal elimination of CO through a non-carbene pathway involving a cyclic intermediate as previously postulated. In order for such a scenario to account for the observed ratio of products, however, the thermolysis rate constant for III-3 must be smaller than that for oxadiazoline III-1a but

large enough to lead to a 1:3 ratio of **III-3**:**III-4** after 24 hours of thermolysis. If the thermolysis rate

constants for **III-1a** and **III-3** are not equal then the ratio of **III-3**:**III-4** should change as a function

of thermolysis time. Therefore the thermolysis rate constants for both **III-1a** and **III-3** were

measured.

Thermolysis of 5,5-Dimethyl-2-methoxy-2-triphenylsiloxy-Δ^3-1,3,4-oxadiazoline (**III-1a**) at 110 °C

in a sealed NMR tube was performed and the progress of the reaction was monitored by ^{1}H-NMR.

The thermolysis rate constant was determined to be 8.1 x 10^{-5} s^{-1} for this oxadiazoline at 110 °C by

comparing the signal at δ 1.47 with that of internal standard p-xylene. A log plot of the normalized

data is in Figure III-1.
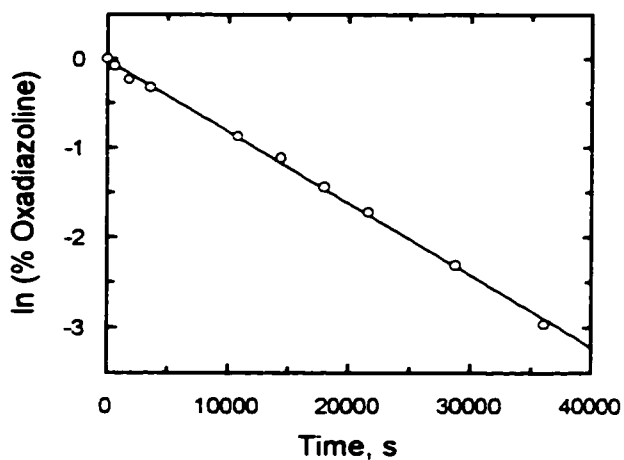
Figure III-1. Extent of thermolysis of oxadiazoline **III-1a** at 110 °C in benzene with the progress
of the reaction monitored by ^{1}H-NMR.

It was also found that the ratio of methyl triphenylsilyl ether (**III-4**) to methyl triphenylsilyl

formate (**III-3**) did not change significantly over the course of the thermolysis which is inconsistent

with formation of **III-4** from oxadiazoline **III-1a** *via* **III-3**, Figure III-2. The thermolysis rate constant

for methyl triphenylsilyl formate was measured independently in benzene in a sealed NMR tube by ^{1}H-

NMR by following the singlet at δ 3.37 (C_6D_6) and comparing the integrations of that signal to that

of internal standard p-xylene. A plot of the log of the data vs. time is in Figure III-3.
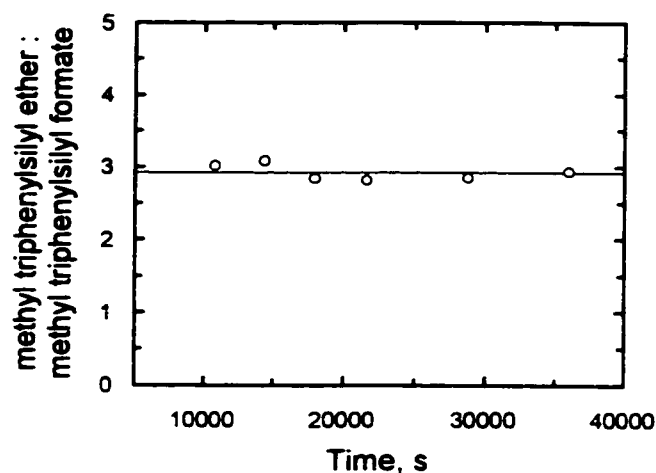
Figure III-2. Ratios of methyl triphenylsilyl ether (**III-4**) : methyl triphenylsilyl formate (**III-3**) during the thermolysis of 5,5-dimethyl-2-methoxy-2-triphenylsiloxy-Δ^3-1,3,4-oxadiazoline at 110 °C in benzene. The progress of the reaction was monitored by ^{1}H-NMR.
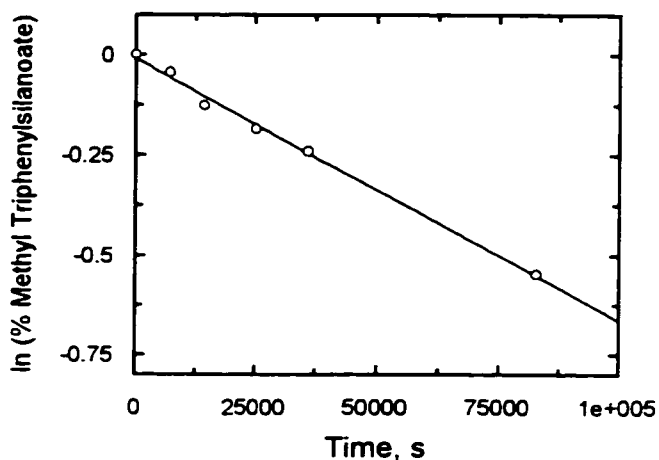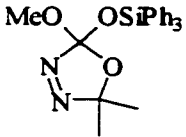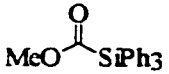
Figure III-3. Extent of Methyl Triphenylsilanoate Thermolysis at 110 °C in Benzene with the Progress of the Reaction Monitored by ^{1}H-NMR.

We found that the rate constant for the conversion of methyl triphenylsilyl formate (**III-3**) to

methyl triphenylsilyl ether (**III-4**) at 110 °C was only 6.5 x 10^{-6} s^{-1}; too small to account for the

formation of **III-4** from oxadiazoline **III-1a** via **III-3** (Table III-1).

Table III-1. Thermolysis Rate Constants Determined by ^{1}H-NMR spectroscopy.

Precursor	Solvent	Thermolysis Rate Constant (110 °C)
MeO OSiPh$_3$ (III-1a)	Benzene	$k_{obs} = 8.1 \times 10^{-5} \text{ s}^{-1}$
	Methanol	$k_{obs} = 6.1 \times 10^{-5} \text{ s}^{-1}$
MeO SiPh$_3$ (III-3)	Benzene	$k_{obs} = 6.5 \times 10^{-6} \text{ s}^{-1}$
	Methanol	$k_{obs} = 8.2 \times 10^{-4} \text{ s}^{-1}$

The thermolysis rate constant data suggest that both methyl triphenylsilyl formate (**III-3**) and methyl triphenylsilyl ether (**III-4**) are derived from methoxytriphenylsiloxycarbene (**MSC:**) with the former being the result of a 1,2-Si migration in **MSC:** and the latter arising by an unknown mechanism.

It is well established that other metallo formates, containing Sn, Se, or Te can undergo thermal or photochemical M-C bond homolysis to give acyl radical/metal radical pairs.[164] Acyl radicals then can undergo either decarboxylation or decarbonylation (eq III-6).

$$\text{M = Se, Sn, or Te}$$

(III-6)
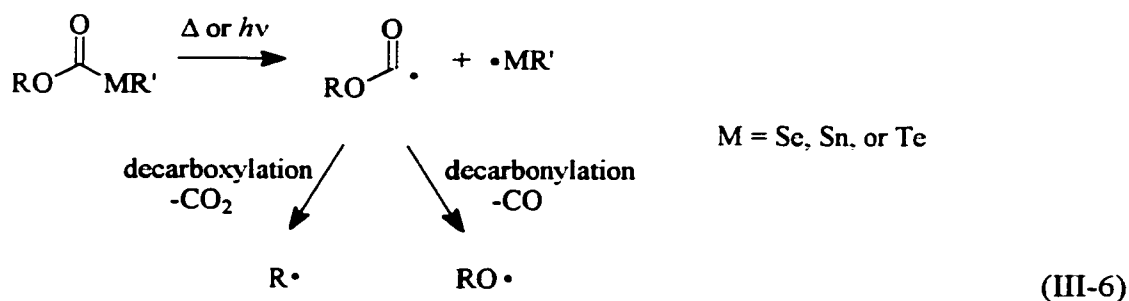
Also, Venneri and Warkentin have recently reported the first clear cases of thermal fragmentation of acyclic dialkoxycarbenes in solution, to radical pairs consisting of methoxycarbonyl and allylic radicals, eq III-7, in which both the carbenes and the radicals could be trapped.[165]

MeO $\overset{\cdot\cdot}{\underset{}{}}$O $\overset{}{\underset{R}{}}$R' ⟶ MeO $\overset{}{\underset{\cdot}{}}$O + $\cdot$ $\overset{}{\underset{R}{}}$R' ⟶ MeO $\overset{O}{\overset{\|}{C}}\overset{}{\underset{R}{}}$R'

R=Ph, R'=H; or R=H, R'=Ph

+

MeO $\overset{O}{\overset{\|}{C}}\overset{}{\underset{R'}{}}$R

(III-7)
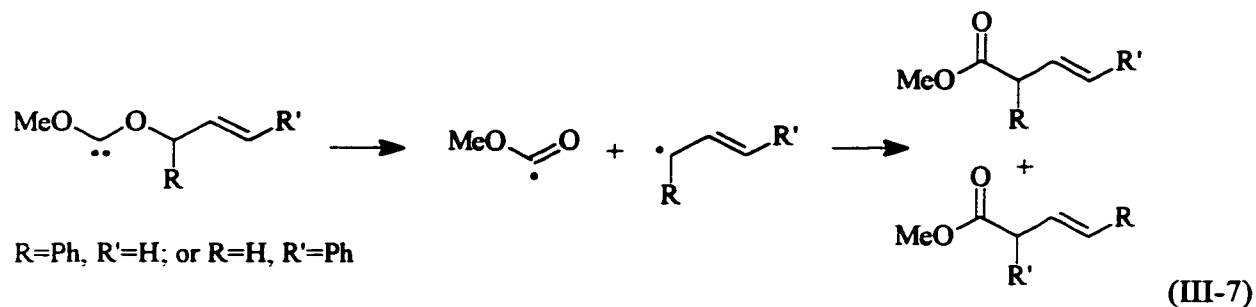
In order to test whether radicals are generated in the themolysis of **III-1a**, oxadiazoline **III-1a** was heated in toluene and, in a separate experiment, in benzene in the presence of added stable free radical TEMPO. It was found that thermolyses in toluene did not afford bibenzyl and added stable free radical, TEMPO, did not lead to any detectable products of radical trapping. It is likely, then, that radical intermediates are not involved in the formation of either **III-3** or **III-4**.

$$MeO \overset{O}{\overset{\|}{C}} SiPh_3$$

III-3

$$MeO \overset{O}{\overset{\|}{C}} \cdot \;+\; \cdot SiPh_3$$

MeO OSiPh₃ (N=N ring structure)

III-1a

MeO OSiPh₃

MSC:
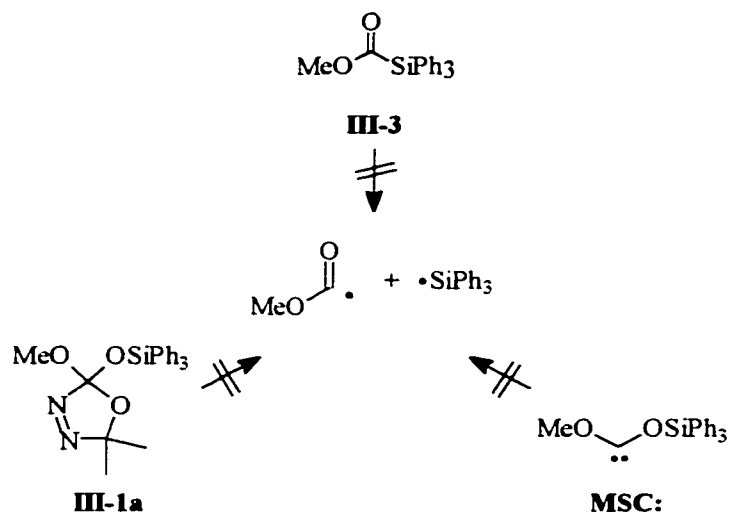
Decarbonylation within carbene **MSC:** is also reminiscent of the rearrangement of alkoxyhalocarbenes, which do so by fragmentation to carbon monoxide, carbocation, and halide ion (eq III-8).

$$X \diagdown OR \longrightarrow \left[X^{\ominus} \overset{\overset{\displaystyle O}{\parallel}}{C} \; {}^{\oplus}R \right] \longrightarrow RX + CO$$

$$(III-8)$$
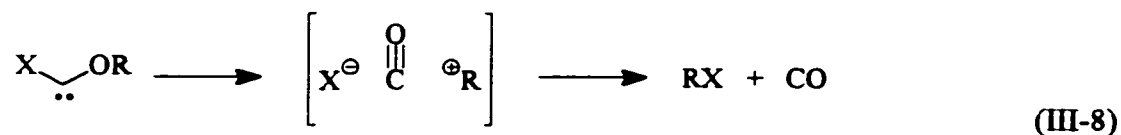
The latter then combine, in the absence of carbocation scavengers, to afford alkyl halide in high yield.[166] An analogous process in case of **MSC:** is unlikely because it would require formation of the triphenylsilyl cation/ methoxide anion pair (eq III-9) in benzene.

$$\underset{\textbf{MSC:}}{MeO \diagdown OSiPh_3} \longrightarrow \left[MeO^{\ominus} \overset{\overset{\displaystyle O}{\parallel}}{C} \; {}^{\oplus}SiPh_3 \right] \longrightarrow \underset{\textbf{III-4}}{MeOSiPh_3}$$

$$(III-9)$$
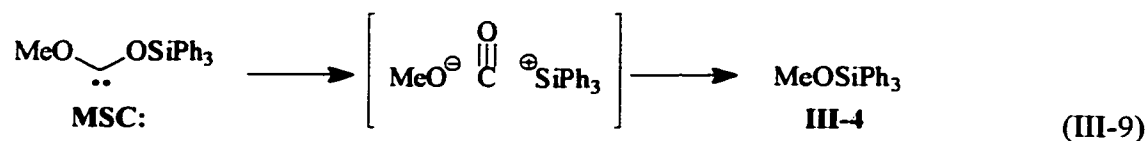
The greater basicity of methoxide ions, compared to halide ions, makes that mechanism unlikely. Moreover, such a mechanism fails to account for **III-3**.

III.1.c. Trapping of Methoxytriphenylsiloxycarbene (MSC:).

Thermolysis of **III-1a** in methanol-d_4 did afford orthoformate **III-5**, as indicated by the ²H-NMR spectrum, which showed both the expected OCD_3 and the orthoformyl CD signals (C_6H_6, δ= 3.19 and 6.93, respectively). However, the yield was low (~8 %) and ether **III-4** was a co-product. Thermolysis of **III-3** in CD_3OD at 110 °C also afforded **III-5**, again in low yield, eq III-10. Thus, rearrangement of the carbene intermediate must be fast relative to trapping with methanol, which we assume occurs with a bimolecular rate constant of *ca.* 1 x 10⁵ M⁻¹ s⁻¹(see Ch. 4); the measured rate constant for trapping dimethoxycarbene. Larger rate constants for OH insertion reactions of alkylsiloxycarbenes have been measured[167] ($k_{ROH} \sim 10^7 - 10^9$ M⁻¹ s⁻¹) but those carbenes, with only one oxygen atom directly bonded to the carbene center, are expected to be more reactive (see next chapter for a more detailed explanation).

$$
\begin{array}{c}
\underset{\text{III-3}}{\text{MeO}\overset{\overset{\displaystyle O}{\|}}{\diagdown}\text{SiPh}_3}
\end{array}
$$

$$
\text{III-1a} \longrightarrow \blacktriangleright \longrightarrow \underset{\textbf{MSC:}}{\text{MeO}\diagdown\diagup\text{OSiPh}_3} \xrightarrow[\text{110 °C}]{\text{CD}_3\text{OD}} \underset{\textbf{III-5}}{\text{Ph}_3\text{SiO}\overset{\text{MeO}}{\underset{\text{D}}{\diagup\!\!\diagdown}}\text{OCD}_3} \qquad \text{(III-10)}
$$
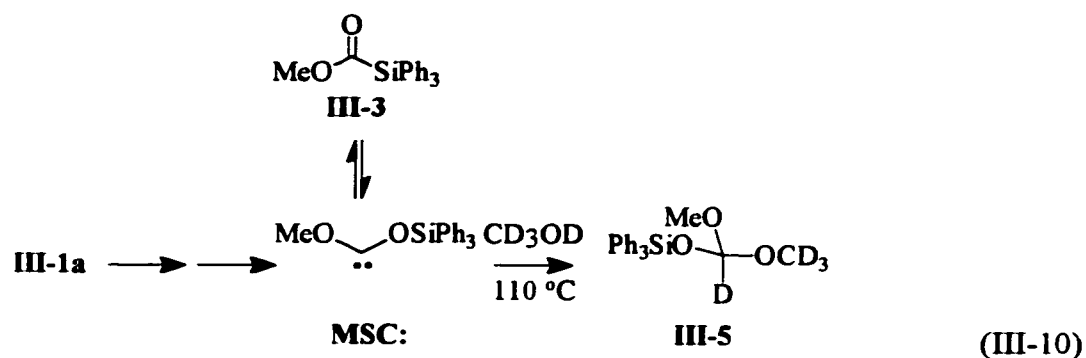
Significantly, no crossover products involving the capture of triphenylsilyl cations by methanol-d_4 were observed, suggesting that the inert molecule separated ion pair in eq III-9 is not formed. Trapping of **MSC:** was also attempted with *p*-cresol, a more acidic carbene trap, was unsuccessful, probably because the oxadiazoline underwent acid catalyzed decomposition in the presence of *p*-cresol.

The thermolysis rate constant of oxadiazoline **III-1a** and the thermolysis rate constant of ester **III-3** were also determined in methanol-d_4, in separate experiments as described earlier, by monitoring the resonance at δ 3.18 ppm, and δ 3.73 ppm, respectively. The thermolysis rate constants are summarized in Table III-1. Although the thermolysis rate constant for oxadiazoline **III-1a** does not change dramatically in more polar solvents, the rate constant for conversion of **III-3** to **III-4** was 126-fold larger in methanol than in benzene (Table III-1) suggesting that this process occurs through a polar transition state.

III.1.d. Proposed Mechanisms for 1,2 Si Migration and Decarbonylation within MSC:.

The most straightforward interpretation of these results involves thermal cycloreversion of **III-1a**, to generate nitrogen gas and a carbonyl ylide, as in Scheme III-2. The ylide fragments rapidly to acetone and **MSC:**,[168] and the latter rearranges by migration of the triphenylsilyl group from oxygen to carbon.

Scheme III-2.
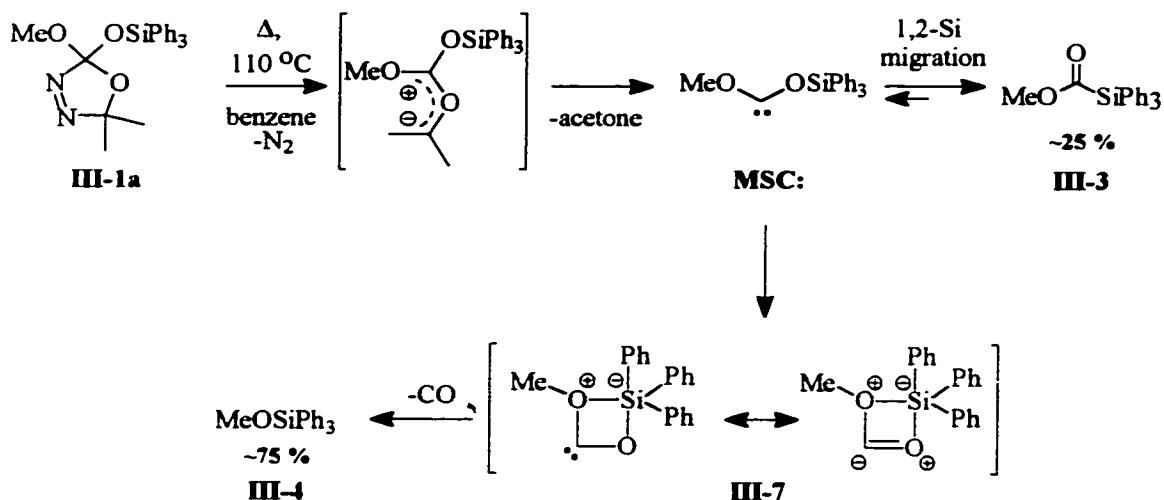
There are several reported cases of migrations of alkyl groups from oxygen to carbon of dialkoxycarbenes in the gas phase, where the migrating group develops negative charge during its migration, as inferred from the migration of 2,2,2-trifluoroethyl in preference to methyl or ethyl.[169] Those dialkoxycarbenes do not rearrange appreciably in solution, however, suggesting that triphenylsilyl is a better migrating group than trifluoroethyl. A concerted mechanism is proposed in which the Ph₃Si group migrates from O to C through a transition state in which the silicon atom has been attacked by the carbene's unshared electron pair and has become pentacoordinate, with some negative charge, rather than a "hydride-like" migration of silicon into the empty p-orbital of the carbene carbon. Nucleophilic attack at silicon to generate pentacoordinate silyl intermediates or transition states such as **III-6** are well known[170] and, because dialkoxycarbenes are nucleophiles,[14a,b] **III-6** is an appropriate model. The fact that carbene dimers were not obtained implies that rearrangement of **MSC:** to **III-3** is fast.
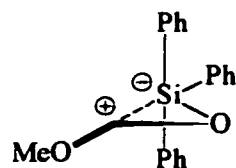
III-6

The mechanism by which the carbene and the ester are decarbonylated is more complex, Scheme III-2. We propose that the ester is decarbonylated *via* the carbene,[171] which cyclizes to afford the 4-membered intermediate **III-7** by attack of the silophilic methoxy oxygen at silicon. This mechanism is supported by the fact that both **III-1a** and **III-3** gave the same product from apparent trapping of MSC: with CD_3OD. Moreover, the conversion of ester **III-3** to ether **III-4** is more than 10 fold slower than thermolysis of **III-1a** in benzene, but **III-1a** gives rise to **III-3** and **III-4** in a 1:3 ratio. Scheme III-2 accounts for this if decarbonylation (**MSC:** → **III-4**) is faster than rearrangement (**MSC:** → **III-3**).

The Brook rearrangement of methyl triphenylsilylformate (**III-3**) to methyl triphenylsilyl ether (**III-4**) and CO, was never firmly connected to the intermediacy of methoxy(triphenylsiloxy)carbene, because that carbene had never been generated independently. The results described above indicate that ester **III-3** must pass through **MSC:**, and that ester and carbene are equilibrated thermally at ≥ 110 °C. This discovery has large implications for the thermal generation of other carbenes by rearrangements of silyl analogues. It may also be possible to design systems with other double bonds, such as C=N, that will rearrange similarly (i.e. diaminocarbenes, $R_2NC(=NR)SiR_3$ → $R_2N(NRSiR_3)C$: and alkoxyaminocarbenes, $ROC(=NR)SiR3$ → $RO(NRSiR_3)C$:, or $R_2NC(=O)SiR3$ → $R_2N(OSiR_3)C$:).

Also, the proposed mechanism by which carbene **MSC:** decarbonylates (Scheme III-2) is novel. It has been shown that a polar solvent enhances the rate of decarbonylation of methyl

triphenylsilylformate and it is postulated that decarbonylation occurs from a 4-membered ring that is itself a dialkoxycarbene, except that one of the oxygens is actually at the oxonium oxidation state.

Chapter 3. Section 2.

Reactions of Dimethoxycarbene with Polychlorinated Olefins and Ketones.

III.2. Introduction.

This section describes the intermolecular chemistry of dimethoxycarbene (**DMOC:**), generated thermally from oxadiazoline **III-1b** (Scheme III-1), with polychlorinated substrates. The solution chemistry of **DMOC:** has been studied previously and has shown that **DMOC:** prefers to react with electron deficient olefins, such as dimethylfumarate, dimethylmaleate,[172] and styrene,[173] as well as strained olefins[53c] over more electron rich olefins such as tetramethylethylene,[14,174] in keeping with its nucleophilic character. Dimethoxycarbene (**DMOC:**) also undergoes conjugate [1+4]cycloadditions with tetraphenylcyclopentadienone (eq III-11),[175] with tropone (eq III-12),[175] and with tetrazines.[176] Such conjugate additions may occur by concerted mechanisms or by stepwise additions.

(III-11)

(III-12)
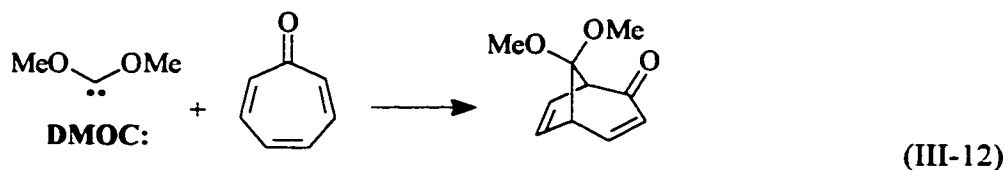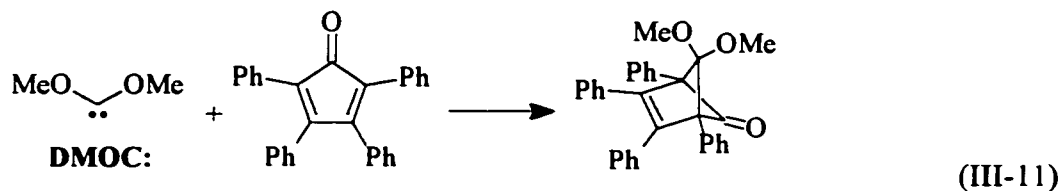
Dimethoxycarbene (**DMOC:**) also adds to electron deficient alkynes such as dimethyl acetylenedicarboxylate (DMAD)[177] giving intermediate dioxyvinylcarbenes either directly or by thermal ring opening of cyclopropenone ketals from [1+2]cycloaddition (eq III-13). The synthetic

utility of reactions involving the thermal ring opening of cyclopropenone ketals, has been demonstrated in the construction of complex products including the natural product colchicine as well as its analogues, *via* Boger cycloadditions.[178, 179, 180]

Colchicine

(III-13)
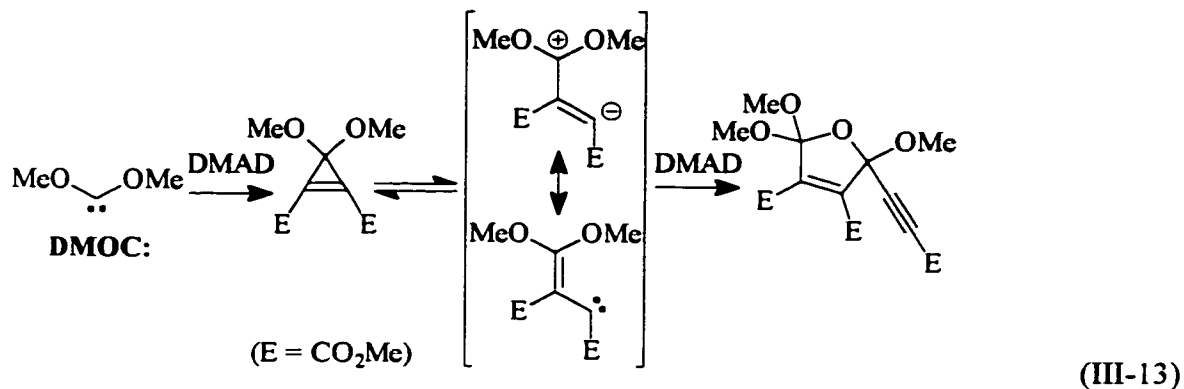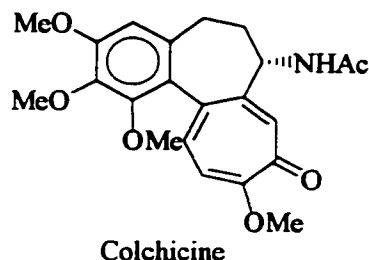
In fact, dipolar intermediates in reactions involving nucleophilic attack by dimethoxycarbene are commonly inplicated. Thermal reactions of **DMOC:** with either aryl isocyanates (ArNCO) or aryl isothiocyanates (ArNCS) yield 5,5-dimethoxyhydantoins or 5,5-(dimethoxythio)hydantoins, respectively.[181] The proposed mechanism for the formation of these products involves the nucleophilic attack of **2** onto the central carbon atom of the isocyanate or isothiocyanate to give a dipolar intermediate (eq III-14) which then reacts with a second molecule of ArNCO or ArNCS.

$$
\text{MeO} \underset{\overset{\cdot\cdot}{}}{\diagup} \text{OMe} \quad + \quad \underset{\underset{R}{\diagdown}{N}}{\overset{\overset{X}{\parallel}}{\underset{\parallel}{C}}} \quad \longrightarrow \quad \left[\begin{array}{c} \text{MeO} \overset{\oplus}{\diagdown}{\diagup} \text{OMe} \\ \overset{\ominus}{N} \diagdown X \\ \underset{R}{} \end{array} \right]
$$

DMOC: X = O, S   (III-14)
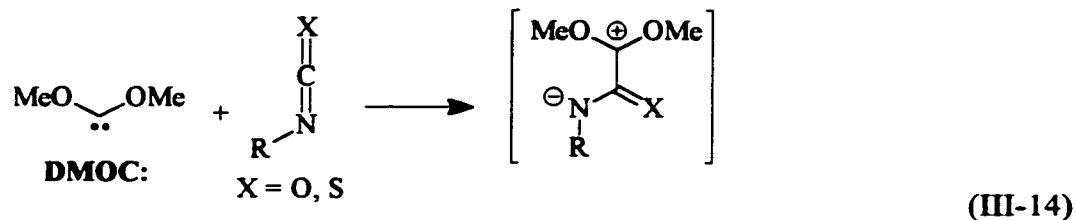
A Hammett plot, constructed from the results of competition experiments involving aryl isocyanates,[182] gave a ρ value of +2.0 which is consistent with the proposed mechanism. Reactions of dimethoxycarbene (**DMOC:**) with vinylisocyanates have been used for the construction of highly functionalized pyrrolinones *via* formal [1+4] cycloadditions.[183]

$$
\text{MeO} \underset{\overset{\cdot\cdot}{}}{\diagup} \text{OMe} \quad + \quad \underset{\underset{R^2}{\diagdown}{R^1}}{\overset{\overset{O}{\diagup}{C}}{\diagdown}{N}} \quad \longrightarrow \quad \cdots \quad \longrightarrow \quad \cdots
$$

III-2b   (III-15)
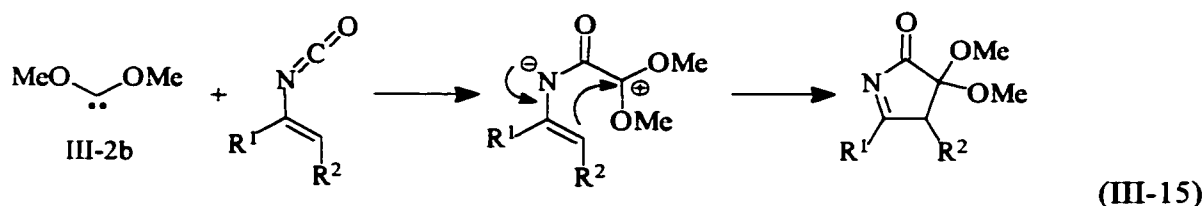
This methodology is currently being used for the preparation of the natural product tazettine as well as functional analogues.[183]
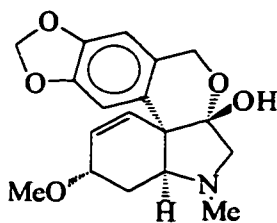
Tazettine

Dimethoxycarbene (**DMOC:**) has also been shown to attack 2,4-dinitro-fluorobenzene and hexafluorobenzene, by nucleophilic aromatic substitution, to afford acetals of aroyl fluorides.[184] Understanding the reactivity patterns of **DMOC:** not only expands our understanding of the innate properties of a typical nucleophilic carbene but also expands its synthetic utility as a masked carbonyl equivalent.

MeO OMe C_6F_6 → structure → structure (III-16)

DMOC:
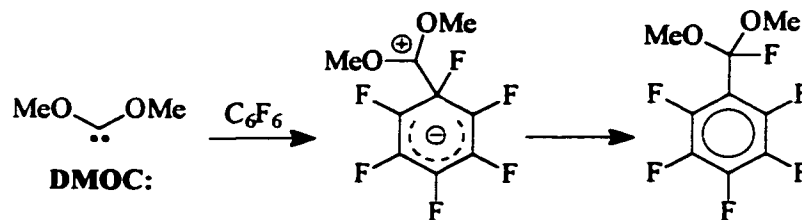
III-2a. Reaction of 2b with hexachlorocyclopentadiene (III-8).

Thermolysis of oxadiazoline **III-1b** at 110 °C in benzene containing hexachlorocyclopentadiene (**III-8**) at an initial concentration of 0.1 M (1.1 equivalents relative to **III-1b**) afforded products **III-12**, **III-14**, and **III-16** (Scheme III-3) which were isolated by radial chromatography in 24, 29, and 34 % yield, respectively. Hexachlorocyclopentadiene (**III-8**) was also recovered from the reaction. The GC-MS analysis of the thermolysis mixture prior to chromatography revealed that products **III-12**, III-14, and **III-16** were formed in 1.2:1.8:1 ratios. Other minor products were detected by GC-MS; integration of the GC trace revealed that they were formed in sufficiently low quantities relative to III-12, **III-14**, and **III-16** to preclude their isolation and characterization. However, the GC-MS analysis indicated that the minor products were isomers of **III-14**, and **III-16**. Surprisingly, we did not observe any products with molecular weights corresponding to [1+2] or [1+4] cycloaddition adducts, and none of the minor products were of higher molecular weight than that of **III-16**. Since the location of the ester substituents in the isolated products, **III-14** and **III-16**, could not be assigned unambiguously by conventional spectroscopic techniques their structures were determined by X-ray crystallography, as shown in Figures III-4, and III-5.

Scheme III-3.
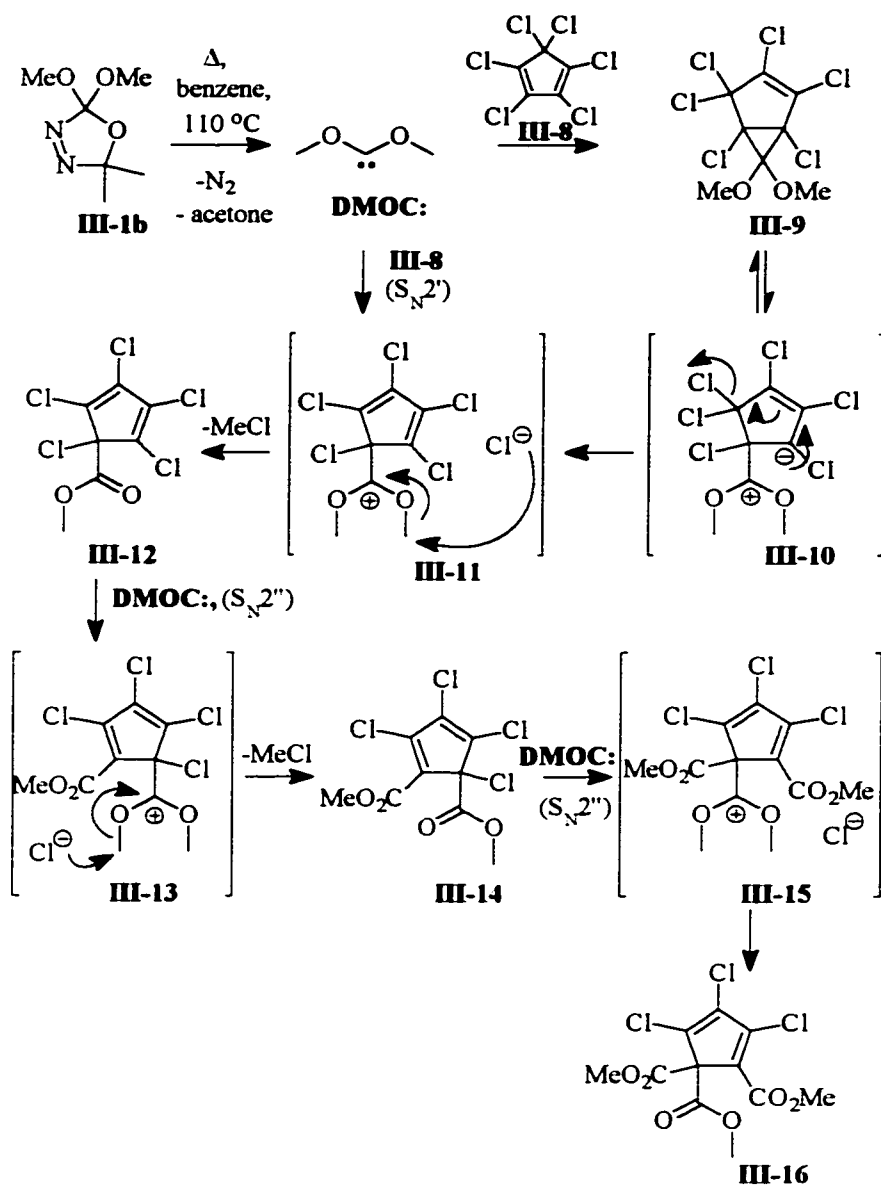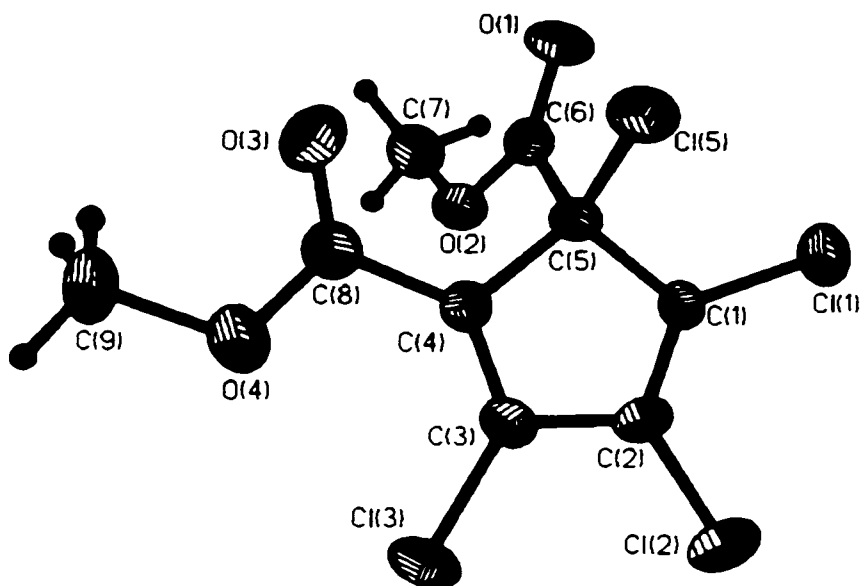
Figure III-4. X-ray crystal structure of III-14.
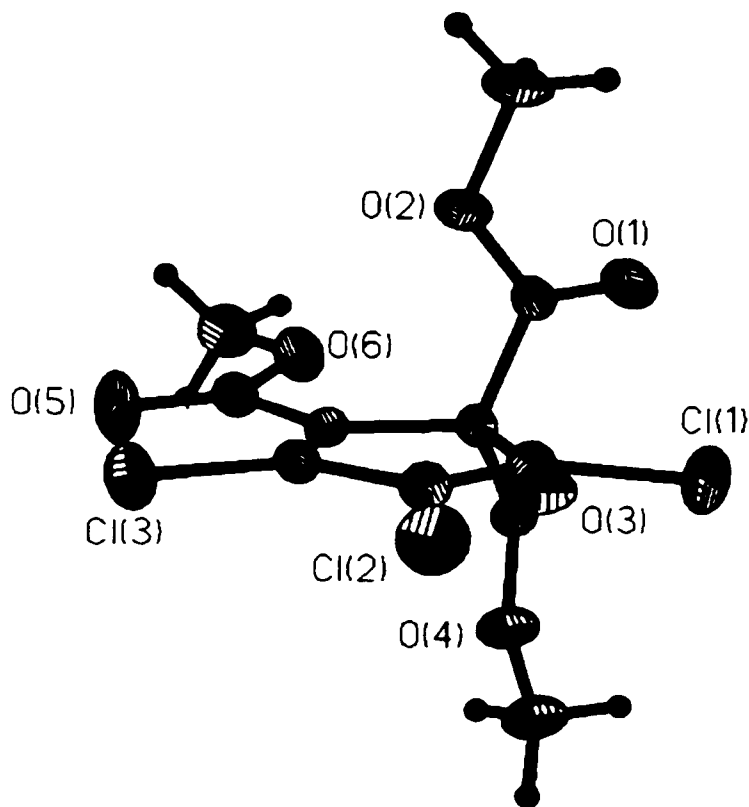
Figure III-5. X-ray crystal structure of III-16.

Initially we were surprised at the regioselectivity of the reaction and speculated that all the possible isomers were in fact formed in the reaction and that the identified products were the result of either 1,5-chlorine or 1,5-ester migrations. Therefore, we performed variable temperature ^{1}H-NMR experiments on **III-12**, **III-14**, and **III-16**, from -80 to 0 °C (CD$_2$Cl$_2$) and from 25 to 110 °C (toluene-d_8) by monitoring the methoxy signals. Ester groups attached to an sp^2 site , ~3.85, were distinguishable from those on sp^3 hybridized centers, ~3.75. Fluxionality in either **III-12**, **III-14**, or **III-16** under these conditions was not observed. Compound **III-16** was found to be stable in solution over a period of 24 hours at 110-140 °C and only at temperatures of 160 °C or higher were products associated with 1,5-ester migrations observed (NMR, sealed tubes). These results are in keeping with high barriers for ester migrations in cyclopentadiene systems. For example, the barrier for a [1,5]-sigmatropic ester shift in 5-chloro-1,2,3,4,5-pentakis(carbomethoxy)cyclopentadiene has been calculated to be ~32 kcal mol^{-1} in dichlorobenzene.[185]

Thermolysis of a ten-fold excess of oxadiazoline **III-1b** relative to **III-8** (0.1 M, 0.1 equivalents) at 110 °C in benzene resulted in a change in the ratios of products **III-12**, **III-14**, and **III-16**. Under these reaction conditions, products **III-14** and **III-16** were formed in 12 and 76 % yields (isolated), respectively, whereas **III-12** was observed only in trace amounts (GC-MS).

There are a number of mechanisms that could lead to the formation of products **III-12**, **III-14**, and **III-16** in the thermal reaction of dimethoxycarbene (**DMOC:**) with hexachlorocyclopentadiene (**III-8**). The intermediacy of dimethoxy acetals of acyl chlorides, arising from "formal" insertion of dimethoxycarbene into C-Cl bonds in **III-8**, could lead to the observed ester products by way of thermally activated ionization and subsequent elimination of methyl chloride (eq III-17).

$$
\begin{array}{c}
\underset{\underset{Cl}{\overset{MeO}{\diagup}}\overset{OMe}{\diagdown}}{\overset{}{\diagdown}R} \longrightarrow \left[\underset{R\quad Cl^{\ominus}}{\overset{MeO\_\oplus\_OMe}{\diagup\diagdown}}\right] \xrightarrow{-MeCl} \underset{R}{\overset{O}{\diagdown}}\overset{}{\diagup}OMe
\end{array} \qquad \text{(III-17)}
$$
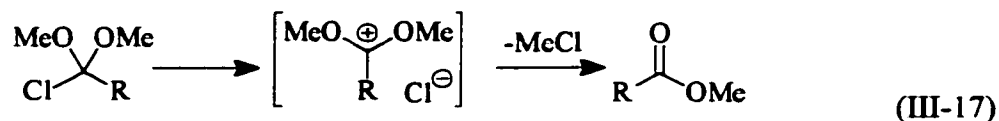
Such insertions can occur by a variety of possible mechanisms which are summarized in Scheme III-4.

Scheme III-4.
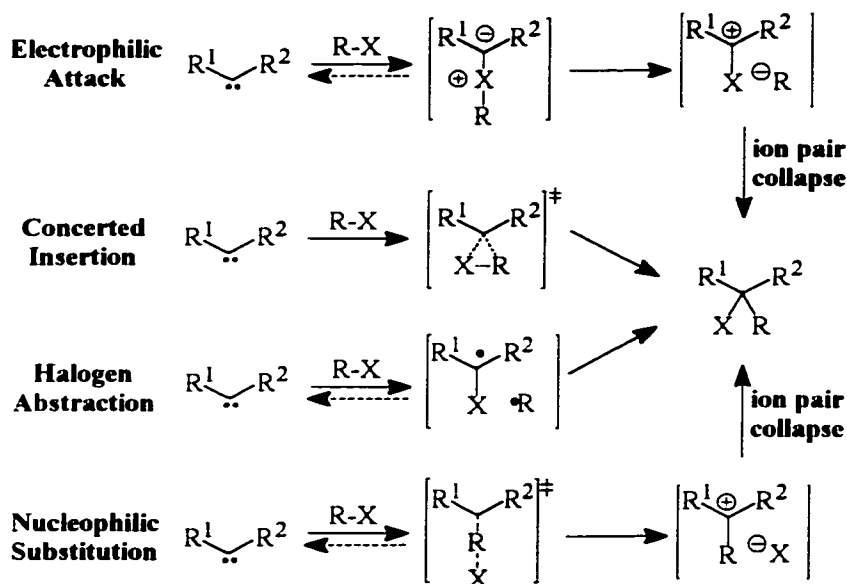
Although there is precedence for halonium ylide intermediates in the reactions of nucleophilic diaminocarbenes,[186] it is unlikely that the observed products come about by such a mechanism in this case. Carbenes, such as **DMOC:**, with one or two oxygen atoms attached directly to the carbene center are slow to react with lone pairs on heteroatoms.[70] Furthermore, a chloronium ylide mechanism would not account for the regioselectivity of the reaction. Thermolyses of **III-1b** in the presence of saturated compounds such as chloroform and tetrachloroethane do not yield products other than the

carbene dimer, tetramethoxyethylene. Although we cannot rule out a concerted mechanism for C-Cl bond insertion entirely, indiscriminate insertion into C-Cl bonds located on both sp^3 and sp^2 hybridized carbon atoms would not account for the products observed. The singlet/triplet energy gap ($\Delta\varepsilon_{ST}$) of **DMOC:** has been calculated[15] to be ~ 76 kcal/mol and, because of this high gap, the chemistry exhibited by **DMOC:** must be predominantly that of the singlet state. Chlorine atom abstraction would be expected to occur from triplet carbenes rather than singlets,[187] although singlet methylene has been shown to abstract chlorine from chloroform to form radical pairs as was shown by CIDNP techniques.[188] The fact that radical derived products were not observed from the reaction of **DMOC:** with fully saturated chlorocarbons and that no cross coupling products (e.g. decachlorobi(2,4-cyclopentadien-1-yl) or octachloropentafulvalene)[189] were seen in the reaction of **DMOC:** with **III-8** suggests that chlorine abstraction by singlet dimethoxycarbene is not an accessible pathway. Therefore, the most likely mechanism for the formation of products **III-12**, **III-14**, and **III-16** is nucleophilic attack by dimethoxycarbene. The lack of substitution products from **2** and saturated substrates such as tetrachloroethane precludes a direct (S_N2) displacement of a chloride anion by **DMOC:** in hexachlorocyclopentadiene (**III-8**). We propose that dimethoxycarbene attacks one of the double bonds in **III-8** to give the ion pair intermediate **III-11**. This S_N2' (or S_N2'') displacement may occur directly, or *via* thermal equilibration of either cyclopropane adduct **III-9** or a [1+4] cycloaddition product with zwitterion **III-10** (Scheme III-3). Dechloromethylation in ion pair **III-11** then gives product **III-12**. The conversion of **III-12** (which must be more reactive towards **DMOC:**) to **III-14** can occur in a similar manner. The regioselectivity of this transformation may be understood in terms of the relative stabilities of zwitterionic intermediates (or transition states) **III-17** and **III-19** (Scheme III-5). The latter is an allylic anion whereas **III-17** is unconjugated. Intramolecular participation of the ester moiety may give added stability to **III-19**, however a *cis*

configuration would be required. Similar arguments may account for the regioselective formation of

III-16 from **III-14**.

Scheme III-5.
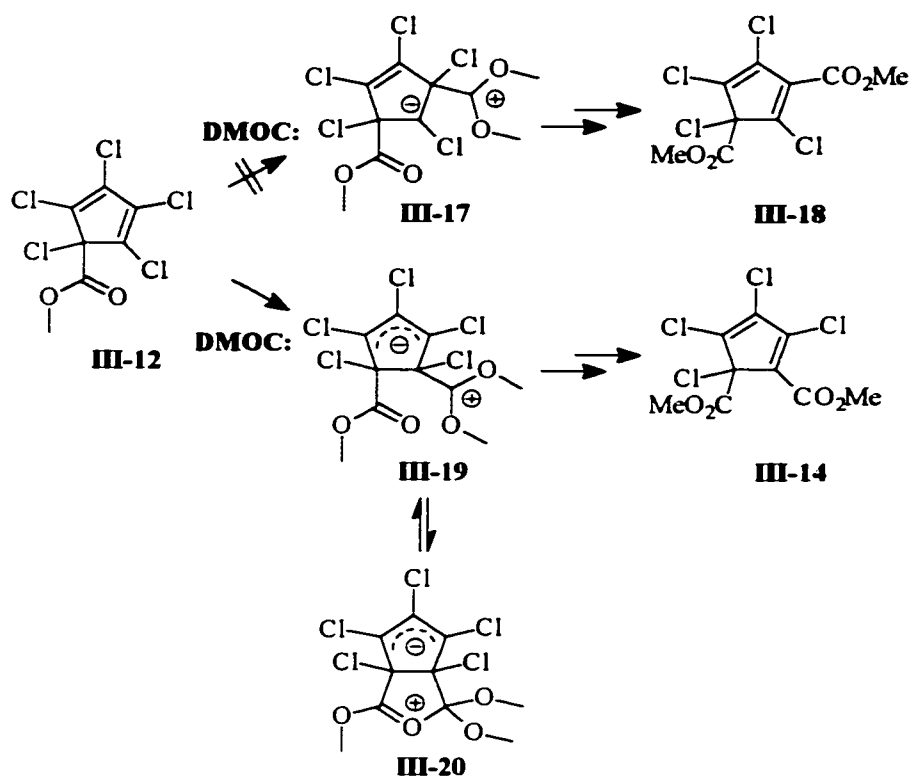
The fact that no products of molecular weight higher than that of **III-16** were observed suggests

that a chlorine atom (or other leaving group) on an sp^3 carbon adjacent to a double bond is required

for these types of reactions.[190] The proposed ionic intermediates, such as **III-11** and **III-13**, where

positive charge resides on the former carbene carbon and a chlorine atom is located directly adjacent

to it, can be written as chloronium ions. In the case of **III-11** and **III-13**, additional stabilization of

positive charge from the adjacent chlorine is not expected owing to the anti-aromatic nature of the

cyclopentadienyl cation; any weakening/lengthening of this sp^3 hybridized C-Cl bond in a chloronium

ion structure would necessarily put positive charge onto both those atoms (eq III-18).

(III-18)
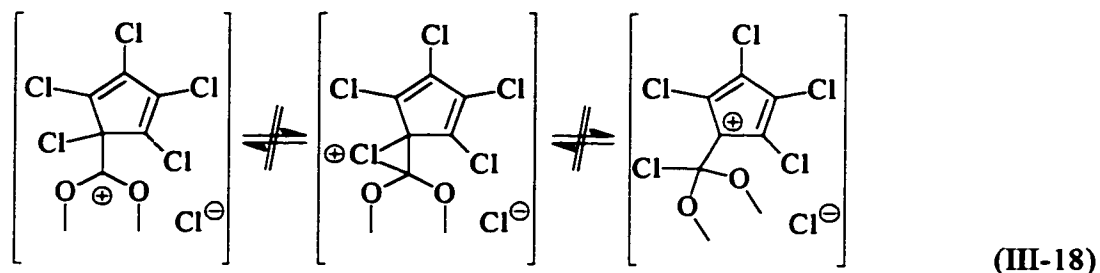
James Dunn found that reactions of **DMOC:** with octachlorocycloheptatriene (**III-21**) and with octachlorobicyclo[3.2.0]hepta-3,6-diene (**III-22**), both yielded ketene acetal **III-23** and perchloroheptafulvalene **III-24** (eq III-19).[a]

(III-19)
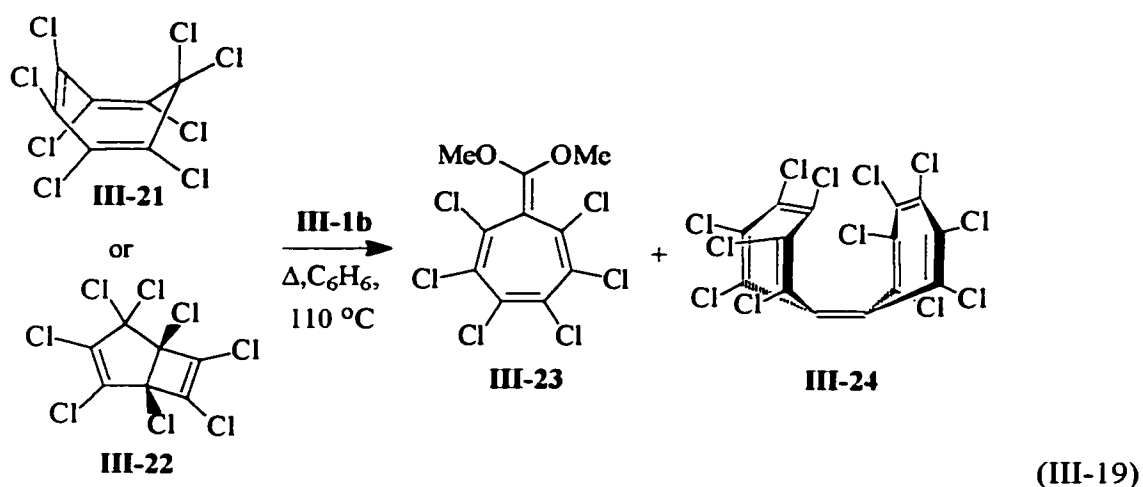
A mechanism similar to that for reaction with **III-8** was postulated for the formation of ketene acetal **III-23** involving attack by dimethoxycarbene (**DMOC:**) at one of the double bonds of **III-21** (or **III-22**, S_N2', or S_N2'', or S_N2''') leading to the formation of an ion pair with three possible structures in equilibrium (eq 20).

---

[a] Part of a collaborative effort. See James A. Dunn's Ph. D. thesis (McMaster) for results and discussion.
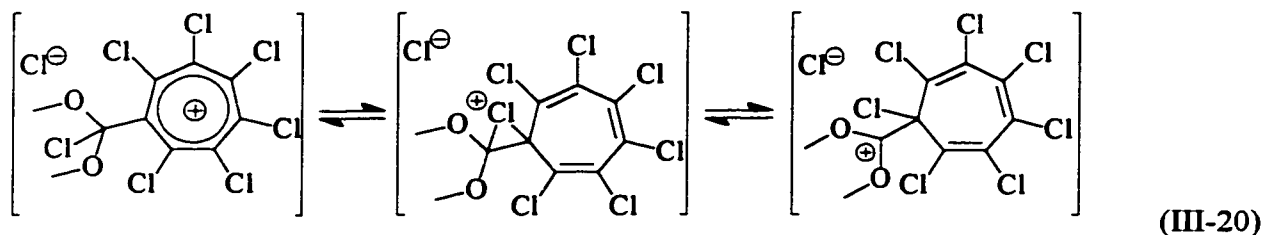
$$(III\text{-}20)$$

The relative stabilities these ion pairs are not known, but the chloronium ion intermediate (center structure, eq III-20) is expected to be more stable than the analogous structures in the reaction of **DMOC:** with hexachlorocyclopentadiene (center structure, eq III-18). One of the ion pairs in eq III-20 undergoes dechlorination to give ketene acetal **III-23**, rather than dechloromethylation which predominates in the analogous reaction with C_5Cl_6 (**III-8**). Dechlorination vs demethylation is consistent with a more stable chloronium ion structure in eq III-20 as compared with that in eq III-18 that has more positive charge on chlorine rather than on the former carbene carbon.

III.2.b. Reaction of 2 and hexachlorobicyclo[3.2.0]-3,6-dien-2-one (III-25).

The reaction of **DMOC:** with hexachlorobicyclo[3.2.0]-3,6-dien-2-one (**III-25**) was also examined. Hexachlorobicyclo[3.2.0]-3,6-dien-2-one (**III-25**) is known to react with anions (e.g. MeLi) to afford the corresponding alcohols[191] with no evidence for Michael-type addition products. When oxadiazoline **DMOC:** and **III-25** (1.1 equiv., 0.1 M **III-25**) were heated at 110 °C in benzene, a single product was isolated in quantitative yield. ^{1}H- and ^{13}C-NMR spectroscopic data indicated the presence of two distinct methoxy resonances and infra-red data ($v_{CO} = 1740$ cm^{-1}) suggested that the α,β unsaturated carbonyl unit remained intact. X-ray crystallography revealed that the product

was 1,4,5,6,7,8-hexachloro-2,2-dimethoxybicyclo[4.2.0]octa-4,7-dien-3-one (III-28), shown in Figure III-6.
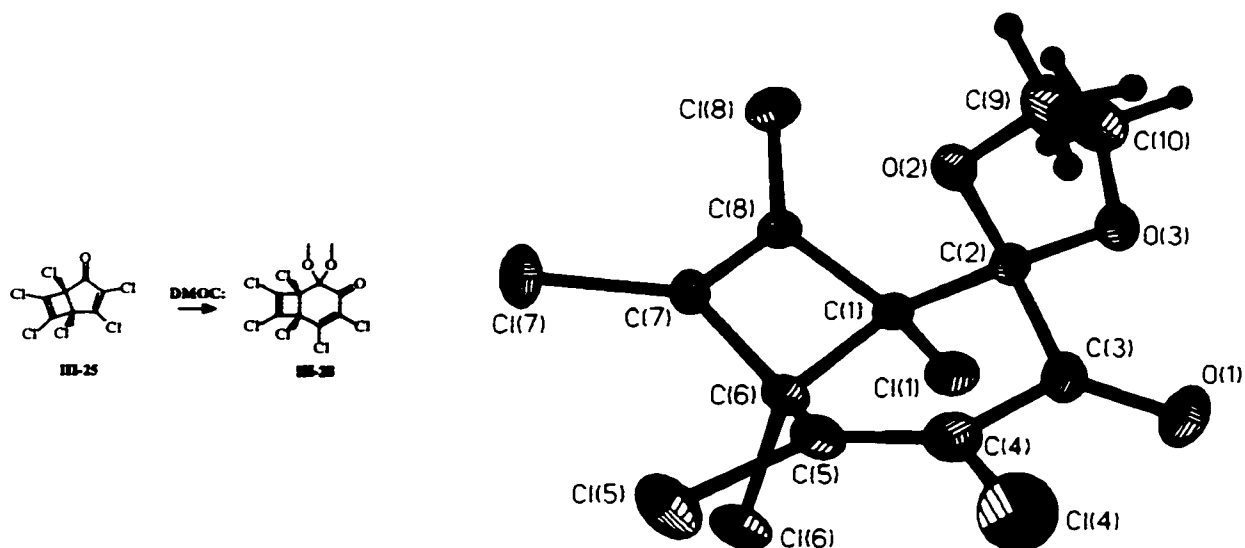
Figure III-6. X-ray crystal structure of III-28.

Compound III-28 is the result of a formal carbene insertion into a carbon-carbon bond. Reactions of DMOC: with carbonyl groups of anhydrides (eq 21),[200] biacetyl, and benzoyl chloride[201] have been reported. The products which result from these reactions arise from the nucleophilic addition of DMOC: at the carbonyl carbon, followed by the rearrangement of the resulting dipolar intermediates such as III-30 in eq 21. These are examples of formal insertion of DMOC: into carbon-oxygen bonds; analogous insertions into carbon-sulfur bonds have also been observed.[202]

(III-21)
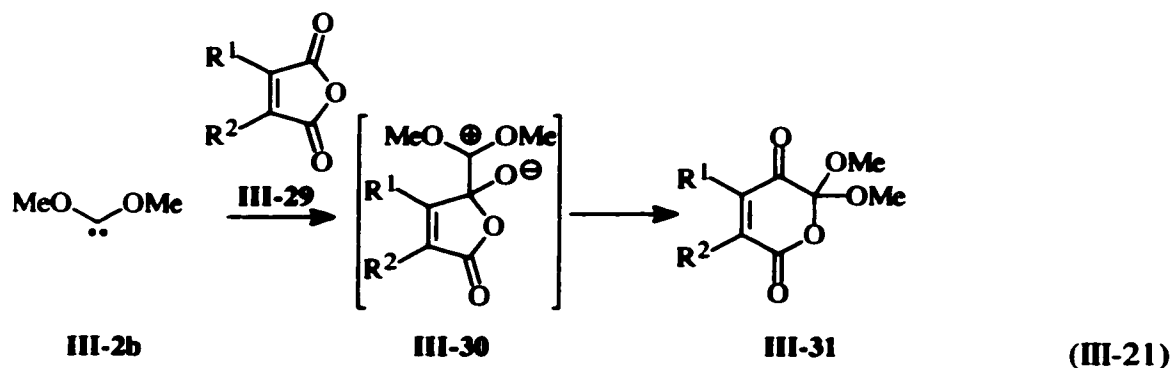
The mechanism for the formation of **III-28** probably involves similar nucleophilic attack by dimethoxycarbene (**DMOC:**) at the carbonyl carbon to yield intermediate **III-26** (Scheme III-6), which rearranges by a 1,2-carbon migration with retention of stereochemistry to form **III-28**.

Scheme III-6.
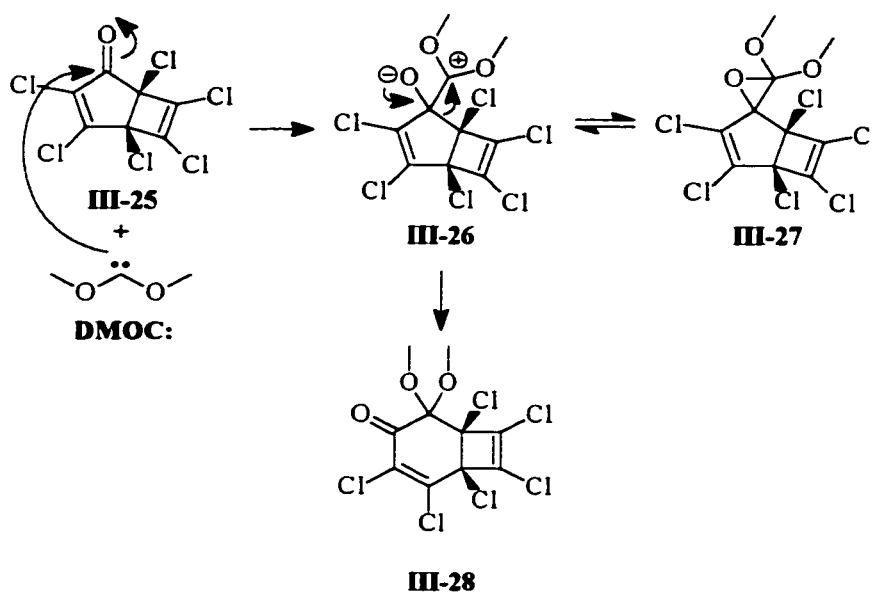
Although reactions of dialkoxycarbenes with carbonyl compounds have been shown to give formal carbene insertion products, the reaction of **DMOC:** with **III-25** is the first example of a formal carbon-carbon insertion reaction for an alkoxy or dialkoxycarbene. It is interesting to note that the product arising from the formal insertion of **DMOC:** into the carbon-carbon bond on the other side of the carbonyl group was not observed. Presumably migration of a carbon atom within a dipolar species, such as **III-26**, involves development of negative charge on the migrating carbon atom which would be more favorable at the sp^3 hybridized carbon atom in **III-26** rather than at the sp^2 site,

because of the relative stabilities of the allyl and vinyl carbanions. We are currently exploring such C-C bond insertions of **DMOC:** into other α-haloketones.

III.2.c. Reaction of DMOC: with tetrachloro-1,4-benzoquinone (III-32).

Thermolysis of oxadiazoline **III-1b** at 110 °C in benzene containing tetrachloro-1,4-benzoquinone (**III-32**) at an initial concentration of 0.1 M (1.1 equivalents) for 24 hours yielded three products. These products were isolated by radial chromatography and identified as 4-methoxy-2,3,5,6-tetrachlorophenyl methyl carbonate (**III-36**, 82% isolated yield), biscarbonate **III-37** (5%), and 1,4-dimethoxy-2,3,5,6-tetrachlorobenzene (**III-38**, 1%). The GC-MS analysis of the thermolysis mixture, prior to chromatography, revealed that products **III-36: III-37: III-38** were formed in ratios of *ca.* 57: 4: 1, respectively.

It is well known that tetrachloro-1,4-benzoquinone (**III-32**) is a good one electron acceptor,[195] but an electron transfer mechanism for the formation of the observed products is unlikely because the energy difference between dihydroxycarbene, a reasonable model for **DMOC:**, and its radical cation is ~120 kcal mol^{-1}.[196] The aromatization and formal oxidation of **III-32** occurs *via* initial attack of **DMOC:** onto the carbonyl carbon to yield dipolar structure **III-33** which is presumably in equilibrium with oxirane **III-34** and dipole **III-35** (Scheme III-7). Structure **III-35** can then react with another molecule of **III-35** by way of a methyl transfer to give **III-39** and **III-40** which undergo a subsequent intermolecular methyl transfer to yield the major product **III-36** (Scheme III-8).

Scheme III-7.
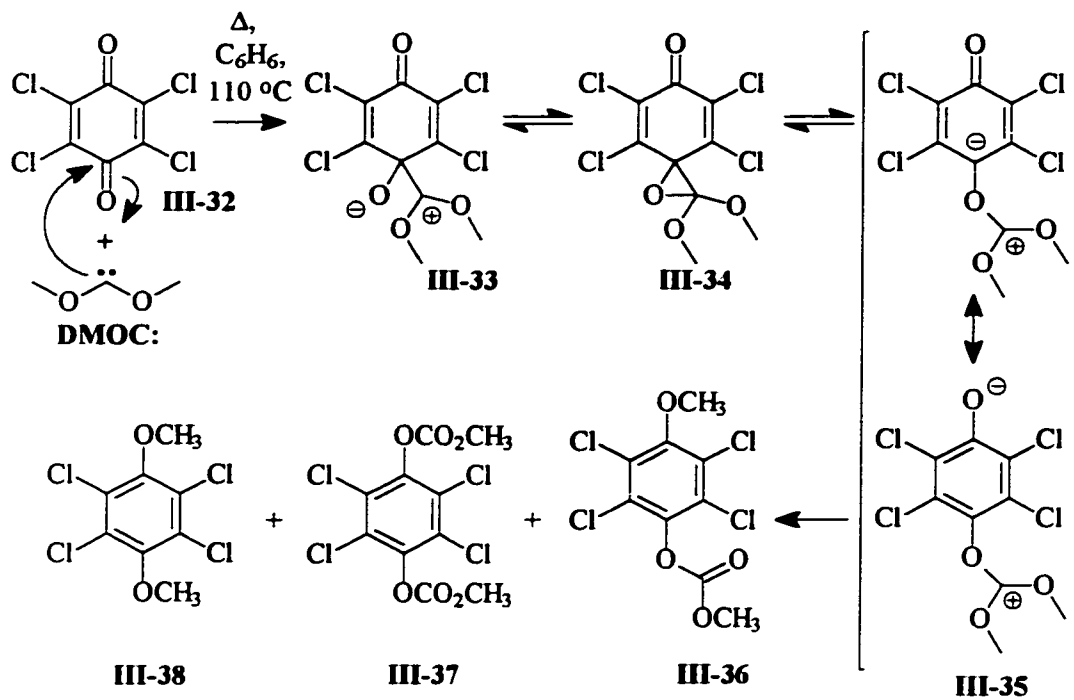
Scheme III-8.
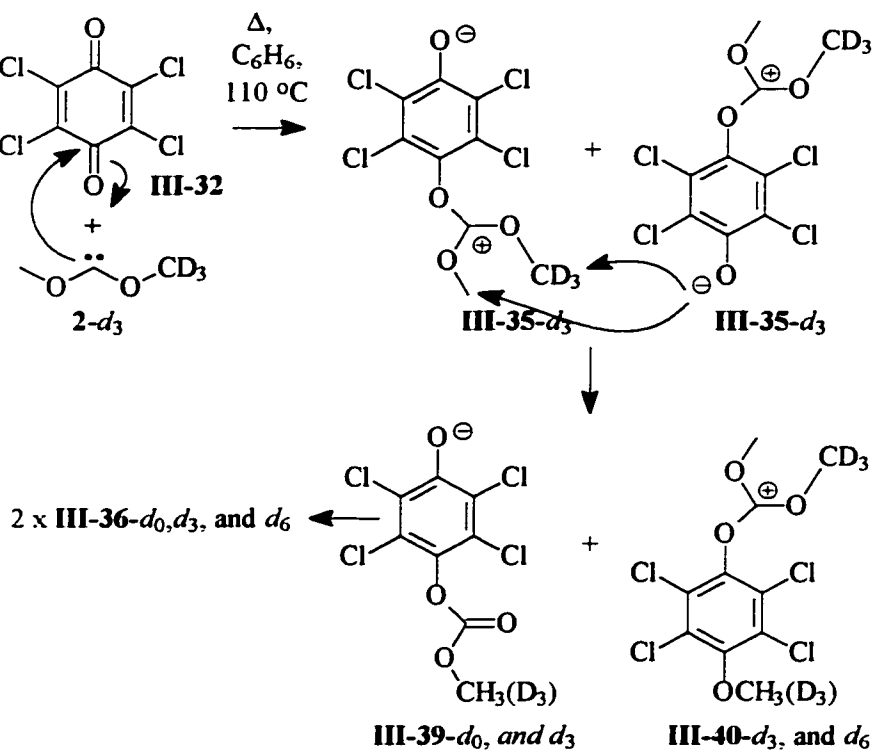
In order to determine whether products **III-36**, **III-37**, and **III-38** are formed *via* intermolecular or intramolecular methyl transfers we performed the reaction with isotopically labeled carbene precursor 1-d_3, possessing a single OCD_3 group. The expectation was that methyl group transfer with crossover would lead to the formation of deuterium labeled products **III-36**, **III-37**, and **III-38**, with the isotopomer distribution ~25% d_0, ~50% d_3, and ~25% d_6, based on a statistical distribution and ignoring kinetic isotope effects. The GC-MS analysis of the resulting thermolysis mixture showed that products **III-36**, **III-37**, and **III-38** all had molecular ion isotopic distributions consistent with such a CD_3 crossover (Figure III-7). Although the isotopic distributions in the molecular ions of **III-36**, **III-37**, and **III-38** are complicated somewhat by the $^{35}Cl/^{37}Cl$ isotopomers, the overlap in the d_3, and d_6 isotopomers could be corrected for. Based on these findings a cascade of intermolecular methyl transfers is implicated.

We are unsure of the origins of the minor products **III-37** and **III-38**; one possibility which is consistent with the labeling studies is that they arise from the reaction of anion **III-40** with a molecule of **III-36** to yield **III-37** and a new anion **III-41** which then demethylates either **III-35** or **III-39** to give **III-38** (eq III-22).

$$\text{(III-22)}$$
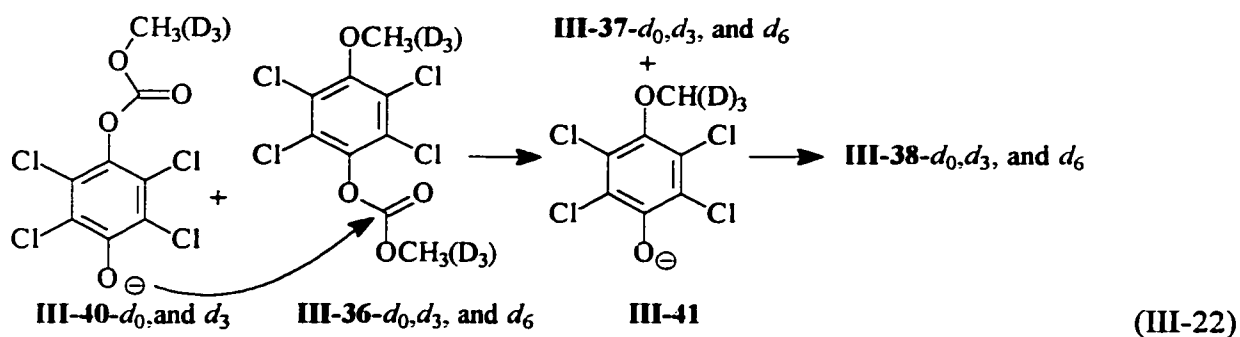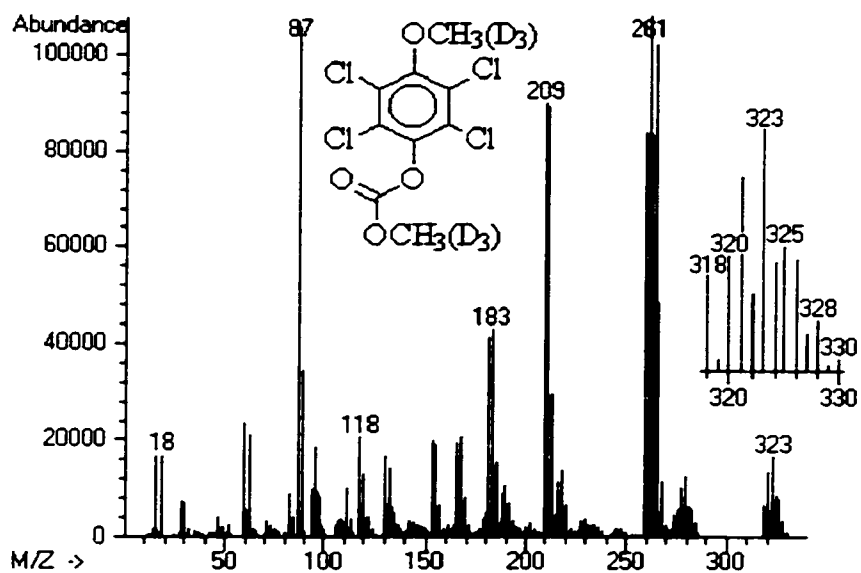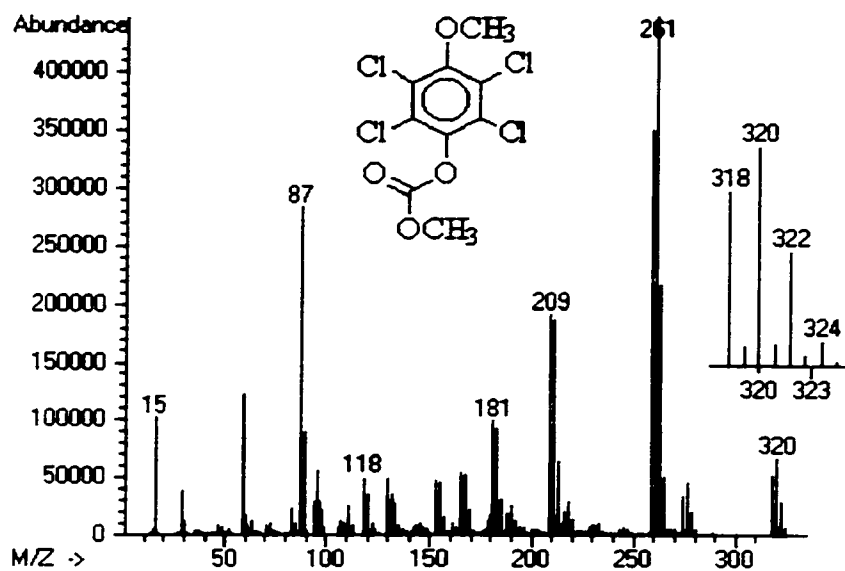
Figure III-7. Electron impact mass spectra for **III-36** and isotopically labeled **III-36**. Insets show the expanded region of the molecular ions.

III.2.d. Conclusions.

Dimethoxycarbene reacts with perchlorinated olefins containing leaving groups in the alpha position by nucleophilic substitution (S_N2' or S_N2'') leading to ion pair intermediates. The latter undergo nucleophilic substitution by Cl^- at Me of $(MeO)_2C^+R$ to afford esters and MeCl. Unsaturated perchloroketones and tetrachloro-1,4-benzoquinone are attacked at the carbonyl carbon atom to afford dipolar intermediates that can rearrange without loss of a Cl^- moiety. Alternatively, such intermediates can form ion pairs that also lead to MeCl and esters.

Chapter 4.

Normal Acid/Base Behaviour in Proton Transfer Reactions to Alkoxy Substituted Carbenes: Estimates for Intrinsic Barriers to Reaction and pK_a Values.

IV. General Introduction.

Proton transfer reactions to and from carbon atoms are usually quite different from those to and from heteroatoms (commonly referred to as "normal" Brönsted acids and bases).[197] Carbon centered acids and bases usually undergo proton transfer reactions more slowly than do their heteroatom counterparts and are believed to do so directly rather than through a solvent molecule in aqueous solvents.[198,199] "Normal" Brönsted acids and bases are thought to donate or accept a proton through one or more water molecules, according to the Swain-Grunwald mechanism, [198, 199] as well as directly from acid to base. Furthermore, Brönsted plots for proton transfer reactions between "normal" acids and bases follow *Eigen curves* with slopes (α) equal to zero when proton transfer is thermodynamically favourable, with rate constants for proton transfer being at or near the diffusion controlled limit. When proton transfer is thermodynamically unfavourable then diffusion-controlled separation of the products is rate limiting[200] and the slopes (α) equal one. There is only a small region near $\Delta pK = 0$ where proton transfer is partially rate limiting and deuterium isotope effects are observed. Carbon centered acids and bases generally give Brönsted plots which are not as sharply curved by comparison, if they show curvature at all. This lack of curvature in Brönsted plots for carbon acids and bases is presumably the result of changes in hybridization, changes in heavy atom bond lengths and angles, desolvation in the rate limiting transition state, differences in hydrogen-bonding ability, and changes in delocalization of charge. Any or all of these effects are believed to

result in higher activation barriers, even when proton transfer is thermodynamically favourable (i.e. higher intrinsic barriers), and therefore smaller changes in transition state position (and in slope α) as a function of ΔpK for the reaction.[197] However, nearly all of the studies related to the acid/base chemistry at carbon atoms have been restricted to carbanions and their conjugate acids; the acid/base chemistry of divalent carbon atoms, carbenes, and their conjugate acids is not well established by comparison.

As stated in the Introduction (chapter 1, section I.7.1), the formal insertions of carbene intermediates into O-H bonds are well known processes and can occur by different mechanisms depending on the nature of the carbene intermediate.[113] Carbenes may insert into O-H bonds from the singlet spin state by a concerted mechanism, or by initial formation of an oxonium ylide intermediate followed by a 1,2-hydrogen shift, or by proton transfer (Chapter 1, Scheme 14). The proton transfer mechanism has been implicated in several systems based on direct observations of resulting carbocations, or on product distributions, or on slopes of Brönsted plots. Non-zero slopes in Brönsted plots suggest that the reactions depend on the acidity of the O-H containing substrate with the rate constants for O-H insertion (assuming that proton transfer is rate limiting) and are proportional to the pK_a's of the protonating acid. Often overlooked is the fact that such rate constants will also depend on the thermodynamics of the overall reaction, according to the Hammond postulate, and the pK_a's of the conjugate acids of carbene intermediates are also important in determining how fast a given proton transfer event will occur. Unfortunately, for most carbenes such thermodynamic parameters are unknown and virtually impossible to measure directly with present day equipment. However, in some cases, when the conjugate acids of carbenes are stable and unreactive, it is possible to gain information about their pK_a values.

A pK_a value of ca. 16 has been estimated for thiamin,[201] and those for thiazolium ions fall between ca. 16 and 22.[202] Also, "normal" acid/base behaviour has been implicated in proton transfer reactions

of thiazolium ions including thiamin.[201-203] More recently, a pK_a of 24 for the conjugate acid of the stable carbene 1,3-diisopropyl-4,5-dimethylimidazol-2-ylidene has been measured by ^{1}H-NMR in DMSO solvent by monitoring hydrocarbon acids (such as 2,3-benzofluorene, eq IV-1) and their conjugate bases.[204] Alder and co-workers also noted that while the carbon acids and their conjugate bases were distinguishable by ^{1}H-NMR, suggesting that proton transfer is slow compared to the NMR timescale, proton transfer between 1,3-diisopropyl-4,5-dimethylimidazol-2-ylidene and its conjugate acid is fast as evidenced by the fact that the carbene and its conjugate acid appear as an averaged spectrum in the presence of base.[204]
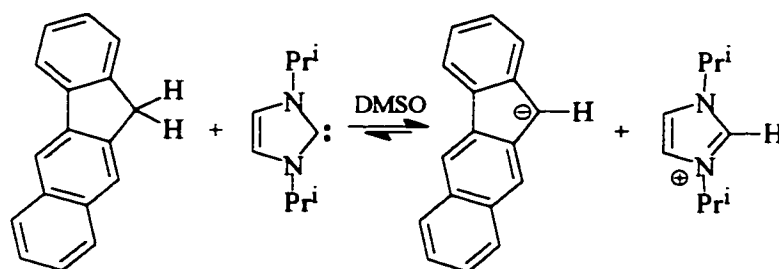
(IV-1)

The reported acid/base reactivity of diamino and aminothiocarbenes suggest that other π-donor substituents may also behave as "normal" Brönsted bases and that equilibria between carbenes and their conjugate acids may be established in solution. The application of proton transfer theories to rate data for proton transfer reactions to dimethoxycarbene (**DMOC:**) and for four aryltrimethylsiloxycarbenes (**IV-3a** to **d**) were performed. The evaluation of the acid/base chemistry of dimethoxycarbene (**DMOC:**) and four aryltrimethylsiloxycarbenes (**IV-3a** to **d**) as well as the first estimates of the pK_a values for their conjugate acids are presented in this chapter.

IV.1 Brönsted Relations and Eigen Curves.

IV.1.a. Proton Transfer to Dimethoxycarbene.

Like diamino and aminothiocarbenes, dimethoxycarbene (**DMOC:**) is considered to be a *nucleophilic* carbene due to conjugative stabilization through donation by the lone pairs on the oxygen atoms of the methoxy substituents to the formally vacant virtual p-orbital at the carbene carbon.[4,15] Resonance stabilization in the ground state of **DMOC:**, in the transition states, and in carbocationic intermediates makes proton transfer to dimethoxycarbene (**DMOC:**) the most likely mechanism for formal OH insertion reactions. Such a proton transfer mechanism is supported by observed kinetic isotope effects.[205]

In a previous investigation,[206] rate constants for the reactions of dimethoxycarbene with a series of oxygen centered acids were measured by LFP and a Brönsted plot, based on the linear free energy relationship in eq IV-2 or its differential form in equation IV-3, was constructed based on the data in Table IV-1.

$$\log(k_a) = \alpha \cdot \log(K_a) + \text{constant} \tag{IV-2}$$

$$\delta \log(k_a) = \alpha \cdot \delta \log(K_a) \tag{IV-3}$$

A slope of $\alpha \sim 0.66$ was determined by Du *et al.*[206] The pK_a values used for the Brönsted reported by Du *et al.*[206] and for all Brönsted correlations reported here are those determined in water[207] as a result of a lack of appropriate thermodynamic data for these acids in acetonitrile solvent.[208] Therefore correlations of the data should be considered to be semi-quantitative, although the pK_a values for phenols and carboxylic acids in acetonitrile and in water may be approximated by eq IV-4,[197a] which is assumed to be valid for the acidic species in Tables IV-1 and 2. Knowledge of the pK_a's in acetonitrile would make the interpretation of these data quantitative. However, it is the difference in pK_a values (i.e. $\Delta\Delta G^\circ$) and not the absolute values of the individual equilibrium constants which are important

here and the differences between the thermodynamic data in water and those in acetonitrile are not

expected to change the calculated values or the interpretations dramatically.

$$pK_a^{MeCN} - pK_a^{H_2O} \approx 14.0 \qquad\qquad (IV-4)$$

Table IV-1. Observed proton transfer rate constants (k_a) for the protonation of dimethoxycarbene by oxygen acids in acetonitrile at 20 °C.[206]

Acid	pK_a [a]	k_a, M^{-1} s^{-1} [b]
CH_3CH_2OH	15.9	3.2×10^4
CH_3OH	15.54	8.8×10^4
$ClCH_2CH_2OH$ [b]	14.31	9.1×10^5
FCH_2CH_2OH [b]	14.2	2.3×10^6
F_3CCH_2OH (TFE) [b]	12.37	6.3×10^7
$(CF_3)_2CHOH$ (HFIP)	9.3	6.7×10^8
CH_3CO_2H	4.76	2.4×10^9

[a] pK_a values in water (Reference 207).
[b] Plots for quenching of dimethoxycarbene by $ClCH_2CH_2OH$, FCH_2CH_2OH, and 2,2,2-trifluoroethanol (TFE) were found to be concave upward due to the contribution of oligomeric alcohol to the rate constants for the decay of this carbene. The rate constants for these acidic species therefore represent upper limits for the rate constants for reaction with the monomeric form.

Slopes of Brönsted plots (α) are considered to be a measure of the extent of proton transfer at the transition state for the reaction, with $\alpha=0$ representing the structure of the reactants and $\alpha=1$ representing that of the products. An α value of 0.66 suggests that the transition state for proton transfer to dimethoxycarbene is more product like than reactant like over the pK_a range studied. However, the structure of the transition state may change with pK_a, following the thermodynamics of the reaction, according to the Hammond postulate.[209] Reactions which are exothermic have transition states that are more reactant-like and those which are endothermic have transition states that are more product-like. Such changes in transition state structure lead to curvature in Brönsted plots. Curvature

in Brönsted plots can be evaluated with Marcus rate theory[210,211] and such evaluations are in a following section.

When proton transfer reactions are fast, as in those to and from electronegative atoms ("normal" Brönsted acids and bases), then diffusion becomes a limiting factor except for small values of ΔpK when proton transfer is, at least partially, rate determining. Curvature in Brönsted plots for proton transfers to and from "normal" Brönsted acids and bases then arise from changes in the rate determining step. When proton transfer is thermodynamically unfavourable then diffusional separation of the products is rate limiting (α approaches 1) and when proton transfer is thermodynamically favourable then diffusional encounter becomes rate limiting (α approaches 0). In such cases, the rate determining proton transfer step can itself be divided into three steps as described by Eigen.[200]

The reactions of dimethoxycarbene (**DMOC:**) with oxygen-centered acids (the forward reaction in eq IV-5) appear to be at least partially diffusion controlled when proton transfer is thermodynamically favourable, given that the observed rate constants for proton transfer to these carbenes reach a maximum at values greater than 10^9 M^{-1} s^{-1}. If dimethoxycarbene behaves as a "normal" Brönsted base, then it should be possible to draw an Eigen curve[200] through the data points in the Brönsted plot, based on the three step mechanism for proton transfer in eq IV-5, where k_d is the rate constant for diffusion together of the reactants, k_{-d} is the rate constant for diffusional separation of the products, and k_p and k_{-p} are the rate constants for proton transfer within the encounter complex.

$$\text{ROH} + \text{X}\diagdown\diagup\text{Y} \underset{k_{-d}}{\overset{k_d}{\rightleftharpoons}} \left[\begin{array}{c} \text{X}\diagdown\diagup\text{Y} \\ \cdots \\ \text{ROH} \end{array} \right] \underset{k_{-p}}{\overset{k_p}{\rightleftharpoons}} \left[\begin{array}{c} \text{X}\overset{\oplus}{\diagdown}\diagup\text{Y} \\ | \\ \text{H} \quad {}^{\ominus}\text{OR} \end{array} \right] \underset{k_d}{\overset{k_{-d}}{\rightleftharpoons}} \begin{array}{c} \text{X}\overset{\oplus}{\diagdown}\diagup\text{Y} \\ | \\ \text{H} \end{array} + {}^{\ominus}\text{OR}$$

(IV-5)
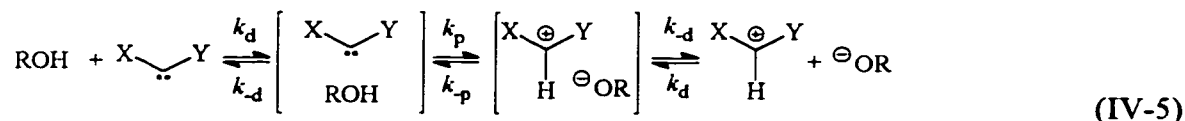
The steady-state solution to equation IV-5, where k_a (eq IV-6) are the observed bimolecular rate constants for proton transfer to **DMOC:** by the oxygen centered acids, is in eq IV-7. The values for k_p

and k_{-p} are defined in equations IV-8 and IV-9, respectively.[202, 212]

$$ ROH \ + \ X\overset{\cdot\cdot}{\diagdown}Y \quad \xrightarrow{\ k_a\ } \quad X\overset{\oplus}{\diagup}Y \ + \ ^{\ominus}OR $$

$$\hspace{9cm}(\text{IV-6})$$
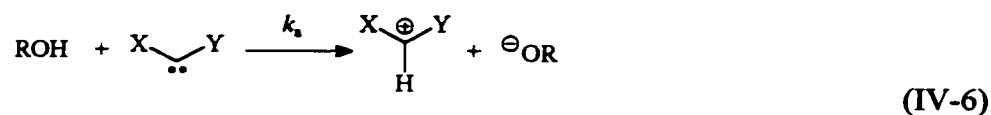
$$ k_a \ = \ \frac{k_d k_p k_{-d}}{k_p k_{-d} \ + \ k_{-d} k_{-d} \ + \ k_{-d} k_{-p}} \hspace{3cm}(\text{IV-7}) $$

$$ k_p \ = \ k_{p(\Delta pK = 0)} \cdot 10^{0.5(\Delta pK)} \hspace{4cm}(\text{IV-8}) $$

$$ k_{-p} \ = \ k_{p(\Delta pK = 0)} \ / \ 10^{0.5(\Delta pK)} \hspace{4cm}(\text{IV-9}) $$

The values for ΔpK are defined by the relation in eq IV-10, where pK_a^{AH} are the pK_a's of the oxygen acids, $pK_a^{CH^+}$ is the pK_a for the conjugate acid of the carbene and α for the proton transfer (PT) step is assumed to be 0.5 at $\Delta pK = 0$ (and in the adjacent region in which proton transfer contributes to $k_a^{CH^-}$).

$$ \Delta pK \ = \ pK_a^{AH} \ - \ pK_a^{CH^-} \hspace{4cm}(\text{IV-10}) $$
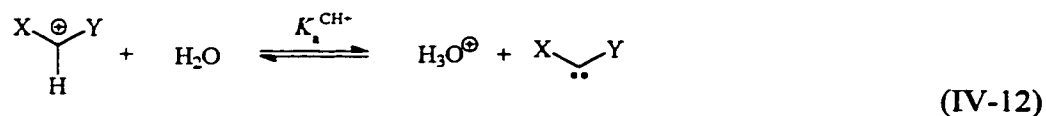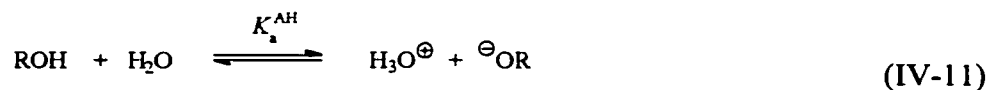
$$ ROH \ + \ H_2O \quad \underset{}{\overset{K_a^{AH}}{\rightleftharpoons}} \quad H_3O^{\oplus} \ + \ ^{\ominus}OR $$

$$\hspace{9cm}(\text{IV-11})$$

$$ X\overset{\oplus}{\diagup}Y \ + \ H_2O \quad \overset{K_a^{CH^-}}{\rightleftharpoons} \quad H_3O^{\oplus} \ + \ X\overset{\cdot\cdot}{\diagdown}Y $$

$$\hspace{9cm}(\text{IV-12})$$

After statistical correction for the number of equivalent acidic sites on the protonating species (q),

and substituting values of k_d = 3.2 x 10^9 $M^{-1}s^{-1}$ and k_{-d} = 1 x 10^{10} s^{-1}, least-squares fitting of the data in

Table IV-1 to the expression in eq IV-13 yielded a smooth Eigen curve (middle curve in Figure IV-1)

with $pK_a^{CH^+}$ = 11.0 ± 0.1 (water, ~25 in MeCN) and log $k_{p(\Delta pK=0)}$ = 8.92 ± 0.23 $M^{-1}s^{-1}$.

$$\log k_a = \log \left(\frac{k_d \cdot (k_{p(\Delta pK=0)} \cdot 10^{0.5(pK_a^{AH} - pK_a^{CH^+})}) \cdot k_{-d}}{(k_{p(\Delta pK=0)} \cdot 10^{0.5(pK_a^{AH} - pK_a^{CH^+})}) \cdot k_{-d} + k_{-d}k_{-d} + k_{-d} \cdot (k_{p(\Delta pK=0)} / 10^{0.5(pK_a^{AH} - pK_a^{CH^+})})} \right) \quad \text{(IV-13)}$$

Similar least-squares fitting of the expression in eq IV-13 to the data in Table IV-1, with k_{-d} = 1 x

10^{10} s^{-1} yielded a different Eigen curve (lower curve in Figure IV-1) with computed values of pK_a^{CH-}

= 11.2 ± 0.2 (water, ~25 in MeCN), log k_d = 9.27 ± 0.16 $M^{-1}s^{-1}$, and log $k_{p(\Delta pK=0)}$ = 9.18 ± 0.31 $M^{-1}s^{-1}$

from the fit. Analogous least-squares fitting (upper curve in Figure IV-1) with k_d = 5 x 10^9 $M^{-1}s^{-1}$, k_{-d}

= 1 x 10^{11} s^{-1}, and $k_{p(\Delta pK=0)}$ = 10^{12} $M^{-1}s^{-1}$ (essentially no intrinsic barrier) yielded a value for $pK_a^{CH^+}$ of

10.6 ± 0.2 (water, ~25 in MeCN). A summary of the results of obtained from other least-squares fits

are in Table IV-3.

Kirmse and coworkers[103] have suggested that proton transfers to aryltriphenylsiloxycarbenes

occur *via* a pre-association mechanism. Such proton transfers would obey the relation in eq IV-14,

where K_{ass} is the association constant.

$$k_a = \frac{K_{ass} k_d k_p k_{-d}}{k_p k_{-d} + k_{-d}k_{-d} + k_{-d}k_{-p}} \quad \text{(IV-14)}$$

The least-squares fitting of the data in Table IV-1 to the logarithmic form of the expression in eq

IV-14, assuming k_d = k_{-d} = 4 x 10^{10} s^{-1} yielded a smooth Eigen curve through the data with coefficients

yielding values of $pK_a^{CH^+}$ = 11.2 ± 0.2 (water, ~25 in MeCN), log $k_{p(\Delta pK=0)}$ = 9.78 ± 0.32 M^{-1} s^{-1}, and

K_{ass} = 4.6 x 10^{-2} M (assuming the proton is transferred from a second molecule of acid through solvent

and that the overall reaction is pseudo-bimolecular where k_d is pseudo first order).
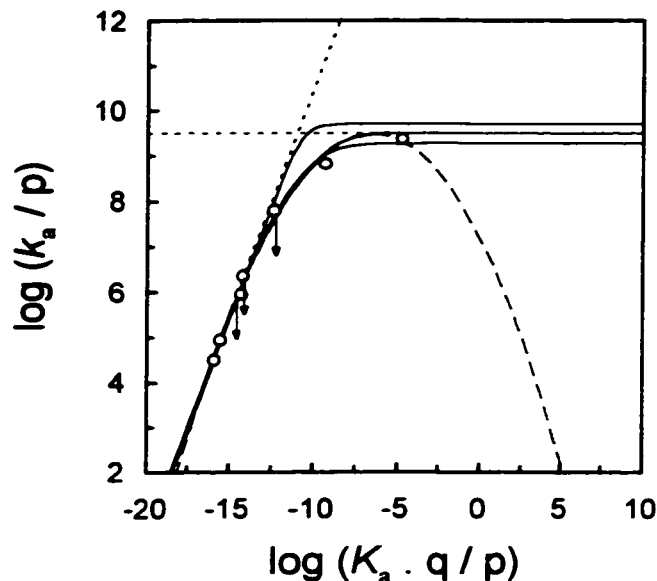
FIGURE IV-1. Brönsted plot for the protonation of dimethoxycarbene in acetonitrile at 20 °C. Arrows indicate that the corresponding data points are upper limits for the log k_a values (see text). The solid lines are theoretical Eigen curves (see text), the dotted lines are extrapolated from the portions of the middle Eigen curve where $\alpha_{obs} = 0$ and $\alpha_{obs} = 1$. These dotted lines cross at $pK_a^{AH} = pK_a^{CH^+}$ ($\Delta pK = 0$).[208] The dashed line is the Marcus curve through the data.

In all cases, least-squares fitting of the data, using the Eigen model with reasonable assumptions regarding rate constants for diffusional encounter and separation,[212] yielded reasonable curves through the data and computed values of ~11 (water, ~25 in MeCN) for the pK_a of the conjugate acid of dimethoxycarbene, and computed intrinsic barriers[a] (the barrier to reaction at $\Delta pK = 0$) of 2.4-3.7 kcal/mol (again with reasonable assumptions regarding rate constants for diffusional processes). The small variation within each theoretical model then depends on what values of k_d and k_{-d} are used.[213] The magnitude of the "apparent" intrinsic barrier (larger than 1 kcal/mol) suggests that the proton transfer step (k_b) may be coupled with other molecular events that contribute to this barrier which are not accounted for by this model.[200] The fact that reasonable Eigen curves can be drawn through the

---

[a] There are many potential factors which may influence the magnitudes of apparent intrinsic barriers to reaction[197,200] so that the computed values for the intrinsic barriers should be viewed with caution.

Brönsted data suggests that dimethoxycarbene is a "normal" Brönsted base and that the pK_a of its conjugate acid is between those of 2,2,2-trifluoroethanol (TFE) and 1,1,1,3,3,3-hexafluoroisopropanol (HFIP) in acetonitrile. Thiazolium ions and thiamin (which itself is a thiazolium cation) have pK_a's ~14-20 in aqueous solution solution.[201-203] As well, the pK_a of a conjugate acid of a diaminocarbene has been measured to be 24 in DMSO.[204] Since the conjugate bases of these cations may be written as carbenes, they are good model systems for comparison. The cations are stable species and the carbene/ylide conjugate bases would be more stable/less reactive than oxygen substituted carbenes. The computed pK_a of the conjugate acid of **DMOC:** suggests that it is more acidic than thiazolium ions which is expected as a result of the increased electronegativity of oxygen as compared with nitrogen and sulfur. Oxazolium ions are known to be more acidic than their imidazolium and thiazolium ion counterparts.[214] Interestingly, the pK_a's of the electron deficient 4-biphenylnitrenium ion and 4-aminobiphenyl dication in 20 % aqueous acetonitrile have been estimated as 16 and 0.1,[215] respectively, suggesting that these species are more acidic than the conjugate acid of **DMOC:**.[a]

IV.1.b. Proton Transfer to Aryltrimethylsiloxycarbenes.

Aryltrimethylsiloxycarbenes (**IV-3**) have been generated from the corresponding acylsilanes (**2**) both thermally and photochemically.[47] Rate constants for the protonation of **IV-3a** to **d** by hydroxylic acids in organic media have been measured by LFP.[102,103] The direct observation of carbocationic intermediates **IV-4a** to **d** unambiguously proves that proton transfer to arylsiloxycarbenes **IV-3a** to **d** is the initial step in formal OH insertion reactions of these carbenes.

---

[a] Nitrenium ions are isoelectronic with carbenes.

$$\underset{\textbf{IV-2}}{\overset{O}{\underset{Ar}{\|}}\underset{}{\overset{}{C}}SiMe_3} \xrightarrow{h\nu} \underset{\textbf{IV-3}}{Ar\diagdown\diagup OSiMe_3} \xrightarrow{ROH} \underset{\textbf{IV-4}}{\overset{Ar\diagdown\overset{\oplus}{\underset{H}{C}}\diagup OSiMe_3}{}} + RO^{\ominus}$$

(IV-15)
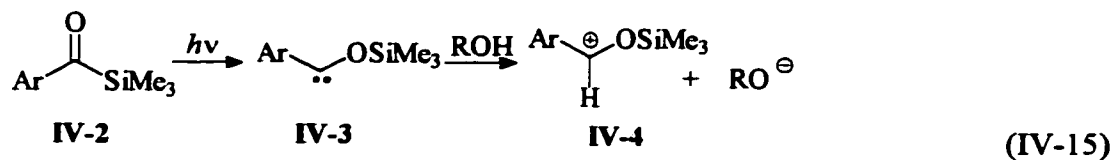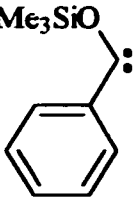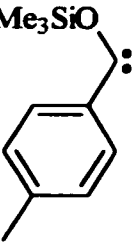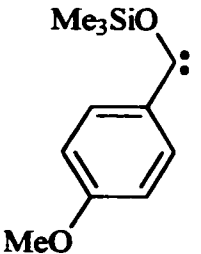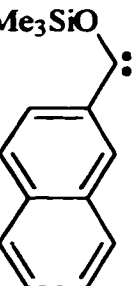
IV-3a: Ar = Ph;
IV-3b: Ar = 4-methylphenyl;
IV-3c: Ar = 4-methoxyphenyl;
IV-3d: Ar = β-naphthyl.

Arylsiloxycarbenes are expected to be *nucleophilic* in character. Evidence for this comes from addition reactions with carbonyl compounds (presumably at carbon).[47] Conjugative stabilization presumably occurs in carbenes IV-3a to d through donation from the aryl substituents and by the lone pairs on the oxygen atoms of the trimethylsiloxy substituents to the formally vacant p-orbital at the carbene carbon. Additional stabilization of carbenes IV-3a to d and cations IV-4a to d results from hyperconjugation of the trimethylsilyl group, with resulting positive charge on silicon and negative charge at the carbene carbon.

$$R\diagdown\diagup OSiMe_3 \longleftrightarrow \overset{\oplus}{R\diagdown\diagup OSiMe_3}_{\ominus} \longleftrightarrow R\diagdown\diagup O_{\ominus}\ \ ^{\oplus}SiMe_3$$

The analysis of the kinetic data for proton transfer to aryltrimethylsiloxycarbenes IV-3a to d, obtained by W. Kirmse *et al.*, according to Eigen theory and to Marcus theory[210,211] is presented here. The relevant kinetic data may be found in Table IV-2.

Table IV-2. Observed proton transfer rate constants (k_a) for the protonation of arylsiloxycarbenes by oxygen acids in acetonitrile at 20 °C.[103]

Acid	pK_a[a]	k_a, M^{-1} s^{-1}			
		Me$_3$SiO carbene (IV-3a)	Me$_3$SiO carbene (IV-3b)	Me$_3$SiO / MeO carbene (IV-3c)	Me$_3$SiO naphthyl carbene (IV-3d)
H$_2$O	15.7	9.3 x 10^7	9.2 x 10^7	1.0 x 10^8	1.2 x 10^8
CH$_3$OH	15.5	3.0 x 10^8	2.7 x 10^8	3.8 x 10^8	2.2 x 10^8
CH$_3$CH$_2$OH	15.9	-	-	2.0 x 10^8	-
HOCH$_2$CH$_2$OH	15.1	9.1 x10^8	1.5 x 10^9	3.0 x 10^9	-
CH$_3$OCH$_2$CH$_2$OH	14.8	1.6 x 10^8	2.6 x 10^8	6.3 x 10^8	-
ClCH$_2$CH$_2$OH	14.3	1.1 x 10^9	-	2 x 10^9	-
Cl$_2$CHCH$_2$OH	12.9	2.0 x 10^9	-	2.1 x 10^9	-
F$_3$CCH$_2$OH (TFE)	12.8	1.5 x 10^9	1.8 x 10^9	1.5 x 10^9	1.5 x 10^9
Cl$_3$CCH$_2$OH	12.2	1.6 x 10^9	-	2.0 x 10^9	-
(CF$_3$)$_2$CHOH (HFIP)	9.3	1.2 x 10^9	1.0 x 10^9	1.2 x 10^9	9.6 x 10^8
CH$_3$CO$_2$H	4.76	1.1 x 10^9	1.2 x 10^9	1.0 x 10^9	9.9 x 10^8
4-O$_2$NC$_6$H$_4$OH	7.15	~3 x 10^9	-	-	-

[a] pK_a values in water (Reference 207).

From the data in Table IV-2, Brönsted plots for the proton transfer reactions to aryltrimethylsiloxycarbenes **IV-3a** to **d** by oxygen acids were constructed by plotting log $(k_a$ / p) *vs.* log $(K_a^{AH}$ q/p) (Figure IV-2) for each carbene, where p and q are statistical factors for the number of equivalent basic sites on the carbene (always 1) and the number of equivalent acidic sites on the protonating acid. Linear least-squares fittings of these data to eq IV-13 and IV-14 were performed in a fashion analogous to that for the data for dimethoxycarbene protonation. The results are summarized in Table IV-3.
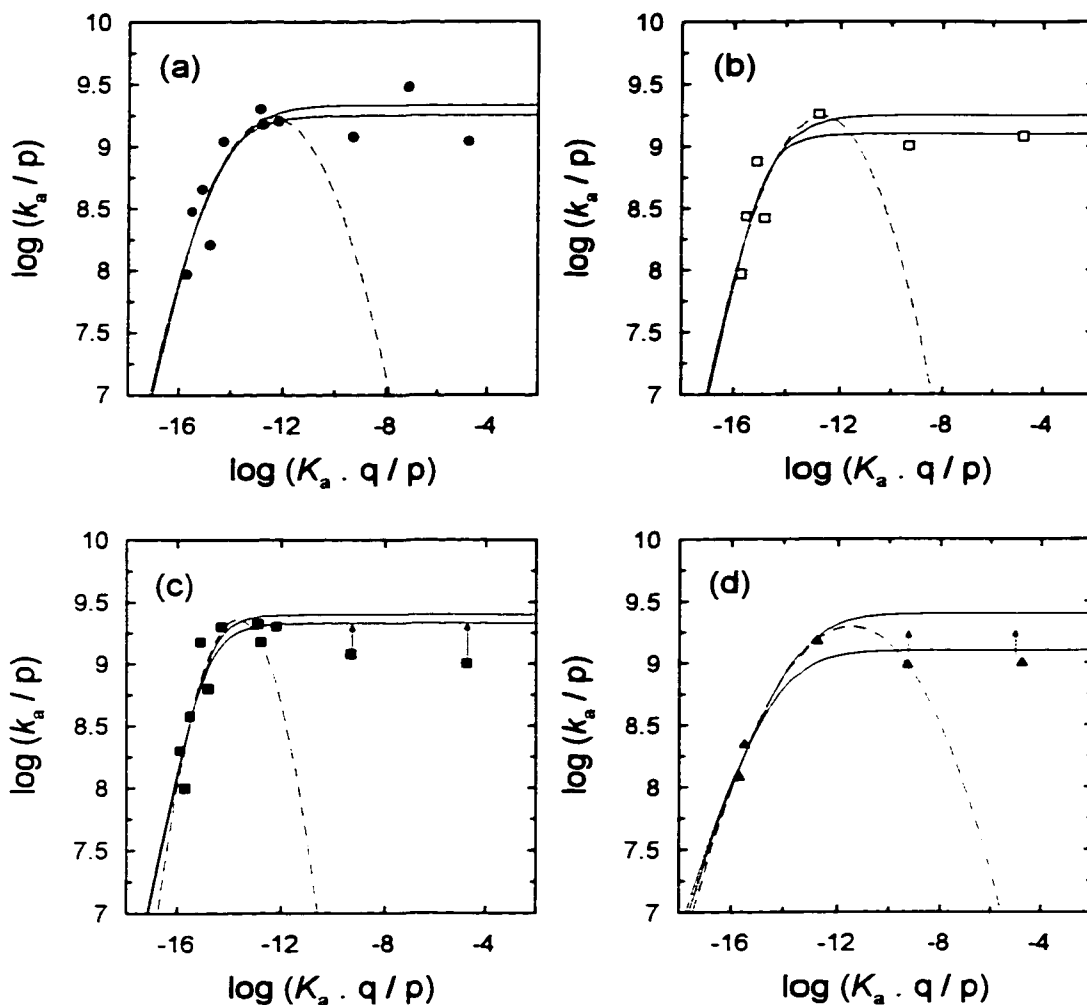
FIGURE IV-2. Brönsted plot for the protonation of (a) Ph(Me₃SiO)C: (filled circles, ●), of (b) 4-MeC₆H₄(Me₃SiO)C: (open squares, □), of (c) 4-MeOC₆H₄(Me₃SiO)C: (filled squares, ■), and of (d) β-C₁₀H₇(Me₃SiO)C: (filled triangles, ▲), all in acetonitrile at 20 °C. The upper solid lines are theoretical Eigen curves (see text) where $k_d = 3.2 \times 10^9$ M^{-1} s^{-1} and $k_{-d} = 1 \times 10^{10}$ s^{-1} (see Table 3), the lower solid lines are theoretical Eigen curves where $k_{-d} = 1 \times 10^{10}$ s^{-1} (see Table 3), and the dashed line is the Marcus curve through the data.

Table IV-3. Parameters derived from curve fitting of the data for proton transfer to oxygen substituted carbenes to Equation IV-18.

Carbene	log k_d	log k_{-d}[b]	log k_p (at $\Delta pK = 0$)	K_{ass}	pK_a^{CH+} in water (in MeCN)
DMOC:	9.27 ± 0.26	8.0	7.19 ± 0.31[a]	-	11.2 ± 0.2 (~25)
	9.27 ± 0.16	9.0	8.18 ± 0.31[a]	-	11.2 ± 0.2 (~25)
	9.5[b]	10.0	8.92 ± 0.23	-	11.0 ± 0.1 (~25)
	9.27 ± 0.16	10.0	9.18 ± 0.31[a]	-	11.2 ± 0.2 (~25)
	9.27 ± 0.16	11.0	10.2 ± 0.32[a]	-	11.2 ± 0.2 (~25)
	9.5[b]	10.0	9.19 ± 0.32	5.8 ± 2.2 x 10^{-1}	11.2 ± 0.2 (~25)
	10.6[b]	10.6	9.78 ± 0.32	4.6 ± 1.7 x 10^{-2}	11.2 ± 0.2 (~25)
	9.5[b]	10.0	8.0[b]	-	11.6 ± 0.3 (~26)
	9.5[b]	10.0	9.0[b]	-	11.0 ± 0.1 (~25)
	9.5[b]	10.0	10.0[b]	-	10.9 ± 0.1 (~25)
	9.5[b]	10.0	11.0[b]	-	10.9 ± 0.1 (~25)
	9.5[b]	10.0	12.0[b]	-	10.9 ± 0.1 (~25)
	9.7[b]	11.0	12.0[b]	-	10.6 ± 0.2 (~25)[c]
	10.6[b]	10.6	12.0[b]	-	9.7 ± 0.4 (~24)[c]
IV-3a	9.25[b]	10.0	9.69 ± 0.72	-	14.8 ± 0.6 (~29)
	10.2 ± 2.5	10.0	9.45 ± 0.10	-	14.9 ± 0.6 (~29)
	9.5[b]	10.0	9.45 ± 1.1	6.8 ± 4.0 x 10^{-1}	14.9 ± 0.9 (~29)
	10.6[b]	10.6	10.1 ± 1.1	5.4 ± 3.6 x 10^{-2}	14.9 ± 0.9 (~29)
IV-3b	9.25[b]	10.0	9.8 ± 1.8	-	14.8 ± 0.7 (~29)
	9.10 ± 0.16	10.0	10.3 ± 2.5	-	14.9 ± 0.9 (~29)
	9.5[b]	10	10.3 ± 2.5	4.0 ± 1.5 x 10^{-1}	14.9 ± 0.6 (~29)
	10.6[b]	10.6	10.9 ± 2.5	3.2 ± 1.2 x 10^{-2}	14.9 ± 0.6 (~29)
IV-3c	9.25[b]	10.0	10.7 ± 2.7	-	14.7 ± 2.6 (~29)
	9.33 ± 0.12	10.0	10.3 ± 2.2	-	14.9 ± 0.23 (~29)
	10.6[b]	10.6	10.9	5.4 ± 1.5 x 10^{-2}	14.9 ± 0.22 (~29)
IV-3d	9.25[b]	10.0	~8.9	-	~16 (~30)
	9.10[b]	10.0	~9.1	-	~16 (~30)

[a] These Eigen curves are identical graphically. See reference 221 for discussions on the coupling of diffusion and apparent intrinsic barriers to reaction.
[b] These values were defined and not results from curve fitting of the data.
[c] These curves clearly do not go through the data points.

Although Kirmse, Guth, and Steenken[103] have suggested that the proton transfer reactions to carbenes **IV-3a** to **d** are probably not diffusion controlled because the largest rate constants measured are at least an order of magnitude lower than that of diffusion in acetonitrile $(2-4 \times 10^{10} \text{ M}^{-1} \text{ s}^{-1})$, according to the Eigen model, these proton transfers can be diffusion controlled even when the rate constants are far below the diffusion controlled limit provided that the reactions are reversible. In fact, the actual proton transfer step may never be fully rate determining, even at small values of ΔpK, provided that the reactions are intrinsically fast. Normal acid/base behaviour in these carbenes and their conjugate acids also explains the lack of significant isotope effects.[a]

For carbenes **IV-3a** to **d**, the computed intrinsic barriers were 1-3.7 kcal/mol. The pre-equilibrium model predicted lower values for the intrinsic barriers to proton transfer (1-2.4 kcal/mol) as compared to those predicted by the three step model. The variation within each model then depends on what values of k_d and k_{-d} are used. Within experimental error, the pK_a's for the conjugate acids of carbenes **IV-3a** to **d** were all ~15 (water, ~ 29 in acetonitrile), regardless of which theoretical model was used, suggesting that there isn't a significant substituent effect on the acid dissociation constant for phenyl(trimethylsiloxy)carbenium ion (the conjugate acid of phenyltrimethylsiloxycarbene). This is not surprising since π-donor substituents interact favourably with both the empty p-orbital of the carbene and the conjugate acid carbenium ion, resulting in ground state stabilization of both the reactant and

---

[a] Kirmse and coworkers[103] measured rate constants for the protonation of α- and β-naphtholate anions by $HClO_4$ in acetonitrile $(k_{H^+} \sim 4 \times 10^{10} \text{ M}^{-1} \text{ s}^{-1})$. Larger intrinsic barriers for proton transfers to carbenes **3a-d**, compared with those for the protonation of α- and β-naphtholate anions, combined with pre-association mechanisms for carbenes **3a-d** would explain the apparent discrepancy. The pre-association mechanism proposed by Kirmse and coworkers involves proton transfer through a second molecule of alcohol. This type of mechanism is analogous to the Swain-Grunwald mechanism for "normal" acids/bases in water.[198,199] Such mechanisms do not display detectable kinetic isotope effects. However, at low concentrations of alcohol, the pre-association mechanism probably doesn't occur in favour of a direct mechanism since the carbenes have a finite lifetime (~100-200 ns) in solution. A pre-association mechanism, where the acid is not bulk solvent, requires two molecules of acid and two diffusional steps prior to proton transfer.

the product and a small change in $\Delta\Delta G°$. Conversely, π-acceptor substituents should cause ground state destabilization of both carbene and conjugate acid carbenium ion. In both cases the bond order between the carbene carbon and the attached group (aryl in this case) bearing the substituent doesn't change dramatically after proton transfer. The situation is quite different from that of the acid dissociation constants for benzoic acids or phenols where the stabilities of the protonated forms are not dramatically affected by the presence of substituents.
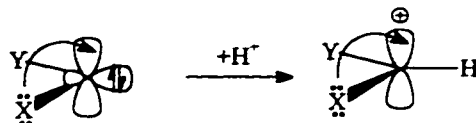
Since the carbenes (**DMOC:,3a-d**) have finite lifetimes in solution, the reactions may not be reversible (i.e. no internal return). For such cases Marcus theory can be used to explain curvature in Brönsted plots. It is important to note that both models give similar values for the pK_a^{CH-}'s of each carbene conjugate acid.

IV.2. Brönsted Relations and Marcus Theory.

IV.2.a. Proton Transfer to Dimethoxycarbene

Curvature in Brönsted plots can also be evaluated with Marcus rate theory[210,211] by taking advantage of the relation in eq IV-16, where w^r is the work required to bring the reactants into a reaction complex, $\Delta G_o^{\ddagger}$ is the intrinsic reaction barrier, $\Delta G^{\ddagger}$ is the overall free energy of activation, and $\Delta G°$ is the difference in free energy between the reactants and the products.[211] The slope parameter α is defined by the differential in equation 8, and differentiation of $\Delta G^{\ddagger}$ with respect to $\Delta G°$ in eq IV-16 gives an alternative mathematical representation for α in eq IV-17. The second derivative in eq IV-18 reflects the change in α as a function of the intrinsic barrier for reaction ($\Delta G_o^{\ddagger}$), implying that intrinsically fast reactions will show more distinct curvature in Brönsted plots than will those with

large intrinsic barriers.

$$\Delta G^{\ddagger} = w^r + \left(1 + \frac{\Delta G^{\circ}}{4 \Delta G_o^{\ddagger}}\right)^2 \Delta G_o^{\ddagger} \qquad \text{(IV-16)}$$

$$\alpha = \frac{\partial \Delta G^{\ddagger}}{\partial \Delta G^{\circ}} = \left(1 + \frac{\Delta G^{\circ}}{4 \Delta G_o^{\ddagger}}\right) / 2 \qquad \text{(IV-17)}$$

$$\frac{\partial \alpha}{\partial \Delta G^{\circ}} = \frac{1}{8 \Delta G_o^{\ddagger}} \qquad \text{(IV-18)}$$

For proton transfer reactions that are bimolecular and are highly exoenergetic, the maximum rate constants for reaction are limited by the rate constants for diffusional encounter of the reactants, usually approximated to be ~ 10^{10} $M^{-1} s^{-1}$. A value of 2.4×10^9 $M^{-1} s^{-1}$ for the rate constant for reaction between dimethoxycarbene and acetic acid in acetonitrile implies that the reaction is partially diffusion controlled and more than likely exothermic, which is inconsistent with the calculated value of α = 0.66[206] from eq IV-2.

After statistical correction for the number of equivalent acidic sites on the protonating species (q), least-squares fitting of the quadratic expression in eq IV-19 to the data in Table 1 yielded a smooth curve (Figure 1) with the following coefficients: a = 7.17, b = -0.715 , c = -0.0552. The data do not follow the inverted region of the Marcus parabola presumably because of a change in rate determining step (i.e. diffusion controlled encounter). The correlation coefficient (R) is 0.996, which is statistically a better fit than that to a straight line (R = 0.929). Eq IV-19, is a form of eq IV-16, after substitution of eqs IV-20 and 21, followed by rearrangement.

$$\log (k_a / p) = a + b \log (K_a \cdot q / p) + c \log (K_a \cdot q / p)^2 \qquad \text{(IV-19)}$$

$$\Delta G^\circ = -RT \ln K \qquad \text{(IV-20)}$$

$$k = \frac{k_B T}{h} e^{\left(-\frac{\Delta G^{\ddagger}}{RT}\right)} \qquad \text{(IV-21)}$$

After substitution and rearrangement in eq IV-16 and IV-19, coefficients a, b, and c yielded values

of the Marcus theory parameters[210,211] for the work required to bring the reactants into a reaction

complex, $w^r \approx 4.5$ kcal mol^{-1}, and for the intrinsic reaction barrier, $\Delta G_o^{\ddagger} \approx 1.5$ kcal mol^{-1}. The

calculated value for the intrinsic barrier to proton transfer to dimethoxycarbene, although semi-

quantitative due to the lack of thermodynamic data for the protonating acids in acetonitrile solutions,

indicates that proton transfer to the carbene carbon is an intrinsically fast reaction akin to those of

normal acids/bases. The value of the intrinsic barrier computed here may in fact be too low as the

influence of diffusion may not be accounted for properly in the Marcus model.[213] Presumably the work

term accounts for diffusional encounter but does not account for the diffusional separation of the

products.

IV.2.b. Proton Transfer to Aryltrimethylsiloxycarbenes.

Marcus rate theory[210,211] was also applied to the data in Table IV-2 in a fashion analogous to that

applied to the data for dimethoxycarbene protonation. In each case, the rate constants for proton

transfer by acids with pK_a's of 12 and higher (in water) were essentially the same; this is the portion of

the Brönsted plots where $\alpha \approx 0$ and diffusion is at least partially rate determining. Therefore, data for

only those acids with p$K_a \leq 12$ were fitted to the quadratic expression in eq IV-19. The data do not

follow the inverted region of the Marcus parabola presumably because of a change in rate determining

step (i.e. rate limiting diffusion controlled encounter). Least-squares fitting of the data to the quadratic expression in eq IV-19 gave coefficients a, b, and c which yielded values of the Marcus theory parameters of 0.8, 0.7, 0.3, and 1 kcal mol^{-1} for the intrinsic reaction barriers ($\Delta G^{\ddagger}_o$), and 4.9, 4.8, 4.7, and 7 kcal mol^{-1} for the work terms (w^r), for phenyltrimethylsiloxycarbene (**IV-3a**), 4-methylphenyl(trimethylsiloxy)carbene (**IV-3b**), 4-methoxyphenyl(trimethylsiloxy)carbene (**IV-3c**), and β-naphthyl(trimethylsiloxy)carbene (**IV-3d**), respectively.

Although the differential in eq IV-17 is correct, it cannot be applied directly to the Brönsted plots in Figures IV-1 and 2 because ΔG^o in eq IV-16 and IV-17 is the free energy change for the reaction whereas log K_a^{AH} (see eqs IV-11 and 12), which can be converted to free energy using eq IV-20, is representative of the free energy for only part of the reaction. These values are proportional because the pK_B (or the pK_a of the conjugate acid) of the carbene is constant throughout, however, without the knowledge of the pK_a of the conjugate acid of the carbene the free energies for proton transfer to carbenes **DMOC:**, and **IV-3a** to **d** (ΔG^o which is equal to -RT ln $K_{C:}$, $K_{C:}$ is defined in eqs IV-22 and 23) remain unknown.

$$\text{AH} + \text{X}\underset{\cdot\cdot}{\diagup}\text{Y} \xrightleftharpoons{K_{C:}} \underset{H}{\text{X}\overset{\oplus}{\diagup}\text{Y}} + \text{A}^{\ominus}$$

(IV-22)
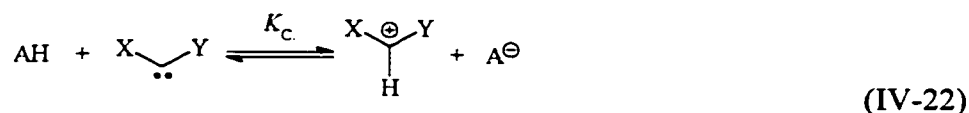
$$K_{C:} = \frac{K_a^{AH}}{K_a^{CH+}}$$

(IV-23)

Instead, one can determine the tangents to the curves in the Brönsted plots in figures IV-1 and 2 by determining the first derivative of the quadratic expression in eq IV-19 (eq IV-24). Coefficients b and c come from the least-squares fitting of the data to eq IV-24 and substituting those values and values for log (K_a q/p) into eq IV-24 yields values for α (the slope of the tangent at a point on the graph).

Likewise, one may substitute values for b, c, and α into eq IV-24 and determine which point on the curve corresponds to a particular value of α.

$$\alpha = \frac{\partial\,[\log\,(k_{HA}\,/\,p)]}{\partial\,[\log\,(K_{A}\,.\,q\,/\,p)]} = b + 2c\,.\,[\log\,(K_{A}\,.\,q\,/\,p)] \qquad\qquad \text{(IV-24)}$$

In this manner log (K_a q/p) values where α equals 0, 0.5, and 1 were computed using the quadratic expression (eq IV-19) for the Brönsted curve for the protonation of dimethoxycarbene. These values of α are the slopes of the tangent lines to the curve at points (log K_a , log k_a) = (-6.48 , 9.49), (-11.0 , 8.34), and (-15.5 , 4.99) respectively, Figure IV-3. Since α can be considered to be a measure of transition state structure, a reasonable approximation for the point on the Brönsted curve where the acid/base reaction is thermoneutral (i.e. ΔG° = 0) is the point where the transition state lies exactly half way between reactants and products (α = 0.5).[216] If the proton transfer reaction between an oxygen centered Brönsted acid and dimethoxycarbene reaction is to be considered thermoneutral then K_C in eq IV-22 must equal unity, and $K_a{}^{AH}$ must equal the acid dissociation constant for the conjugate acid of dimethoxycarbene, $K_a{}^{CH+}$ (eq IV-23). The tangent to the curve with slope of α = 0.5 at the point (-11.0 , 8.34) therefore suggests that the log $K_a{}^{CH+}$ for the conjugate acid of dimethoxycarbene is approximately -11.0 (water) and that the pK_a for dimethoxycarbenium ion is ~ 11.0 (water, ~ 25 in acetonitrile). In fact, substituting the calculated values for the intrinsic barrier and work term for proton transfer to dimethoxycarbene into eq IV-16, with ΔG° = 0, gives a value of ~ 6 kcal/mol for the free energy of activation ($\Delta G^{\ddagger}$) when the reaction is thermoneutral. This value corresponds to a bimolecular rate constant of k_a $\approx$ 2.0 x 10^8 M^{-1} s^{-1} (log k_a = 8.30), which corresponds to the point (-11.1 , 8.30) on the Brönsted curve (by solving the quadratic expression in equation 24) indicating that the interpretations here are, at least, self-consistent.
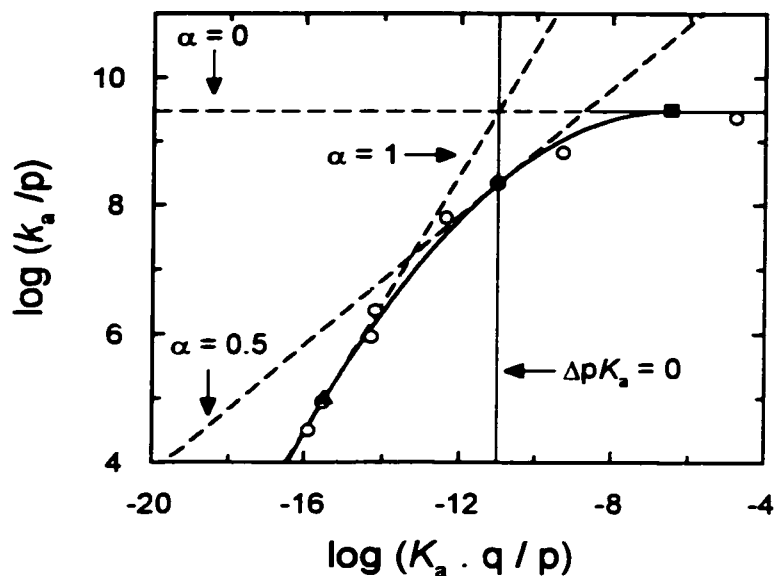
Figure 3. Tangents to the Brönsted curve for the protonation of dimethoxycarbene at $\alpha = 0$, 0.5, and 1.0 (dashed lines). The equations for the tangent lines were determined using equations 4, 10, and 18. The points on the Brönsted curve where the slope of the tangent equals 0, 0.5, 1.0 (i.e. $\alpha = 0$, 0.5, and 1) are indicated by the filled square (■), the filled circle (●), and the filled triangle (▲), respectively. Where the slope of the tangent to the curve equals 0.5 ($\alpha = 0.5$, thermoneutral reaction) $\log K_a$ for a protonating acid equals the $\log K_a$ for the conjugate acid of dimethoxycarbene ($\Delta pK_a = 0$, solid vertical line).

Table IV-4. Intrinsic barriers ($\Delta G^{\ddagger}_o$) and Marcus work terms (w^r) for proton transfer to oxygen substituted carbenes and the pK_a values of the conjugate acids.

Carbene	$\Delta G^{\ddagger}_o$, kcal mol^{-1}	w^r, kcal mol^{-1}	pK_a of conjugate acid in water (in MeCN)
1	1.5	4.5	~11 (~25)
IV-3a	0.8	4.9	~15 (~29)
IV-3b	0.7	4.8	~15 (~29)
IV-3c	0.3	4.7	~15 (~29)
IV-3d	~1	~7	~15 (~29)

Similarly, points on the Brönsted plots pertaining to **IV-3a** to **d** (Figure IV-2), where the slopes of the tangents to the curves (α) are equal to 0.5, were calculated and estimates for the pK_a's of the conjugate acid carbenium ions were computed as described above. These values are summarized in Table IV-4. All the $pK_a^{CH^+}$ values are consistent with those determined using the Eigen theoretical model.

II.3. Variation in Transition State Structure.

Substitution of the intrinsic barriers determined for dimethoxycarbene and aryltrimethylsiloxycarbenes **IV-3a** to **d**, from the coefficients of quadratic Brönsted correlations, into the partial derivative in eq IV-18 allow for the evaluation of the change in α as a function of the change in ΔG° for proton transfer reactions to these carbenes. For dimethoxycarbene, α is predicted to change from a value of 1 to a value of 0 over a $\Delta\Delta G^\circ$ range (12 kcal / mol) which corresponds to a range of ~9 pK_a units for the protonating acids. This change in α corresponds to a change in transition state structure, from very product-like (α=1) to essentially reactant-like (α=0). Similarly, α values for arylsiloxycarbenes **IV-3a** to **d** are predicted to change from $\alpha \approx 1$ to $\alpha \approx 0$ over pK_a ranges of ~5, ~4, ~2, and ~6, respectively. Such dramatic changes in the slope parameter α and in transition state structure are typical for "normal" acids and bases where α changes from near 0 to near 1 over a $\Delta\Delta G^\circ$ range which corresponds to ~4 pK_a units,[200] but are rarely observed in carbon acids and bases.

IV.4. "Normal" Acid/Base Behaviour.

The fact that the Brönsted plots for carbenes **DMOC:** and **3a-d** are all curved and that theoretical Eigen curves or Marcus parabolas can be drawn through these data provides strong evidence that these π-donor substituted carbenes behave as "normal" Brönsted bases. The dramatic change in the

slope parameter α (and in transition state structure) over a narrow range of ΔpK of the protonating acids for these carbenes is also consistent with normal acid/base behaviour. Brönsted plots for the protonation of normal bases typically change slope from unity to zero over a ΔpK$_a$ range of ~4 units.[197, 200]

Small intrinsic barriers to proton transfer are also common for "normal" acids and bases and intrinsic barriers of 1-5 kcal/mol, computed for carbenes **DMOC:** and **3a-d**, are consistent with their "normal" acid/base behaviour. Examples of other carbon bases, which have small intrinsic barriers to proton transfer reactions and show some "normal" acid/base behaviour, include cyanide,[212c, 217] acetylide,[218] C-2 thiazolium ions,[201-203] the C-2 ylide of thiamin,[203] and C-2α anions of covalent intermediates of thiamin.[219] The small intrinsic barriers determined here for dimethoxycarbene and carbenes **IV-3a** to **d** support the idea that electron delocalization, rehybridization (carbenes do not undergo a change in hybridization either during or after proton transfer), changes in bond lengths and angles of heavy atoms, and changes in solvation do not significantly effect the barriers to proton transfer to these π-donor substituted carbon bases as is the case for other carbon acids and bases with larger intrinsic barriers to proton transfer. Presumably the most stable ground state conformations of these carbenes are those where the π-donor substituents (methoxy and aryl) are already aligned with, and are already donating electron density to, the vacant p-orbital at the carbene carbon so that bond angles, lengths and electron delocalization do not change dramatically at the transition state for proton transfer.

Other criteria for evaluating "normal" acid/base behaviour such as acid inhibition cannot be evaluated in acetonitrile solvent because of the increased rate constants for reaction by oligomeric acids at higher concentrations of acid, and clearly the Swain-Grunwald mechanism does not apply in this solvent system although the participation of a second molecule of acid in a reaction complex has been proposed previously.[103] It is evident that oxygen substituted carbenes behave very much like

"normal" Brönsted bases.

IV.5. Conclusions.

Brönsted plots for proton transfer data for dimethoxycarbene and for aryltrimethylsiloxycarbenes **IV-3a** to **d** show distinct Eigen curvature which is characteristic of reactions between "normal" acids and bases. Values of α that are near 1 when proton transfer is thermodynamically unfavourable and near 0 when proton transfer is thermodynamically favourable, combined with rate constants of $\sim 10^9$ M^{-1} s^{-1} for thermodynamically favourable proton transfer reactions, support the notion that these carbenes behave as "normal" Brönsted bases. Values for intrinsic barriers $(\Delta G^{\ddagger}_o)$, calculated from Eigen curves and using the Marcus theory formalism, indicate that these reactions are intrinsically fast, which provides further support for "normal" acid/base behaviour. A consequence of "normal" acid/base behaviour is that proton transfers in the thermodynamically favourable direction proceed with maximum rate constants of $\sim 10^9$ M^{-1} s^{-1}, and that proton transfer may be reversible depending on the lifetimes of the carbenes and their conjugate acids (carbocations) in solution. Ultimately, curvature in the Brönsted plots for dimethoxycarbene and for aryltrimethylsiloxycarbenes **IV-3a** to **d** can be explained by changes in the rate determining step for proton transfer as a function of the pK_a for the protonating acid and/or by variation in transition state structure, near $pK = 0$, according to the Hammond postulate. Estimates for pK_a values of the conjugate acids of carbenes **DMOC:** and **3a-d** have been computed directly from Eigen curves and from tangents to Marcus parabolas (α values at individual points on the curves). The pK_a values computed by both methods are roughly the same for each carbene. These pK_a values are 11 (water, ~ 25 MeCN) for dimethoxymethyl cation and ~ 15 (water, ~ 29 in MeCN) for aryltrimethylsiloxymethyl cations **IV-4a** to **d**.

Chapter 5.

Alkanediazonium ions and Carbocations Generated Photochemically from Oxadiazoline Precursors in Acidic Media.

V. General Introduction.

This chapter contains results and discussions regarding rate constants for proton transfer to diazoalkanes and rate constants and products from the ensuing cations. Oxadiazolines were used as a convenient photochemical source of diazoalkanes according to the general Scheme below (Scheme V-1).

Scheme V-1.

Scheme V-1 continued.

V-1a: R³= Me;
V-1b: R³= OMe.   **V-1c**   **V-1d**   **V-1e**

V-1f   **V-1g**   **V-1h**   **V-1i**
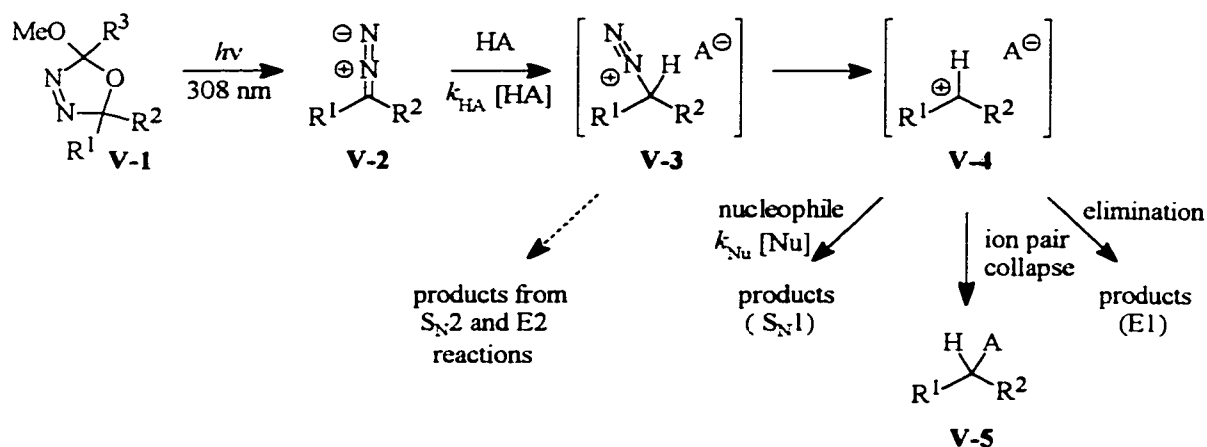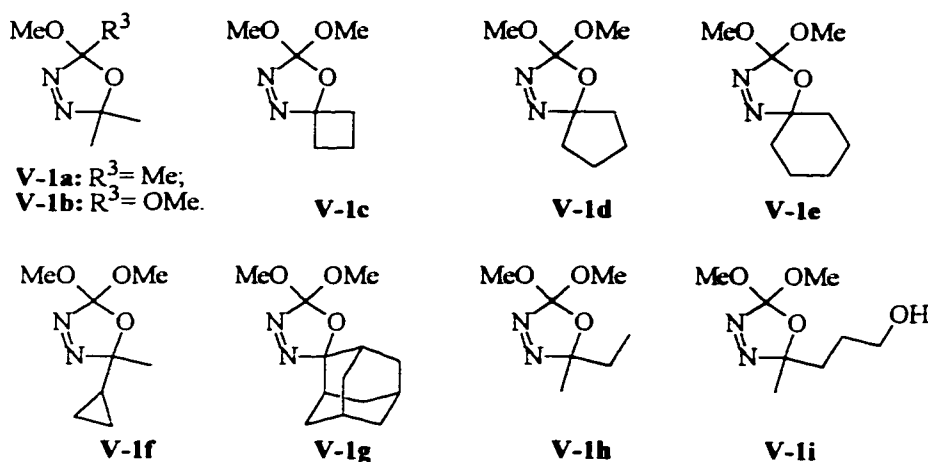
Although oxadiazolines were used as precursors, the chemistry and background literature is quite different from that found in other chapters. The relevant background is presented in the following section.

V.1. Background.

Diazonium ion intermediates have been of considerable interest since their discovery by Griess in 1861.[220] Diazoalkanes and their conjugate acids, diazonium ions, are important reactive intermediates which have been implicated in the carcinogenicity and mutagenicity of N-alkyl-N-nitroso compounds.[221] It has been postulated that N-alkyl-N-nitroso compounds are oxidatively converted to alkanediazoates and alkanediazoic acids, in biological organisms, and that these intermediates then decompose to give alkanediazonium ions which react with biological nucleophiles, including DNA, giving rise to intracellular damage. The carcinogenic properties of N-alkyl-N-nitrosamines were first recognized in the late 1960's.[222] There are several different classes of carcinogenic nitroso compounds

including N-nitrosamines, N-nitrosamides, N-nitrosoureas, and N-nitro-N-nitrosoguanidines. The metabolism of N-nitrosamines is thought to occur by enzymatic hydroxylation (cytochrome P_{450} dependant) of one of the α-aminocarbons.[223] The intermediate then undergoes a heterolytic cleavage resulting in an alkanediazoic acid and an aldehyde[223,224] as in eq V-1. The (E)- and (Z)-isomers[225] of alkanediazoates and their conjugate acids (alkanediazoic acids) have been shown to decompose in aqueous medium yielding alkanediazonium ions.[226]

(V-1)
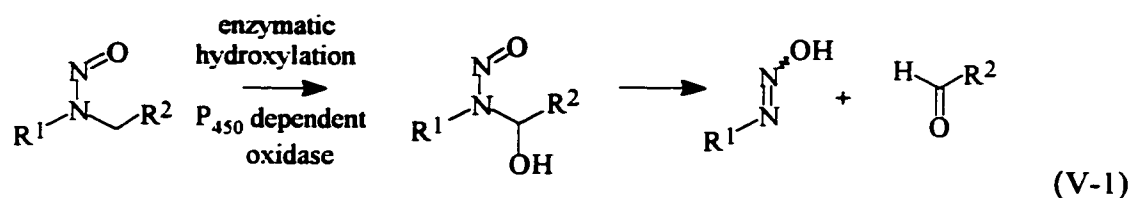
N-Alkyl-N-nitroso compounds of the type in Scheme V-2 can lead to the formation of diazoalkanes in biological systems.[227] There are several examples of methylation of DNA bases by compounds of this general type in biological systems. Those compounds decompose to give diazomethane and not methanediazonium ion (at least not directly), which was proven by isotopic labeling of the starting material.

Scheme V-2. Formation of Diazoalkanes from N-Alkyl-N-Nitroso Compounds.
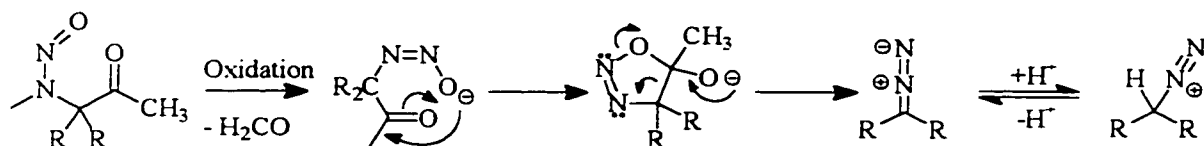
Alkylation of the DNA bases adenine, guanine, cytosine, and thymine can occur at both ring nitrogen atoms and at oxygen. The O-alkylation of guanine is apparently more harmful than N-alkylation.[228]
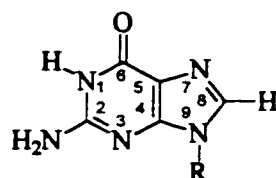
Guanine Residue

N-Methyl-N-nitrosourea,   N-methyl-N-nitro-nitrosoguanidine,   N-nitroso(1-

acetoxyethyl)methylamine, and diazomethane all show identical alkylation patterns with a sequence

characterized DNA restriction fragment.[229] It has been shown that methylation by N-nitroso

compounds occurs selectively at N^7 of guanine[230] with sequence selectivity attributed to the sequence

dependent changes in nucleophilicity.[228] This is in contrast to patterns of ethylation which occurs at

both oxygen and nitrogen. It has been postulated that *secondary*, and *benzyl* derivatives decompose

via cationic intermediates, rather than diazonium ions, and that observed selectivities are the result of

preferential solvation of alkanediazoates prior to decomposition.[226b] Notable exceptions are diazonium

ions which contain trifluoroethyl substituents.

Detailed kinetic studies on methyl, primary, and secondary alkanediazoates in aqueous medium of

varying pH have been performed (Scheme V-3).[226]

Scheme V-3.
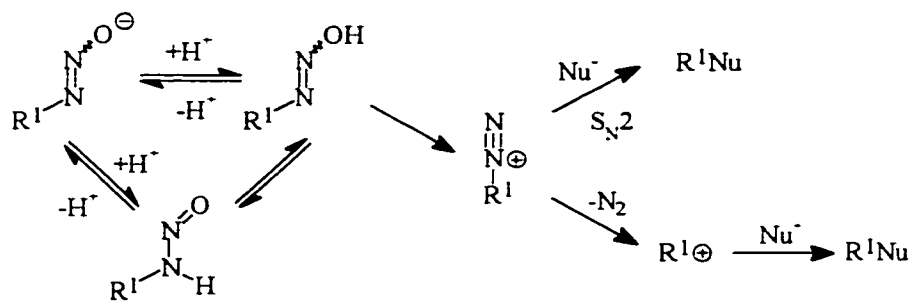
These studies focus mainly on mechanisms for the decomposition of alkanediazoates. In general, both

(E) and (Z) alkanediazoates decompose *via* protonation at diazoate oxygen which is followed by loss

of hydroxide ion to give diazonium ion/hydroxide ion pairs. It is important to note that 2,2,2-trifluoroethanediazonium ion,[226d] 3,5-bis(trifluoromethyl)phenylmethanediazonium ion,[234b] and 1-aryl-2,2,2-trifluoroethanediazonium ions[226a] have been implicated as "free" intermediates with significant lifetimes in solution based on deuterium incorporation from D_2O and on observed selectivities toward nucleophiles (azide ion vs. solvent), whereas other diazonium ions are thought to give rise to carbocations which then react within the solvent cage.[226]

Understanding aliphatic diazonium ion reactivities has been challenging, because they are highly reactive electrophilic intermediates which are difficult to observe directly as a result of their proclivity for molecular nitrogen loss, leading to the formation of carbocations.[231] Additional complexities arise due to difficulties in distinguishing between S_N2, S_N1, and intermediate mechanisms.[232] As a result, reactivities of these biologically relevant electrophiles are not well understood. In general, diazonium ion stabilities as a function of substituent are thought to be opposite to those of carbocations. That is, alkanediazonium ions (dinitrogen stabilized carbocations) will lose N_2 more readily as the stability of the resulting carbocations increases.

Direct observation of the methanediazonium ion has been accomplished in superacidic media (eq V-2).[233] In solutions of FSO_3H/SO_2ClF protonation occurs only at carbon, however, in stronger superacids (FSO_3H-SbF_5/SO_2ClF), protonation was observed to occur at both carbon and at nitrogen to give methylenediazenium ion as a minor species.

$$(V-2)$$
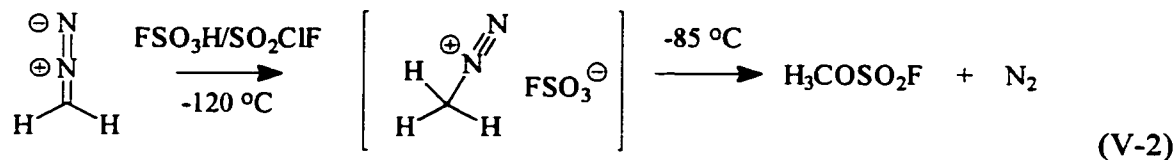
2,2,2-Trifluoroethanediazonium ion has been observed in superacid solutions.[234] This is the only example of an observable primary alkanediazonium ion, indicating that dediazotization is generally too facile even at low temperatures. It is possible that a hydride shift concerted with loss of N_2, a pathway not available in the 2,2,2-trifluoroethanediazonium ion, is responsible for vanishingly small lifetimes of these intermediates.

McGarrity and Smyth performed kinetic studies on the hydrolysis of diazomethane using a stopped-flow spectrometer and a novel continuous flow pH meter.[235] The reaction between diazomethane and hydronium ion was studied in THF-water (60:40 v/v) solutions and the bimolecular rate constant for protonation of diazomethane by hydronium ion was estimated to be $k_{H^-} \approx 4 \times 10^8$ M^{-1}s^{-1}, at 25 °C. Based on results obtained from both instruments, the rates of nucleophilic attack of water and hydroxide ion onto methanediazonium ion were also estimated to be 1.8 s^{-1} and 1×10^4 M^{-1} s^{-1}, respectively. The magnitudes of these rate constants for reaction of methanediazonium ion imply that it has a considerable lifetime in aqueous solution and that there is a significant barrier to nucleophilic substitution of molecular nitrogen (S_N2). The results of isotope-exchange studies show that water is a better nucleophile than a base with respect to methanediazonium ion, whereas hydroxide reacts more rapidly as a base than as a nucleophile. Fishbein et al. have also measured the rates of reaction of methanediazonium ion with water in basic media.[226c]

The heat of formation of methanediazonium ion (223 kcal/mol) was first measured by Foster and Beauchamp by ion cyclotron resonance spectroscopy,[236] and has since been re-measured to be 209.4 kcal/mol,[237] and 212.9 kcal/mol,[238] by photoionization. With a value of 261.2 kcal/mol for the heat of formation of the methyl cation,[239] the three heats of formation given correspond to methyl cation affinities for N_2 of 38.2, 51.2, and 48.3 kcal/mol, respectively, indicating that the dissociation of

molecular nitrogen from methanediazonium ion to form methyl cation is an energetically unfavourable process. Calculations performed using *ab initio* methods agree closely with those determined experimentally giving a value of 42.2 kcal/mol for the methyl cation affinity for N_2.[240] The ethyl cation affinity for N_2 was calculated to be 11.5 kcal/mol which corresponds to a difference of 30.7 kcal/mol for the dissociation of molecular nitrogen from methane- and ethanediazonium ions. This difference is attributed to the intervention of the nonclassical (bridged) ethyl cation as well as differences in the electrostatic contribution to CN binding and smaller stabilization of the cation by N_2. Calculations also indicate that charge transfer between the hydrocarbon fragment of alkanediazonium ions and N_2 is small and that most of the charge remains localized on the CN carbon atom.[241]

Although methanediazonium ion is known to undergo nucleophilic attack via an S_N2 process, much controversy has surrounded the mechanisms by which *primary*-alkanediazonium ions partake in nucleophilic substitution.[221,226] The idea that products from *primary*-alkanediazonium ions arise from *primary* carbocations has endured, despite strong theoretical evidence that the dissociation of molecular nitrogen is endothermic. Recently, the stereochemical investigation of nucleophilic substitution on optically active [1-^{2}H]butanediazonium ion and [1-^{2}H]-2-methylpropanediazonium ion has shown that these intermediates undergo nucleophilic substitution by an S_N2 pathway (complete inversion of configuration, >92 % ee, Scheme V-4).[242]

The observation of 2-butyl products from the nitrous acid deamination of 1-butylamine indicates that dissociation of molecular nitrogen is competitive with nucleophilic substitution (eq V-3).

$$(V-3)$$
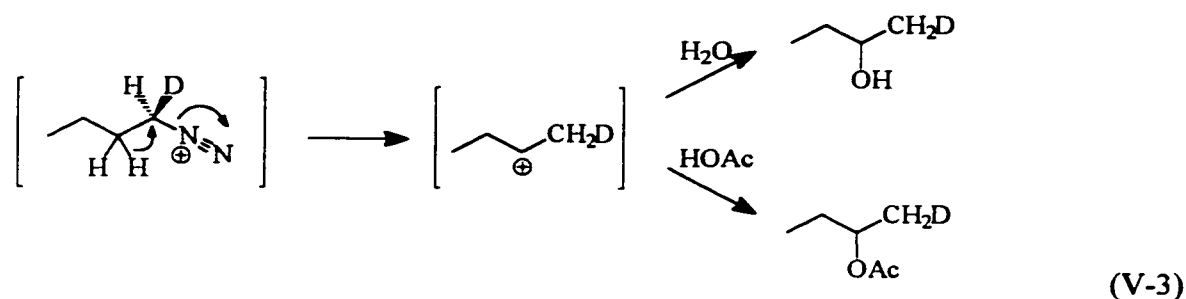
Scheme V-4. Stereochemical Cycle for Determining the Mechanism of Nucleophilic Attack onto *Primary*-Alkanediazonium ions.
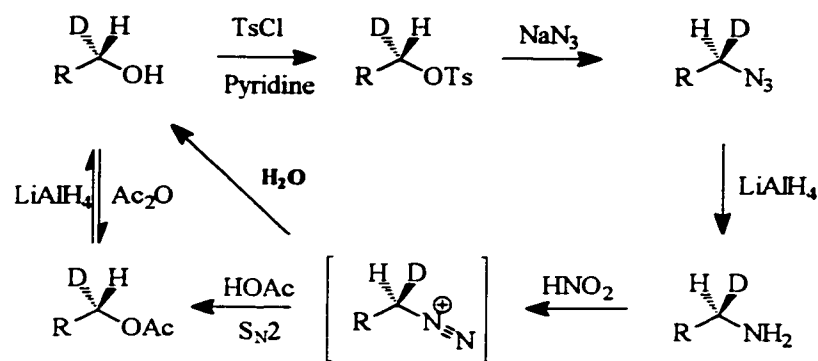
However, since racemization was not observed at the primary center, it is likely that N_2

dissociation is concerted with a hydride shift resulting in the formation of a *secondary* carbocation.

Favorable conformations for this hydride shift are illustrated with the Newman projections below.
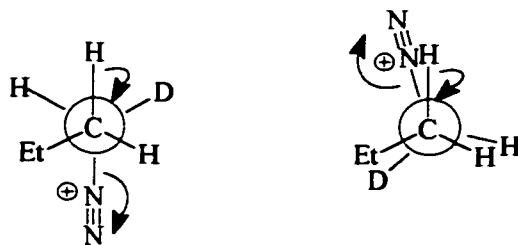
Also, it has been shown that the ratio k_{LiN3} / k_{MeOH} for 1-butanediazonium ion and 1-

hexanediazonium ion are 17.6 and 18.4 respectively which are higher (i.e. more selective) than would

be expected for primary or secondary carbocations.[243] These numbers are close to that found for solvolysis of t-BuBr.[243]

In contrast to methanediazonium ion and *primary* alkanediazonium ions which undergo nucleophilic substitution by a coupled process (S_N2), *secondary* diazonium ions have been considered to be too unstable relative to the corresponding cation intermediate to exist as intermediates themselves.[221,244] Exceptions include 1-phenyl-2,2,2-trifluoroethanediazonium ion[245] and bis(trifluoromethyl)methanediazonium ion[246] which have been observed at low temperatures by NMR in superacids, and 1-cyano-1-propanediazonium ion which partitions between S_N1 and S_N2 mechanisms.[247] The consequence of the diminished lifetimes of diazonium ions is that they alkylate via carbocation intermediates which, depending on their stability will be less sensitive to the relative nucleophilicities of the incipient attacking groups than diazonium ions which react by a concerted mechanism.[a]

Rate constants for protonation of several different *sec*-diazoalkanes by various acids in aqueous and acetonitrile solutions have been measured by laser flash photolysis of the corresponding oxadiazoline precursor (**V-1**, Scheme V-1). These rate constants and the methods by which they were obtained are presented in a following section.

To evaluate the reactivity of a particular carbocation by direct kinetic methods such as LFP the cations require a UV-visible chromophore in a useful (monitorable) region of the spectrum. In the absence of such a chromophore, or a suitable photochemical precursor,[248] indirect methods based either on competition kinetics[249] or on a kinetic probe reaction[76,69,250] are required. An example of

---

[a]. For examples of such arguments see: ref. 226a and references therein.

such a probe reaction is the "pyridine probe" method,[76,69] which is used to evaluate the reactivities of carbenes which lack suitable chromophores in the UV-visible spectrum.

It was found that 1,3,5-trimethoxybenzene reacts with highly electrophilic carbocations to yield substituted cyclohexadienyl cations which are easily monitored by UV-LFP. The reactions of cations derived from diazonium ions, generated photochemically from oxadiazoline precursors using this probe method, have been investigated. Estimates of the lifetimes of four alkanediazonium ions in 1,1,1,3,3,3-hexafluoro-2-propanol (HFIP), trifluoroethanol (TFE), and acetonitrile have been made. Although we have used 1,3,5-trimethoxybenzene as a probe for specific purposes, we think that the 1,3,5-trimethoxybenzene probe methodology should be applicable in a more general sense.

V.2. Protonation of Diazoalkanes.

Rate constants for proton transfer to the diazo carbon can be conveniently measured by TRIR-LFP by monitoring the diazo stretching band at ~2040 cm^{-1}, or by UV-LFP by monitoring the UV absorption of the diazoalkane at ~230-250 nm. Both absorptions are persistent in solution in the absence of acidic substrates. In the presence of acids, these absorptions decay with pseudo-first order kinetics. Bimolecular rate constants for protonation can then be obtained as the slopes of linear plots of observed rate constants[b] *vs* acid concentration. Dialkylcarbenes have also been generated from oxadiazoline precursors in LFP experiments, however, the major products of steady state irradiations are diazoalkanes (~95-99% yield) and carbene formation can effectively be eliminated by using lower laser power.

---

[b]. It is assumed that protonations are irreversible in all cases, $k_{obs} = k_1$ [HA], based on the propensity for N_2 loss from *sec*-alkanediazonium ions.

The formation of the two products upon 308 nm LFP of **V-1a** in acetonitrile at 25 °C, is readily confirmed with use of time-resolved infrared (TRIR) detection. Absorptions assigned to the diazo band of 2-diazopropane, centered at 2036 ± 3 cm⁻¹, and to the carbonyl band of methyl acetate, centered at 1744 cm⁻¹ (not shown), were formed instantaneously (within the response time of the instrument) from **V-1a**, Figure V-1. Both absorptions were persistent under the experimental conditions. Under identical conditions, 308 nm LFP (UV-VIS detection) of **V-1a** resulted in an instantaneous bleaching of its absorption at 322 nm and was accompanied by the instantaneous appearance of a strong persistent band, centered at 250 nm, assigned to **V-2a**. Both the UV and the IR absorptions assigned to **V-2a** decayed with first order kinetics (τ = 30μs) when trifluoroacetic acid (TFA, 3.0 mM) was present (Figure V-1).
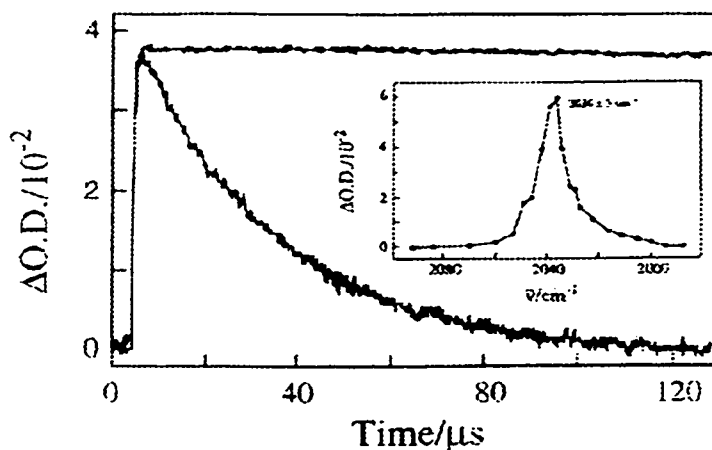
FIGURE V-1. Time-resolved IR absorption traces and spectrum (inset) observed following 308-nm laser flash photolysis of **V-1a** in acetonitrile and in acetonitrile containing 3.0 mM TFA. Decay of absorption of **V-2a** monitored at 2037 cm⁻¹.

Rate constants for protonation of **V-2a** by carboxylic acids with pK_a's ranging from 10 to 23 in acetonitrile,[208] at 25 °C, μ = 0 M, are listed in Table V-1. They were obtained as the slopes of linear plots of observed rate constants (determined from LFP TRIR measurements) *vs* acid concentration. The linear least-squares analysis of log k_a *vs* log K_a of the acids (data adjusted for statistics) by the

Brönsted procedure gave $\alpha \approx 0.25$ (Figure V-2). Alternatively, least-squares fitting of the data to a quadratic expression gave coefficients which yielded values of the Marcus theory parameters[210,211] for the work required to bring the reactants into a reaction complex, $w^r \approx 9$ kcal mol^{-1}, and for the intrinsic reaction barrier, $\Delta G_o^{\ddagger} \approx 7$ kcal mol^{-1}. However, the resulting curve was statistically indistinguishable from a straight line, which best describes the reactivity of V-2a toward the carboxylic acids that were studied.
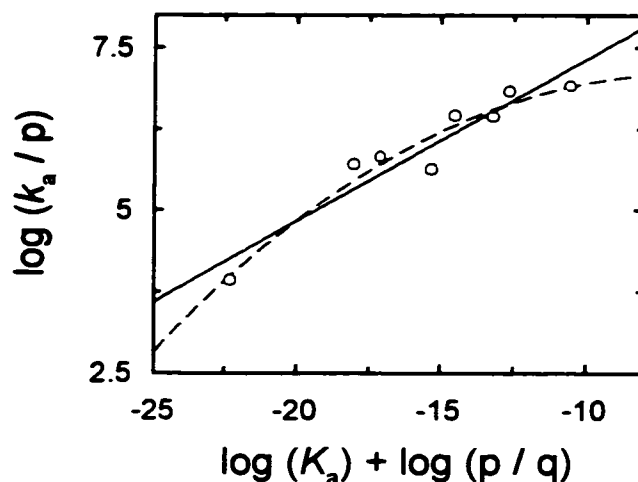
FIGURE V-2. Brönsted Plot for 2-propanediazonium ion formation in acetonitrile. Solid line from linear fit of the data, and dashed line from curve fit of the data.

The reaction between V-2a and hydronium ion was also studied by monitoring decay of the UV absorption of V-2a in aqueous perchloric acid solutions at 25°C, $\mu = 1.0$ M (NaClO$_4$) and the rate constants found were $k_{H^-} = 2.46 \pm 0.07 \times 10^6$ M^{-1} s^{-1} in H$_2$O and $k_{D^-} = 1.32 \pm 0.04 \times 10^6$ M^{-1} s^{-1} in D$_2$O (Figure V-3). The primary kinetic isotope effect for the reaction of hydronium ion with V-2a is $k_{H^-}/k_{D^-} = 1.86$. A Brönsted correlation for the protonation of V-2a with carboxylic acids in aqueous solutions showed a slope ($\sim$0.22) similar to that found in acetonitrile solutions (Table V-1 and Figure V-4).

Table V-1. Observed proton transfer rate constants (k_a) for the reaction of **V-2a** with carboxylic acids in acetonitrile and in water at 25 °C.[a]

Acid	Acetonitrile		Water	
	pK_a[b]	k_a, M⁻¹·s⁻¹	pK_a[c]	k_a, M⁻¹·s⁻¹
Trichloroacetic	10.57	8.2×10^6	0.70	2.2×10^6
Trifluoroacetic	12.65	6.8×10^6	---	2.2×10^6
		6.9×10^6 [d]		
Dichloroacetic	13.20	2.8×10^6	1.48	1.8×10^6
Oxalic	14.50	2.9×10^6	1.23	---
Malonic	15.3	4.3×10^5	2.83	1.6×10^6
2,3-Dibromopropionic	17.1	6.7×10^5	---	---
Cyanoacetic	18.04	5.1×10^5	2.45	1.2×10^6
Acetic	22.30	8.5×10^3 [e]	4.75	2.9×10^5

[a] Measured by TRIR at 2037 cm⁻¹. Some of the data points were determined by Dr. Brian Wagner (NRC).
[b] The pK_a values of the various acids in acetonitrile were obtained from *The IUPAC Chemical Data Series*No. 35, **1990**, compiled by K. Izutsu.
[c] From (a) Ballinger, P.; Long, F. A. *J. Am. Chem. Soc.***1960**, *82*, 795. (b) Dyatkin, B. L.; Mochalina, E. P.; Knunyants, I. L. *Tetrahedron* **1965**, *21*, 2991. (c) Takahashi, S.; Cohen, L. A.; Miller, H. K.; Peake, E. G. *J. Org. Chem.* **1971**, *36*, 1205.
[d] Measured by UV at 250 nm.
[e] From quadratic fit of k_{obs} vs [acid].
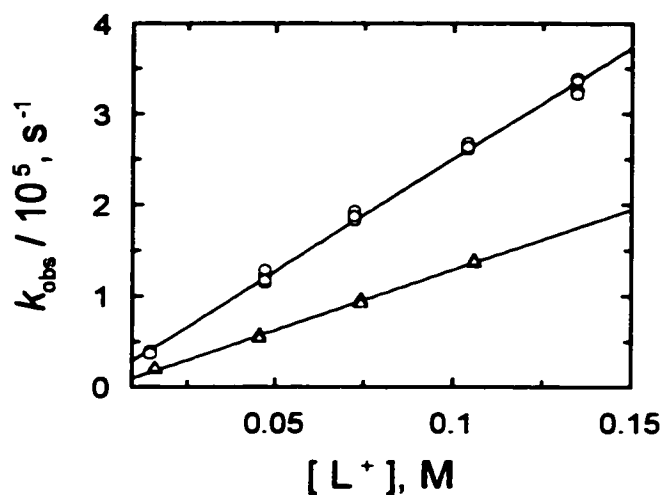
FIGURE V-3. Plots of the change in k_{obs}, for the decay of V-2a, as a function of H$^+$ concentration (○), and as a function of D$^+$ concentration (△), in aqueous perchloric acid solutions, at 25 °C, ionic strength 1.0 M (NaClO$_4$).
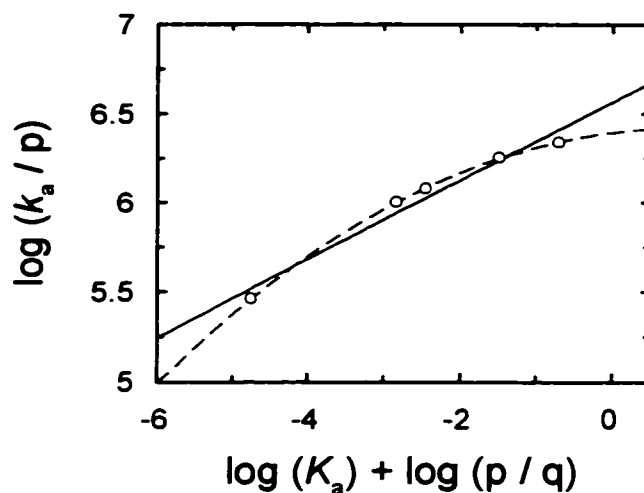
FIGURE V-4. Brönsted plot for 2-propanediazonium ion formation in water. Solid line from linear fit of the data, and dashed line from curve fit of the data.

Rate constants for protonation of diazocyclobutane (V-2c), diazocyclopentane (V-2d), and diazocyclohexane (V-2e) by TFA in acetonitrile at 25 °C were determined from the decays of their UV absorptions upon 308 nm LFP of V-1c to e in acetonitrile. The linear plots of k_{obsd} vs [HA] gave

bimolecular rate constants (k_a) equal to 4.28 ± 0.10 x 10^7 M^{-1} s^{-1}, 1.19 ± 0.03 x 10^7, and 9.17 ± 0.12 x

10^6 for the reaction of TFA with **V-2c** to **e**, respectively.

It is unlikely that the magnitudes of rate constants of proton transfer are governed by diazonium

ion stabilities, given that the observed Brönsted coefficient is consistent with an early, reactant-like,

transition state.[197] It also seems that torsional effects are not dominant since larger eclipsing

interactions for the smaller rings are expected for hybridization changes at the diazocarbon in the

transition state, which would give a trend opposite to that observed experimentally.[216] Thus, it is

concluded that the relative reactivities, **V-2c>V-2d>V-2e**, of the cyclic diazo compounds largely

reflect differences in their ground state stabilities. They relate to the ring strain which is relieved at the

transition state by a change in hybridization, from sp^2 to sp^3.

Our results are consistent with those of McGarrity and Smyth[235] in that the bimolecular rate

constants for proton transfer to the diazo carbon by strong acids are large, although still 2-3 orders of

magnitude below the limit for diffusion control. A Brönsted coefficient of ~0.25 for the protonation of

V-2a suggests an early transition state, and may indicate that the reaction is exothermic.[251] Another

implication is that the pK_a's of carboxylic acids and of 2-propyl diazonium ions are significantly

different.[197]

It has been suggested that the carbon atom of diazomethane is a good hydrogen-bond

acceptor.[235,252] Stabilization of carbon bases by hydrogen bonding is expected to be most favorable

when negative charge is localized at carbon. Examples of such bases are cyanide[217] and acetylide[218]

ions and C-2 of the ylide thiamin.[203] However, Washabaugh and Jencks have shown that hydrogen

bonding is not important in proton transfer reactions of C-2 thiazolium ions,[203] and rate constants for

protonation at carbon can reach the diffusion controlled limit even when a lone pair on carbon is

delocalized, at least formally, as in phenyl ynolate ions.[253] Thus, the effects of hydrogen bonding in formally neutral diazoalkanes, on rates of proton transfer, remain unclear. Whatever the reasons, protonations of dialkyldiazo compounds are intrinsically fast, as indicated by our estimate of the intrinsic barrier to protonation of 2-diazopropane.
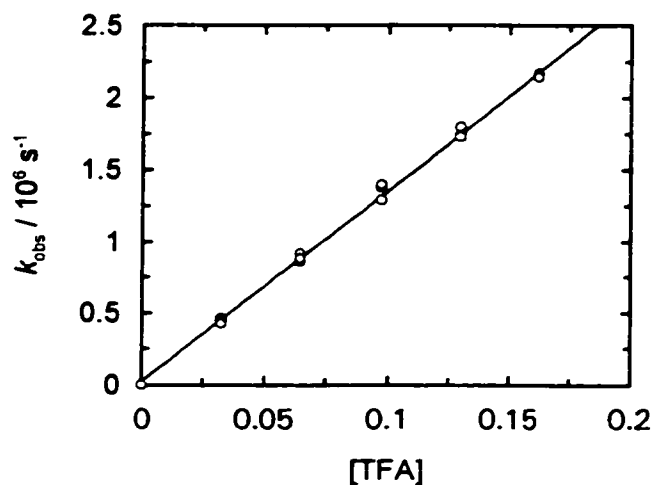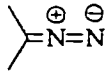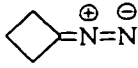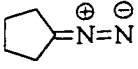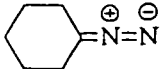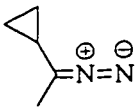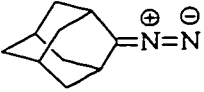
Figure V-5. Plot of k_{obs} vs. [TFA] in acetonitrile for the protonation of diazoadamantane (**V-2g**) in acetonitrile at 22 °C.

Phenyldiazomethane is *ca* 70-fold less reactive than **V-2a** toward H_3O^+, and α-diazocarbonyl compounds are slower yet by several orders of magnitude.[254] Such structural effects on rate constants for protonation at the diazo carbon atom presumably include effects from changes in the structure of the ground states (conjugation, H-bonding as well as other solvation) and in the structure of corresponding transition states.

In order to estimate the lifetimes of *sec*-alkanediazonium ions in solution, we measured rate constants for proton transfer from trifluoroacetic acid (TFA) to diazoalkanes **V-2a** to **g** (Scheme V-1) in acetonitrile, trifluoroethanol (TFE), and 1,1,1,3,3,3-hexafluoroisopropanol (HFIP) by monitoring the decays of the diazo bands at 250 nm in UV-LFP experiments (example in Figure 5). The rate

constants are those for diazonium ion formation (**V-3**) in these solvents and the results are summarized in Table V-2.

Table V-2. Rate constants for proton transfer to diazoalkanes (k_a) in acetonitrile, TFE, and HFIP at 22 °C[a].

Diazoalkane	Solvent	Bimolecular Rate Constants for Protonation of Diazo Compounds **2a-d**, $M^{-1} s^{-1}$
(V-2a)	MeCN	$k_{TFA} = (6.84 \pm 0.43) \times 10^{6}$ [b]
	TFE	$k_{TFE} < 10^{4}$
		$k_{TFA} = (1.19 \pm 0.34) \times 10^{7}$
	HFIP	$k_{HFIP} < 10^{4}$
		$k_{TFA} = (4.03 \pm 0.69) \times 10^{7}$
(V-2c)	MeCN	$k_{TFA} = (4.28 \pm 0.10) \times 10^{7}$
	TFE	$k_{TFE} < 10^{4}$
		$k_{TFA} = (1.18 \pm 0.08) \times 10^{8}$
	HFIP	$k_{HFIP} < 10^{4}$
		$k_{TFA} = (2.87 \pm 0.67) \times 10^{8}$
(V-2d)	MeCN	$k_{TFA} = (4.28 \pm 0.10) \times 10^{7}$
(V-2e)	MeCN	$k_{TFA} = (9.17 \pm 0.12) \times 10^{6}$
(V-2f)	MeCN	$k_{TFA} = (4.83 \pm 0.25) \times 10^{6}$
	TFE	$k_{TFE} < 10^{4}$
		$k_{TFA} = (5.53 \pm 0.64) \times 10^{6}$
	HFIP	$k_{HFIP} < 10^{4}$
		$k_{TFA} = (8.03 \pm 0.49) \times 10^{6}$
(V-2g)	MeCN	$k_{TFA} = (1.35 \pm 0.09) \times 10^{7}$
	TFE	$k_{TFE} < 10^{4}$
		$k_{TFA} = (2.90 \pm 0.32) \times 10^{7}$
	HFIP	$k_{HFIP} < 10^{4}$
		$k_{TFA} = (5.14 \pm 0.43) \times 10^{7}$

[a] Measured by UV-LFP at 250 nm. [b] Measured by TRIR-LFP at 2037 cm^{-1}.

V.3. Cyclohexadienyl Cations by Laser Flash Photolysis.

Relatively non-nucleophilic polar solvents were chosen in order to maximize the lifetimes of the cationic intermediates generated upon protonation of diazoalkanes **V-2**. Highly reactive cations such as benzyl cations[255] or the 9-fluorenyl cation[256] have been observed in LFP experiments in HFIP suggesting that this solvent is sufficiently polar to allow ionic intermediates to exist and sufficiently inert to preclude fast nucleophilic attack.

V.3.1. 1,3,5-Trimethoxybenzene Probe Reactions.

Attempts to observe alkanediazonium ions directly after 308 nm LFP of oxadiazolines **V-1** by TRIR or UV-visible detection proved to be fruitless. Instead we sought trapping reactions which would be compatible with the solvent system and lead to a product with a UV-visible chromophore that would be easily detected by UV-LFP. It is well established that π-nucleophiles react readily with carbocations[257] and cyclohexadienyl cations are relatively stable unreactive cationic intermediates[258] with UV absorptions ranging from 340 to 400 nm,[257] with high extinction coefficients[257b] ($\epsilon \sim 10000$). The use of arenes as π-nucleophiles would lead to cyclohexadienyl cations. The "anti-aromatic" fluorenyl cation (**FL**$^+$) has been shown to react with mesitylene as well as other electron rich aromatics *via* electrophilic aromatic addition and rate constants for these reactions have been measured by LFP according to eq V-4.[259] It is well known that oxygen substituted cations are more stable than their analogous alkyl substituted counterparts and therefore the electron rich 1,3,5-trimethoxybenzene was chosen as the probe π-nucleophile. Although we did look at other arenes, we found that the best results were obtained with 1,3,5-trimethoxybenzene (TMB).

$$(V\text{-}4)$$
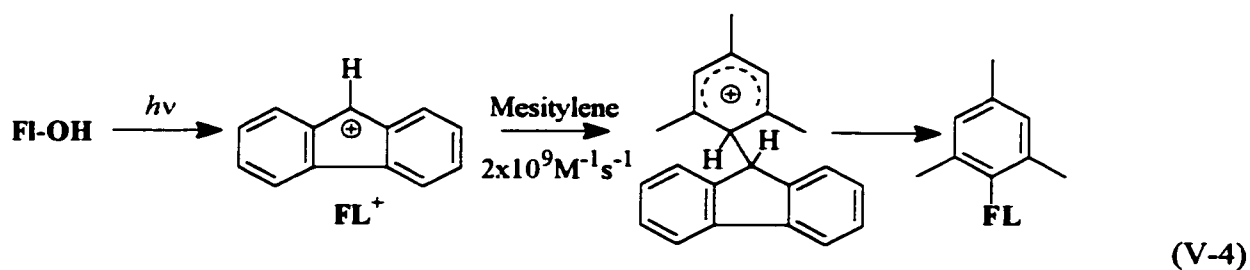
Rate constants for reactions of TMBH⁺ with nucleophiles such as halide ions and alcohols have been studied previously by excited state protonation of TMB (eq V-5). This low reactivity of TMBH⁺ towards nucleophiles ($k_{Nu} \sim 10^2$ - 10^3 or smaller in HFIP) suggests that cations resulting from electrophilic aromatic addition reactions (TMBR⁺), which should have similar reactivities towards nucleophiles, should be good probes for the study of more reactive cations (R⁺) since the more reactive cations can be quenched by added nucleophiles without affecting the TMBR⁺ cations.

$$(V\text{-}5)$$
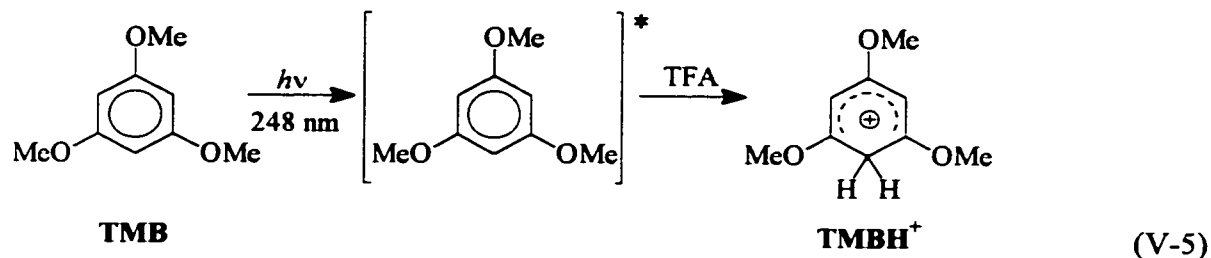
The LFP of oxadiazolines V-1b, c, f, and g, individually at 308 nm, in the presence of 1.34 M TMB and 2.0 x 10⁻³ M TFA in HFIP led to the observation of persistent (stable on the timescales of the experiments) absorptions with $\lambda_{max} \sim$ 350-370 nm, assigned to the cyclohexadienyl cations. The time-resolved UV-visible spectrum acquired (300-700 nm) after 308 nm LFP of oxadiazoline V-1c in the presence of 1.34 M TMB and 2.0 x 10⁻³ M TFA in HFIP is in Figure V-6. The transients, assigned to the cyclohexadienyl cations V-6b, c, f, g (eq V-6 and Scheme V-5), grew in with the same rate constants (within experimental error) as those for the decay of the diazo band observed at 250 nm by UV-LFP or at 2037 cm⁻¹ by TRIR-LFP. The growths and decays were not affected by the presence of

molecular oxygen. Time-resolved UV-visible spectra acquired (300-700 nm) after 308 nm LFP, under identical conditions in the absence of oxadiazoline, did not show any signals associated with excited state protonation of TMB.

(V-6)
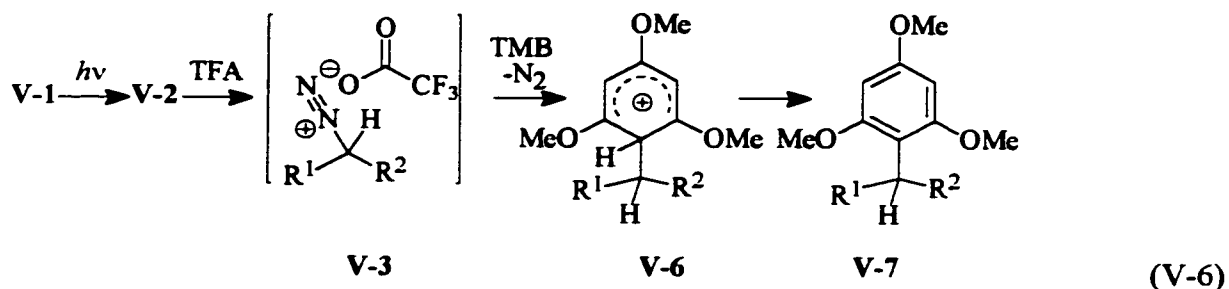
Scheme V-5.
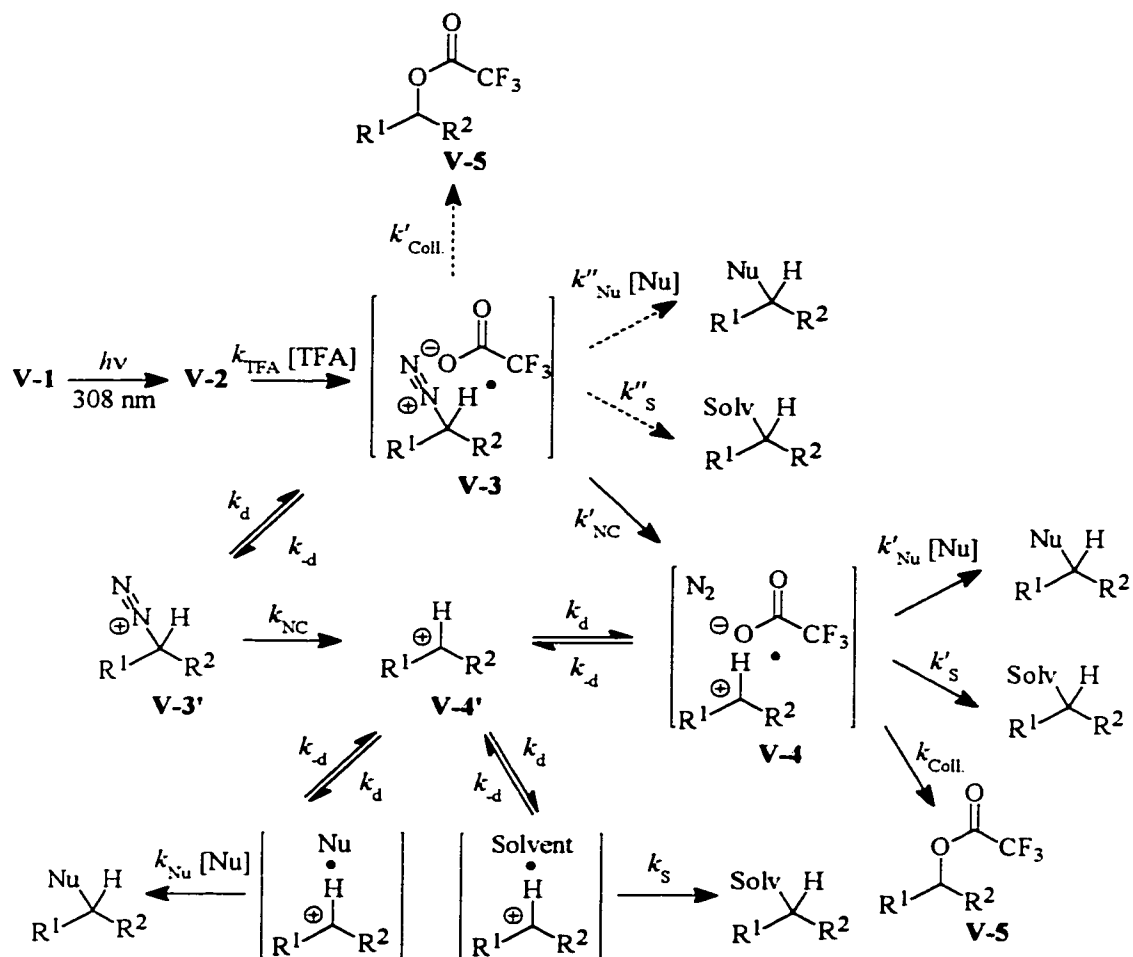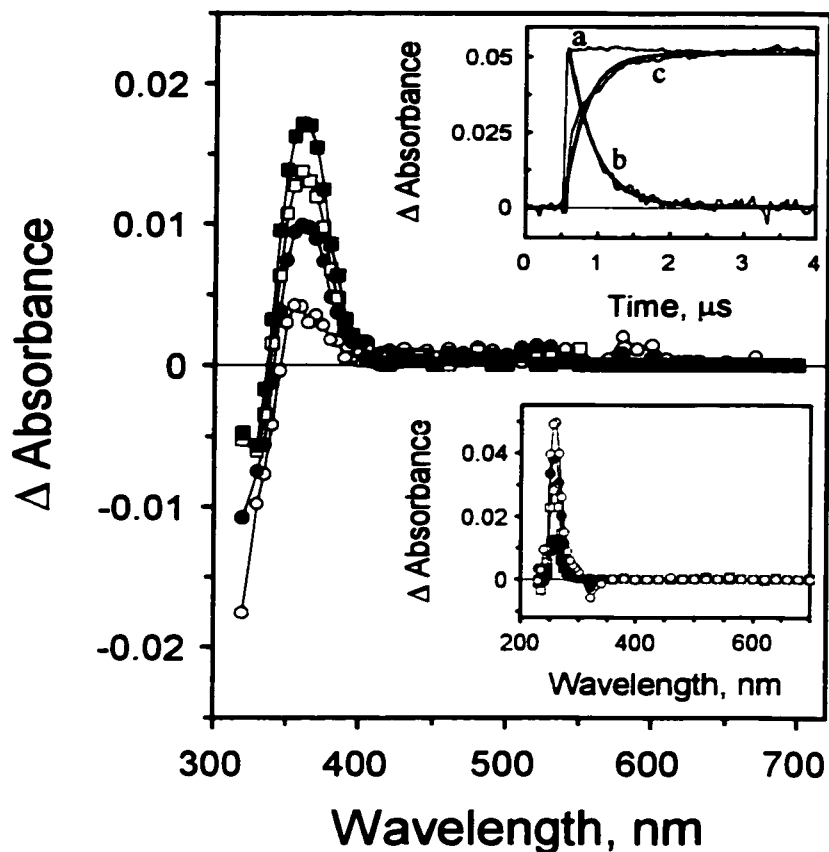
FIGURE V-6. Time resolved UV-visible spectra of 1-cyclobutyl-2,4,6-trimethoxybenzenium ion obtained after 308 nm LFP of **V-1c** in HFIP containing 1.34 M 1,3,5-trimethoxybenzene and 0.002 M TFA at 22 °C. The data were collected at intervals of 260 ns (O), 620 ns (●), 720 μs (□), and 2.3 μs (■) after the laser pulse. Lower inset shows the time resolved UV-visible spectra obtained after 308 nm LFP of **V-1c** in HFIP containing 0.002 M TFA at 22 °C with the data collected at the same time intervals. Upper inset shows the time resolved UV-Visible absorption traces (overlayed and normalized) observed at 250 nm (a, stable intermediate and b, decay) and 355 nm (c, growth) of wavelengths following 308 nm LFP of **V-1c** in HFIP, in HFIP containing 0.002 M TFA, and in HFIP containing both 1.34 M 1,3,5-trimethoxybenzene and 0.002 M TFA.

Absorbances with $\lambda_{max} \sim$ 350-370 nm for cyclohexadienyl cations **6a, c, f, g** were also observed

after 308 nm LFP of solutions of oxadiazolines **1b, c, f, g**, individually, in the presence of 1.34 M

TMB and various concentrations of TFA in 2,2,2-trifluoroethanol (TFE) and in aqueous acetonitrile

solvent. Again the UV-visible signals, assigned to cyclohexadienyl cations **6a, c, f, g**, appeared with

the same rate constants (within experimental error) as those of the disappearance of the corresponding

diazoalkane (Figure V-7). It was found that the absorbances associated with cyclohexadienyl cations

6a-d were stable on the millisecond time scale in both solvents.

Analogous experiments performed at various TFA concentrations, in each case showed that the

rate constants for the disappearance of diazoalkanes **V-2b, c, f, g** were the same (within experimental

error) as those for the formation of cyclohexadienyl cations **V-6a, c, f, g**. These observations

confirmed that the transients, assigned to cations **V-6a, c, f, g**, are derived from protonation of the

corresponding diazoalkane and that proton transfer is the rate determining step in the formation of

cyclohexadienyl cations **V-6a, c, f, g**.
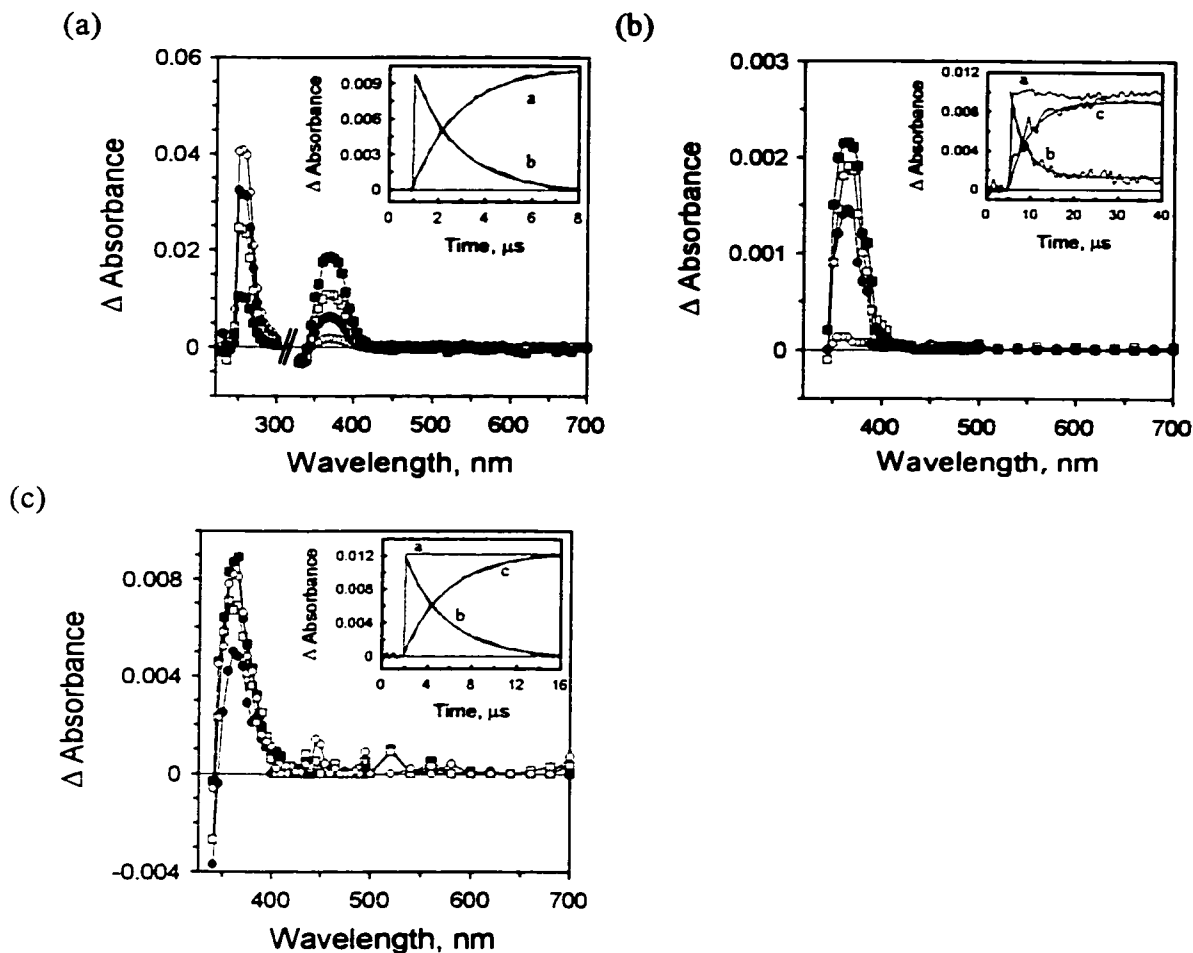
FIGURE V-7. (a) Time resolved UV-visible spectra of 1-(2-adamantyl)-2,4,6-trimethoxybenzenium ion obtained after 308 nm LFP of **V-1g** in acetonitrile containing 1.34 M 1,3,5-trimethoxybenzene and 0.04 M TFA at 22 °C. The data were collected at intervals of 460 ns (O), 1.9 μs (●), 3.2 μs (□), and 6.9 μs (■) after the laser pulse. The points between 230-320 nm were collected in a separate experiment in the absence of TMB because of the strong absorption of TMB in this region of the UV-visible spectrum. (b) Time resolved UV-Visible Spectra of 2-(1-cyclopropylethyl)-1,3,5-trimethoxybenzonium ion obtained after 308 nm LFP of **V-1f** in acetonitrile containing 1.34 M 1,3,5-trimethoxybenzene and 0.04 M TFA at 25 °C. The data were collected at intervals of 2.6 μs (O),11.4 μs (●), 19.4 μs (□), and 32.6 μs (■) after the laser pulse. (c) Time resolved UV-visible spectra of 2-*iso*-propyl-1,3,5-trimethoxybenzenium ion obtained after 308 nm LFP of **V-1b** in acetonitrile containing 1.34 M 1,3,5-trimethoxybenzene and 0.04 M TFA at 25 °C. The data were collected at intervals of 1.0 μs (O), 4.6 μs (●), 7.8 μs (□), and 13.2 μs (■) after the laser pulse. * Insets show the time resolved UV-visible absorption traces (overlayed and normalized) observed at 250 nm (stable intermediates and decays) and 360-370 nm (growths) wavelengths following 308 nm LFP **V-1b, c, f, g.**

The excited state protonations of TMB (UV-LFP, 266 nm) were repeated in aqueous acetonitrile

and in TFE in the presence of 0.01-0.05 M TFA to measure λ_{max} for TMBH$^+$ in the solvent systems

which we have employed. We confirmed the low reactivity of TMBH$^+$ towards nucleophiles in both

solvent systems and also found that the reactions of TMBH$^+$ with Cl$^-$ and with Br$^-$ were too slow to

measure by LFP consistent with the results reported by McClelland and Steenken.[258] Values of λ_{max}

for TMBH$^+$ in TFE and in aqueous acetonitrile containing TFA were found to be ~345-350 (broad

absorption maxima). Broad absorptions between ~500 and 630 nm (λ_{max} ~ 595 nm) were also

observed and assigned to the TMB radical cation (TMBH$^{\bullet}$). The absence of these absorptions in the

electrophilic aromatic addition reactions described earlier suggest that they do not proceed *via* an

electron transfer mechanism.

V.3.2. Stern-Volmer Quenching Experiments.

It was observed in all cases that the cyclohexadienyl cations **V-6a, c, f, g** were formed with the

same rate constants as those for the disappearance of the corresponding photochemically generated

precursor diazoalkane. The rate law for the disappearance of diazoalkane is given in eq V-7.

$$\frac{-d\ [R^1R^2CN_2]}{d\ t} = k_{obs}\ [R^1R^2CN_2];\ \ k_{obs} = k_o + k_{HA}\ [HA] \tag{V-7}$$

However, the yields of cyclohexadienyl cations as a function of TMB concentration, which are

proportional to the intensities of the UV-visible absorbances of these cations, are governed by the

relative rate constants in the product determining steps. Products may arise from reaction of the

alkanediazonium ions *via* a concerted process (S_N2 displacement of molecular nitrogen) or from

reaction of dialkyl carbocations within ion pair **4** (scheme V-5), or from diffusionally equilibrated

"free" dialkyl carbocations. These mechanistic possibilities are discussed in more detail in a following section. If we assume that products arise from diffusionally equilibrated "free" dialkyl carbocations then eq V-8 reflects the rate law for the reaction of the carbocation and eqs V-9 and 10 represent the rate constants leading to products.

$$\frac{-d\ [R^1R^2CH^-]}{dt} = k_{obs}\ [R^1R^2CH^+] \tag{V-8}$$

$$k_{obs} = k_o + k_{TMB}\ [TMB] \tag{V-9}$$

$$k_o = k_{coll} + k_S\ [Solvent] + \sum k_B\ [B] + \sum k_{Nu}\ [Nucleophile] \tag{V-10}$$

Stern-Volmer type analyses[69] relate the yields of product of a trapping reaction as a function of trap concentration to that for the trapping reaction at infinite trap concentration. Such an analysis is based on the competition of all other reactions of an intermediate (k_o) with the trapping reaction (k_{TMB} [TMB] in this case) and assumes that all of the intermediate is consumed in the trapping reaction at infinite trap concentration. The lifetimes of cations **V-4a, c, f, g** were determined by Stern-Volmer analysis of the maximum amplitudes of the cyclohexadienyl cation absorptions as a function of [TMB]. The data were analyzed by linear least squares fitting of the curve to eq V-11, and by double reciprocal treatment of the data (eq V-12). A typical plot is in Figure V-8. In eq V-11 and 12, A_{Cation} is the amplitude of absorbance of the cyclohexadienyl cation in the present of various amounts of added TMB, A^∞_{Cation} is the amplitude of absorbance of the cyclohexadienyl cation at infinite [TMB], k_o is the sum of all the rate constants leading to the disappearance of the transient cation, $\tau = 1/k_o$ is the lifetime of the transient cation, and k_{TMB} is the bimolecular rate constant for the reaction of the cation

with TMB. Fitting the data to the curve in eq V-11 allows one to solve for the product $k_{TMB}\tau$ directly without using intercept:slope ratios (which are equal to k_{TMB} / k_o) from double reciprocal plots (eq V-12).

$$\frac{A_{Cation}}{A^{\infty}_{Cation}} = \frac{k_{TMB}\,[TMB]}{k_o + k_{TMB}\,[TMB]} = \frac{k_{TMB}\,\tau\,[TMB]}{1 + k_{TMB}\,\tau\,[TMB]}$$ (V-11)

$$\frac{1}{A_{Cation}} = A^{\infty}_{Cation} \cdot \frac{k_o}{A_{Cation} \cdot k_{TMB}\,[TMB]} + \frac{1}{A_{Cation}}$$ (V-12)

The lifetimes of cations **V-4a, c, f, g** determined in aqueous acetonitrile, TFE, and HFIP are summarized in Table V-3.
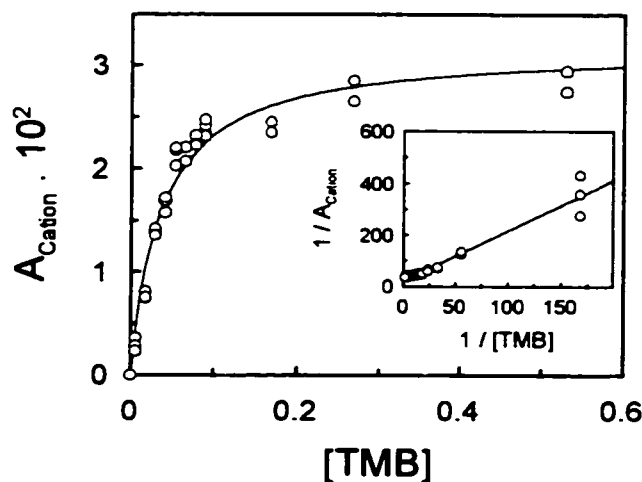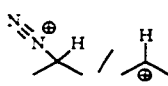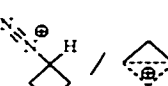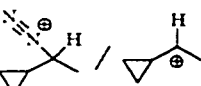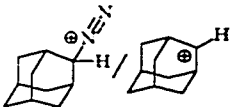
FIGURE V-8. Absorbance of 1-cyclobutyl-2,4,6-trimethoxybenzenonium ion *vs.* TMB concentration in HFIP at 22° C. Inset shows the double reciprocal plot of 1 / Absorbance of 1-cyclobutyl-2,4,6-trimethoxybenzenonium ion *vs.* 1 / TMB concentration in HFIP at 22° C.

Table V-3. Rate constants (k_o) for carbenium ion reactions with solvent deduced using the trimethoxybenzenium ion probe technique.

Cation	Solvent	k_{TMB}/k_o (Curve Fit)	k_o, s^{-1} [a]	λ_{max} for the cyclohexadienyl cation
(structure) **V-3a / V-4a**	MeCN (aq.)	0.25 ± 0.12	$(0.4\text{-}2.0) \times 10^{10}$	~360
	TFE	0.68 ± 0.14	$(1.5\text{-}7.4) \times 10^{9}$	~355
	HFIP	0.70 ± 0.22	$(1.4\text{-}7.1) \times 10^{9}$	~355
(structure) **V-3c / V-4c**	MeCN (aq.)	0.30 ± 0.04	$(0.3\text{-}1.7) \times 10^{10}$	~360
	TFE	2.3 ± 0.21	$(0.4\text{-}2.1) \times 10^{9}$	~355
	HFIP	27.5 ± 1.50	$(0.4\text{-}1.8) \times 10^{8}$	~355
(structure) **V-3f / V-4f**	MeCN (aq.)	0.89 ± 0.07	$(1.1\text{-}5.6) \times 10^{9}$	~360
	TFE	20.4 ± 0.21	$(0.5\text{-}2.5) \times 10^{8}$	~355
	HFIP	183 ± 27	$(0.5\text{-}2.7) \times 10^{7}$	~355
(structure) **V-3g / V-4g**	MeCN (aq.)	0.62 ± 0.09	$(1.6\text{-}8.1) \times 10^{9}$	~375
	TFE	1.63 ± 0.44	$(0.6\text{-}3.1) \times 10^{9}$	~370
	HFIP	1.71 ± 0.35	$(0.6\text{-}2.9) \times 10^{9}$	~365

[a] Assuming $k_{TMB} = 1\text{-}5 \times 10^{9}$ M^{-1} s^{-1}.

V.3.3. Azide Clock.

Bimolecular rate constants for the reactions of cations **V-4a, c, f, g** with nucleophilic traps were determined by keeping the TMB concentration constant and varying the concentration of nucleophile (eq V-13). Linear least-squares analysis of the ratio (A°_{Cation} / A_{Cation}) vs nucleophilic trap concentration, with the y-intercept defined as 1, according to the Stern-Volmer[79] relation in eq V-14, gives a slope which is equal to k_{Nu} / $k_{TMB}[TMB]$. In eq V-14, A°_{Cation} is the amplitude of absorbance of cyclohexadienyl cation in the absence of added nucleophile, A_{Cation} is the amplitude of its absorbance

in the presence of nucleophile and k_{Nu} is the bimolecular rate constant for the reaction of the nucleophile with the cation.

$$(V-13)$$
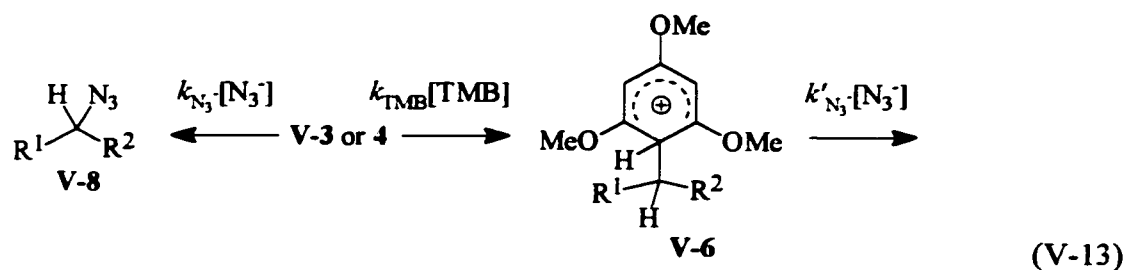
$$\frac{A^{o}_{Cation}}{A_{Cation}} = \frac{k_{Nu}}{k_{TMB}[TMB]} \cdot [\text{Nucleophile}] + 1 \qquad (V-14)$$

Such quenching plots were constructed for the reactions of cations **V-4a, c, f, g** with azide ion (Figure V-9) and bromide anion. The azide ion, which reacts with highly electrophilic carbocations at the diffusion-controlled rate [260,261,262] with $k_{azide} \approx 5 \times 10^{9}$ M^{-1} s^{-1},[263] was used to clock the electrophilic aromatic addition reactions and the results are summarized in Table V-4.
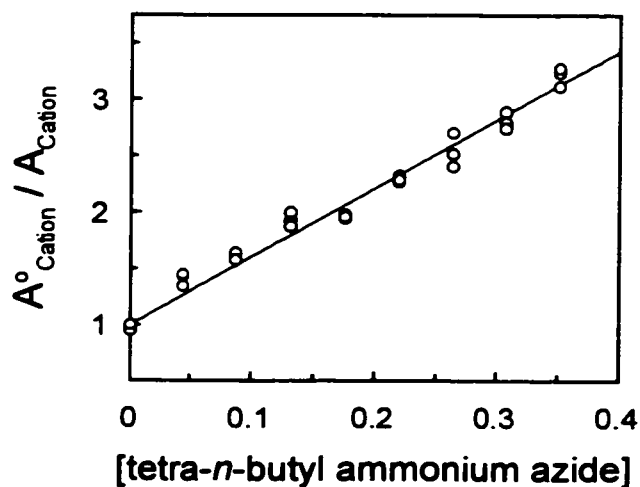
FIGURE V-9. Stern-Volmer quenching plot for the reaction of cyclobutonium ion with azide ion in the presence of 0.16 M TMB in HFIP at 22 °C.

Table V-4. Rate constants and rate constant ratios in TFE at 22 °C.

Cation	Nucleophile			
	N$_3^-$		Br$^-$	
	k_{TMB}/k_{azide}	k_{Nu}, M^{-1} s^{-1}	k_{TMB}/k_{Nu}	k_{Nu}, M^{-1} s^{-1}
V-4a	0.89[a]	4.5 x 10^{9b}	1.0	5 x 10^9
V-4c	0.94[a]	4.7 x 10^{9b}	0.99	4.7 x 10^9
V-4f	0.92[a]	4.6 x 10^{9b}	1.0	5 x 10^9
V-4g	0.93[a]	4.6 x 10^{9b}	1.0	5 x 10^9
V-6a	---	3.8 x 10^6	---	c
V-6c	---	4.0 x 10^6	---	c
V-6f	---	2.5 x 10^6	---	c
V-6g	---	3.7 x 10^6	---	c

[a] May be an underestimation as a result of azide/hydrazoic acid equilibration in solutions of 0.002 M TFA in TFE. [b] Assuming k_{azide} = 5 x 10^9 M^{-1} s^{-1}. [c] Too small to measure.

It was observed that cations **V-6a, c, f, g** decayed with *pseudo*-first-order kinetics in the presence of added azide ion. The quenching of these cations occurred with much lower rate constants (k_{Azide} = 1-4 x 10^6 M^{-1} s^{-1}) than those of cations **V-3a, c, f, g**. The formation of cations **V-6a, c, f, g** and their decay in the presence of added azide were resolvable in LFP experiments (Figure V-10).

The rate constants of reactions of Br$^-$ with cations **V-3a, c, f, g** were of the same order of magnitude as those for their reactions with N$_3^-$. On the other hand, cyclohexadienyl cations **V-6a, c, f, g** do not react with Br$^-$ at an appreciable rate. The low reactivity of 1-alkyl-2,4,6-trimethoxybenzenium ions towards nucleophiles, exemplified by the slow reactions of **V-6a, c, f, g** with N$_3^-$ and Br$^-$, makes electrophilic addition reactions to TMB a versatile kinetic probe reaction.
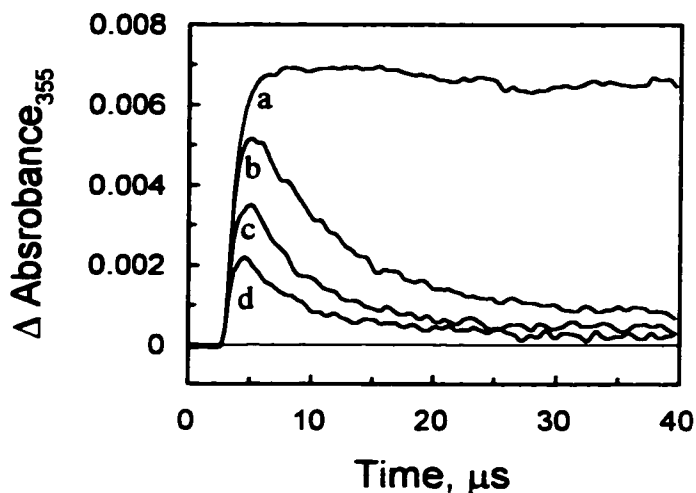
FIGURE V-10. Time-resolved UV-visible traces observed following 308-nm laser flash photolyses of V-1c in TFE containing 0.20 M TMB, 0.02 M TFA, and (a) 0 M, (b) 0.10 M, (c) 0.25 M, and (d) 0.5 M tetra-n-butyl ammonium azide at 22° C.

V.3.4. Electrophilic Aromatic Addition/Substitution.

Solutions of 2.0 M TMB in HFIP, in TFE, and in benzene were prepared containing 0.01 M of oxadiazoline V-1a, c, f or g. These solutions were placed in Pyrex reaction vessels (1 mL each) fitted with septa, degassed with N_2, and irradiated for 2 hours in a Rayonet reactor fitted with 6-12 300 nm bulbs. HFIP and TFE were both acidic enough to protonate the resulting diazoalkanes V-2a, c, f, g, whereas 0.01 M TFA was added to the benzene solutions after photolysis. The resulting solutions were analyzed by GC-MS and, in some cases, by ¹H-NMR. In each case, products of electrophilic aromatic substitution (7a-d) were observed in addition to solvent derived products, elimination products and ion pair collapse products (when TFA was used as the proton source). The fact that products associated with electrophilic aromatic substitution were observed together with products of ion pair collapse and capture by solvent strongly support the assignments of the transient signals in LFP experiments to cyclohexadienyl cations V-6a, c, f, g. However, there does seem to be a discrepancy between the ratios of rate constants (k_{TMB} / k_s) measured by LFP and those determined by product studies for precursors V-1a and V-1g. Smaller ratios of k_{TMB} / k_s determined by product

studies may reflect an increase in k_s resulting from ion pair collapse (when HFIP or TFE is the protonating acid) which would artificially deflate the k_{TMB} / k_s ratios. Those ratios measured by LFP may reflect the lifetimes of only those cations which escape the ion pair ($k_s \approx k_o = k_{coll} + k_s'[\text{solvent}]$). The apparent discrepancy may also reflect a redistribution of products within a cation-arene π-complex. This possibility is discussed further in a following section.

V-7a   **V-7f**   **V-7g**
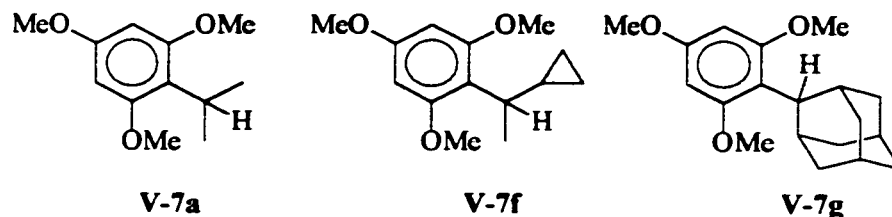
No ion pair collapse or solvent derived products were detected from precursors **V-1c** and **V-1f** in HFIP solvent (AH = solvent or TFA) for solutions of 2.0 M TMB. For the reactions involving diazocyclobutane protonation in the presence of TMB, three electrophilic aromatic substitution products were observed in HFIP, TFE and in benzene solvents. Those products were identified as **V-7c(1)**, **V-7c(2)**, and **V-7c(3)** (Scheme V-6). The ratios of products are listed in Table V-5 and 6.

Table V-5. Product distributions from protonation of diazocyclobutane.

Solvent	V-7c(1): 7c(2): 7c(3)	% cyclobutene
HFIP	21.3: 7.1: 1.0	trace, < 0.1 %
TFE	25.0: 9.7: 1.0	trace, < 0.1 %
Benzene	2.3: 1.0ᵃ	trace, < 0.1 %
Solvent	9: 10: 11	% cyclobutene
Benzene	6.3: 6.9: 1.0	trace, < 0.1 %
Acetonitrile	3.9: 5.1: 1.0	trace, < 0.1 %

ᵃ V-7c(3) not detected.

Scheme V-6.
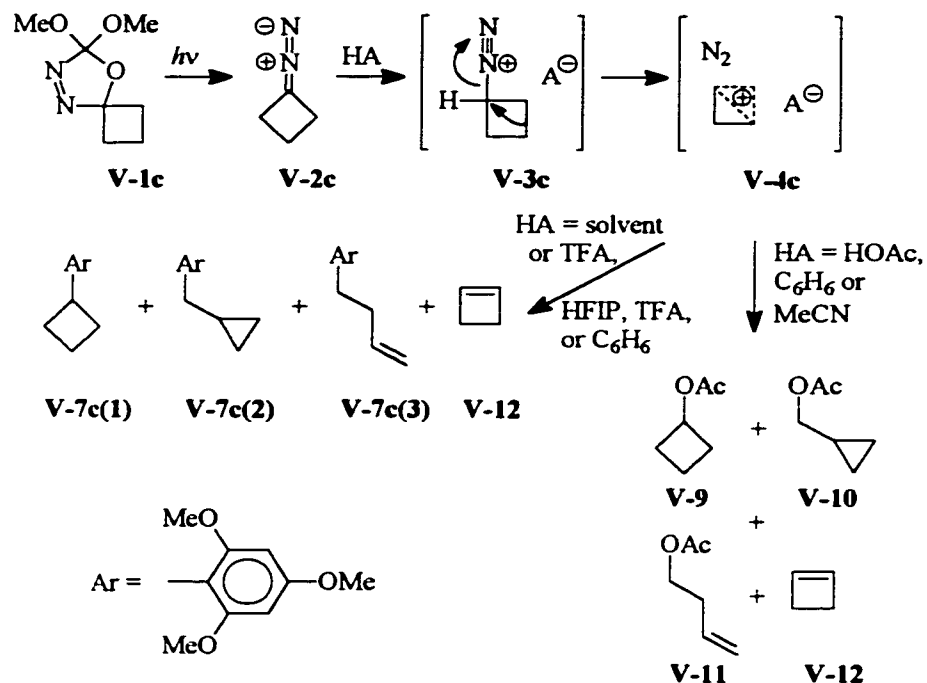
Table V-6. Yields of products from steady state photolysis experiments.[a, b]

Cation	Solvent	% TMB adduct	% Solvent adduct	% Elimination Product	k_{TMB} / k_s
4a	HFIP	6.9	90	< 1	3.9×10^{-2}
	TFE	8.6	92	< 1	4.7×10^{-2}
	Benzene[d]	8.0	—	—	—
4c	HFIP	> 95	c	< 1	—
	HFIP[e]	21[e]	69[e]	< 1	30[e]
	TFE	80	16	< 1	2.5
	Benzene[d]	> 50	c	< 1	—
4f	HFIP	> 95	c	< 1	—
	HFIP[e]	74[e]	26[e]	< 1[e]	280[e]
	TFE	> 95	c	< 1	—
	Benzene[d]	> 90	c	< 1	—
4g	HFIP	7.4	90	< 1	4.1×10^{-2}
	TFE	14.5	82	< 1	8.9×10^{-2}
	Benzene[d]	15.5	c	3.8	—

[a] Minor side products from the photolysis of oxadiazolines were detected is some cases. [b] Solutions contained 2.0 M TMB. [c] Not detected in the GC-MS experiments. [d] Solutions contained 4.5 M TMB. [e] Solutions were 0.01 M in TMB.

Steady state photolyses of oxadiazoline **V-1c** in benzene or acetonitrile containing 0.1M acetic acid gave products **V-9** to **12** (Scheme V-6). These observations are consistent with decomposition *via* the bicyclobutonium ion intermediate **V-4c**. The unimolecular dissociation of N_2 from cyclobutyldiazonium ion (**V-3c**) may proceed with "anchimeric assistance" from the adjacent carbon atom in the transition-state for N_2 loss (Scheme V-6). The observed product ratios are all in close agreement with those observed for the deamination of cyclobutyl amine.[264] There does appear to be an enrichment in the cyclobutyl adduct **V-7c(1)** which could reflect either the incursion of a concerted mechanism (S_N2), or a preference for the electrophilic addition step as compared with of solvent capture or ion pair collapse.

V.3.5. Elimination vs. Electrophilic addition / Ion Pair Collapse.

Only trace amounts of elimination products[265,266] propene, cyclobutene, ethylenecyclopropane, and dehydroadamantane were detected from photolyses of oxadiazolines **1a**, **c**, **f**, and **g**, respectively in HFIP, in TFE, or in benzene. The lack of elimination products from **V-4c** and **V-4f** is presumably the result of ring strain in the products. The 2-adamantyl cation apparently shows little propensity for 1,2-shifts and 1,2-elimination is not favored due to ring strain in the bridgehead alkene product; however, 1,3-elimination can occur.[267]

Studies of the products of reaction of 2-diazobutane (**V-2h**) with acetic acid, including both low and high conversions, using steady-state photolytic techniques in sealed, degassed tubes are described in the Experimental Section. The products were identified by means of standard NMR techniques, and spectra were compared to those in the literature. Products of this reaction in solvents of different polarity as summarized in Table V-7. The major product in all cases was 2-butyl ethanoate; however, in contrast to the reactions of **V-2a**, **c**, **f**, **g**, elimination products were formed in significant yield. It

has been suggested that 1,2-hydride shifts can occur in concert with the loss of N_2 in alkanediazonium ions.[242] The elimination from a hydrogen bridged species below[268] might explain the product distributions observed.
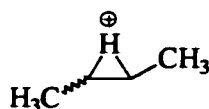
Further support for this hypothesis comes from the products of the reactions of diazocyclopentane (V-2d) and diazocyclohexane (V-2e) with acetic acid (0.1 M) in benzene and acetonitrile solutions (Table V-7), where only two products are formed in each reaction. Again, high yields of elimination products were observed which is in keeping with a concerted 1,2-hydride shift occurring in concert with the loss of molecular nitrogen.

Table V-7. Product distributions from protonation of **V-2d**, **V-2e**, & **V-2h** by acetic acid in various solvents.

Solvent	%2-butyl ethanoate: % 1-butene: % 2-butene	% methylcyclopropane
Cyclohexane	3.1: 0.9: 1.0	≤0.1
Benzene	2.0: 1.0: 1.0	0.5
Dichloromethane	2.1: 0.9 : 1.0	0.5
DMSO[a]	2.2: 0.8: 1.0	≤0.1
Acetonitrile[a]	1.8: 1.0: 1.0	0.6

Solvent	%cyclohexyl ethanoate: % cyclohexene	
Benzene	1.3: 1	
Acetonitrile	1.3: 1	

Solvent	%cyclopentyl ethanoate: % cyclopentene	
Benzene	1.4: 1	
Acetonitrile	1.5: 1	

[a] Solvent derived products were observed.

The steady-state photolysis of 2,2-dimethoxy-5-methyl-5-(3-hydroxypropyl)-Δ^3-1,3,4-oxadiazoline (**V-1i**) in the presence of 0.1 M acetic acid in benzene was also performed. The major product formed in the reaction of 5-hydroxy-2-diazopentane (**V-2i**) with acetic acid was 5-hydroxy-2-pentyl ethanoate (~40%), with the minor products being 1-penten-5-ol, and (*E* & *Z*)-2-penten-5-ol (~50% combined yield of alkene products), as well as methyltetrahydrofuran resulting from intra-molecular cyclization. The fact that the ester product **V-13** was observed in excess of the tetrahydrofuran **V-14** (~3:1, eq 15) suggests that ion pair collapse occurs at a very rapid rate, with molecular reorganization being the only impediment to product formation and that elimination is competitive with ion pair collapse.

$$\text{(V-15)}$$
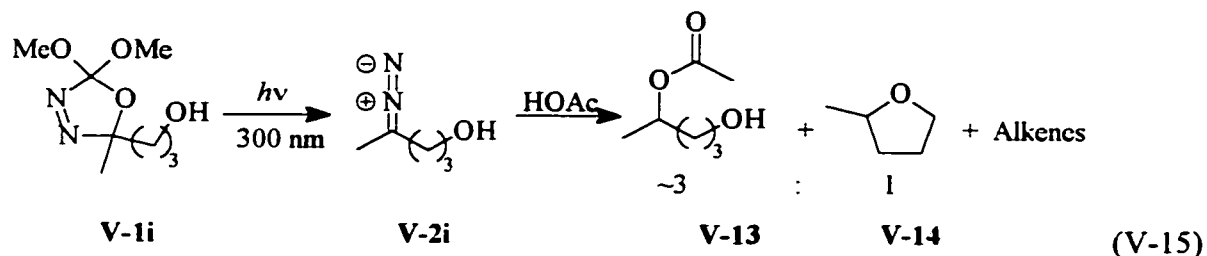
V.3.6. π-Complexes.

It has been suggested that transition states for aromatic substitution involving highly reactive electrophiles resemble π-complexes.[269] However, it is clear that electrophilic aromatic substitution products observed in this study ultimately derive from cyclohexadienyl cations (σ-complexes). However, cation-π interactions can be considerable[270] so that such interactions cannot be discounted. It is possible that, prior to electrophilic attack and σ-bond formation, either alkanediazonium ions **V-3** and/or carbenium ions **V-4** may form π-complexes with TMB and, from these complexes, partition between electrophilic addition and reaction with solvent and counterion. Such an interaction would

also lead to extended lifetimes in solution and explain differences in product distributions in the presence and absence of arene. There is precedence for such behavior in carbene chemistry.[82]

V.4. Lifetimes of Cations.

The lifetimes reported in Table V-3 may be those for the alkanediazonium ions which react *via* a concerted process (S_N2 displacement of molecular nitrogen), or those of dialkyl carbocations within ion pair **V-4**, or from diffusionally equilibrated "free" dialkyl carbocations according to Scheme 1. As stated earlier, the lifetimes of alkanediazonium ions **3a, c, f, g** are expected to be inversely proportional to those of carbocations **4a, c, f, g**. The lifetimes of alkanediazonium ions then should be governed by the rate constants for dissociation of molecular nitrogen which should be proportional to the relative stabilities of the corresponding carbocations. Other factors such as solvent polarity and solvent nucleophilicity will undoubtably affect these lifetimes as well. Lifetimes of alkanediazonium ions should be the longest in solvents of low polarity and low nucleophilicity. When the dissociation of molecular nitrogen is dominant over bimolecular nucleophilic substitution (S_N2), the reactions will proceed though carbocationic intermediates. Such cases are analogous to the thermally activated dissociation of other leaving groups such as alkyltosylates or alkylhalides. The lifetimes measured from precursors **V-1a, c, f, g** are consistent with the relative stabilities of the dialkylcarbocations as measured by solvolysis rate constants for the corresponding alkyltosylates[271] or alkylhalides.[272] Figure V-11 shows linear free energy relationships between the k_o determined from precursors **V-1a, c, f, g** and solvolysis rate constants of analogous alkyltosylates and alkylchlorides.
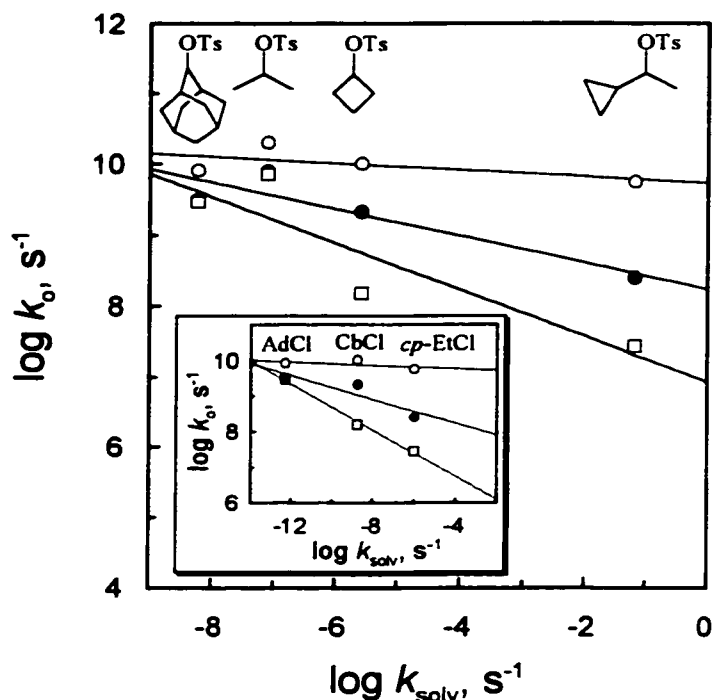
Figure V-11. Plots of log k_o determined by the TMB kinetic probe method *vs.* log k_{solv} for the acetolyses of the analogous alkyltosylates at 25 °C. The open circles, filled circles, and open squares represent the log k_o data in HFIP, TFE and 10 % aqueous MeCN, respectively. The solid lines represent the linear least-squares fits of each set of data. Inset shows the plots of log k_o determined by the TMB kinetic probe method *vs.* log k_{solv} for the solvolyses of the analogous alkylchlorides in 80% aqueous acetone at 25 °C (see text).

The solvolysis rate constants for 2-propyltosylates and halides in Figure V-11 are larger than expected because of solvent assistance in the rate limiting step,[271i-k] which probably doesn't occur for 2-propanediazonium ion. The fact that the observed lifetimes correlate with analogous solvolysis rate constants and that the products from diazocyclobutane are attributable to the trapping of cyclobutonium ion at high trap concentrations suggest that the lifetimes measured here represent those of the carbocations and should be viewed as *upper limits* for the lifetimes of the corresponding alkanediazonium ions.

V.5. Cyclobutyl and 1-cyclopropylethyl carbocations.

The cyclobutyl cation is thought to exist as the non-classical bicyclobutonium ion which is postulated to be in rapid equilibrium with the bisected cyclopropylcarbinyl cation. The most energetically favorable conformer of (α-methylcyclopropyl)carbinyl cation is the *trans* bisecting structure below.[273, 274]
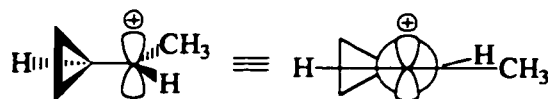
Although there is much controversy regarding the relative stabilities of cyclopropyl and phenyl substituted carbocations, cyclopropylcarbinyl cations are thought to be at least as stable as the analogous phenyl substituted carbocations thermodynamically, based on gas phase data[275] and pK_R- values.[276] Chemical shift data for cyclopropyl and phenyl substituted carbocations, however, suggest that phenyl is slightly better at stabilizing positive charge.[277] Recently, the kinetic stabilities of substituted arylcyclopropylcarbenium ions have been investigated by LFP.[17c] Kirmse and co-workers showed that cyclopropyl and phenyl groups are very similar in their ability to stabilize carbocations, however, the cyclopropyl group was found to be more sensitive to electron demand according to the slopes of Hammett plots for the reactions of the cations with TFE (for diarylcarbenium ions $\rho^* = 2.64$, whereas for arylcyclopropylcarbenium ions $\rho^* = 4.34$).

Although the lifetime of benzylcarbenium ion in HFIP is not known, McClelland and co-workers predict that it should be 2-20 ns,[255] and the lifetime measured for the cyclobutylcarbenium ion using the TMB probe method is certainly of the same magnitude. Direct comparison of the lifetime of 1-cyclopropylethyl cation with that of 1-phenylethyl cation[255] in HFIP suggests that the phenyl substituted cation is more kinetically stable than the cyclopropyl substituted one. This result, when compared with those of Kirmse and coworkers,[17c] may reflect differences in steric, electronic, and

solvation effects between the various substrates. It is unclear whether the twist angles of aryl groups in diaryl and arylcyclopropyl cations vary with substituent,[a] and whether such structural changes affect the reactivity of these species. Calculations regarding Ph_2C^+H show that the minimum energy structure has C_2 symmetry and that both phenyls are rotated 18.59° out of the plane which is defined by the sp^2 hybridized carbocation carbon and the atoms directly attached to it,[278] whereas the phenyl group in arylcyclopropylcarbenium ions can be out of plane by as much as 27°.[274d] Figures V-12 and V-13 summarize the relative reactivities of some other carbenium ions in non-aqueous media[17c,248,255,256,258] with those measured here.

It is concluded that the lifetimes observed are those of cations **V-4a, c, f, g** which are at least partially, if not completely, diffusionally separated from the trifluoroacetate counterion based on the magnitudes of the observed lifetimes.[c] There also appears to be a solvent effect on the lifetimes of cations **V-4a, c, f, g**, in accord with the relative nucleophilicities of the different solvent systems, consistent with previous observations.[248] In an aqueous environment, cations **V-4a, c, f, g** most probably react within the first solvation shell.[248, 226b] The solvolysis reactions of alkanediazonium ions, proceeding through carbocationic intermediates, represent the extreme in terms of leaving group ability. To illustrate this point we can compare the rates of dissociation of tosylate from 2-adamantyltosylate ($k_{solv} \sim 4 \times 10^{-10}$ s^{-1}, 25 °C in ethanol) and that of the dissociation of N_2 from 2-adamantanediazonium ion ($k_{solv} \geq 3 \times 10^9$ s^{-1}, 22 °C in TFE); the relative rate for the dissociation of N_2 vs. tosylate is $k_{rel} \sim 10^{19}$!

---

[a] One might consider, for example. whether the twist angles are the same for Ph_2C^+H and say Phenyl(4-methoxyphenyl) carbocation, and also for c-pr(Ph)C^+H and c-pr(4-MeO-Ph)C^+H? One might very well expect the 4-methoxyphenyl substituents to be more in plane as a result of greater resonance interactions.

[c]. It is possible that the alkanediazonium ions may live long enough to allow for partial diffusional separation from the least coordinating trifluoroacetate counterion for the most reactive cations.

Figure V-12. Reactivities of some Carbocations towards HFIP at ~-20 °C.[a]
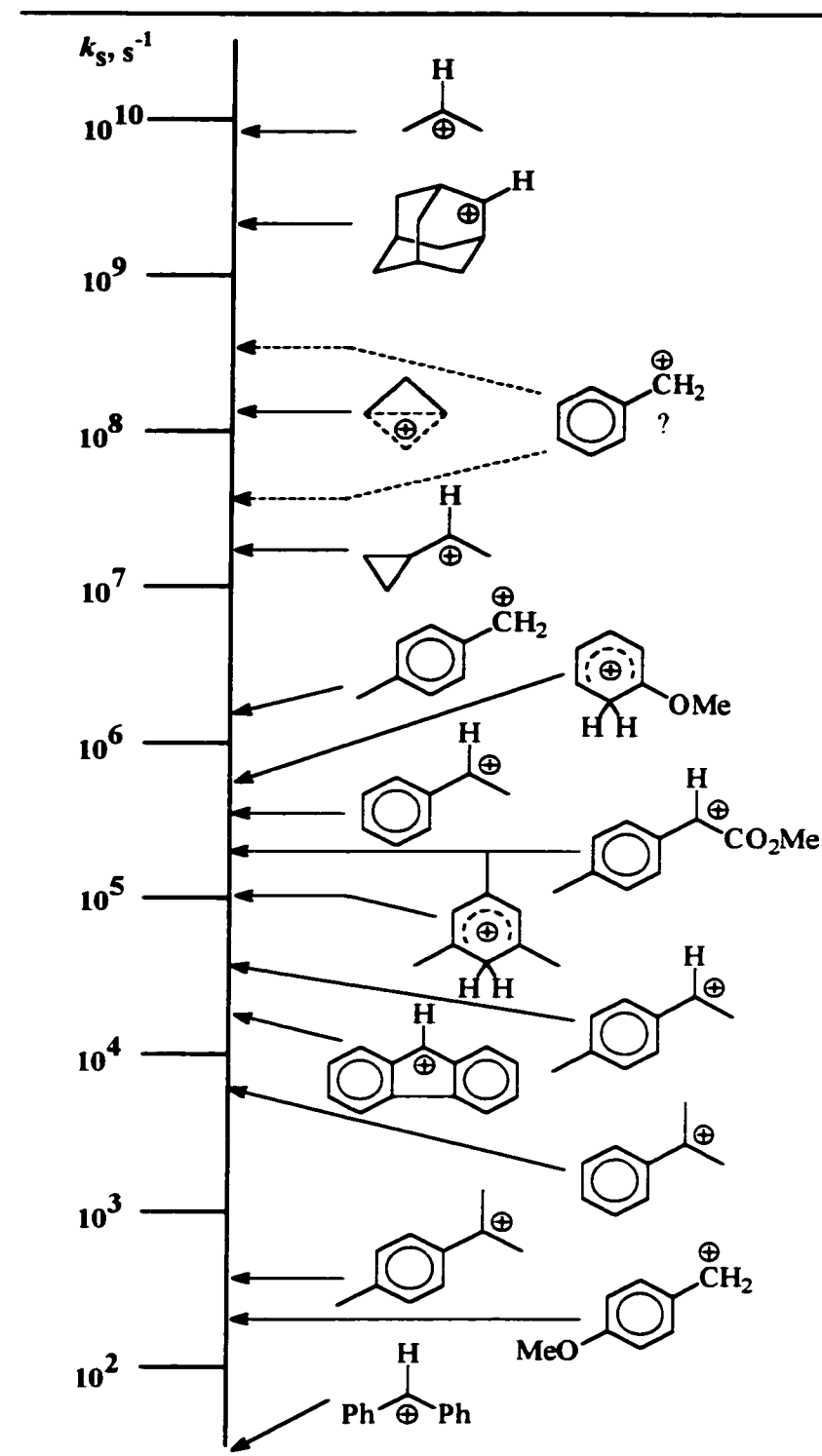
[a] Rate constants are from references 248, 255, 256, and 258.

Figure V-13. Reactivities of some Carbocations towards TFE at ~20 °C.[a]

k_s, s^{-1}

10^{10}

10^9

10^8

10^7

10^6

10^5

10^4

10^3

10^2

10^7

10^6

10^5

10^4
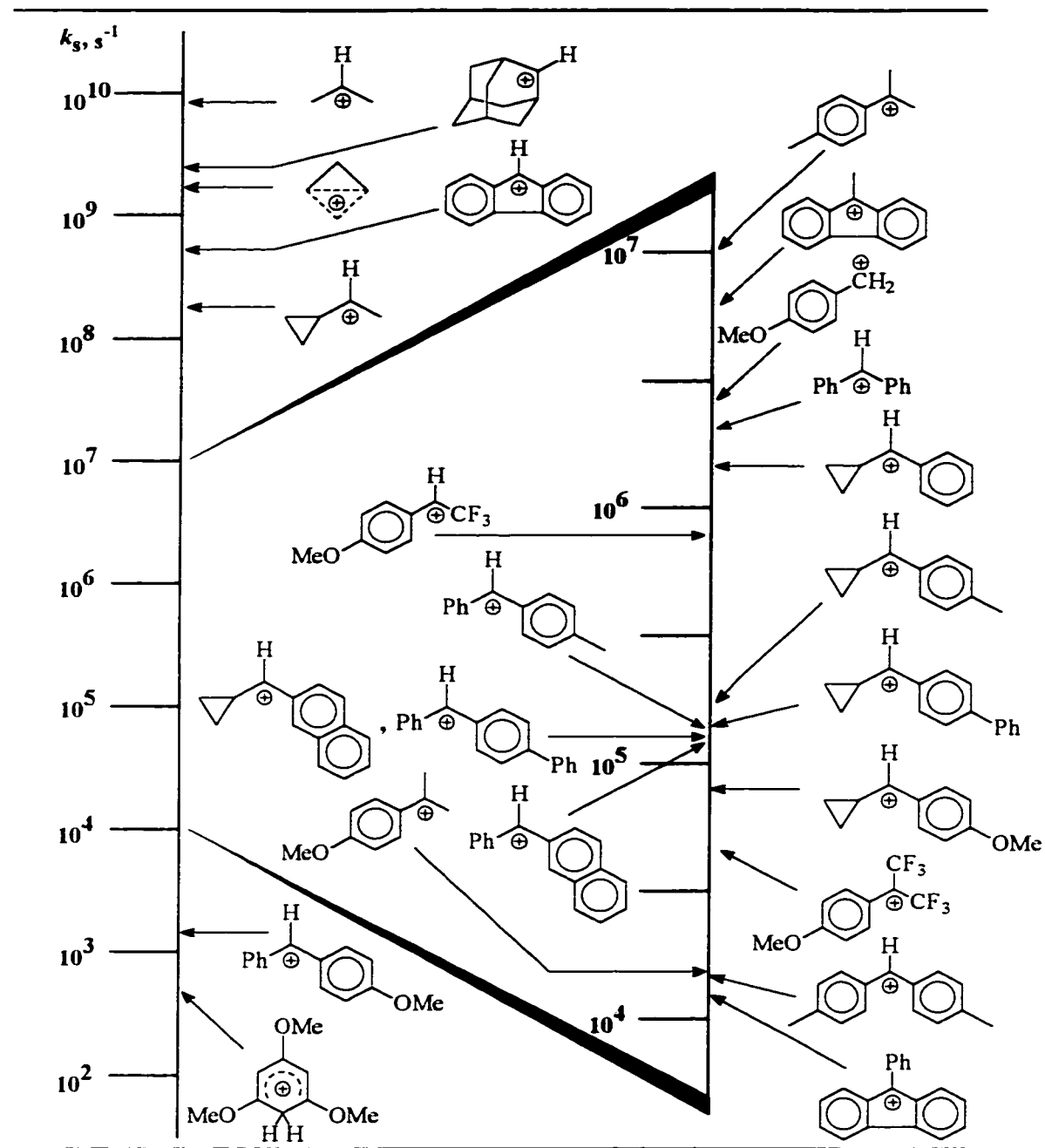
[a] Rate constants are from references 17c, 248, 255, 256, and 258.

V.6. Biological Significance.

Photochemical generation of diazoalkanes (V-2) from oxadiazolines (V-1) in a variety of media containing a proton source represents an alternative and convenient method for determining rate constants for diazoalkane protonation reactions. Secondary aliphatic diazo compounds undergo rate-determining proton transfer to form alkanediazonium ions with bimolecular rate constants which can approach the diffusion controlled limit. The major alkylating pathway involves collapse of ensuing intimate ion pairs and diffusion controlled reactions with nucleophiles. The lifetimes of simple sec-alkanediazonium ions are too small, even in relatively non-nucleophilic solvents such as HFIP, to allow for diffusional encounters with DNA unless the generation of sec-alkanediazonium ion intermediates occur at almost contact distances. Therefore alkanediazonium ions must be formed in very close proximity to DNA for alkylation to occur. Pre-association of the alkanediazoate precursors probably occurs and favourable π–π interactions may be responsible for pre-association. Our results and interpretations are entirely consistent with those of Fishbein and co-workers.[226] The major fate of simple sec-alkanediazonium ion intermediates outside contact distances with DNA should be the reaction with water or nucleophilic residues which may lead to intra-cellular damage. Site specificity of DNA alkylation could arise from different environments according to DNA sequence, depending on the local environment and the degree to which that environment is solvated. It is fortuitous that sec-alkanediazonium ion intermediates show such behavior given the deleterious effects of DNA alkylation.

Chapter 6.

Experimental.

VI.1. General.

NMR spectra were determined with Bruker spectrometers; DRX 500, AC 300 or AC 200. Chemical shifts are reported in parts per million relative to internal TMS. The GC-MS analyses were carried out with a Hewlett-Packard 5890 gas chromatograph equipped with a HP-5971A mass selective detector and a DB-1 capillary column (12m x 0.2 mm; Chromatographic Specialties, Inc.). High resolution mass spectra were obtained on a VG Analytical ZAB-E double-focusing mass spectrometer. Infrared spectra were obtained with a Bio-Rad FTS-40 spectrometer from samples in KBr windows.

Thermolyes of oxadiazoline precursors were performed in vessels which were degassed by successive freeze-pump-thaw cycles and sealed prior to heating. All thermolyses were performed in a constant temperature oil bath. Photolyses were performed in quartz or Pyrex tubes fitted with septa. Solutions were deoxygenated using a stream of N_2 or Argon. Photolyses were performed in a Rayonet reactor fitted with either RPR253.7, RPR300, RPR350 nm UV lamps.

VI.2. Materials.

Pyridine (Aldrich) was distilled from either calcium hydride or barium oxide and stored under nitrogen over potassium hydroxide. In some cases it was necessary to purify pyridine by Zn complexation.[141] Cyclohexane and benzene (BDH Omnisolv) were distilled from sodium prior to use.

Acetonitrile (BDH Omnisolv) was distilled under nitrogen after refluxing over calcium hydride for several days. Oxiranes and thiiranes were commercial samples of the highest purity available (Aldrich) and were distilled prior to use. Tetramethylethylene was purified by passing it through an alumina column prior to use. All other solvents and reagents were of the highest purity commercially available and were used as received or purified using standard distillation techniques. Purities of reagents and solvents were determined using GC and GC-MS techniques. 1,3,5-Trimethoxybenzene was purified by repeated re-crystallizations from hexanes.

VI.2.a. Oxadiazolines.

Acetyl- or carbomethoxyhydrazones were prepared from the appropriate ketones and hydrazides by refluxing in benzene (4-12 hours) using a Dean-Stark apparatus. In some cases, hydrazones were used without purification. All oxadiazolines were prepared by oxidative cyclization of the corresponding hydrazones using either lead tetraacetate or iodobenzene diacetate as described previously.[49-59] The products were purified by column chromatography on silica gel using hexane/ethyl acetate (24:1) as eluents or by radial chromatography using gradients of hexanes and hexanes/ethyl acetate combinations. Reported yields were determined from hydrazones.
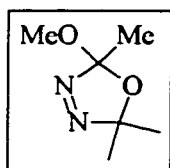
2-Methoxy-2,5,5-trimethyl-Δ^3-1,3,4-oxadiazoline (15, II-1a, and V-1a);[59] Yield 72%, Clear colourless oil; ^{1}H NMR (200 MHz, CDCl$_3$) δ 1.46 (s, 3 H), 1.59 (s, 3 H), 1.61 (s, 3 H), 3.10 (s, 3 H); ^{13}C NMR (50.3 MHz, CDCl$_3$) δ 23.4, 23.9, 25.0, 50.4, 119.8, 133.5; UV (pentane) λ_{max} = 322nm (ϵ = 500).
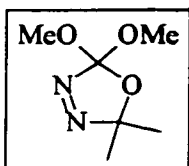
2,2-Dimethoxy-5,5-dimethyl-Δ³-1,3,4-oxadiazoline (24, II-1b, III-1b, and V-1b).[51] Yield 70 %, Clear colourless oil; ^{1}H NMR (200 MHz, CDCl₃) δ 1.53 (s, 6 H), 3.45 (s, 6 H); ^{13}C NMR (50.3 MHz, CDCl₃) δ 23.7, 51.5, 118.8, 137.0; IR (neat, KBr) 2982, 2949, 2887, 2847, 1577, 1459, 1448, 1376, 1137, 1078, 930, 862 cm⁻¹ ; MS (e.i.) m/z: (molecular ion not observed),129 [M - OMe]⁺, 105, 91, 90, 75, 74, 73, 59 (100%), 43; MS (c.i., NH₃) m/z: 178 [M + NH₄]⁺; UV (pentane) λ_max = 328 nm (ε = 500).
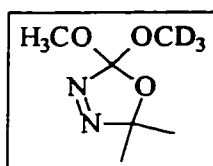
2-Methoxy-2-methoxy-d₃-5,5-dimethyl-Δ³-1,3,4-oxadiazoline (III-1a-d₃). Oxadiazoline 2 was prepared by LTA oxidation of the carbomethoxyhydrazone of acetone in CH₂Cl₂ to yield 2-acetoxy-2-methoxy-5,5-dimethyl-Δ³-1,3,4-oxadiazoline which was then treated with methanol-d₄ as described previously.[192]
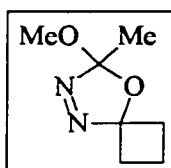
3,4-Diaza-2-methoxy-2-methyl-1-oxa[4.3]spirooct-3-ene (II-1d). Yield 42 %, Clear colourless oil; ^{1}H NMR (200 MHz, CDCl₃) δ: 1.62 (s, 3 H), 1.80-2.1 (m, 1 H), 2.15-2.45 (m, 1 H), 2.40-2.70 (m, 4 H), 3.13 (s, 3 H); ^{13}C NMR (50.3 MHz, CDCl₃) δ: 11.1 (+) (CH₂), 24.8 (-) (CH₃), 30.6 (+) (CH₂), 30.8 (+) (CH₂), 51.6 (-) (OCH₃), 119.9 (+) (C), 132.8 (+) (C); MS (e.i.) m/z: (molecular ion not observed), 125 [M - OMe]⁺, 101, 74, 59 (100%); MS (c.i., NH₃) m/z: 190 [M + NH₄]⁺; UV (pentane) λ_max = 322 nm (ε = 500).
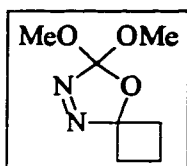
3,4-Diaza-2,2-dimethoxy-1-oxa[4.3]spirooct-3-ene (II-1e and V-1c).

Yield 42 %, Clear colourless oil; ^{1}H NMR (200 MHz, CDCl$_3$) δ: 1.82-2.05 (m, 1 H), 2.10-2.38 (m, 1 H), 2.41-2.70 (m, 4 H), 3.29 (s, 6 H); ^{13}C NMR (50.3 MHz, CDCl$_3$) δ: 11.6 (+) (CH$_2$), 31.0 (+) (CH$_2$), 51.7 (-) (OCH$_3$), 117.9 (+) (C), 138.2 (+) (C); IR (neat, KBr) 2990, 2951, 2847, 1565, 1443, 1240, 1122, 1071, 1031, 898, 823 cm^{-1}; MS (e.i.) m/z: (molecular ion not observed), 141 [M - OMe]$^+$, 117, 91, 74, 59 (100%), 54, 43; MS (c.i., NH$_3$) m/z: 190 [M + NH$_4$]$^+$; UV (pentane) λ$_{max}$ = 328 nm (ε = 500).
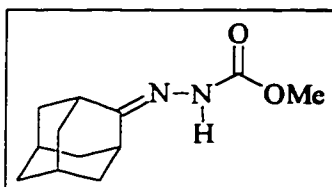
Preparation of Carbomethoxyhydrazone of 2-adamantanone. The carbomethoxyhydrazone of 2-adamantanone was prepared by refluxing 3.01 g of 2-adamantanone (0.020 moles) with 1.98 g of carbomethoxyhydrazide (1.1 eq., 0.022 moles) in benzene using a Dean-Stark apparatus for 8 hours. The crude product was isolated as a white solid after evaporation of the solvent (by rotary evaporation) and was recrystallized from ethanol to give 3.65 g (82%) of product as a white solid. ^{1}H NMR (200 MHz, CDCl$_3$) δ: 1.66-1.83 (m, 12 H), 2.69-2.93 (m, 2 H), 3.80 (s, 3 H), 7.74 (s, 1 H).
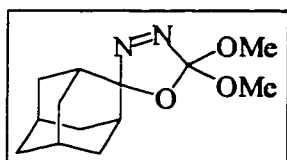
Preparation of 5',5'-Dimethoxyspiro[adamantane]-2,2'-[Δ^3-1,3,4-oxadiazoline] (II-1f and V-1g). 5',5'-Dimethoxyspiro[adamantane]-2,2'-[Δ^3-1,3,4-oxadiazoline] was prepared by dissolving 3.65 g of the carbomethoxyhydrazone of 2-adamantanone (0.0164 moles) in 125 mL of methanol. The resulting solution was then cooled to 0 °C in an ice bath and 7.27 g of lead tetraacetate (1 eq.), dissolved in 25 mL of methanol, was added to the solution slowly over a period of 45 minutes using a dropping flask. This solution was then allowed to stir for a period of one hour

at 0 °C before it was allowed to warm to room temperature. Methanol was then removed by rotary evaporation and the product was dissolved in CH_2Cl_2 and extracted 3 times with 4 % sodium bicarbonate. The organic layer was then dried over magnesium sulfate and the solvent removed by rotary evaporation. The product was then purified by centrifugal chromatography on silica gel using a gradient of hexane to 9:1 hexane:ethyl acetate as the eluant to yield 2.32 g (56%) of clear viscous oil. ^1H NMR (500 MHz, $CDCl_3$) δ: 1.70-2.53 (m, 14 H), 3.44 (s, 6 H); ^{13}C NMR (50.3 MHz, $CDCl_3$) δ: 26.4 (-) (CH), 27.1 (-) (CH), 34.3 (+) (CH_2), 34.7 (+) (CH_2), 36.9 (+) (CH_2), 51.6 (-) (OCH_3), 124.2 (+) (C), 135.3 (+) (C); MS (e.i.) m/z: (molecular ion not observed), 221 [M - OMe]⁺, 165, 134, 119, 106, 105, 93, 92 (100%), 90, 79, 59; MS (c.i., NH_3) m/z 270 [M + NH_4]⁺; UV (pentane) λ_{max} = 328 nm (ε = 300); Anal. Calcd for $C_{13}H_{20}N_2O_3$: C 61.88, H 7.99, N 11.10. Found: C 61.60 , H 8.08 , N 10.71.
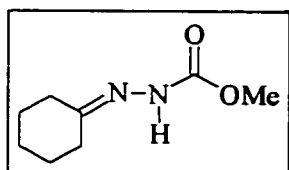
Carbomethoxyhydrazone of cyclohexanone.[279] Yield 91 %; ^1H NMR (200 MHz, $CDCl_3$) δ 1.5-1.8 (m, 6H), 2.20 (dd, J = 5.4, 6.4 Hz, 2H), 2.34 (dd, J = 5.5, 6.3 Hz, 2H), 3.80 (s, 3H), 7.5-7.7 (br s, 1H).
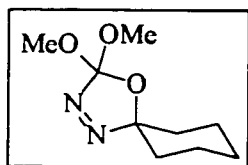
3,4-Diaza-2,2-dimethoxy-1-oxa[4.3]spirodec-3-ene (II-1g and V-1e). Yield 66 %; clear oil: ^1H NMR (500 MHz, $CDCl_3$) δ 1.47-2.01 (m, 10H), 3.42 (s, 6H); ^{13}C NMR (50.3 MHz, $CDCl_3$) δ 22.7 (+) (CH_2), 24.6 (+) (CH_2), 33.5 (+) (CH_2), 51.8 (-) (CH_3), 121.0 (+) (C), 136.1 (+) (C); IR (neat, KBr) 3003, 2945, 2862, 1576, 1447, 1226, 1145, 1097, 900, 848 cm⁻¹; UV λ_{max} = 328 nm (ε = 400); MS (e.i.) m/z: (mol. ion not obsd), 169 [M - OMe]⁺, 113, 91, 90, 81, 67, 59 (100%), 41; MS (c.i., NH_3)

m/z: 218 [M + NH$_4$]$^+$, 201 [M + H]$^+$; Anal. Calcd. for C$_9$H$_{16}$N$_2$O$_3$: C 53.99, H 8.05, N 13.99. Found: C 53.75, H 8.18, N 13.40.
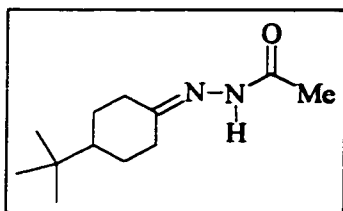
Acetylhydrazone of 4-t-butylcyclohexanone. Yield 95 %: ^{1}H NMR (200 MHz, CDCl$_3$) δ 0.86 (s, 9H) 1.5-1.8 (m, 5H), 2.02 (dd, J = 5.5, 6.4 Hz, 2H), 2.23 (dd, J = 5.5, 6.4 Hz, 2H), 2.15 (s, 3H), 8.4-8.6 (br s, 1H).
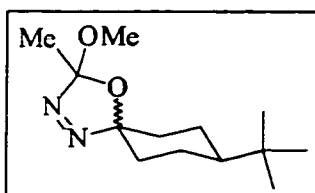
8-t-Butyl-3,4-diaza-2-methoxy-2-methyl-1-oxa[4.3]spirodec-3-ene (II-1h). Yield 71%; 4 diastereomers (10:10:1:1 estimated by integration of the methoxy signals); white solid, m.p. 15-20 °C: ^{1}H NMR (500 MHz, CDCl$_3$) δ 0.83 (s, minor isomer), 0.87 (s, minor isomer), 0.89 (s, major isomer), 0.92 (s, major isomer), 1.21-2.25 (m) overlapping with 1.60 (s) and 1.62 (s), 3.08 (s, minor isomer), 3.10 (s, minor isomer), 3.12 (s, major isomer), 3.17 (s, major isomer); ^{13}C NMR (50.3 MHz, CDCl$_3$) δ 23.1, 23.3, 23.6, 23.8, 24.0, 25.1, 27.5, 27.7, 32.4, 32.8, 33.1, 34.2, 35.2, 36.9, 46.8, 47.3, 50.3, 50.5, 120.1, 133.8; UV λ$_{max}$ = 328 nm (ε = 300); MS (e.i.) m/z: (mol. ion not obsd), 209 [M - OMe]$^+$, 167, 155, 139, 123, 75, 59, 43 (100%); MS (c.i., NH$_3$) m/z: 258 [M + NH$_4$]$^+$, 241 [M + H]$^+$; Anal. Calcd. for C$_{13}$H$_{24}$N$_2$O$_2$: C 64.97, H 10.06, N 11.66. Found: C 64.72, H 9.76, N 11.46.

Carbomethoxyhydrazone of 4-t-butylcyclohexanone.[279] Yield 81%; ^{1}H NMR (200 MHz, CDCl$_3$) δ 0.89 (s, 9H), 1.5-1.8 (m, 6H), 2.19 (dd, J = 5.5, 6.3 Hz, 2H), 2.35 (dd, J = 5.5, 6.3 Hz, 2H), 3.80 (s, 3H), 7.5-7.7 (br s, 1H).
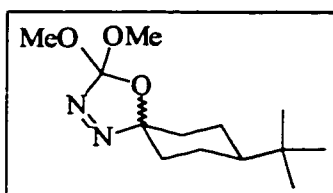
8-*t*-Butyl-3,4-diaza-2,2-dimethoxy-1-oxa[4.3]spirodec-3-

ene (II-1i). Yield 77 %, 2 diastereomers (1.3:1 estimated by

integration of the methoxy signals); viscous liquid: ^{1}H NMR (500

MHz, CDCl$_3$, integrations normalized for each isomer) δ 0.86 (s,

minor isomer, 9 H), 0.91 (s, major isomer, 9 H), 1.12-2.15 (m), 3.44 (s, minor isomer, 6 H); 3.46 (s,

major isomer, 6 H); ^{13}C NMR (50.3 MHz, CDCl$_3$) δ 23.3, 24.8, 27.5, 27.6, 32.4, 33.2, 35.2, 46.5,

47.1, 51.9, 120.9, 136.4; UV λ$_{max}$ = 328 nm (ε = 300); MS (e.i.) m/z: (mol. ion not obsd), 225 [M -

OMe]$^-$, 204, 167, 109, 101, 75, 57, 43 (100%); MS (c.i., NH$_3$) m/z: 257 [M + H]$^+$; Anal. Calcd. for

C$_{13}$H$_{24}$N$_2$O$_3$: C 60.91, H 9.44, N 10.93. Found: C 60.56, H 9.66, N 10.32.
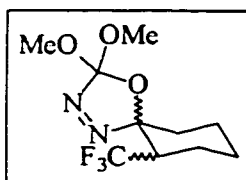
6-Trifluoromethyl-3,4-diaza-2,2-dimethoxy-1-oxa[4.3]spirodec-3-

ene (II-1j). A two-necked, 500 mL round-bottom flask was fitted with

an acetone-dry ice condenser and CF$_3$I, *ca* 6 g, was transferred into the

flask. Pentane (75 mL) was added, followed by 9.0 g (60 mmol, 0.5

equiv.) of the pyrrolidine enamine of cyclohexanone (II-24, Scheme II-7) in 75 mL of pentane. The

solution was stirred at room temperature for 3 h. The precipitate was then filtered off and washed

with pentane, and the solvent was removed with a rotary evaporator. The resulting oil was acidified

with 5M H$_2$SO$_4$ and stirred at room temperature for another 3 h. Extraction with ether (3 x 50 mL)

was followed by washing of the organic layer with water (20 mL), 5% sodium bicarbonate (3 x 25

mL), and brine (25 mL). After the solution was dried over magnesium sulfate it was filtered, and the

solvent was removed by rotary evaporation. The product, 2-trifluoromethylcyclohexanone (II-25) was

purified by fractional distillation at *ca* 25 torr. The fraction collected at 85-87 °C (2.0 g) consisted of

85 % II-25 and 15% cyclohexanone as determined by GC; overall yield 33 %. A solution of benzene

(50 mL) containing 2-trifluoromethylcyclohexanone (II-25, 1.77 g, 9 mmol, weight adjusted for

cyclohexanone impurity), methyl hydrazinocarboxylate (1.24 g, 13.8 mmol) and acetic acid (2 drops) was refluxed for 24 h using a Dean-Stark apparatus. The crude product containing II-26 was isolated as an oil and attempts to crystallize II-26 from it (various solvent mixtures) failed. ^{1}H NMR (500 MHz, CDCl$_3$) δ 1.2-2.1 (m, 8H), 2.1-2.3 (m, 3H), 3.80 (s, 3H), 7.6-7.8 (br s, 1H). Hydrazone II-26 (2.92 g, 1.23 mmol, weight adjusted for carbomethoxyhydrazone of cyclohexanone) dissolved in 20 mL of methanol under N$_2$ was added from a dropping funnel during 30 min to an ice-cold solution of lead tetraacetate (LTA, 5.55g, 12.5 mmol) in 25 mL of methanol. The solution was kept at ca -10 °C for 5 days with occasional stirring. The solvent was then removed by rotary evaporation and methylene chloride (50 mL) was added to the residue. The solution was filtered to remove inorganic salts and it was washed with 5% sodium bicarbonate (4 x 25 mL) before the organic layer was dried over magnesium sulfate. Removal of the solvent left oxadiazoline II-1j which was purified from minor amounts of oxadiazoline II-1g by repeated radial chromatography on silica, eluting with 5 - 20% ethyl acetate in hexane. Yield of II-1j, 12%, isolated as a mixture of 2 diastereomers (2:1 estimated by integration of the methoxy signals); clear liquid: ^{1}H NMR (500 MHz, CDCl$_3$, integrations normalized for each diastereomer) δ 1.42-2.03 (m), 2.05-2.15 (m), 2.25-2.40 (m), 3.45 (s, major isomer, 3H), 3.52 (s, minor isomer, 3H), 3.54 (s, minor isomer, 3H), 3.55 (s, major isomer, 3H); ^{13}C NMR (125 MHz, CDCl$_3$) δ 22.8, 22.9, 23.3, 23.4, 24.1, 24.8, 33.7, 36.1, 46.0 (q, J= 26.3 Hz), 48.2 (q, J= 26.0 Hz), 51.9, 52.0, 52.1, 118.1, 118.6, 120.3 (q, J= 299 Hz), 125.4 (q, 280 Hz), 136.2, 137.4; ^{19}F NMR (470 MHz, CDCl$_3$ referenced to CFCl$_3$) δ -64.9 (major isomer, d, J=7.5 Hz), -66.3 (minor isomer, d, J=7.5 Hz); UV λ_{max} = 328 nm (ε = 300); MS (e.i.) m/z: (mol. ion not obsd), 237 [M - OMe]$^-$, 219, 169, 150, 131, 119, 100, 69 (100%); Anal. Calcd. for C$_{10}$H$_{15}$F$_3$N$_2$O$_3$: C 44.78, H 5.64, N 10.44. Found: C 44.67, H 5.53, N 10.05.

Carbomethoxyhydrazone of tropinone. Yield 91 %: ^{1}H NMR (200 MHz, CDCl$_3$) δ 1.4-1.6 (m,

2H), 1.9-2.1 (m, 4H), 2.40 (s, 3H), 2.62 (dd, J = 4.4, -14 Hz, 4H), 3.3-3.5 (m, 2H), 3.80 (s, 3H), 7.5-

7.7 (br s, 1H).
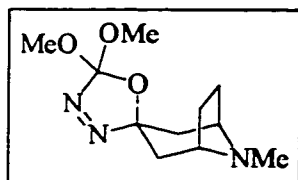
(1α,3β,5α)-5',5'-Dimethoxy-8-methylspiro[8-

azabicyclo[3.2.1]octane]-3,2'-[Δ^3-1,3,4-oxadiazoline] (II-1k).

Yield 32 %, one diastereomer, presumably because of

participation of the amino group during oxidative cyclization,

clear liquid: ^{1}H NMR (500 MHz, CDCl$_3$) δ 1.23 (d, J = 13.8 Hz, 1H), 1.35 (d, J = 13.9 Hz, 1H), 1.76

- 1.91 (m, 4H), 2.08 (s, 3H), 2.09 (s, 3H), 2.10-2.17 (m, 1H), 2.65 (dd, J = 13.9, 3.5 Hz, 1H), 2.82-

2.89 (m, 2H) 3.24 (s, 6H); ^{13}C NMR (125 MHz, CDCl$_3$) δ 25.5, 25.8, 26.9, 37.7, 38.8, 39.3, 39.7,

51.3, 51.5, 59.4, 59.9, 118.8, 138.9; UV λ$_{max}$ = 328 nm (ε = 400); MS (e.i.) m/z: (mol. ion not obsd),

210 [M - OMe]$^-$, 198, 162, 155, 138, 108, 95, 82 (100%), 59, 42; MS (c.i., NH$_3$) m/z: 259 [M +

NH$_4$]$^-$, 242 [M + H]$^-$; Anal. Calcd. for C$_{11}$H$_{19}$N$_3$O$_3$: C 54.76, H 7.94, N 17.41. Found: C 54.38, H

8.23, N 17.20.

Carbomethoxyhydrazone of 3-pentanone.[279] Yield 82 %: ^{1}H NMR (200 MHz, CDCl$_3$) δ 1.06 (t,

J = 7.5 Hz, 6H), 2.32 (q, J = 7.5 Hz, 4H), 3.80 (s, 3H), 7.5-7.7 (br s, 1 H).
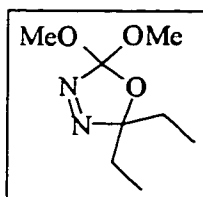
5,5-Diethyl-2,2-dimethoxy-Δ^3-1,3,4-oxadiazoline (II-m). Yield 66 %;

clear oil: ^{1}H NMR (500 MHz, CDCl$_3$) δ 0.88 (t, J = 7.5 Hz, 6H), 1.86 (q, J

= 7.5 Hz, 4H), 3.53 (s, 6H); ^{13}C NMR (125 MHz, CDCl$_3$) δ 7.3, 28.3, 51.6,

124.9, 136.6; UV λ$_{max}$ = 328 nm (ε = 500); MS (e.i.) m/z: (mol. ion not

obsd), 157 [M - OMe]⁺, 129, 91, 75, 59 (100%), 43; MS (c.i., NH₃) m/z: 206 [M + NH₄]⁺, 189 [M +

H]⁺; Anal. Calcd. for C₈H₁₆N₂O₃: C 51.05, H 8.57, N 14.88. Found: C 50.96, H 8.27, N 14.80.

Acetylhydrazone of 3-pentanone.[59] Yield 93 %: ¹H-NMR (200 MHz, CDCl₃) δ 1.02 (t, J = 7.5

Hz, 6H), 1.95 (q, 4H), 2.14 (s, 3H) 8.2-8.4 (br s, 1H).
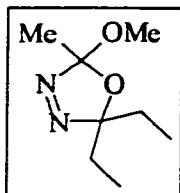
5,5-Diethyl-2-methoxy-2-methyl-Δ³-1,3,4-oxadiazoline (II-1l). Yield

68 %; clear oil: ¹H NMR (500 MHz, CDCl₃) δ 0.86 (t, J = 7.5 Hz, 6H),

0.95 (t, J = 7.5 Hz, 6H), 1.59 (s, 3H), 1.65 - 2.05 (m, 4H), 3.18 (s, 3H);

¹³C NMR (125 MHz, CDCl₃) δ 8.1, 14.4, 22.1, 29.4, 29.6, 50.3, 122.8,

133.1; UV λ$_{max}$ = 328 nm (ε = 500); MS (e.i.) m/z: (mol. ion not obsd), 141 [M - OMe]⁺, 113, 91, 75,

59 (100%), 43; MS (c.i., NH₃) m/z: 190 [M + NH₄]⁺,173 [M + H]⁺.

Carbomethoxyhydrazone of 2-butanone. Yield 88 %; ¹H NMR (200 MHz, CDCl₃) δ 1.08 (t, J

= 7.5 Hz, 3H), 1.78 (s, 3H), 2.31 (q, J = 7.5 Hz, 2H), 3.80 (s, 3H), 7.5-7.7 (br s, 1H).
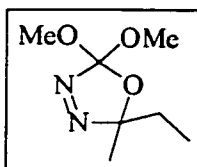
5-Ethyl-2,2-dimethoxy-5-methyl-Δ³-1,3,4-oxadiazoline (II-1n and

V-1h). Yield 70 %; clear oil: ¹H NMR (500 MHz, CDCl₃) δ 0.81 (dd, J =

7.6 Hz, 3H), 1.36 (s, 3H), 1.69 (ABX₃, J = 7.6, -14.3 Hz, 1H), 1.79

(ABX₃, J = 7.6, -14.3 Hz, 1H), 3.44 (s, 3H), 3.49 (s, 3H); ¹³C NMR (125

MHz, CDCl₃) δ 7.4, 21.4, 30.3, 51.4, 51.6, 121.8, 136.7; IR (neat, KBr) 2982, 2949, 2887, 2847,

1577, 1459, 1448, 1376, 1137, 1078, 930, 862 cm⁻¹; UV λ$_{max}$ = 328 nm (ε = 500); MS (e.i.) m/z:

(mol. ion not obsd), 143 [M - OMe]⁺, 91, 74, 59 (100%), 43; MS (c.i., NH₃) m/z: 192 [M + NH₄]⁺,

175 [M + H]⁺; Anal. Calcd. for C₇H₁₄N₂O₃: C 48.26, H 8.10, N 16.08. Found: C 48.20, H 8.14, N

15.79.
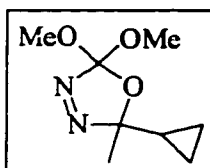
5-Cyclopropyl-2,2-dimethoxy-5-methyl-Δ³-1,3,4-oxadiazoline (V-1f). Yield 68 %, Clear viscous oil; ¹H NMR (500 MHz, CDCl₃) δ: 0.42-0.56 (m, 4 H), 1.32 (tt, J=9.6, 4.0 Hz, 1 H), 1.53 (s, 3 H), 3.43 (s, 3 H), 3.53 (s, 3 H); ¹³C NMR (125 MHz, CDCl₃) δ: 1.60, 17.0, 22.5, 51.7, 52.0, 121.2, 137.1; MS (e.i.) m/z: (molecular ion not observed), 155 [M - OMe]⁺, 143, 131, 123, 115, 91 (100%), 67, 53, 43; MS (c.i., NH₃) m/z 204 [M + NH₄]⁺; UV (pentane) λₘₐₓ = 328 nm (ε = 500); Anal. Calcd for C₈H₁₄N₂O₃: C 51.60, H 7.58, N 15.04. Found: C 51.75, H 7.22, N 14.99.
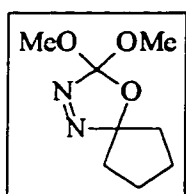
3,4-Diaza-2,2-dimethoxy-1-oxa[4.4]spironon-3-ene (V-1d);Yield 74%, Clear oil; ¹H NMR (200 MHz, CDCl₃) δ 1.74-2.20 (m, 8 H), 3.44 (s, 6 H); ¹³C NMR (50.3 MHz, CDCl₃) δ 24.9 (+) (CH₂), 35.3 (+) (CH₂), 51.6 (-) (CH₃), 127.7 (+) (C), 136.8 (+) (C); IR (neat, KBr) 2969, 2952, 2877, 2847, 1571, 1444, 1329, 1235, 1200, 1157, 1140, 1115, 1079, 1037, 1012, 948, 913, 862 cm⁻¹; MS (e.i.) m/z: (molecular ion not observed), 155 [M - OMe]⁺, 131, 115, 91 (100%), 59, 43; MS (c.i., NH₃) m/z 204 [M + NH₄]⁺; UV (pentane) λₘₐₓ = 328 nm (ε = 300); Anal. Calcd for C₈H₁₄N₂O₃: C 51.60, H 7.58, N 15.04. Found: C 51.45, H 7.76, N 15.06.
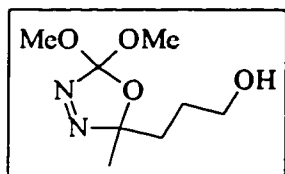
5-(3-Hydroxypropyl)-2,2-dimethoxy-5-methyl-Δ³-1,3,4-oxadiazoline (V-1i); Yield 23 %, Clear oil; ¹H NMR (500 MHz, CDCl₃) δ1.46-1.59 (m) with 1.52 (s) and 1.57 (t) superimposed, 6 H total,1.61-1.74 (m, 2 H), 1.80-1.94 (m, 2 H), 3.45 (s, 3 H), 3.52 (s, 3 H), 3.64 (dt, J=6.1, 5.8 Hz, 2 H); ¹³C NMR (125 MHz, CDCl₃) δ 22.1, 26.6, 33.8,51.4, 51.6, 62.3, 121.4, 136.9; IR (neat, KBr) 3450, 2988, 2953, 2879, 2848, 1578, 1448, 1209, 1136, 1075,

1027, 957, 907 cm^{-1}; Anal. Calcd for $C_8H_{16}N_2O_4$: C 47.05, H 7.90, N 13.72. Found: C 47.10, H 8.08, N 13.82.
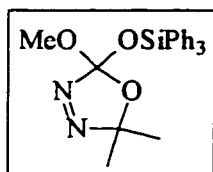
5,5-Dimethyl-2-methoxy-2-triphenylsiloxy-Δ^3-1,3,4-oxadiazoline(III-1a): 5,5-Dimethyl-2-methoxy-2-triphenylsiloxy-Δ^3-1,3,4-oxadiazoline was prepared by acid catalyzed exchange of 2-acetoxy-5,5-dimethyl-2-methoxy-Δ^3-1,3,4-oxadiazoline with triphenylsilanol. 2-Acetoxy-5,5-dimethyl-2-methoxy-Δ^3-1,3,4-oxadiazoline (2.0 g, 0.011 mol), triphenylsilanol (1.1:1, 3.2 g, 0.012 mol) and 40 mL of dichloromethane and 3 drops of trifluoroacetic acid were mixed in a 100 mL round bottom flask. The mixture was stirred for 5 days at room temperature. The solvent was then removed under vacuum and the crude product was purified by centrifugal chromatography on silica gel using hexane as the eluant to yield 1.4 g (32.3 % from 2-acetoxy-5,5-dimethyl-2-methoxy-Δ^3-1,3,4-oxadiazoline) of white solid (m.p. 74.5 °C). ^{1}H NMR (200 MHz, CDCl$_3$) δ 1.24 (s, 3 H), 1.47 (s, 3 H), 3.22 (s, 3 H), 7.32-7.45 (m, 9 H), 7.63-7.66 (m, 6 H); ^{13}C NMR (50.3 MHz, CDCl$_3$) δ 23.8, 23.9, 51.6, 118.4, 127.7, 130.1, 132.2, 133.7, 135.6; ^{29}Si NMR (59.6 MHz, CH$_2$Cl$_2$) δ -14.6; MS (e.i.) m/e: (molecular ion not observed), 317, 287, 259 (M- 145)* (100%), 213, 181, 105, 77, 43. Anal. Calcd for C$_{23}$H$_{24}$N$_2$O$_3$Si: C 68.28, H 5.98, N 6.93. Found: C 68.0 , H 6.03 , N 6.76.

VI.3. Diazirines (II-34).

3-Benzyl-3-chlorodiazirine (**II-34a**) and 3-phenyl-3-chlorodiazirine (**II-34b**) were prepared by Graham oxidations and characterized as described previously.[30] 3-Methoxy-3-phenyldiazirine (**II-34c**) was prepared by the exchange reaction of 3-bromo-3-phenyldiazirine with sodium methoxide in dimethylformamide (DMF) and characterized as described previously.[14c,30,151]

VI.4. Steady State Photolyses (Chapter II).

Steady state photolyses (300 nm) were performed on solutions of oxadiazoline (II-1a, II-1b, and

II-1c) (each solution 0.1 M in benzene-d_6, deoxygenated with dry N_2) in Pyrex NMR tubes and the

reactions were monitored by ^{1}H-NMR. In each case, a signal at $\delta 1.20$ ppm, assigned to 2-

diazopropane, was observed and the starting material was completely converted after 1 h of exposure

to 300 nm light in the Rayonet chamber (6-12 300 mn bulbs). The slow growth of acetone azine

(identified by comparison with an authentic sample by ^{1}H-NMR and GC co-injection techniques) was

observed (two singlets δ 1.86 and 1.81) over time and trace amounts of propene were detected only

after more than 12 hours had elapsed (11 hours in the dark). Ester or carbonate products were also

identified by comparison with authentic materials. For the case of oxadiazolines II-1a,b, no signals

associated with either methoxydiazoethane or dimethoxydiazomethane or their corresponding azines

were detected. The results of this study suggest that if alkoxycarbenes are formed in the laser

experiments, then they are most probably the result of a multiphoton process.

VI.4.a. Steady state photolysis of oxadiazoline II-1a and b with 250/300 nm light.

Steady state photolyses of oxadiazoline II-1a,b with both 250 and 300 nm light (each solution 0.1

M in benzene-d_6, deoxygenated with dry N_2) in quartz NMR tubes showed the growth of a signal at

$\delta 1.20$ ppm, assigned to 2-diazopropane. However, under these conditions significant amounts of

propene (ca. 5%) were formed after 5 minutes of photolysis. After 1 hr of photolysis only signals

associated with methyl acetate or dimethylcarbonate, propene, and acetone azine were observed

(propene:azine=2:1). Optimal conditions for the generation of dimethylcarbene from oxadiazolines II-

1a,b by steady state photolysis were found when 10-14 300 nm bulbs were used to convert

oxadiazoline precursors to 2-diazopropane completely, which was then irradiated using 6-12 250 nm

bulbs, or when solutions of oxadiazolines were irradiated simultaneously using 10-12 250 nm and 1-2 300 nm bulbs. In either case, full photochemical conversion of the oxadiazolines was required because the oxadiazolines also absorb at 250 nm. It was found that acetone azine formation was minimized (< 5%) when the initial oxadiazoline concentrations were between 0.01 and 0.001 M.

VI.4.b. Steady state photolysis of 3,4-diaza-2,2-dimethoxy-1-oxa[4.3]spirooct-3-ene with 300 nm light.

Upon photolysis of oxadiazoline **II-1d** or **II-1e** with 300 nm light in benzene (0.1 M, deoxygenated with dry N_2) the appearance of triplets at 2.94 ppm (J = 5.3 Hz) and at 2.75 ppm (J = 5.3 Hz), and a pentet at 1.49 ppm (J = 5.3 Hz) were observed and assigned to diazocyclobutane. Methyl acetate (from **II-1d**) or dimethylcarbonate (from **II-1e**) were formed in nearly quantitative yields as determined by ^{1}H-NMR. As was the case for oxadiazolines **II-1a** to **c**, the starting material was completely converted to diazoalkane after 1 hr of photolysis. Cyclobutanone azine (GC-MS, m/z: 136 [M]$^+$, 119, 108, 81, 55, 39) was formed slowly and only trace amounts of methylenecyclopropane (pentet at 5.46 ppm (J = 2.1 Hz) and a triplet at 0.88 ppm (J = 2.1 Hz) were observed after 12 hours of photolysis.

VI.4.c. Steady state photolysis of 3,4-diaza-2,2-dimethoxy-1-oxa[4.3]spirooct-3-ene with 250/300 nm light.

Steady state photolyses of oxadiazolines **II-1d, e** with both 250 and 300 nm light (0.1-0.001 M in benzene-d_6) in quartz NMR tubes led to the growth of signals assigned to diazocyclobutane. Significant amounts of methylenecyclopropane and cyclobutene (two singlets at 5.91 and 2.44 ppm) were also formed after 30 minutes of photolysis. It appeared that the photolysis of diazocyclobutane

was less efficient than that of 2-diazopropane. The ratio of methylenecyclopropane to cyclobutene

(5.5:1) was determined based on integrations of unobscured peaks in the vinyl region of the spectrum

which did not change dramatically as a function of photolysis time. GC-MS analysis of the photolysis

mixtures (oven temperature of 30°C) showed a broad peak with a retention time of ca. 2 minutes

(before solvent) with a molecular ion of mass 54 (C_4H_6) and a base peak of 39 (M-15) which could be

attributed to either cyclobutene or methylenecyclopropane or both.

Photolysis of oxadiazoline **II-1e** in neat tetramethylethylene (TME) with 250/300 nm light in a

quartz NMR tube (deoxygenated with dry N_2, with a drop of benzene-d_6 for locking) was followed by

500 MHz ^{1}H-NMR spectroscopy using solvent suppression routines. The growth of a signal at 0.80

ppm was assigned to formation of the adduct of **CB:** with TME. Methylenecyclopropane and

cyclobutene were also observed. Ratios of cyclobutene:methylenecyclopropane:adduct were

determined to be 1:5:5.5, respectively. The GC-MS analysis of the photolysis mixtures (oven

temperature of 30°C) showed the same broad peak with a retention time of ca. 2 minutes (molecular

ion 54 and base peak of 39) and a peak with a retention time of ca. 12 minutes with a molecular ion

of mass 138 ($C_{10}H_{18}$). The TME adduct was isolated by preparative GC. ^{1}H-NMR (microprobe,

C_6D_6, 500 MHz) δ: 1.87 (m, 6H) and 0.88 (s, 12H). Single peak in the GC-MS trace (oven 30 °C) at

retention time *ca* 12 min, GC-MS (e.i.) m/z: 138 [M]$^+$, 123 [M-15]$^+$, 95, 81, 67, 53, 41.

Trapping of **CB:** with tetramethylethylene (TME)   also occurred in cyclohexane-d_{12} and

acetonitrile-d_3 solutions as above with various concentrations of TME present using the

photochemical precursor 3,4-diaza-2,2-dimethoxy-1-oxa[4.3]spirooct-3-ene (**II-1e**). Preparatory GC

allowed for the isolation of methylenecyclopropane, cyclobutene, and the TME adduct and proton

NMR chemical shifts and GC-MS traces confirmed their structure. These experiments were

performed in sealed and deoxygenated quartz NMR tubes and product yields and ratios were determined using a 500 MHz NMR spectrometer and by GC. Integrations of peaks assigned to photolysis products were compared with an internal standard of known concentration. A merry-go-round Rayonet apparatus ensured that all solutions were photolyzed under identical conditions. Yields at high conversion were by 500 MHz ^{1}H NMR spectroscopy with suppression of the TME singlet as well as digital filtering of that singlet outside the spectral window. Integrations of unobscured signals were compared with that of internal standard hexamethyldisilane. Yields and product ratios of photolysis products were determined and the results are summarized in chapter II. In order to ensure that yields of TME adduct were the result of carbene addition to TME, a solution of precursor II-1e was irradiated with only 300 nm light in a solution of neat TME. The resulting photolysis mixture showed no adduct formation with an irradiation time of 2.5 hours as determined by ^{1}H-NMR and GC-MS.

VI.4.d. Steady state photolysis of 5',5'-Dimethoxyspiro[adamantane-2,2'-[Δ^3-1,3,4]oxadiazoline] (II-1f) with 250/300 nm light.

Steady state photolyses of oxadiazoline II-1f with both 250 and 300 nm light (each solution 0.1-0.001 M in benzene and cyclohexane, deoxygenated with dry N$_2$) in quartz NMR tubes as described above were also performed. In benzene dehydroadamantane and adamantanone azine were found to be the major products and the ratios of these products were found to be dependant on the concentration of oxadiazoline starting material (<1:12 dehydroadamantane: adamantanone azine when [II-1f]=0.1M, >2:1 dehydroadamantane: adamantanone azine when [II-1f]=0.001M). Approximately 3-4 % adamantanone was also detected (yields not sensitive to precursor concentration). Saturation of the solutions with O$_2$ prior to photolysis resulted in significant increases in the yield of adamantanone

(~18% relative to the internal standard). Dehydroadamantane, adamantanone, and adamantanone azine were identified by their mass spectra obtained by GC-MS of the photolysis mixtures. **Dehydroadamantane** MS (e.i.) m/z: 134 [M]⁺, 119, 115, 105, 91 (100 %), 79, 65, 51, 39. **Adamantanone** MS (e.i.) m/z: 150 [M]⁺, 134, 117, 104, 93, 79, 67, 53, 39. **Adamantanone azine** MS (e.i.) m/z: 296 [M]⁺, 281, 267, 253, 239, 228, 215, 201, 190, 175, 150, 134, 121, 106, 91, 79 (100 %), 67, 55, 41.

In cyclohexane, dehydroadamantane, adamantanone, and adamantanone azine were also formed during two colour irradiation. In addition, a product with a molecular ion of mass m/z=218, which is thought to be from a C-H insertion adduct of adamantylidene (**AD:**) with solvent, was detected.

VI.5. Cyclohexylidenes Generated by Steady State Photolysis of Oxadiazolines.

Steady-state photolyses were carried out in a Rayonet photochemical reactor equipped with a "merry-go-round" apparatus. Photolytic conversions of oxadiazolines to diazo compounds were performed by irradiating 0.001 M solutions of oxadiazolines **II-1g** to **n** in deoxygenated (N₂ or argon) benzene-d₆ in Pyrex reaction vessels (NMR tubes in some cases) with 10-14 300 nm lamps. Under these conditions, irradiation for 15-45 minutes was sufficient to convert each oxadiazoline completely to its corresponding diazoalkane. Diazoalkanes **II-2g** to **n** were stable for several hours at room temperature in dilute solution but thermal azine formation occurred at room temperature over a period of 4-5 days, after which the solutions were analyzed by ¹H-NMR and GC-MS. Photolytic conversion of oxadiazolines **II-1g** to **n** to the corresponding cycloalkyl- or dialkylcarbenes were performed by irradiating 0.01 M solutions of oxadiazolines in deoxygenated (N₂ or argon) cyclohexane-d₁₂ in quartz reaction vessels (NMR tubes in some cases) with 8-12 250 nm lamps and 1-2 300 nm lamps. Dual wavelength irradiation was required to convert each oxadiazoline to the

corresponding carbene efficiently and typical reaction times for complete conversion of the starting materials were 2-4 h. The reaction times were shortest when 12 250 nm lamps were used in conjunction with 2 300 nm lamps. Short reaction times were preferable to minimize azine formation. Dual wavelength irradiations of solutions of oxadiazolines in hexadecane allowed for GC and GC-MS analyses of reaction mixtures. Compounds II-1g, i, j, k, m, and n afforded dimethyl carbonate as a co-product, whereas compounds II-1h and II-1l afforded methyl acetate as a co-product.

Photolysis of oxadiazoline II-1g with 300 nm light.

Diazocyclohexane: ^{1}H NMR (500 MHz, C_6D_6) δ 1.45-1.60 (m, 6H), 1.85-1.95 (m, 2H), 2.15-2.25 (m, 2H). Dimethylcarbonate: ^{1}H NMR (500 MHz, C_6D_6) δ 3.38 (s). IR (solution, KBr) 2942, 2853, 2038 (C=N=N), 1754 (dimethylcarbonate).

After 5 days at room temperature cyclohexanone azine was obtained in 92 % yield: ^{1}H NMR (500 MHz, C_6D_6) δ 1.2-1.6 (m, 12H), 1.65-1.85 (m, 4H), 2.34 (dd, J = 6.5, 6.2 Hz, 2H), 2.60 (dd, J = 6.6, 6.3 Hz, 2H). MS (e.i,, photolysis in benzene) m/z: 192 [M]⁺, 177, 163, 149, 136, 129, 110, 96, 82, 69, 55, 41 (100%), 27. Cyclohexene (1.4 %) was estimated by ^{1}H NMR relative to internal standard hexamethyldisilane.

Photolysis of oxadiazoline II-1g with 250/300 nm light.

Cyclohexene: ^{1}H NMR (500 MHz, C_6D_{12}) δ 1.60 (s, 4H), 1.96 (s, 4H), 5.60 (s, 2H), unresolved coupling in each case; MS (e.i., photolysis in hexadecane) m/z: 82 [M]⁺, 67 (100 %), 54, 50, 39, 27, 15. Dimethylcarbonate : ^{1}H NMR (500 MHz, C_6D_{12}) δ 3.63 (s). Cyclohexanone azine was not detected.

Photolysis of oxadiazoline II-1h with 300 nm light.

4-*t*-Butyldiazocyclohexane[280]: ¹H NMR (500 MHz, C₆D₆) δ 0.87 (s, 9H), 0.95-1.85 (m, 5H), 1.85-2.30 (m, 4H). Methyl acetate: ¹H NMR (500 MHz, C₆D₆) δ 3.27 (s, 3H), 1.61 (s, 3H).

Photolysis of oxadiazoline II-1i with 300 nm light.

4-*t*-Butyldiazocyclohexane: ¹H NMR (500 MHz, C₆D₆) δ 0.87 (s, 9H), 0.95-1.85 (m, 5H), 1.85-2.30 (m, 4H). Dimethylcarbonate: ¹H NMR (500 MHz, C₆D₆) δ 3.38 (s). IR (solution, KBr) : 2954, 2849, 2037 (C=N=N), 1755 (dimethylcarbonate).

After 5 days at room temperature 4-*t*-butylcyclohexanone azine was present in 86 % yield: ¹H NMR (300 MHz, C₆D₆) δ 0.82 (s, 18H), 0.90-1.45 (m, 10H), 1.50-2.20 (m, 8H). MS (ei, photolysis in benzene) m/z: 304 [M]⁺, 289, 275, 261, 247, 233, 219, 205, 192, 180, 163, 152, 135, 121, 96, 82, 67, 57 (100%), 41, 29. 4-*t*-Butylcyclohexene(1.5 %) was estimated relative to internal standard hexamethyldisilane.

Photolysis of oxadiazoline II-1i with 250/300 nm light.

4-*t*-Butylcyclohexene: ¹H NMR (500 MHz, C₆D₁₂) δ 0.86 (s , 9H), 1.1-1.3 (m, 3H), 1.75-1.80 (m, 2H), 1.95-2.00 (m, 2H), 5.61 (m, 2H). Dimethylcarbonate : ¹H NMR (500 MHz, C₆D₁₂) δ 3.63 (s). 4-*t*-Butylcyclohexanone azine was not detected.

Photolysis of oxadiazoline II-1j with 300 nm light.

2-Trifluoromethyldiazocyclohexane: ^{1}H NMR (500 MHz, C_6D_6) δ 0.85-1.0 (m, 2H, C_4-H, C_5-H),

1.0-1.2 (m, 3H, C_3-H$_e$, C_4-H, C_5-H), 1.45-1.52 (m, 1H, C_3-H$_a$), 1.62 (ddd, J = 3.9, 6.5, -15.1 Hz, 1H,

C_6-H$_e$), 2.01 (ddd, J = 11.0, 4.5, -15.0 Hz, 1H, C_6-H$_a$), 2.37 (qdd, J = 10.0, 7.1, 3.3 Hz, 1H, C_2-H$_a$).

Dimethylcarbonate: ^{1}H NMR (500 MHz, C_6D_6) δ 3.38 (s). IR (solution, KBr): 2955, 2856, 2052

(C=N=N), 1756 (dimethylcarbonate), 1453, 1282.

Photolysis of oxadiazoline II-1j with 250/300 nm light.

3-Trifluoromethylcyclohexene and 1-trifluoromethylcyclohexene were not separated for

acquisition of the NMR spectra but they were examined separately by GC/MS. The signals in the

proton NMR spectrum are normalized for each isomer. 3-Trifluoromethylcyclohexene[141b]: ^{1}H NMR

(500 MHz, C_6D_{12}) δ 1.2-2.1 (m overlapping with signals of the other isomer), 2.73 (qddd, J = 9.1,

6.5, 3.6, 1.6 Hz, 1 H), 5.60 (dd, J = 9.6, 1.6 Hz, 1 H), 5.89 (m, 1 H); ^{19}F NMR (280 MHz, C_6D_{12}

referenced to $CFCl_3$) δ -73.78 (d, 9.1 Hz); MS (e.i., photolysis in hexadecane) m/z: 150 [M]$^+$, 135,

115, 81 (100 %), 53, 39. 1-Trifluoromethylcyclohexene[141a]: ^{1}H NMR (500 MHz, C_6D_{12}) δ 1.2-2.1 (m

overlapping with signals of the other isomer), 6.2-6.25 (br s, 1 H); ^{19}F NMR (280 MHz, C_6D_{12}

referenced to $CFCl_3$) δ -70.99 (s); MS (e.i., photolysis in hexadecane) m/z: 150 [M]$^+$, 131, 122, 81

(100 %), 53, 39. Dimethylcarbonate : ^{1}H NMR (500 MHz, C_6D_{12}) δ 3.63 (s). Azines were not

detected.

Photolysis of oxadiazoline II-1k with 300 nm light.

8-Aza-3-diazo-8-methylbicyclo[3.2.1]octane: ^{1}H NMR (500 MHz, $CDCl_3$) δ 1.3-1.4 (m, 2H), 1.53

(dd, J = 1.9, -14.3 Hz, 2H), 1.70-1.75 (m, 2H), 1.97 (s, 3H, N-CH$_3$), 2.53 (dd, J = 2.8, -14.6 Hz, 2H),

2.73 (m, 2H). Dimethylcarbonate: ^{1}H NMR (500 MHz, C_6D_6) δ 3.38 (s). IR (solution, KBr): 2977, 2942, 2855, 2037 (C=N=N), 1755 (dimethylcarbonate).

Photolysis of oxadiazoline II-1k with 250/300 nm light.

8-Aza-8-methylbicyclo[3.2.1]oct-2-ene: ^{1}H NMR (500 MHz, C_6D_{12}) δ 1.4-2.5 (m, 6H, C_4-H_2, C_6-H_2, and C_7-H_2), 2.95-3.20 (m, 2H, C_1-H and C_5-H), 3.26 (s, 3H, N-CH$_3$), 5.85-6.0 (m, 1H, C_3-H), 6.19 (ddd, J = 12.9, 9.8, 1.8 Hz, 1H, C_2-H). Dimethylcarbonate : ^{1}H NMR (500 MHz, C_6D_{12}) δ 3.63 (s).

Photolysis of oxadiazoline II-1l with 300 nm light.

3-Diazopentane: ^{1}H NMR (500 MHz, C_6D_6) δ 0.83 (t, J = 7.6 Hz, 3H), 1.73 (q, J = 7.6 Hz, 2H). Methyl acetate: δ 1.61 (s, 3 H), 3.27 (s, 3H).

Photolysis of oxadiazoline II-1m with 300 nm light.

3-Diazopentane: ^{1}H NMR (500 MHz, C_6D_6) δ 0.78 (t, J = 7.6 Hz, 6H), 1.68 (q, J = 7.6 Hz, 4H). Dimethylcarbonate: ^{1}H NMR (500 MHz, C_6D_6) δ 3.38 (s). IR (solution, KBr): 2948, 2846, 2037 (C=N=N), 1755 (dimethylcarbonate).

During 5 days 3-pentanone azine was formed in 99 % yield: ^{1}H NMR (500 MHz, C_6D_6) δ 0.91 (t, J= 7.5 Hz, 3H), 1.11 (t, J= 7.5 Hz, 3H), 2.16 (q, J= 7.5, 2H), 2.31 (q, J= 7.5 Hz, 2H). Alkene products were barely detectable; estimated at < 1% by ^{1}H NMR, relative to internal standard hexamethyldisilane. MS (e.i., photolysis in benzene) m/z: 168 (M+), 157, 153, 139, 125, 113, 98, 84, 68, 56 (100%), 41, 29.

Photolysis of oxadiazoline II-1m with 250/300 nm light.

NMR spectra of the products were gleaned, insofar as possible, from the composite spectrum of the mixture. (E)-2-Pentene: ^{1}H NMR (500 MHz, C_6D_{12}) δ 0.943 (t, J = 7.3 Hz, 3H), 1.595 (m, 3H), 2.02 (m, 2H), 5.2-5.5 (br s, 2H). (Z)-2-Pentene: δ 0.944 (t, J = 7.3 Hz, 3H), 1.560 (m, 3H), 1.96 (m, 2H), 5.2-5.5 (br s, 2H). The presence of 1,2-dimethylcyclopropane was inferred from a signal near δ 0.4 ppm corresponding to the methylene group. The ratios (E)-2-pentene:(Z)-2-pentene:1,2-dimethylcyclopropane were *ca* 15:10:1 (58%, 38%, 3.8%) as estimated by integration of the resolved signals at 2.02, 1.96 and 0.4 ppm. Dimethylcarbonate : δ 3.63 (s). 2-Pentanone azine was not detected.

Photolysis of oxadiazoline II-1n with 300 nm light.

2-Diazobutane: ^{1}H NMR (500 MHz, C_6D_6) δ 0.78 (t, J = 7.6 Hz, 3H), 1.23 (s, 3H), 1.70 (q, J = 7.6, 2H). IR (solution, KBr): 2975, 2848, 2037 (C=N=N), 1756 (dimethylcarbonate).

After 5 days a mixture of isomeric 2-butanone azines (E,E), (E,Z) and (Z,Z) was obtained in 99 % combined yield: ^{1}H NMR (300 MHz, C_6D_6, signals nomalized separately for each isomer, which were assigned on the basis of expected relative abundances[281]) δ 0.87 ((E,Z) isomer, t, J = 7.5 Hz, 3H), 0.89 ((E,E) isomer, t, J = 7.5 Hz, 3H), 1.05 ((E,Z) isomer, t, J = 7.6 Hz, 3H), 1.07 ((Z,Z) isomer, t, J = 7.5 Hz, 3H), 1.76 ((Z,Z) isomer, s, 3H), 1.78 ((E,Z isomer), s, 3H), 1.81 ((E,E) isomer, s, 3H), 1.85 ((E,Z) isomer, s, 3H), 2.11 ((E,Z) isomer, q, J = 7.5 Hz, 2H), 2.13 ((E,E) isomer, q, J = 7.5 Hz, 2H), 2.32 ((E,Z) isomer, q, J = 7.5 Hz, 2H), 2.37 ((Z,Z) isomer, q, J = 7.5 Hz, 2H). Dimethylcarbonate: ^{1}H NMR (500 MHz, C_6D_6) δ 3.38 (s). Alkene products were estimated at < 1% by ^{1}H NMR, relative to internal standard hexamethyldisilane. The (E,E), (E,Z), and (Z,Z) isomers of

2-butanone azine were found by GC in 10.8: 7.9: 1 ratios. All three isomers have the same mass spectrum with slightly different relative intensities of the fragment signals. MS (ei, photolysis in benzene) m/z: 140 [M]$^+$, 125, 111, 108, 99, 84, 70, 56, 42 (100%), 27.

Photolysis of oxadiazoline II-1n with 250/300 nm light.

(E)-2-Butene: ^{1}H NMR (500 MHz, C_6D_{12}) δ 1.56 (s, 6H), 5.39 (br s, 2H). (Z)-2-Butene: ^{1}H NMR (500 MHz, C_6D_{12}) δ 1.59 (s, 6H), 5.36 (br s, 2H). 1-Butene: ^{1}H NMR (500 MHz, C_6D_{12}) δ 0.98 (t, J = 7.4 Hz, 3H), 2.0-2.1 (m, 2H), 4.85 (d, J = 10.1 Hz, 1H), 4.94 (d, J = 17.1 Hz, 1H), 5.70-5.85 (m, 2H). The presence of 1-methylcyclopropane was inferred from signals near δ = 0.4 ppm (C_6D_{12}). The ratios (E)-2-butene:(Z)-2-butene:1-butene:methylcyclopropane were *ca* 45:34:20:1 as estimated by integrations of resolved signals (sealed NMR tubes). Dimethylcarbonate : ^{1}H NMR (500 MHz, C_6D_{12}) δ 3.63 (s). 2-Butanone azine was not detected.

IV.6. Laser Flash Photolysis.

The nanosecond laser flash photolysis system at NRC has been described previously.[150] A Lumonics EX-530 excimer laser (XeCl, 308 nm, 6 ns pulses, ≥ 40 mJ/pulse) was used for photolyses of oxadiazoline precursors. Sample solutions were prepared with absorbances (A) of 0.3-0.6 at the excitation wavelength (308 nm) as described below. These solutions were irradiated in 7 x 7 mm quartz cells. Stock solutions of oxadiazolines II-1a to n were prepared in freshly distilled benzene or cyclohexane containing various concentrations of pyridine (typically between 0.1 - 5.0 M) so that the values of A_{308} were approximately 0.4-0.6. Typical concentrations of oxadiazolines required to accomplish this were ~ 2-3 x 10^{-3} M. For each oxadiazoline, solutions without pyridine were degassed with N_2, and the time-resolved UV-Vis spectra for each were acquired (300-700 nm) after

308 nm LFP to ensure that signals assigned to pyridinium ylides did not arise from intermediates other than pyridinium ylides. Stern-Volmer kinetics were obtained from values of A_{360} of solutions of oxadiazolines **II-1a** to **n** containing various amounts of pyridine, after 308 nm-LFP.

For each pyridine quenching experiment, UV-visible spectra were taken of each solution prior to LFP, to ensure that the absorbances of the solutions at the excitation wavelength remained constant. Residual absorption of impurities in pyridine at the excitation wavelength can lead to errors in Stern-Volmer quenching, and the stock solutions of pyridine and LFP solutions were carefully monitored to eliminate this possibility.

Diazirines II-34a to c . The absolute rate constants for the reaction of **BCC:**, **PCC:**, and **MPC:** with oxygen and sulfur atom donors were measured by UV-LFP. Stock solutions of diazirines **II-34a** to c were prepared in freshly distilled cyclohexane and in freshly distilled acetonitrile so that A_{355} were approximately 0.2 to 0.6 depending on the precursor. Stock solutions of 1.0 M pyridine in cyclohexane and in acetonitrile were also prepared. The stock solution of diazirines **II-34a to c** were diluted by a factor of 2 in 2 mL cuvettes (so that $A_{355} \sim 0.1$ - 0.3) with 1.0 M pyridine in cyclohexane and in acetonitrile respectively. Solutions were degassed with N_2, and the time-resolved UV-Vis spectra were acquired (250-700 nm) after 355 nm LFP. Upon 355 nm LFP of diazirine **II-34a** , in the presence of pyridine, a long-lived absorption centered at ~370 nm was observed and assigned to the pyridine ylide of benzylchlorocarbene, as well as an absorption centered at ~270 nm assigned to E- & Z-β-chlorostyrenes.

For kinetic studies, stock solutions of diazirines **II-34a to c** were prepared in freshly distilled cyclohexane and in freshly distilled acetonitrile so that $A_{355} \sim 0.2$ to 1.2. For diazirines **II-34a to c** , the stock solution was diluted by a factor of 2 (so that $A_{308} \sim 0.6$, 50 mL solutions) with various

concentrations of pyridine in cyclohexane and in acetonitrile respectively. These solutions were further diluted by a factor of 2 with solutions containing various concentrations of oxygen and sulfur atom donors, purged with N_2, and the time-resolved absorption traces (at 370 nm, or 480 nm) were acquired after 355 nm LFP.

Oxygen and sulfur atom transfers to DMC:, CB:, and Ad:. Stock solutions of oxadiazolines II-1b, II-1e, and II-1f were prepared in freshly distilled cyclohexane so that the A_{308} were approximately 1.2. Typical concentrations of oxadiazolines required to accomplish this were ~ 2-3 x 10^{-3} M. A stock solution of 1.0 M pyridine in cyclohexane was also prepared. For each oxadiazoline, stock solutions were similarly diluted by a factor of 2 with 1.0 M pyridine in cyclohexane (total volume 2 mL, A_{308} ~ 0.6), degassed with N_2, and the time-resolved UV-Vis spectra for each were acquired (300-700 nm) after 308 nm LFP.

Solutions of oxadiazolines II-1b, II-1e, and II-1f (A_{308} = 1.2, path length 7 mm, 2-3 x 10^{-3} M) were prepared containing 0.2 M pyridine in cyclohexane and diluted by a factor of 2 with solutions containing various amounts of oxiranes and and thiiranes. Solutions were purged with N_2 prior to photolysis. The traces of these solutions were measured at 360 nm for **DMC:** and **CB:**, and at 380 nm for carbene **Ad:**, after 308 nm-LFP, with data analysis as described for benzylchlorocarbene.

For each quenching experiment UV-visible spectra were taken of solutions to ensure that the absorbances of the precursors **II-34**, as well as oxadiazolines **II-1b**, **II-1e**, and **II-1f**, at the excitation wavelength remained constant. Residual absorption of traps at the excitation wavelength can lead to errors in Stern-Volmer quenching, and concentration ranges were chosen to eliminate this possibility.

(b) Infrared.[152] For these experiments, samples contained in quartz flow cells with either 1 or 3 mm pathlengths were excited at 308 nm with a Lumonics EX-530 excimer laser (XeCl, 308 nm, 6 ns pulses, $\geq$ 40 mJ/pulse).

IV.7. Thermolysis of II-1b in the presence of an oxirane and a thiirane.

Solutions of 0.1 M **II-1b** (0.0160 g in 1 mL) in benzene-d_6 were prepared containing 0.1 M cyclohexene oxide (0.00981 g) or propylene sulfide (0.00741 g). These solutions were placed into NMR tubes, degassed by means of three successive freeze-pump-thaw cycles, and the tubes were flame sealed. The sealed tubes were heated at 110 °C in a constant temperature oil bath for 24 hours and the resulting product mixtures were analyzed by 500 MHz ^{1}H-NMR spectroscopy. The seals were then broken and the reaction mixtures were analyzed by GC-MS.

IV.8. Experimental details for Chapter III.

A solution of 5,5-dimethyl-2-methoxy-2-triphenylsiloxy-Δ^3-1,3,4-oxadiazoline (**III-1a**, 0.6 g, 0.1 M in dry benzene) was heated in a sealed degassed tube for 24 hours at 110 °C. The benzene was then removed by rotary evaporation and the products of the reaction were separated by radial chromatography using a gradient of hexanes to 10% ethyl acetate in hexanes. Two products were identified as methyl triphenylsilyl formate (12 % isolated yield) and methyl triphenylsilyl ether (40 % isolated yield).
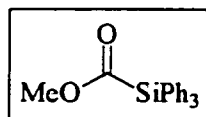
Methyl Triphenylsilyl formate (III-3): m.p. 98-102 °C, lit. 110-111 °C;[161] ^{1}H-NMR (200 MHz, CDCl$_3$) δ 3.74 (s, 3 H), 7.34-7.64 (m, 15 H); ^{13}C-NMR (50.3 MHz, CDCl$_3$) δ 49.9, 128.1, 130.5, 130.6, 135.1,

183.8; MS (e.i.) *m/z*: 318, 287, 259 (100 %); MS (CI, NH$_3$) *m/z*: 336 (M + NH$_4$$^+$); IR (cm^{-1}): 3071-2836, 1683.

Methyl Triphenylsilyl Ether (III-4): m.p. 52.1-52.3, lit. 52-55 °C,[161] ^{1}H-NMR (200 MHz, CDCl$_3$) δ 3.64 (s, 3 H), 7.33-7.65 (m, 15 H); ^{13}C-NMR (50.3 MHz, CDCl$_3$) δ 51.8, 127.9, 130.0, 133.9, 135.4; MS (e.i.) *m/z*: 290, 259, 213 (100 %); MS (CI, NH$_3$) *m/z*: 308 (M + NH$_4$$^+$).

Trapping of **MSC**: with methanol-d$_4$ was accomplished by thermolysis of oxadiazoline **III-1a** (0.1 M in methanol-d$_4$) in a sealed degassed NMR tube for 24 hours at 110 °C in a constant temperature oil bath. The reaction progress was monitored by NMR. It was found that products **III-3** and **4** were formed initially but product **III-3** was rapidly converted to **III-4** (ca. 90% yield at the end of the thermolysis). Orthoformate **III-5** was detected with ^{1}H-NMR (500 MHz, C$_6$D$_6$) δ 7.2-7.5 (m, 18 H), 3.17 (s, 3 H); ^{2}H-NMR (500 MHz, C$_6$H$_6$) δ 6.93 (s, 1D), 3.19 (s, 3D); GC-MS (e.i.): m/z: 354 [M]$^+$, 330, 259 (100 %).

Chapter III, Section 2.

All masses quoted for polychlorinated compounds are the lowest value of *m/z* in the envelope and correspond to ^{35}Cl; the observed signal intensities correctly matched the pattern required for the number of chlorine atoms in the fragment ion.
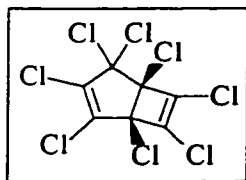
Octachlorobicyclo[3.2.0]hepta-3,6-diene.

Octachlorobicyclo[3.2.0]hepta-3,6-diene was synthesized according to literature procedures[282] and identified by conventional spectroscopic techniques. White solid, mp 53-54 °C (lit.[282] 53 °C); ^{13}C NMR (50.3 MHz,

CDCl₃) δ 137.4, 134.2, 133.4, 132.2, 89.0, 81.8, 78.7; MS (e.i.) m/z: 364 [M]⁺, 329 (100%) [C₇Cl₇]⁺, 294

[C₇Cl₆]⁺, 259 [C₇Cl₅]⁺, 189 [C₇Cl₃]⁺, 154 [C₇Cl₂]⁺, 119 [C₇Cl]⁺; MS (c.i., NH₃) m/z: 382 [M + NH₄]⁺.
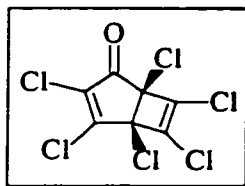
Hexachlorobicyclo[3.2.0]hepta-3,6-dien-2-one (III-25). III-25 was prepared using a modified literature procedure.[282] Excess conc. sulfuric acid (5.0 mL) was added to octachlorobicyclo[3.2.0]hepta-3,6-diene (1.947 g, 5.30 mmol) and the solution was heated at 80 °C for 20 h.

The solution was cooled, poured over ice, and extracted with ether. Radial chromatography of the extract using petroleum ether eluent yielded **II-25** as a white powder (1.034 g, 63 %), mp 84.5-85 °C (lit.[290] 85-86

°C); ¹³C NMR (50.3 MHz, CDCl₃) δ 182.5, 157.0, 136.1, 132.1, 131.6, 75.6, 73.7; IR (neat, KBr) 1746,

1622, 1573, 1226, 1155, 1129, 1030, 988, 800, 763, 736, 712, 648, 607 cm⁻¹; MS (e.i.) m/z: 310 [M]⁺,

282 [M-CO]⁺, 247 [C₆Cl₅]⁺, 212 [C₆Cl₄]⁺, 177 [C₆Cl₃]⁺, 142 (100%) [C₆Cl₂]⁺, 107 [C₆Cl]⁺; MS (c.i., NH₃)

m/z: 328 [M+NH₄]⁺, 311 [M+H]⁺; HRMS calcd for C₇Cl₆O 309.8080, found 309.8092.

Reaction of dimethoxycarbene with C₅Cl₆ (III-8). A solution of **III-1b** (0.268 g, 1.68 mmol) in

freshly distilled benzene (18.3 mL) containing 0.1 M C₅Cl₆ (**III-8**, 0.500 g, 1.83 mmol), in a 40 mL

thermolysis tube fitted with teflon valves was degassed by means of three successive freeze-pump-

thaw cycles. The sealed tube was then heated at 110 °C in a constant temperature oil bath for 24 h.

The reaction mixture, analyzed immediately by GC-MS, revealed three major products consistent with

III-12, III-14, and **III-16** in 1.2:1.8:1 ratios, respectively. These products were isolated using radial

chromatography with hexanes and 1:1 hexanes/CH₂Cl₂ as the eluent. Isomers of **III-14** and **III-16**

were detected by GC-MS as minor products and could not be isolated by chromatography. A

degassed solution of **III-1b** (0.587 g, 3.67 mmol) in benzene (3.7 mL) containing C₅Cl₆ (**III-8**, 0.100

g, 0.37 mmol) was also heated in a thermolysis tube at 110 °C for 24 h. Analysis of the reaction

mixture by GC-MS gave **II-16** : **III-14** ≈ 4:1 with only trace amounts of **III-12** present. The

identities of **III-14** and **III-16** were confirmed by isolation of those products.
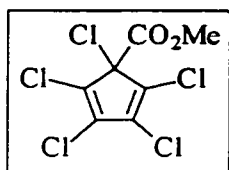
5-Carbomethoxy-1,2,3,4,5-pentachlorocyclopentadiene (III-12). Yield 24 %, white solid, mp 93-94 °C; ^{1}H NMR (500 MHz, CD_2Cl_2) δ 3.82 (s); ^{13}C NMR (125.7 MHz, CD_2Cl_2) δ 162.5, 131.0, 130.1, 72.6, 55.1; IR (neat, KBr) 2956, 2920, 2850, 1756, 1648, 1601, 1448, 1441, 1283, 1234, 1179, 1148, 1123, 1010, 976, 881, 791, 685 cm^{-1}; MS (e.i.) m/z: 294 [M]$^+$ (100%), 259 [$C_7H_3O_2Cl_4$]$^+$, 235 [$C_5H_3O_2Cl_4$]$^+$ (based on the isotopic distribution within the fragment envelope), 215 [$C_6H_3Cl_4$]$^+$, 180 [$C_6H_3Cl_3$]$^+$, 165 [C_5Cl_3]$^+$, 141, 130 [C_5Cl_2]$^+$, 117 [CCl_3]$^+$, 95 [C_5Cl]$^+$, 59 [CO_2Me]$^+$; MS (c.i., NH_3) m/z: 312 [M+NH$_4$]$^+$; HRMS calcd for $C_7H_3O_2Cl_5$ 293.8576, found 293.8573.
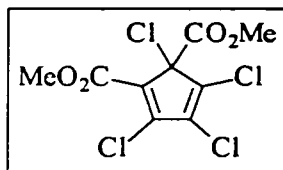
4,5-Dicarbomethoxy-1,2,3,5-tetrachlorocyclopentadiene (**III-14**). Yield 28 %, white solid, mp 84-85 °C; ^{1}H NMR (500 MHz, CD_2Cl_2) δ 3.84 (s, 3 H), 3.75 (s, 3 H); ^{13}C NMR (125.7 MHz, CD_2Cl_2) δ 163.4, 159.9, 143.7, 137.0, 132.3, 132.0, 68.4, 54.9, 52.7; IR (neat, KBr) 3007, 2956, 2848, 1783, 1756, 1697, 1681, 1653, 1628, 1603, 1557, 1436, 1327, 1289, 1254, 1226, 1161, 1120, 1094, 1048, 993 cm^{-1}; MS (e.i.) m/z : 318 [M]$^+$, 287 [$C_8H_3O_3Cl_4$]$^+$, 274 [$C_8H_6O_2Cl_4$]$^+$ (based on isotopic distribution within the fragment envelope), 259 [$C_7H_3O_2Cl_4$]$^+$, 228 [C_6OCl_4]$^+$, 180 [$C_6H_5Cl_3$]$^+$, 165 [C_5Cl_3]$^+$, 130 [C_5Cl_2]$^+$, 95 [C_5Cl]$^+$, 59 [CO_2Me]$^+$ (100 %), 43; MS (c.i., NH_3) m/z: 338 [M+NH$_4$]$^+$; HRMS calcd for $C_9H_6O_4Cl_4$ 317.9020, found 317.9012.
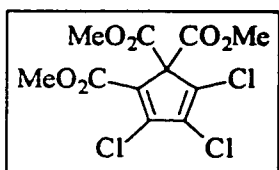
4,5,5-Tricarbomethoxy-1,2,3-trichlorocyclopentadiene (III-16). Yield 33 %, white solid, mp 104-105 °C; ^{1}H NMR (200 MHz, CD_2Cl_2) δ 3.80 (s, 3 H), 3.75 (s, 6 H); ^{13}C NMR (50.3 MHz, CD_2Cl_2) δ 162.8, 160.5 ($CO_2Me's$), 142.4, 133.2, 132.0, 129.0, 71.1, 54.5, 52.3; IR (neat, KBr) 3013, 2959, 2848, 1785, 1754, 1625, 1597, 1552, 1437, 1325, 1290, 1255, 1228, 1161, 1055, 1043, 991, 967, 953, 897, 841, 794, 782, 743, 694 cm^{-1}; MS (e.i.) m/z : 342 [M]$^+$, 298 [$C_{10}H_9O_4Cl_3$]$^+$, 267 [$C_{11}H_9O_6Cl_3$]$^+$, 221, 209, 165 [C_5Cl_3]$^+$, 130 [C_5Cl_2]$^+$, 95 [C_5Cl]$^+$, 59 (100 %) [CO_2Me]$^+$, 43; MS (c.i., NH_3) m/z: 360 [M+NH$_4$]$^+$, 343 [M+H]$^+$; HRMS calcd for $C_{11}H_9O_6Cl_3$ 341.9465, found 341.9463.

Reaction of dimethoxycarbene with octachlorobicyclo[3.2.0]hepta-3,6-diene-2-one (III-25). A 0.1 M solution of **III-1b** (0.116 g, 0.73 mmol) in benzene (8.0 mL) containing 0.1 M octachlorobicyclo[3.2.0]hepta-3,6-dien-2-one (0.250 g, 0.80 mmol) was heated as described above for 24 h at 110 °C. Analysis of the reaction mixture by TLC suggested that only one product was formed during the thermolysis. The product, **III-28**, was purified by recrystallization from a 19:1 hexanes:CH_2Cl_2 solvent mixture.
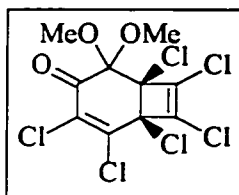
2,2-Dimethoxy-1,4,5,6,7,8-hexachlorobicyclo[4.2.0]octa-4,7-dien-3-one (III-28). Yield 98 %, white solid, mp. 154.5-155 °C; ^{1}H NMR (500 MHz, CD_2Cl_2) δ 3.52 (s, 3H), 3.18 (s, 3H); ^{13}C NMR (125.7 MHz, CD_2Cl_2) δ 183.2, 143.3, 133.5, 132.3, 129.8, 100.3, 80.0, 77.0, 52.0, 51.4; IR (neat, KBr) 2996, 2986, 2944, 2984, 1740, 1637, 1592, 1530, 1458, 1441, 1249, 1194, 1181, 1161, 1086, 1019, 976, 920, 899, 835, 780, 738, 694, 642, 623 cm^{-1} ; MS (e.i.) m/z: (Molecular ion not observed) 349 (100 %) [$C_{10}H_6O_3Cl_5$]$^+$, 321 [$C_9H_6O_2Cl_5$]$^+$, 301, 275 [C_7OCl_5]$^+$,

247 [C₆Cl₅]⁺, 212 [C₆Cl₄]⁺, 177 [C₆Cl₃]⁺, 142 [C₆Cl₂]⁺, 135, 107 [C₆Cl]⁺, 59 [CO₂Me]⁺; MS (c.i.,

NH₃) m/z: 402 [M+NH₄]⁺; HRMS calcd for fragment ion C₁₀H₆O₃Cl₅ 348.8760, found 348.8762.

Reaction of dimethoxycarbene with tetrachloro-1,4-benzoquinone (III-32). A solution of III-

1b (0.296 g, 1.85 mmol) in benzene (20.3 mL) was prepared containing 0.1 M III-32, (0.500 g, 2.03

mmol) was heated as described above for 24 h at 110 °C. Analysis of the reaction mixture by TLC

indicated the formation of three products, which was confirmed by GC-MS analysis. These products,

III-36, III-37, and III-38 were found in a ratio of 57.3: 4.1: 1 (GC-MS), and purified by radial

chromatography using a gradient of solvents ranging from hexanes to 20% CH₂Cl₂ in hexanes as the

eluents.
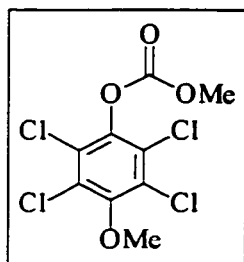
4-Methoxy-2,3,5,6-tetrachlorophenyl methyl carbonate (III-36).
Yield 82 %, yellow solid, mp 106.5-108 °C; ¹H NMR (500 MHz,
CD₂Cl₂) δ 3.95 (s, 3 H), 3.91 (s, 3 H); ¹³C NMR (125.7 MHz, CD₂Cl₂)
δ 152.8, 152.1, 142.2, 128.3, 127.5, 61.3, 57.0; IR (neat, KBr) 2952,
1784, 1462, 1443, 1408, 1383, 1316, 1254, 1199, 1166, 1031, 964,

930, 857, 771, 720 cm⁻¹; MS (e.i.) m/z: 318 [M]⁺, 274 [C₈H₆O₂Cl₄]⁺, 259 (100 %) [C₇H₃O₂Cl₄]⁺, 228

[C₆OCl₄]⁺, 209, 181, 167, 153, 130, 118, 87, 59 [CO₂Me]⁺, 43; MS (c.i., NH₃) m/z: 336 [M+NH₄]⁺;

HRMS calcd for C₉H₆O₄Cl₄ 317.9020, found 317.9004.
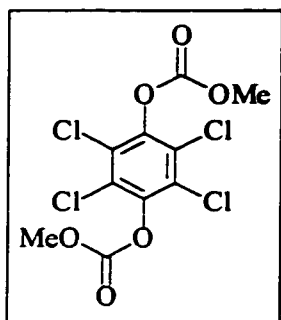
1,4-(2,3,5,6-tetrachlorophenyl) bis(methyl carbonate) (III-37). Yield 5 %, orange solid, mp 169-170.5 °C; ^{1}H NMR (500 MHz, CD$_2$Cl$_2$) δ 3.95 (s, 6 H); ^{13}C NMR (50.3 MHz, CD$_2$Cl$_2$) δ 151.8, 144.0, 127.9, 57.2; IR (neat, KBr) 3005, 2847, 1779, 1715, 1688, 1574, 1455, 1442, 1414, 1384, 1330, 1247, 1194, 1171, 931, 881, 860, 805, 774, 720 cm^{-1}; MS (e.i.) m/z: 362 [M]$^+$, 318 [C$_9$H$_6$O$_4$Cl$_4$]$^+$, 274 [C$_8$H$_6$O$_2$Cl$_4$]$^+$, 259 (100 %)[C$_7$H$_3$O$_2$Cl$_4$]$^+$, 209, 181, 167, 153, 118, 87, 59 [CO$_2$Me]$^+$, 43; MS (c.i., NH$_3$) m/z: 380 [M+NH$_4$]$^+$; HRMS calcd for C$_{10}$H$_6$O$_6$Cl$_4$ 361.8918, found 361.8933.
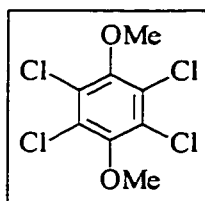
1,4-Dimethoxy-2,3,5,6-tetrachlorobenzene (III-38). Yield 1 %, Yellow solid, mp 98-99 °C; ^{1}H NMR (500 MHz, CD$_2$Cl$_2$) δ 3.92; ^{13}C NMR (50.3 MHz, CD$_2$Cl$_2$) δ 61.5, 128.7, 152.0; MS (e.i.) m/z: 274 [M]$^+$, 259 (100 %) [C$_7$H$_3$O$_2$Cl$_4$]$^+$, 209, 181, 167, 153, 130, 118, 87, 59, 43.

Reaction of dimethoxycarbene-d$_3$ with III-32. A solution of 2-methoxy-2-methoxy-d$_3$-5,5-dimethyl-Δ^3-1,3,4-oxadiazoline (III-1b-d$_3$, 0.120 g, 0.74 mmol) in benzene (8.1 mL) containing 0.1 M III-32 (0.200 g, 0.82 mmol) was heated as described above for 24 h at 110 °C. The GC-MS analysis of the product mixture revealed that products III-36, III-37, and III-38 were again formed in ratios of 57: 4: 1, respectively. The isotopic distribution of the molecular ion envelope from III-36 was consistent with a 1:2:1 distribution of isotopomers containing all hydrogens (m/z = 318), 3 deuterium atoms (m/z = 321), and 6 deuterium atoms (m/z = 324), respectively. The relative intensities for the isotopic distribution in the molecular ion were: 318 (8.1 %), 319 (0.9 %), 320 (9.7 %), 321 (16.4%), 322 (6.6 %), 323 (20.5 %), 324 (9.2 %), 325 (10.5 %), 326 (9.4 %), 327 (3.1 %), 328 (4.2 %), 329 (0.5 %), and 330 (1.0 %). The isotopic distribution for the molecular ion envelope of III-37 was also

consistent with a 1:2:1 distribution of isotopomers containing all hydrogens (m/z = 362), 3 deuterium

atoms (m/z = 365) and, 6 deuterium atoms (m/z = 368), respectively. The relative intensities for the

various isotopes of the molecular ion were: 362 (5.8 %), 363 (< 0.1 %), 364 (13.1 %), 365 (19.4 %),

366 (5.5 %), 367 (29.4 %), 368 (3.2 %), 369 (11.3 %), 370 (9.4 %), 371 (<0.1 %), 372 (2.9 %), 373

(< 0.1 %), and 374 (< 0.1 %). Again, the isotopic distribution for the molecular ion envelope of III-

38 was consistent with a 1:2:1 distribution of isotopomers containing all hydrogens (m/z = 274), 3

deuterium atoms (m/z = 277), and 6 deuterium atoms (m/z = 280). The relative intensities for the

isotopes of the molecular ion were: 274 (4.4 %), 275 (< 0.1 %), 276 (10.9 %), 277 (19.1 %), 278

(5.6 %), 279 (22.4 %), 280 (11.8 %), 281 (12.5 %), 282 (10.2 %), 283 (< 0.1 %), 284 (3.1 %), 285

(< 0.1 %), and 286 (< 0.1 %).

IV.9. Experimental details for Chapter V.

300 nm Steady-State Photolysis.

Steady-state photolyses were carried out in a Rayonet photochemical reactor equipped with a

"merry-go-round" apparatus. Samples were prepared in Pyrex tubes. Photolyses were performed in

oxygenated and deoxygenated (N_2 or argon) solutions with 8-10 350 nm lamps.

Photolysis of 1a in the presence of 2.0 M TMB in HFIP. Product V-7a. ^{1}H NMR (500 MHz,

C_6D_6) δ 1.24 (d, J = 7.1 Hz, 6H), 1.26 (septet, J = 7.1 Hz, 1H), 3.64 (s, 3H), 3.78 (s, 6H), 6.12 (s,

2H); MS (e.i., photolysis in HFIP) m/z: 210 $[C_{12}H_{18}O_3]^-$, 195 $[C_{11}H_{15}O_3]^-$(100%), 181 $[C_{12}H_{18}O_3]^-$,

165, 150, 137, 121, 109, 105, 91, 79, 77, 69, 63, 51, 39.

Photolysis of 1b in the presence of 2.0 M TMB in HFIP. Adducts V-7c(1), V-7c(2), and V-7c(3) were not separated for acquisition of the ^{1}H NMR spectra but they were examined separately by GC/MS. **V-7c.** ^{1}H NMR (500 MHz, C$_6$D$_6$) δ 0.05-0.4 (m), 1.5-2.9 (m), 3.54 (s), 3.68 (s), 3.74 (s), 3.78 (s), 3.83 (s), 3.89 (s), 4.91 (dd, J=10.2, 1.0 Hz), 4.98 (dd, J=17.1, 0.9 Hz) 5.12 (m), 6.10 (s), 6.13 (s), 6.14 (s); **V-7c(1)** MS (ei) m/z: 222 [C$_{13}$H$_{18}$O$_3$]$^+$, 207 [C$_{12}$H$_{15}$O$_3$]$^+$, 191 [C$_{12}$H$_{15}$O$_2$]$^+$ (100%), 181 [C$_{10}$H$_{13}$O$_3$]$^+$, 177, 168, 165, 151, 136, 121, 109, 95, 91, 77, 69, 65, 51; **V-7c(2)** MS (ei) m/z: 222 [C$_{13}$H$_{18}$O$_3$]$^+$, 194 [C$_{11}$H$_{14}$O$_3$]$^+$, 179 [C$_{10}$H$_{11}$O$_3$]$^+$ (100%), 165, 151, 135, 121, 105, 91, 77, 69, 51, 39; **V-7c(3)** MS (ei) m/z: 222 [C$_{13}$H$_{18}$O$_3$]$^+$,207 [C$_{12}$H$_{15}$O$_3$]$^+$, 181 [C$_{10}$H$_{13}$O$_3$]$^+$ (100%), 168, 151, 136, 121, 108, 91, 77, 69, 51.

Photolysis of 1c in the presence of 2.0 M TMB in HFIP. Product V-7f. ^{1}H NMR (500 MHz, C$_6$D$_6$) δ 0-0.49 (m, 4H), 1.31 (d, J = 7.1 Hz, 3H), 1.35-1.42 (m, 1H), 2.40 (p, J = 7.1 Hz, 1H), 3.66 (s, 3H), 3.78 (s, 6H), 6.13 (s, 2H); MS (ei, photolysis in HFIP) m/z: 236 [C$_{14}$H$_{20}$O$_3$]$^+$, 221 [C$_{13}$H$_{17}$O$_3$]$^+$ (100%), 205 [C$_{13}$H$_{17}$O$_2$]$^+$, 195, 179, 165, 151, 137, 121, 115, 105, 91, 77, 69, 51.

Photolysis of 1d in the presence of 2.0 M TMB in HFIP. Product V-7g. ^{1}H NMR (500 MHz, C$_6$D$_6$) δ 1.56-1.64 (m, 2H) 1.74-1.82 (m, 4H), 1.90-1.95 (m, 4H), 1.98-2.05 (m, 2H), 2.10 (m, 2H), 2.19 (m, 1H), 3.60 (s, 3H), 3.78 (s, 6H), 6.11 (s, 2H); MS (ei, photolysis in HFIP) m/z: 302 [C$_{19}$H$_{26}$O$_3$]$^+$, 287 [C$_{18}$H$_{23}$O$_3$]$^+$, 271 [C$_{18}$H$_{23}$O$_2$]$^+$, 255 [C$_{18}$H$_{23}$O]$^+$, 245 [C$_{16}$H$_{21}$O$_2$]$^+$, 227 [C$_{16}$H$_{19}$O]$^+$, 213, 207 [C$_{12}$H$_{15}$O$_3$]$^+$, 181 [C$_{10}$H$_{13}$O$_3$]$^+$ (100%), 168, 151, 136, 121, 115, 91, 79, 69, 53, 41.

Photolysis of V-1a and V-1b in the presence of 0.1 M acetic acid.

Photolysis of V-1c in the presence of 0.1 M acetic acid. Cyclobutyl ethanoate; ^{1}H NMR (500 MHz, C$_6$D$_6$) δ 1.18-1.27 (m, 1 H), 1.41-1.58 (m, 1 H), 1.69 (s, 3 H), 1.85-1.97 (m, 2 H), 2.09-2.19

(m, 2 H), 4.94 (pentet, J=7.9, 1 H); ^{13}C NMR (125 MHz, C$_6$D$_6$) δ 10.2, 20.9, 31.2, 68.9, 169.6;

Cyclopropylmethyl ethanoate; ^{1}H NMR (500 MHz, C$_6$D$_6$) δ 0.01-0.03 (m, 2 H), 0.23-0.27 (m, 2 H)

0.88-0.92 (m, 1 H), 1.65 (s, 3 H), 3.76 (d, J=7.2, 2 H); ^{13}C NMR (125 MHz, C$_6$D$_6$) δ 3.3, 13.7, 20.1,

68.6, 169.2; 1-butenyl ethanoate; ^{1}H NMR (500 MHz, C$_6$D$_6$) δ 1.69 (s, 3 H), 2.05-2.15 (m, 2 H),

3.93 (t, J=6.7, 2 H), 4.93 (dd, J=17.0, 1.4 Hz, 1 H), 4.96 (dd, J=10.5, 0.9 Hz, 1 H) 5.58 (J=

17.0,10.5, 6.3 Hz, 1 H); Cyclobutene; ^{1}H NMR (500 MHz, C$_6$D$_6$) δ 2.43 (4H), 5.91(2H).

Photolysis of V-1h in the presence of 0.1 M acetic acid. 2-Butyl ethanoate; ^{1}H NMR (500 MHz,

C$_6$D$_6$) δ 0.72 (t, J=7.5 Hz, 3H), 1.02 (d, J=6.3 Hz, 3H), 1.28 (ddq, J=7.5, 6.3, -13.4 Hz, 1H), 1.44

(ddq, J=7.5, 6.3, -13.4 Hz, 1H), 1.69 (s, 3H), 4.85 (sextet, J=6.3, 1H). 1-Butene; ^{1}H NMR (500

MHz, C$_6$D$_6$) δ 0.87 (t, J=7.5 Hz, 3H), 1.91 (dddq, J=7.5, 6.2, 1.7, 1.2 Hz, 2H), 4.93 (dd, J=10.1, 1.2

Hz, 1 H), 4.98 (dd, J=17.2, 1.7 Hz, 1 H), 5.78 (m, 1 H); (E)-2-Butene: ^{1}H NMR (500 MHz, C$_6$D$_6$) δ

1.49 (s, 6 H), 5.46 (br s, 2H); (Z)-2-Butene: ^{1}H NMR (500 MHz, C$_6$D$_6$) δ 1.52 (s, 6 H), 5.36 (br s,

2H).

Photolysis of V-1e in the presence of 0.1 M acetic acid. Cyclohexyl ethanoate; ^{1}H NMR (500

MHz, C$_6$D$_6$) δ 0.96-1.04 (m, 1 H), 1.05-1.15 (m, 2 H), 1.21-1.28 (m, 1 H) 1.29-1.38 (m, 2 H), 1.48-

1.51 (m, 2 H), 1.71 (s, 3H), 1.72-1.79 (m, 2 H) , 4.82 (tt, J=9.8, 3.9 Hz, 1 H); cyclohexene; ^{1}H NMR

(500 MHz, C$_6$D$_6$) δ 1.49 (br s, 4H), 1.90 (br s, 4H), 5.67 (t, J=1.5, 2H).

Photolysis of V-1d in the presence of 0.1 M acetic acid. Cyclopentyl ethanoate; ^{1}H NMR (500

MHz, C$_6$D$_6$) δ1.23-1.29 (m, 4 H), 1.58-1.62 (m, 4 H), 1.66 (s, 3 H), 5.15 (m, 1 H); ^{13}C NMR (125

MHz, C$_6$D$_6$) δ 20.9, 23.1, 32.8, 76.7, 170.0. Cyclopentene; ^{1}H NMR (500 MHz, C$_6$D$_6$) δ 1.71

(pentet, J=7.5 Hz, 2 H), 2.21 (t, J=7.5 Hz, 4H), 5.69 (s, 2 H); ^{13}C NMR (125 MHz, C_6D_6) δ 23.8, 32.6, 130.7.

IV.10. X-ray Crystallographic data.

The crystal data and structure refinement parameters are given in a following section of the appendix. All crystals were grown by slow evaporation of the solvent and were mounted on fine glass fibers with epoxy cement. X-ray crystallographic data was collected using a P4 Siemens diffractometer, equipped with a Siemens SMART 1K charge-coupled device (CCD) area detector (employing the program SMART[a]) and a rotating anode utilizing graphite-monochromated Mo-Kα radiation (λ = 0.71703 Å). The crystal-to-detector distance was 3.991 cm, and the data collection was carried out in 512 x 512 pixel mode, employing 2 x 2 pixel binning. In all cases, the initial unit cell parameters were determined by a least-squares fit of the angular settings of the strong reflections, collected using three 4.5° scans (15 frames each) over three different parts of reciprocal space and one complete hemisphere of data was collected, to better than 0.8 Å resolution. Processing of the data was carried out using the program SAINT,[b] which applied Lorentz and polarization corrections to three dimensionally integrated diffraction spots. The program SADABS[c] was employed for the scaling of diffraction data, the application of a decay correction, and an empirical absorption correction based on redundant reflections. All structures were solved by using the direct methods routine outlined in the Siemens SHELXTL program library[d] followed by full-matrix least squares refinement on F^2 with anisotropic thermal parameters for all non-hydrogen atoms.

---

[a] SMART, Release 4.05; Siemens Energy and Automation Inc., Madison, WI 53719, 1996.
[b] SAINT, Release 4.05; Siemens Energy and Automation Inc., Madison, WI 53719, 1996.
[c] Sheldrick, G. M. SADABS (Siemens Area Detector Absorption Corrections), unpublished, 1994.
[d] Sheldrick, G. M. SHELXTL, Release 5.03; Siemens Analytical X-Ray Instruments, Madison, WI, 1994.

References and Notes.

1. For older reviews see: (a) Jones, M., Jr.; Moss, R. A., Eds. "Carbenes"; Wiley Interscience Inc.: New York, 1973; Vol. 1; 1975, Vol. 2. (b) Jones, M., Jr.; Moss, R.A., Eds. "Reactive Intermediates"; Wiley Interscience Inc.: New York, 1978, Vol. 1; 1981, Vol. 2; 1985, Vol. 3.

2. (a) Hoffmann, R.; Zeiss, G. D.; Van Dine, G. W.; *J. Am. Chem. Soc.*, **1968**, *90*, 1485. (b) Hoffmann, R.; Zeiss, G. D.; Van Dine, G. W.; *J. Am. Chem. Soc.*, **1968**, *90*, 5457. (c) Pauling, L.; *J. Chem. Soc., Chem. Comm.*, **1980**, 688. (d) Mueller, P. H.; Rondan, N. G.; Houk, K. N; Harrison, J. F.; Hooper, D.; Willen, B. H.; Liebman, J. F. *J. Am. Chem. Soc.*, **1981**, *103*, 5049.

3. Nickon, A. *Acc. Chem. Res.* **1993**, *26*, 84.

4. Rondan, N. G.; Houk, K. N.; Moss, R. A.; *J. Am. Chem. Soc.*, **1980**, *102*, 1770.

5. (a) Bauschlicher, C. W., Jr.; Langhoff, S. R.; Taylor, P. R. *J. Chem. Phys.* **1987**, *87*, 387. (b) Leopold, D. G.; Murray, K. K.; Miller, A. E. S.; Lineberger, W. C. *J. Phys. Chem.* **1985**, *83*, 4866. (c) Leopold, D. G.; Murray, K. K.; Miller, A. E. S.; Lineberger, W. C. *J. Chem. Phys.* **1984**, *83*, 4849. (d) Shavitt, I. *Tetrahedron* **1985**, *41*, 1531.

6. Hoffmann, R.; Zeiss, G. D.; VanDine, G. W. *J. Am. Chem. Soc.* **1968**, *90*, 1485.

7. (a) Wasserman E. J.; Hutton, S. *Acc. Chem. Res.* **1977**, *10*, 27. (b) Wasserman E. J. *J. Chem. Phys.* **1964**, *41*, 1763.

8. (a) Tomioka, H.; Watanabe, T.; Hirai, K.; Furukawa, K.; Takui, T.; Itoh, K. *J. Am. Chem. Soc.* **1995**, *117*, 6376. (b) Tomioka, H. *Acc. Chem. Res.* **1997**, *30*, 315. (c) Tomioka, H. In *Adv. Carbene Chem.*; Brinker, U.; Ed.: JAI Press. Greenwich, **1998**, Vol.2, p 175.

9. Feller, D.; Borden, W. T.; Davidson, E. R.; *J. Phys. Chem.*, **1979**, *71*, 4987 and references therein.

10. Harrison, J. F.; Kiedtke, R. C.; Liebman, J. F. *J. Am. Chem. Soc.*, **1979**, *101*, 7162.

11. Gonzalez, C.; Restrepo-Cossio, A.; Márquez, M.; Wiberg, K. B.; De Rosa, M. *J. Phys. Chem. A* **1998**, *102*, 2732.

12. Garcia, V. M.; Castell, O.; Reguero, M.; Caballol, R. *Mol. Phys.* **1996**, *87*, 1395.

13. (a) Matzinger, S.; Fülscher, M. P. *J. Phys. Chem.* **1995**, *99*, 10747. (b) Richards, C. A., Jr.; Kim, S.-J.; Yamaguchi, Y.; Schaefer, H. F., III *J. Am. Chem. Soc.* **1995**, *117*, 10104. (c) Sulzbach, H. M.; Bolton, E.; Lenoir, D.; Schleyer, P. v. R.; Schaefer, H. F., III *J. Am. Chem. Soc.* **1996**, *118*, 9908.

14. (a) Moss, R. A. *Acc. Chem. Res.* **1989**, *22*, 15. (b) Moss, R. A. *Acc. Chem. Res.* **1980**, *13*, 58. (c) Moss, R. A.; Shen, S.; Hadel, L. M.; Kmiecik–Lawrynowicz, G.; Wlostowska, J.; Krogh-Jespersen, K. *J. Am. Chem. Soc.* **1987**, *109*, 4341. (d) Moss, R. A.; Jang, E. G.; Fan, H.; Wlostowski, M.; Krogh-Jespersen, K. *J. Phys. Org. Chem.* **1992**, *5*, 104. (e) Sheridan, R. S.; Moss, R. A.; Wilk, B. K.; Shen, S.; Wlostowski, M.; Kesselmayer, M. A.; Subramanian, R.; Kmiecik–Lawrynowicz, G.; Krogh-Jespersen, K. *J. Am. Chem. Soc.* **1988**, *110*, 7563.

15. Moss, R. A.; Wlostowski, M.; Shen, S.; Krogh-Jespersen, K.; Matro, A. *J. Am. Chem. Soc.* **1988**, *110*, 4443.

16. Dixon, D. A.; Arduengo, A. J., III *J. Phys. Chem.* **1991**, *95*, 4180.

17. (a) Belt, S. T.; Bohne, C.; Charette, G.; Sugamori, S. E.; Scaiano J. C. *J. Am. Chem. Soc.* **1993**, *115*, 2200. (b) Dix, E. J.; Goodman, J. L. *J. Phys. Chem.* **1994**, *98*, 12609. (c) Kirmse, W.; Krzossa, B.; Steenken, S. *J. Am. Chem. Soc.* **1996**, *118*, 7473. (d) Chateauneuf, J. E. *J. Chem. Soc., Chem. Commun.* **1991**, 1437.

18. (a) Jones, M. B.; Platz, M. S. *J. Org. Chem.* **1991**, *56*, 1694. (b) Jones, M. B.; Platz, M. S. *Tetrahedron Lett.* **1990**, *31*, 953.

19. (a) Modarelli, D. A.; Platz, M. S. *J. Am. Chem. Soc.* **1991**, *113*, 8985. (b) Morgan, S.; Jackson, J. E.; Platz, M. S. *J. Am. Chem. Soc.* **1991**, *113*, 2782. (c) Modarelli, D. A.; Morgan, S.; Platz, M. S. *J. Am. Chem. Soc.* **1992**, *114*, 7034.

20. (a) Curtin, D. Y. *Rec. Chem. Prog.* **1954**, *15*, 111. (b) Seeman, J. I. *Chem. Rev.* **1983**, *83*, 83.

21. (a) Moss, R. A.; Young, C. M.; Perez, L. A.; Krogh-Jespersen, K. *J. Am. Chem. Soc.* **1981**, *103*, 2413. (b) Moss, R. A.; Mallon, C. B.; Ho, C.-T. *J. Am. Chem. Soc.* **1977**, *99*, 4105.

22. Kirmse, W.; Meinert, T.; Modarelli, D. A.; Platz, M. S. *J. Am. Chem. Soc.* **1993**, *115*, 8918.

23. Fleming, I. *Frontier Orbitals and Organic Chemical Reactions*; Wiley-Interscience: New York, 1976.

24. (a) Zollinger, H. In *Diazo Chemistry*; VCH Publ.: New York, 1995; Vol. 2. (b) Regitz, M.; Maas, G. In *Diazo Compounds*; Academic Press: London, 1986. (c) *The Chemistry of Diazonium and Diazo Compounds*; Patai, S., Ed.; Wiley-Interscience: Chichester, 1978.

25. (a) Bamford, W. R.; Stevens, T. S. *J. Chem. Soc.* **1952**, 4735. (b) Dauben, W. G.; Willey, F. G. *J. Am. Chem. Soc.* **1962**, *84*, 1497.

26. Smith, L. I.; Howard, K. L. *Org. Synth.* **1955**, *3*, 351.

27. For a review see: Kirmse, W. *Eur. J. Org. Chem.* **1998**, 201.

28. Müller, R. K.; Felix, D.; Schreiber, J.; Eschenmoser, A. *Org. Synth. Coll. Vol.* **1988**, *6*, 56.

29. For reviews see: (a) Moss, R. A. In *Adv. Carbene Chem.*; Brinker,U.; Ed.; JAI Press, Greenwich, **1994**, Vol.1, p 59. (b) Jackson, J. E.; Platz, M. S. In *Adv. Carbene Chem.*; Brinker,U.; Ed.; JAI Press, Greenwich, **1994**, Vol. 1, p 89. (c) *Chemistry of Diazirines*; Liu, M. T. H., Ed. CRC Press: Boca Raton, FL, 1987, Vol. 1-2.

30. Graham, W. H. *J. Am. Chem. Soc.* **1965**, *87*, 4396.

31. (a) Moss, R. A.; Wlostowski, M.; Terpinski, J.; Kmiecik-Lawrynowicz, G.; Krogh-Jespersen *J. Am. Chem. Soc.* **1987**, *109*, 3811. (b) Moss, R. A.; Shen, S.; Wlostowski, M.; Krogh-Jespersen *J. Am. Chem. Soc.* **1988**, *110*, 4443.

32. (a) Hartwig, J. F.; Jones, M., Jr.; Moss, R. A.; Lawrynowicz, W. *Tetrahedron Lett.* **1986**, *27*, 5907. (b) Le, N. A.; Jones, M., Jr.; Bickelhaupt, F.; deWolf, W. H. *J. Am. Chem. Soc.* **1989**, *111*, 8491. (c) Robert, M.; Toscano, J. P.; Platz, M. S.; Abbot, S. C.; Kirchoff, M. M.; Johnson, R. P. *J. Phys. Chem.* **1996**, *100*, 18426. (d) Chateauneuf, J. E.; Johnson, R. P.; Kirchoff, M. M. *J. Am. Chem. Soc.* **1996**, *112*, 3217. (e) Robert, M.; Snoonian, J. R.; Platz, M. S.; Wu, G.; Hong, H.; Thamattoor, D. M.; Jones, M., Jr. *J. Phys. Chem. A* **1998**, *102*, 587.

33. Thamattoor, D. M.; Jones, M., Jr.; Pan, W.; Shevlin, P. B. *Tetrahedron Lett.* **1996**, *37*, 8333.

34. Huang, H.; Platz, M. S. *J. Am. Chem. Soc.* **1998**, *120*, 5990.

35. For discussions of the problem and for examples of excited state rearrangements leading to products expected from carbenes see: (a) Moss, R. A. In *Adv. Carbene Chem.*; Brinker,U.; Ed.; JAI Press, Greenwich, **1994**, Vol.1, p 59. (b) Modarelli, D. A.; Morgan, S.; Platz, M. S. *J. Am. Chem. Soc.* **1992**, *114*, 7034 (c) Moss, R. A. *Pure & Appl. Chem.* **1995**, *67*, 741. (d) Platz, M. S.; White, W. R. III; Modarelli, D.A.; Celebi, S. *Res. Chem. Intermed.* **1994**, *20*, 175. (e) Chen, N.; Jones, M. Jr.; Platz, M. S. *J.Am. Chem. Soc.* **1991**, *113*, 4981. (f) White, W. R., III; Platz, M. S. *J. Org. Chem.* **1992**, *57*, 2841. (g) Moss, R. A., Ho, G.-H. *J. Phys. Org. Chem.* **1993**, *6*, 126. (h) Moss, R. A.; Liu, W.; Krogh-Jespersen, K. *J. Phys. Chem.* **1993**, *97*, 13413. (i) Chen, N.; Jones, M. Jr. *Tetrahedron Lett.* **1989**, *1*, 305. (j) Eaton, P. E.; Appell, R. B. *J. Am. Chem. Soc.* **1990**, *112*, 4055. (k) Eaton, P. E.; Hoffmann, H.-L. *J. Am. Chem. Soc.* **1987**, *109*, 5285. (l) Wierlacher, S.; Sander, W.; Liu, M.T.H. *J. Am. Chem. Soc.* **1993**, *115*, 8943. (m) Bonneau, R.; Liu, M. T. H.; Kim, K. C.; Goodman, J. L. *J. Am. Chem. Soc.* **1996**, *118*, 3829.

36. Pezacki, J. P.; Pole, D. L.; Warkentin, J.; Chen, T.; Ford, F.; Toscano, J.; Fell, J.; Platz, M. S. *J. Am. Chem. Soc.* **1997**, *119*, 3191.

37. (a) Nigam, M.; Platz, M. S.; Showalter, B. M.; Toscano, J. P.; Johnson, R.; Abbot, S. C.; Kirchoff, M. M. *J. Am. Chem. Soc.* **1998**, *120*, 8055. (b) Robert, M.; Likhotvorik, I.; Platz, M. S.; Johnson, R.; Abbot, S. C.; Kirchoff, M. M. *J. Phys. Chem.* **1998**, *102*, 1507.

38. Moss, R. A.; Cox, D. P. *Tetrahedron Lett.* **1985**, *26*, 1931.

39. Vilsmeier, E.; Kristen, G.; Telzlaff, C. *J. Org. Chem.* **1988**, *53*, 1806.

40. (a) Lemal, D. M.; Lovald, R. W.; Harrington, R. W. *Tetrahedron Lett.* **1965**, 2779. (b) Lemal, D. M.; Gosselink, E. P.; McGregor, S. D. *J. Am. Chem. Soc.* **1966**, *88*, 582. (c) Lemal, D. M.; Gosselink, E. P.; Ault, A. *Tetrahedron Lett.* **1964**, 579. (d) Hoffmann, R. W.; Hauser, H. *Tetrahedron Lett.* **1964**, 197. (e) McDonald, R. M.; Kreuger R. A. *J. Org. Chem.* **1966**, *31*, 488. (f) Hoffmann, R. W. *Acc. Chem. Res.* **1985**, *18*, 248.

41. (a) Frenzen, G.; Kümmell, A.; Meyer-Dulheuer, C.; Seitz, G. *Chem. Ber.* **1994**, *127*, 1803. (b) Hoffmann, R. W.; Hagenbruch, B.; Smith, D. M. *Chem. Ber.* **1977**, *110*, 23. (c) Wanzlick, H.-W.; Esser, F.; Kleiner, H.-J. *Chem. Ber.* **1963**, *96*, 1208. (d) Wanzlick, H.-W.; Schikora, E. *Chem. Ber.* **1961**, *94*, 2289. (e) Wanzlick, H.-W.; Kleiner, H.-J. *Angew. Chem.* **1961**, *73*, 493.

42. (a) Corey, E. J.; Winter, R. A. E. *J. Am. Chem. Soc.* **1963**, *85*, 2677. (b) Corey, E. J.; Carey, F. A.; Winter, R. A. E. *J. Am. Chem. Soc.* **1965**, *87*, 934

43. Varma, K. S.; Bury, A.; Harris, N. J.; Underhill, A. E. *Synthesis* **1987**, 837.

44. (a) Arduengo, A. J., III; Goerlich, J. R.; Marshall, W. J. *J. Am. Chem. Soc.* **1995**, *117*, 11027. (b) Boche, G.; Hilf, C.; Harms, K.; Marsch, M.; Lohrenz, J. C. W. *Angew. Chem. Int. Ed. Engl.* **1995**, *34*, 487.

45. (a) Hoffmann, R. W.; Hagenbruch, B.; Smith, D. M. *Chem. Ber.* **1977**, *110*, 23. (b) Staab, H. A.; Irngartinger, H.; Mannschreck, A.; Wu, M.-T. *Liebigs Ann.* **1966**, *55*. (c) Scherowsky, G.; Dünnbier, K.; Höfle, G. *Tetrahedron Lett.* **1977**, 2095. (d) Olofson, R. A.; Landesberg, J. M. *J. Am. Chem. Soc.* **1966**, *88*, 4263. (e) Olofson, R. A.; Landesberg, J. M.; Houk, K. N.; Michelman, J. S. *J. Am. Chem. Soc.* **1966**, *88*, 4265.(f) Scherowsky, G. *Chem. Ber.* **1974**, *107*, 1092. (g) Arduengo, A. J., III; Goerlich, J. R.; Marshall, W. J. *Liebigs Ann.* **1997**, 365.

46. (a) Breslow, R. *J. Am. Chem. Soc.* **1957**, *79*, 1762. (b) Kluger, R. *Chem. Rev.* **1987**, *87*, 863.

47. For a review of α-siloxy carbenes generated from acylsilanes see: Brook, A.G.; in " The Chemistry of Organic Silicon Compounds"; Patai, S.; Rappoport, Z. Eds.; John Wiley and Sons: New York, 1989, Ch.15, 984-988. Also see: (a) Brook, A. G.; Kucera, H. W.; Pearce, R. *Can. J. Chem.* **1971**, *49*, 1618. (b) Duff, J. M.; Brook, A. G. *Can J. Chem.* **1973**, *51*, 2869. (c) Bourque, R. A.; Davis, P. D.; Dalton, J. C. *J. Am. Chem. Soc.* **1981**, *103*, 697.

48. (a) Brook, A. G.; Kiviskk, R.; Legrow, G. E.; *Can. J. Chem.* **1965**, *43*, 1175. (b) Brook, A. G.; Pierce, J. B. *J. Org. Chem.* **1965**, *30*, 2566.

49. Warkentin, J. *Synthesis* **1970**, 279 and references therein.

50. Yang, R.-Y.; Dai, L.-X. *J. Org. Chem.* **1993**, *58*, 3381.

51. Kassam, K.; Pole, D. L.; El-Saidi, M.; Warkentin, J. *J. Am. Chem. Soc.* **1994**, *116*, 1161.

52. El-Saidi, M.; Kassam, K.; Pole, D. L.; Tadey, T.; Warkentin, J. *J. Am. Chem. Soc.* **1992**, *114*, 8751.

53. (a) Win, W. W.; Kao, M.; Eiermann, M.; McNamara, J. J.; Wudl, F.; Pole, D. L.; Kassam, K.; Warkentin, J. *J. Org. Chem.* **1994**, *59*, 5871. (b) Colomvakos, J. D.; Egle, I.; Ma, J.; Pole, D. L.; Tidwell, T. T.; Warkentin, J. *J. Org. Chem.* **1996**, *61*, 9522. (c) de Meijere, A.; Kozhushkov, S. I.; Yufit, D. S.; Boese, R.; Haumann, T.; Pole, D. L.; Sharma, P. K.; Warkentin, J. *Liebigs Ann.* **1996**, 601. (d) Couture, P.; Pole, D. L.; Warkentin, J. *J. Chem. Soc., Perkin Trans. 2.* **1997**, 1565.

54. (a) Couture; P.; Warkentin, J. *Can. J. Chem.* **1997**, *75*, 1264. (b) Couture, P.; Warkentin, J. *Can. J. Chem.* **1997**, *75*, 1281. (c) Kassam, K.; Venneri, P.; Warkentin, J. *Can. J. Chem.* **1997**, *75*, 1256. (d) Kassam, K.; Warkentin, J. *Can. J. Chem.* **1997**, *75*, 120. (e) Kassam, K.; Warkentin, J. *J. Org. Chem.* **1994**, *59*, 5071. (f) Er, H.-T.; Pole, D. L.; Warkentin, J. *Can. J. Chem.* **1996**, *74*, 1480. (g) Isaacs, L.; Diederich, F. *Helv. Chim. Acta.* **1993**, *76*, 2454.

55. Warkentin, J. In "Advances in Carbene Chemistry"; Vol. 2, Brinker, U. Ed.; JAI Press Inc.: Greenwich, 1998, pp 245-295.

56. (a) Zoghbi, M.; Warkentin, J. *J. Org. Chem.* **1991**, *56*, 3214. (b) Zoghbi, M.; Horne, S. E.; Warkentin, J. *J. Org. Chem.* **1994**, *59*, 4090. (c) Couture, P.; Warkentin, J. *Can. J. Chem.* **1998**, *76*, 241.

57. Couture, P.; El-Saidi, M.; Warkentin, J. *Can. J. Chem.* **1997**, *75*, 326.

58. (a) Couture, P.; Terlouw, J. K.; Warkentin, J. *J. Am. Chem. Soc.* **1996**, *118*, 4214. (b) Couture, P.; Warkentin, J. *Can. J. Chem.* **1997**, *75*, 1264. (c) Couture, P.; Warkentin, J. *Can. J. Chem.* **1997**, *75*, 1281.

59. Majchrzak, M.; Békhazi, M.; Tse-Sheepy, I.; Warkentin, J. *J. Org. Chem.* **1989**, *54*, 1842.

60. (a) Pezacki, J. P.; Wagner, B. D.; Lew, C. S. Q.; Warkentin, J.; Lusztyk, J. *J. Am. Chem. Soc.* **1997**, *119*, 1789. (b) Majchrzak, M. W.; Jefferson, E. A.; Warkentin, J. *J. Am. Chem. Soc.* **1990**, *112*, 1842. (c) Jefferson, E. A.; Warkentin, J. *J. Org. Chem.* **1994**, *59*, 455. (d) Warkentin, J.; Wollard, J. M. R. *Can. J. Chem.* **1997**, *75*, 289.

61. Adam, W.; Finzel, R. *Tetrahedron Lett.* **1990**, *31*, 863.

62. Caldwell, R. A.; Majimu, T.; Poc, C. *J. Am. Chem. Soc.* **1982**, *108*, 629.

63. For reviews see: (a) Newcomb, M. *Tetrahedron* **1993**, *49*, 1151. (b) Griller, D.; Ingold, K. U. *Acc. Chem. Res.* **1980**, *13*, 317.

64. For reviews of azoalkane chemistry see: (a) Dougherty, D. *Acc. Chem. Res.* **1991**, *24*, 88. (b) Engel, P. S. *Chem. Rev.* **1980**, *80*, 99. (c) Berson, J. A. *Acc. Chem. Res.* **1978**, *11*, 446. (d) Dowd, P. *Acc. Chem. Res.* **1972**, *5*, 242.

65. (a) Closs, G. L.; Rabinow, B. E. *J. Am. Chem. Soc.* **1976**, *98*, 8190. (b) Hadel, L. M.; Platz, M. S.; Scaiano, J. C. *J. Am. Chem. Soc.* **1984**, *106*, 283.

66. (a) Grasse, P. B.; Brauer, B. E.; Zupancic, J. J.; Kaufmann, K. J.; Schuster, G. B. *J. Am. Chem. Soc.* **1983**, *105*, 6833. (b) Griller, D.; Hadel, L. M.; Nazran, A. S.; Platz, M. S.; Wong, P. C.; Savino, T. G.; Scaiano, J. C. *J. Am. Chem. Soc.* **1984**, *106*, 2227.

67. (a) Jackson, J. E.; Soundararajan, N.; Platz, M. S. *J. Am. Chem. Soc.* **1988**, *110*, 5595. (b) Gould, I. R.; Turro, N. J.; Butcher, J. J.; Doubleday, C. J.; Hacker, N. P.; Lehr, G. F.; Moss, R. A.; Cox, D. P.; Guo, W.; Munjal, R. C.; Perez, L. A.; Fedorynski, M. *Tetrahedron*. **1985**, *41*, 1587.

68. (a) Clark, J. S.; Dossetter, A. G.; Whittingham, W. G. *Tetrahedron Lett.* **1996**, 37, 605. (b) Olson, D. R.; Platz, M. S. *J. Phys. Org. Chem.* **1996**, *9*, 759.(c) Padwa, A.; Austen, D. J.; Hornbuckle, S. F. *J. Org. Chem.* **1996**, *61*, 63. (d) Padwa, A.; Curtis, E. A.; Sandanayaka, V. P. *J. Org. Chem.* **1996**, *61*, 73. (e) Platz, M. S.; Olson, D. R. *J. Phys. Org. Chem.* **1996**, 9, 689. (f) Sueda, T.; Nagaoka, T.; Goto, S.; Ochiai, M. *J. Am. Chem. Soc.* **1996**, *118*, 10141. (g) Curtis, E. A.; Sandanayaka, V. P.; Padwa, A. *Tetrahedron Lett.* **1995**, *36*, 1989. (h) Bonneau, R.; Reuter, I.; Liu, M. T. H. *J. Am. Chem. Soc.* **1994**, *116*, 3145. (I) Padwa, A.; Hornbuckle, S. F. *Chem. Rev.* **1991**, *91*, 263. (j) Trost, B. M.; Melvin, L. S. *Sulfur Ylides: Emerging Synthetic Intermediates*; Academic Press, New York, 1975.

69. For reviews see: (a) Moss, R. A. In *Adv. Carbene Chem.*; Brinker, U.; Ed.; JAI Press, Greenwich, **1994**, Vol.1, p 59. (b) Jackson, J. E.; Platz, M. S. In *Adv. Carbene Chem.*; Brinker, U.; Ed.; JAI Press, Greenwich, **1994**, Vol. 1, p 89.

70. Ge, C. S.; Jang, E. G.; Jefferson, E. A.; Liu, W.; Moss, R. A.; Wlostowska, J.; Xue, S. *J. Chem. Soc., Chem. Commun.* **1994**, 1479.

71. Bonneau, R.; Liu, M. T. H.; Lapouyade, R. *J. Chem. Soc. Perkin Trans. 1* **1989**, 1547.

72. Jones, M. B.; Platz, M. S. *J. Org. Chem.* **1991**, *56*, 1694.

73. (a) Jackson, J. E.; Soundararajan, N.; Platz, M. S. *J. Am. Chem. Soc.* **1988**, *110*, 5595. (b) Gould, I. R.; Turro, N. J.; Butcher, J. J.; Doubleday, C. J.; Hacker, N. P.; Lehr, G. F.; Moss, R. A.; Cox, D. P.; Guo, W.; Munjal, R. C.; Perez, L. A.; Fedorynski, M. *Tetrahedron*. **1985**, *41*, 1587.

74. (a) Modarelli, D. A.; Platz, M. S. *J. Am. Chem. Soc.* **1991**, *113*, 8985. (b) Morgan, S.; Jackson, J. E.; Platz, M. S. *J. Am. Chem. Soc.* **1991**, *113*, 2782. (c) Modarelli, D. A.; Morgan, S.; Platz, M. S. *J. Am. Chem. Soc.* **1992**, *114*, 7034. (d) Ford, F.; Yuzawa, T.; Platz, M. S.; Matzinger, S.; Fülscher, M. *J. Am. Chem. Soc.* **1998**, *120*, 4430.

75. Robert, M.; Toscano, J. P.; Platz, M. S.; Abbot, S. C.; Kirchhoff, M. M.; Johnson, R. P. *J. Phys. Chem.* **1996**, *100*, 18426.

76. Platz, M. S.; Modarelli, D. A.; Morgan, S.; White, W. R.; Mullins, M.; Celebi, S.; Toscano, J. P. *Prog. React. Kinetics*; Rodgers, M. A. Ed.; Elsevier, **1994**, *19*, 93 and references therein.

77. (a) Jackson, J. E.; Soundararajan, N.; Platz, M. S.; Doyle, M. P.; Liu, M. T. H.; *Tetrahedron Lett.* **1989**, *30*, 1335. (b) Jackson, J. E.; Soundararajan, N.; Platz, M. S.; Liu, M. T. H. *J. Am. Chem. Soc.* **1988**, *110*, 5595. (c) Platz, M. S.; Modarelli, D. A.; Morgan, S.; White, W. R.; Mullins, M.; Celebi, S.; Toscano, J. P. *Prog. React. Kinetics*; Rodgers, M. A. Ed.; Elsevier, **1994**, *19*, 93.

78. (a) Bonneau, R.; Liu, M. T. H.; Rayez, M. T. *J. Am. Chem. Soc.* **1989**, *111*, 5973. (b) Liu, M. T. H.; Bonneau, R. *J. Am. Chem. Soc.* **1989**, *111*, 6873. (c) LaVilla, J. A.; Goodman, J. L. *J. Am. Chem. Soc.* **1989**, *111*, 6877.

79. LaVilla, J. A.; Goodman, J. L. *Tetrahedron Lett.* **1990**, *31*, 5109.

80. Sheridan, R. S.; Moss, R. A.; Wilk, B. K.; Shen, S.; Wlostowski, M.; Kesselmayer, M. A.; Subramanian, R.; Kmiecik-Lawrynowicz, G.; Krogh-Jespersen, K. *J. Am. Chem. Soc.* **1988**, *110*, 7563.

81. Sugiyama, M. H.; Celebi, S.; Platz, M. S. *J. Am. Chem. Soc.* **1992**, *114*, 966.

82. Moss, R. A.; Yan, S.; Krogh-Jespersen, K. *J. Am. Chem. Soc.* **1998**, *120*, 1088.

83. Evanseck, J. D.; Houk, K. N. *J. Phys. Chem.* **1990**, *94*, 5518.

84. (a) Kenar, J. A.; Nickon, A. *Tetrahedron* **1997**, *53*, 14871. (b) Nickon, A. *Acc. Chem. Res.* **1993**, *26*, 84.

85. (a) Nickon, A.; Stern, A. G.; Ilao, M. C. *Tetrahedron Lett.* **1993**, 1391. (b) Stern, A. G.; Ilao, M. C.; Nickon, A. *Tetrahedron Lett.* **1993**, *49*, 8107.

86. Kyba, E. P.; John, A. M. *J. Am. Chem. Soc.* **1977**, *99*, 8329.

87. Seghers, L.; Shechter, H. *Tetrahedron Lett.* **1976**, 1943.

88. Press, L. S.; Shechter, H. *J. Am. Chem. Soc.* **1979**, *101*, 509.

89. Keating, A. E.; Garcia-Garibay, M. A.; Houk, K. N. *J. Phys. Chem.* **1998**, *102*, 8467.

90. Friedman, L.; Shechter, H. *J. Am. Chem. Soc.* **1960**, *82*, 1002.

91. Brinker, U. H.; Schenker, G. *J. Chem. Soc. Chem. Commun.* **1982**, 679.

92. Schoeller, W. W. *J. Am. Chem. Soc.* **1979**, *101*, 4811.

93. Sulzbach, M.; Platz, M. S.; Schaefer, H. F. III.; Hadad, C. *J. Am. Chem. Soc.* **1997**, *119*, 5682.

94. (a) Ando, W.; in "The Chemistry of diazonium and diazo groups"; Patai, S., Ed.; J. Wiley and Sons: Chichester, 1978; Part 1, 458. (b) Meier, H.; Zeller, K.-P. *Angew. Chem., Int. Ed. Engl.*, **1975**, *14*, 32.

95. (a) Toscano, J. P.; Platz, M. S.; Nikolaev, V.; Popic, V. *J. Am. Chem. Soc.* **1994**, *116*, 8146. (b) Toscano, J. P.; Platz, M. S. *J. Am. Chem. Soc.* **1995**, *117*, 4712. (c) Wang, J.-I.; Toscano, J. P.; Platz, M. S.; Nikolaev, V.; Popik, V. *J. Am. Chem. Soc.* **1995**, *117*, 5477. (d) Toscano, J. P.; Platz, M. S.; Nikolaev, V.; Cao, Y.; Zimmt, M. B. *J. Am. Chem. Soc.* **1996**, *118*, 3527.

96. Toscano, J. P. In *Adv. Carbene Chem.*; Brinker, U.; Ed.; JAI Press, Greenwich, **1998**, Vol.2, p 215.

97. Moss, R. A.; Xue, S.; Liu, W.; Krogh-Jespersen, K. *J. Am. Chem. Soc.* **1996**, *118*, 12588 and references within.

98. (a) Moss, R. A.; Ho. G.-J. *J. Am. Chem. Soc.* **1990**, *112*, 5642. (b) Moss, R. A.; Liu, W. *J. Chem. Soc. Chem. Commun.* **1993**, 1597. (c) Moss, R. A.; Munjal, R. C. *J. Chem. Soc. Chem Commun.* **1978**, 775.

99. (a) Morgan, S.; Jackson, J. E.; Platz, M. S. *J. Am. Chem. Soc.* **1991**, *113*, 2782. (b) Bally, T.; Matzinger, S; Truttman, C.; Platz, M. S.; Morgan, S. *Angew. Chem. Int. Ed. Engl.* **1994**, *33*, 1964.

100. Moss, R. A.; Chang, M. J. *Tetrahedron Lett.* **1981**, *22*, 3749.

101. For reviews see: (a) Colvin, E.W. in "Silicon in Organic Synthesis"; Butterworths Publ.: London, 1981 (b) Larson, G.L.. Ed. "Advances in Silicon Chemistry"; JAI Press Inc.: London, 1991; Vol. 1.

102. Perrin, H. M.; White, W. R.; Platz, M. S. *Tetrahedron Lett.*, **1991**, *32*, 4445.

103. Kirmse, W.; Guth, M.; Steenken, S. *J. Am. Chem. Soc.* **1996**, *118*, 10838.

104. Creary, X.; Wang, Y. X *Tetrahedron Lett.* **1989**, *30*, 2493.

105. Creary, X.; Wang, Y. X *J. Org. Chem.* **1994**, *59*, 1604.

106. Bruckmann, R.; Schneider, K.; Maas, G.; *Tetrahedron* **1989**, *45*, 5517. and references therein.

107. Bruckmann, R.; Maas, G. *Chem. Ber.* **1987**, *120*, 635.

108. For examples see: (a) White, W. R., III; Platz, M. S. *J. Org. Chem.* **1992**, *57*, 2841. (b) Moss, R. A., Ho, G.-H. *J. Phys.Org. Chem.* **1993**, 6, 126. (c) Moss, R. A.; Liu, W.; Krogh-Jespersen, K. *J. Phys. Chem.* **1993**, *97*, 13413.

109. (a) Skell, P. S.; Cholod, M. S. *J. Am. Chem. Soc.* **1969**, *91*, 7131. (b) Liu, M. T. H.; Bonneau, R. *J. Am. Chem. Soc.* **1990**, *112*, 3915.

110. (a) Houk, K. N.; Rondan, N. G.; Mareda, J. *Tetrahedron* **1985**, *41*, 1555. (b) Houk, K. N.; Rondan, N. G.; Mareda, J. *J. Am. Chem. Soc.* **1984**, *106*, 4291. (c) Blake, J. F.; Wierschke, S. G.; Jorgensen, W. C. *J. Am. Chem. Soc.* **1989**, *111*, 1919.

111. Khan, M. I.; Goodman, J. L. *J. Am. Chem. Soc.* **1995**, *117*, 6635.

112. Skell, P. S.; Woodworth, R. C. *J. Am. Chem. Soc.* **1956**, *78*, 4496.

113. Kirmse, W. In "Advances in Carbene Chemistry"; Brinker, U. Ed.: JAI Press Inc.: Greenwich, 1994. Vol. 1, p 1 and references therein.

114. Olson, D. R.; Platz, M. S. *J. Phys. Org. Chem.* **1996**, *9*, 759.

115. Kirmse, W.; Loosen, K.; Sluma, H.-D. *J. Am. Chem. Soc.* **1981**, *103*, 5935.

116. Kirmse, W.; Sluma, H.-D. *J. Org. Chem.* **1988**, *53*, 763.

117. Friedrich, K.; Jansen, U.; Kirmse, W. *Tetrahedron Lett.* **1985**, *26*, 193.

118. Moss, R. A.; Maksimovic, L.; Marchand, A. P.; Ramanaiah, K. C. V. *Tetrahedron Lett.* **1996**, *37*, 5849.

119. (a) Parham, W. E.; Groen, S. H. *J. Org. Chem.* **1964**, *29*, 2214. (b) Parham, W. E.; Groen, S. H. *J. Org. Chem.* **1965**, *30*, 728. (c) Parham, W. E.; Groen, S. H. *J. Org. Chem.* **1966**, *31*, 1694.

120. For a review see: Padwa, A.; Hornbuckle, S. F. *Chem. Rev.* **1991**, *91*, 263.

121. Moss, R. A.; Ho. G.-J.; Sierakowski, C. *J. Am. Chem. Soc.* **1992**, *114*, 3128.

122. Wong, P. C.; Griller, D.; Scaiano, J. C. *J. Am. Chem. Soc.* **1982**, *104*, 663.

123. For oxygen atom abstractions from CO_2 see: (a) Chateauneuf, E. J. *Res. Chem. Intermed.* **1994**, *20*, 159. (b) Wierlacher, S.; Sauer, W. W.; Liu, M. T. H. *J. Org. Chem.* **1992**, *57*, 1051. (c) Sander, W. W. *J. Mol. Struct.* **1990**, *222*, 21. (d) Koch, M.; Temp, F.; Wagner, R.; Wagner, H. Gg. *Ber. Bunsen-Ges. Phys. Chem.* **1990**, *94*, 645. (e) Sander, W. W. *J. Org. Chem.* **1989**, *54*, 4265. (f) Laufer, A. H.; Bass, A. M. *Chem. Phys. Lett.* **1977**, *46*, 151. (g) Hsu,

D. S. Y.; Lin, M. C. *Int. J. Chem. Kinet.* **1977**, *9*, 1507. (h) Kistiakowsky, G. B.; Sauer, K. *J. Am. Chem. Soc.* **1968**, *90*, 1066. (i) Milligan, D. E.; Jacox, M. E. *J. Chem. Phys.* **1962**, *36*, 2911.

124. For oxygen atom abstractions from N-oxides see: (a) Field, K. W.; Schuster, G. B.; *J. Org. Chem.* **1988**, *53*, 4000. (b) Schweiter, E. E.; O'Neill, G. J. *J. Org. Chem.* **1963**, *28*, 2460.

125. For oxygen atom abstractions from PF₃O see: Mahler, W. *J. Am. Chem. Soc.* **1968**, *90*, 523.

126. For oxygen atom abstractions from epoxides see: (a) Shields, C. J.; Schuster, G. B. *Tetrahedron Lett.* **1987**, *28*, 853. (b) Wittig, G.; Schlosser, M. *Tetrahedron* **1962**, *18*, 1026. (c) Nozaki, H.; Takaya, H.; Noyori, R. *Tetrahedron Lett.* **1965**, 2563. (d) Nozaki, H.; Takaya, H.; Noyori, R. *Tetrahedron* **1966**, *22*, 3393. (e) Martin, M.; Ganem, B. *Tetrahedron Lett.* **1984**, 251.

127. Hata, Y.; Watanabe, M. *Tetrahedron Lett.* **1972**, 3827 and 4659.

128. Hata, Y.; Watanabe, M.; Inoue, S.; Oae, S. *J. Am. Chem. Soc.* **1975**, *97*, 2553.

129. For oxygen atom abstractions from carbonyl compounds see: Kovacs, D.; Lee, M.-S.; Olson, D.; Jackson, J. E. *J. Am. Chem. Soc.* **1996**, *118*, 8144.

130. Shevlin, P. B.; Martino, P. C. *J. Am. Chem. Soc.* **1980**, *102*, 5430.

131. (a) Frey, H. M. *Adv. Photochem.* **1964**, *4*, 225. (b) Frey, H. M. *J. Am. Chem. Soc.* **1962**, *84*, 2293.

132. Brinker, U. H.; Boxberger, M. *Angew. Chem. Int. Ed. Engl.* **1984**, *23*, 974.

133. For rate constants of cycloaddition reactions see: Fisera, L.; Geittner, J.; Huisgen, R.; Reissig, H.-U. *Heterocycles* **1978**, *10*, 153.

134. Applequist, D. E.; McGreer D. E. *J. Am. Chem. Soc.* **1960**, *82*, 1965.

135. Huisgen, R. In *Advances in Cycloaddition*; Curran, D. P., ed.; JAI Press: New York, **1988**; Vol. 1.

136. Sugiyama, M.H.; Celebi, S.; Platz, M. S. *J.Am. Chem. Soc.* **1992**, *114*, 966.

137. (a) Pezacki, J. P.; Warkentin, J.; Wood, P. D.; Lusztyk, J.; Yuzawa, T.; Gudmundsdóttir, A. D.; Morgan, S.; Platz, M. S. *J. Photochem. Photobiol. A. Chem.* **1998**, *116*, 1. (b) Bonneau, R.; Hellrung, B.; Liu, M. T. H.; Wirz, J. *J. Photochem. Photobiol. A. Chem.* **1998**, *116*, 9.

138. Unpublished results from the Platz group.

139. El-Saidi, M.; Kassam, K.; Pole, D. L.; Tadey, T.; Warkentin, J. *J. Am. Chem. Soc.* **1992**, *114*, 8751, and references therein.

140. 2-Trifluoromethylcyclohexanone was prepared according to the procedure in: Cantacuzène, D.; Wakselman, C.; Dorme, R. *J. Chem. Soc., Perkin Trans. I* **1977**, 1365.

141. Oxadiazoline precursors give the best signals for pyridinium ylides of dialkyl and cycloalkylcarbenes when irradiated 308 nm by LFP. For these experiments pyridine purity was extremely important as impurities (presumably the N-oxide) absorb at the excitation wavelength. In some cases it was necessary to purify pyridine by ZnCl₂ complexation and release to obtain solutions of pyridine which did not absorb light at 308 nm. see Heap, J.; Jones, W. J.; Speakman, J. B. *J. Am. Chem. Soc.* **1921**, *43*, 1936. Very pure pyridine turns yellow over a period of 10-30 minutes at room temperature when exposed to oxygen.

142. (a) Haas, A.; Plümer, R.; Schiller, A. *Chem. Ber.* **1985**, *118*, 3004. (b) Bouillon, J.-P.; Maliverny, C.; Merényi, R.; Viche, H. G. *J. Chem. Soc. Perkin Trans. I* **1991**, 2147.

143. Mansoor, A. M.; Stevens, I. D. R. *Tetrahedron Lett.* **1966**, 1733.

144. Abelt, C. J.; Pleier, J. M. *J. Am. Chem. Soc.* **1989**, *111*, 1795.

145. (a) Jackson, J. E.; Soundararajan, N.; White, W.; Liu, M. T. H.; Bonneau, R.; Platz, M. S. *J. Am. Chem. Soc.* **1989**, *111*, 6874. (b) Bonneau, R.; Liu, M. T. H.; Subramanian, R.; Linkletter, B.; Stevens, I. D. R. *Laser Chem.* **1989**, *10*, 267. (c) Bonneau, R.; Liu, M. T. H.; Kim, K. C.; Goodman, J. L. *J. Am. Chem. Soc.* **1996**, *118*, 3829. (d) Liu, M. T. H.; Suresh, R. V.; Soundararajan, N.; Vessey, E. G. *J. Chem. Soc., Chem. Commun.* **1989**, 12.

146. (a) Liu, M. T. H.; Soundararajan, N.; Paike, N. *J. Org. Chem.* **1987**, *52*, 4223. (b) Liu, M. T. H.; Suresh, R. V.; Soundararajan, N.; Vessy, E. G. *J. Chem. Soc., Chem. Commun.* **1989**, 12. (c) Liu, M.T.H.; Chapman, R.G.; Bonneau, R. *J. Photochem. Photobiol. A. Chem.* **1992**, *63*, 115.

147. Liu, T. H. M.; Subramanian, R. *J. Org. Chem.* **1985**, *50*, 3218.

148. (a) Jackson, J. E.; Soundararajan, N.; Platz, M. S. *J. Am. Chem. Soc.* **1988**, *110*, 5595. (b) Gould, I. R.; Turro, N. J.; Butcher, J. J.; Doubleday, C. J.; Hacker, N. P.; Lehr, G. F.; Moss, R. A.; Cox, D. P.; Guo, W.; Munjal, R. C.; Perez, L. A.; Fedorynski, M. *Tetrahedron.* **1985**, *41*, 1587

149. Liu, M. T. H.; Bonneau, R. *J. Am. Chem. Soc.* **1990**, *112*, 3915.

150. For a description of laser flash photolysis with UV-VIS detection see Kazanis, S.; Azarani, A.; Johnston, L. J. *J. Phys. Chem.* **1991**, *95*, 4430.

151. Wlostowska, J.; Moss, R. A.; Guo, W.; Chang, M. J. *J. Chem. Soc., Chem. Commun.* **1982**, 432.

152. Myers, D. R.; Senthilnathan, V. P.; Platz, M. S.; Jones, M., Jr. *J. Am. Chem. Soc.* **1986**, *108*, 4232.

153. A laser flash photolysis system with a Mutek MPS-1000 diode laser (output 1520-2314 cm-1) as the monitoring source was used. Wagner, B. D.; Arnold, B. R.; Brown, G. S.; Lusztyk, J. *J. Am. Chem. Soc.* **1998**, *120*,1827.

154. (a) Zupancic, J. J.; Schuster, G. B. *J. Am. Chem. Soc.* **1980**, *102*, 5958. (b) Senthilnathan, V. P.; Platz, M. S. *J. Am. Chem. Soc.* **1980**, *102*, 7637. (c) Wong, P. C.; Griller, D.; Scaiano, J. C. *J. Am. Chem. Soc.* **1981**, *103*, 5934. (d) Zupancic, J. J.; Schuster, G. B. *J. Am. Chem. Soc.* **1981**, *103*, 944. (e) Griller, D.; Montgomery, C. R.; Scaiano, J. C.; Platz, M. S.; Hadel, L. M. *J. Am. Chem. Soc.* **1982**, *104*, 6813. (f) Griller, D.; Hadel, L. M.; Nazran, A. S.; Platz, M. S.; Wong, P. C.; Savino, T. G.; Scaiano, J. C. *J. Am. Chem. Soc.* **1984**, *106*, 2227. (g) Scaiano, J. C.; McGimpsey, W. G.; Casal, H. L. *J. Am. Chem. Soc.* **1985**, *107*, 7204. (h) Barcus, R. L.; Wright, B. B.; Leyva, E.; Platz, M. S. *J. Phys. Chem.* **1987**, *91*, 6677.

155. Gash, R. C.; MacCorquodale, F.; Walton, J. C. *Tetrahedron* **1989**, *45*, 5531.

156. (a) Ziegler, F. E.; Petersen, A. K. *J. Org. Chem.* **1995**, *60*, 2666. (b) Ziegler, F. E.; Petersen, A. K. *J. Org. Chem.* **1994**, *59*, 2707. (c) Dickinson, J. M., Murphy, J. A.; Patterson, C. W.; Wooster, N. F. *J. Chem. Soc., Perkin Trans 1* **1990**, 1179. (d) Stogryn, E. L.; Gianni, M. H. *Tetrahedron Lett.* **1970**, 3025.

157. Izraelewicz, M. H.; Nur, M.; Spring, R. T.; Turos, E. *J. Org. Chem.* **1995**, *60*, 470.

158. (a) Alberti, A.; Griller, D.; Nazran, A. S.; Pedulli, G. F. *J. Am. Chem. Soc.* **1986**, *108*, 3024. (b) McGimpsey, W. G.; Scaiano, J. C. *Tetrahedron Lett.* **1986**, *27*, 547.

159. (a) Gaussian 94, Revision D.4, M. J. Frisch, G. W. Trucks, H. B. Schlegel, P. M. W. Gill, B. G. Johnson, M. A. Robb, J. R. Cheeseman, T. Keith, G. A. Petersson, J. A. Montgomery, K. Raghavachari, M. A. Al-Laham, V. G. Zakrzewski, J. V. Ortiz, J. B. Foresman, J. Cioslowski, B. B. Stefanov, A. Nanayakkara, M. Challacombe, C. Y. Peng, P. Y. Ayala, W. Chen, M. W. Wong, J. L. Andres, E. S. Replogle, R. Gomperts, R. L. Martin, D. J. Fox, J. S. Binkley, D. J. Defrees, J. Baker, J. P. Stewart, M. Head-Gordon, C. Gonzalez, and J. A. Pople, Gaussian, Inc., Pittsburgh PA, 1995. (b) Møller, C.; Plesset, M. S. *Phys. Rev.* **1934**, *46*, 618. (b) Krishman, R.; Frisch, M. J.; Pople, J. A. *J. Chem. Phys.* **1980**, *72*, 4244. (c) Hehre, W. J.; Radom, L.; Pople, J. A.; Schleyer, P. v. R. *Ab Initio Molecular Orbital Theory;* Wiley-Interscience: New York, 1986. (d) NBO Version 3.1, Glendening, E.D., Reed, A.E., Carpenter, J.E., and Weinhold, F.

160. (a) Moss, R. A.; Young, C. M.; Perez, L. A.; Krogh-Jespersen, K. *J. Am. Chem. Soc.* **1981**, *103*, 2413. (b) Moss, R. A.; Mallon, C. B.; Ho, C.-T. *J. Am. Chem. Soc.* **1977**, *99*, 4105.

161. (a) Brook, A. G. *J. Am. Chem. Soc.* **1955**, *77*, 4827-4829. (b) Brook, A. G.; Mauris, R. J. *J. Am. Chem. Soc.* **1957**, *79*, 971.

162. (a) Pole, D. L.; Sharma, P. K.; Warkentin, J. *Can. J. Chem.* **1996**, *74*, 1335-1340. (b) Kirmse, W.; Guth, M.; Steenken, S. *J. Am. Chem. Soc.* **1996**, *118*, 10838-10949. (c) González, R.; Wudl, F.; Pole, D. L.; Sharma, P. K.; Warkentin, J. *J. Org. Chem.* **1996**, *61*, 5837-5839. (d) Kirmse, W.; Konrad, W.; Schnitzler, D. *J. Org. Chem.* **1994**, *59*, 3821-3929. (e) Walsh, R.; Wolf, C.; Untiedt, S.; de Meijere, A. *J. Chem. Soc. Chem. Commun.* **1992**, 421-422. (f) Walsh, R.; Untiedt, S.; de Meijere, A. *Chem. Ber.* **1994**, *127*, 237-245. (g) Shimizu, H.; Gordon, M. S. *Organometallics* **1994**, *13*, 186-189. (h) Barton, T. J.; Lin, J.; Ijadi-Maghsoodi, S.; Power, M. D.; Zhang, X.; Ma, Z.; Shimuzu, H.; Gordon, M. S. *J. Am. Chem. Soc.* **1995**, *117*, 11695-11703. (i) Creary, X.; Wang, Y.-X. *J. Org. Chem.* **1994**, *59*, 1604-1605.

163. Baird, M. S.; Dale, C. M.; Dulayymi, J. R. A. *J. Chem. Soc. Perkin Trans. 1.* **1993**, 1373-1374.

164. See Lucas, M. A.; Schiesser, C. H. *J. Org. Chem.* **1996**, *61*, 5754 and references within.

165. Venneri, P. C., Warkentin, J. *J. Am. Chem. Soc.* **1998**, *120*, 11182.

166. (a) Moss, R. A.; Ho, G.-J.; Wilk, B.K. *Tetrahedron Lett.* **1989**, *30*, 2473-2476. (b) Moss, R.A.; Wilk, B. K.; Hadel, L. M. *Tetrahedron Lett.* **1987**, *28*, 1969-1972. (c) Moss, R. A.; Kim, H.-R. *Tetrahedron Lett.* **1990**, *31*, 4715-4718. (d)

Moss, R. A.; Ho, G.-J.; Liu, W. *J. Am. Chem. Soc.* **1992**, *114*, 959-963. (e) Moss, R. A.; Zdrojewski, T. *Tetrahedron Lett.* **1991**, *32*, 5667-5670. (f) Moss, R. A.; Balcerzak, P. *J. Am. Chem. Soc.* **1992**, *114*, 9386-9390. (g) Moss, R. A.; Ge, C.-S.; Maksimovic, L. *J. Am. Chem. Soc.* **1996**, *118*, 9792-9793.

167. (a) Perrin, H. M.; White, W. R.; Platz, M. S. *Tetrahedron Lett.* **1991**, *32*, 4443-4446. (b) Kirmse, W.; Guth, M.; Steenken, S. *J. Am. Chem. Soc.* **1996**, *118*, 10838-10849.

168. A fully concerted mechanism has been proposed for a specific oxadiazoline. Smith, W. B. *J. Org. Chem.* **1995**, *60*, 7456.

169. Suh, D.; Pole, D. L.; Warkentin, J.; Terlouw, J. K. *Can. J. Chem.* **1996**, *74*, 544.

170. (a) Kirmse, W.; Konrad, W.; Özkir, I. S. *Tetrahedron* **1997**, *53*, 9935-9964. (b) Compounds containing SiON fragments have recently been shown to have cyclopropane-like structures with quite short SiN bonds. Mitzel, N. W.; Losehand, U. *Angew. Chem. Int. Ed. Engl.* **1997**, *36*, 2807-2809.

171. Photochemical reactions of acyl silanes are also known to involve silyl migration to carbonyl oxygen, R3SiC(=O)R'→ R3SiO(R')C:. See, for example, (a) Bourque, R. A.; Davis, P. D.; Dalton, J. C. *J. Am. Chem. Soc.* **1981**, *103*, 697-699. (b) Dalton, J. C.; Bourque, R. A. *J. Am. Chem. Soc.* **1981**, *103*, 699-700. (c) Scheller, M. E.; Frei, B. *Helv. Chim. Acta.* **1984**, *67*, 1734-1747.

172. Hoffmann, R.W.; Lilienblum, W.; Dittrich, B. *Chem. Ber.* **1974**, *107*, 3395.

173. Moss, R. A.; Huselton, J. K. *J. Chem. Soc., Chem. Commun.* **1976**, 950.

174. Enders, D.; Breuer, K.; Runsink, Teles, J. H. *Liebigs Ann.* **1996**, 2019.

175. Lilienblum, W.; Hoffmann, R. W. *Chem. Ber.* **1977**, *110*, 3405.

176. (a) Kümmell, A.; Seitz, G. *Tetrahedron Lett.* **1991**, *32*, 2743. (b) Gerninghaus, C.; Kümmell, A.; Seitz, G. *Chem. Ber.* **1993**, *126*, 733. (c) Frenzen, G.; Kümmell, A.; Meyer-Dulheuer, C.; Seitz, G. *Chem. Ber.* **1994**, *127*, 1803.

177. Hoffmann, R.W.; Lilienblum, W.; Dittrich, B. *Chem. Ber.* **1974**, *107*, 3395.

178. Boger, D. L.; Brotherton, C. E. *J. Org. Chem.* **1985**, *50*, 3425.

179. (a) Boger, D. L.; Brotherton-Pleiss, C. E. In *Advances in Cycloaddition*, Vol. 2.; Curran, D. P. Ed.; JAI Press: Greenwich, CT, 1990, pp 147. (b) Boger, D. L.; Brotherton, C. E. *J. Am. Chem. Soc.* **1986**, *108*, 6695. (c) Boger, D. L.; Brotherton, C. E. *Tetrahedron Lett.* **1984**, *25*, 5611.

180. Boger, D. L.; Brotherton, C. E. *J. Am. Chem. Soc.* **1986**, *108*, 6713.

181. Hoffmann, R. W.; Steinbach, K.; Dittrich, B. *Chem. Ber.* **1973**, *106*, 2174.

182. Hoffmann, R. W.; Reiffen, M. *Chem. Ber.* **1976**, *109*, 2565.

183. (a) Rigby, J. H.; Cavezza, A.; Ahmed, G. *J. Am. Chem. Soc.* **1996**, *118*, 12848. (b) Rigby, J. H.; Cavezza, A.; Heeg, M. J. *J. Am. Chem. Soc.* **1998**, *120*, 3664.

184. Ross, J. P.; Couture, P.; Warkentin, J. *Can. J. Chem.* **1997**, *75*, 1331.

185. (a) Hoffmann, R. W.; Schmidt, P.; Backes, J. *Chem. Ber.* **1976**, *109*, 1918. (b) Hoffmann, R. W.; Backes, J. *Chem. Ber.* **1976**, *109*, 1928.

186. Arduengo, A. J., III; Kline, M.; Calabrese, J. C.; Davidson, F. *J. Am. Chem. Soc.* **1991**, *113*, 9704.

187. For some examples of triplet carbene atom abstractions including chlorine atoms see: (a)Platz, M. S. *Acc. Chem. Res.* **1988**, *21*, 236. (b) Griller, D.; Hadel, L. M.; Nazran, A. S.; Platz, M. S.; Wong, P. C.; Savino, T. G.; Scaiano, J. C. *J. Am. Chem. Soc.* **1984**, *106*, 2227.

188. Roth, H. D. *Acc. Chem. Res.* **1977**, *10*, 85.

189. West, R. *Pure & Appl. Chem.* **1971**, *43*, 379.

190. We also thermolyzed 1 in the presence of excess hexachloropropene which yielded a combination of mono-, di, and triester products, however, we have not been able to identify the structures of these adducts unambiguously.

191. Sünkel, R. *J. Organomet. Chem.* **1990**, *391*, 247.

192. Pole, D. L.; Warkentin, J. *Liebigs Ann.* **1995**, 1907.

193. Hoffman, R. W.; Lilienblum, W.; Dittrich, B. *Chem. Ber.* **1974**, *107*, 3395.

194. Reid, D.; Warkentin, J. unpublished results.

195. (a) Eberson, L. "Electron Transfer Reactions in Organic Chemistry"; Springer-Verlag: NY; 1987. (b) "Photoinduced Electron Transfer"; Vol. A-D, Fox, M. A., Chanon, M. Eds.; Elsevier: NY; 1988.

196. (a) Burgers, P. C.; McGibbon, G. A.; Terlouw, J. K. *Chem. Phys. Lett.* **1994**, *224*, 539. (b) Burgers, P. C.; Mommer, A. A.; Holmes, J. L. *J. Am. Chem. Soc.* **1983**, *105*, 5976.

197. For some reviews see: (a) Bell, R. P. *The Proton in Chemistry*, 2nd ed.; Cornell University Press: Ithaca, NY, 1973. (b) Kresge, A. J. *Chem. Soc. Rev.* **1973**, *4*, 475. (c) Kresge, A. J. In *Proton Transfer Reactions*; Caldin, E. F., Gold, V., Eds.; Chapman and Hall: London, 1975; Ch. 7. (d) Jencks, W. P. *Acc. Chem. Res.* **1976**, *9*, 425. (e) Kresge, A. J. *Acc. Chem. Res.* **1975**, *8*, 354. (f) Hine, J. *Adv. Phys. Org. Chem.* **1977**, *15*, 1. (g) Bernasconi, C. F. *Acc. Chem. Res.* **1992**, *25*, 9. (h) Bernasconi, C. F. *Adv. Phys. Org. Chem.*. **1991**, *27*, 119. (i) Bernasconi, C. F. *Acc. Chem. Res.* **1987**, *20*, 301.

198. (a) Emerson, M. T.; Grunwald, E.; Kaplan, M. L.; Kromhout, R. A. *J. Am. Chem. Soc.* **1960**, *82*, 6307. (b) Grunwald, E. *J. Phys. Chem.* **1963**, *67*, 2211. (c) Grunwald, E.; Ralph, E. K. *Acc. Chem. Res.* **1971**, *4*, 107. (d) Grunwald, E. Eustace, D. In "Proton-Transfer Reactions"; Caldin, E., Gold, V., Eds.; Chapman and Hall: London, 1975, pgs 103 - 120.

199. Also see: Guthrie, J. P. *J. Am. Chem. Soc.* **1996**, *118*, 12886 and references therein.

200. Eigen, M. *Angew. Chem., Int. Ed. Engl.* **1964**, *3*, 1.

201. Bordwell, F. G.; Satish, A. V. *J. Am. Chem. Soc.* **1991**, *113*, 985.

202. Washabaugh, M. W.; Jencks, W. P. *J. Am. Chem. Soc.* **1989**, *111*, 674 and 683.

203. Washabaugh, M. W.; Jencks, W. P. *Biochemistry* **1988**, *27*, 5044.

204. Alder, R. W.; Allen, P. R.; Williams, S. J. *J. Chem. Soc. Chem. Commun.* **1995**, 1267.

205. Moss, R.A.; Shen, S.; Wlostowski, M. *Tetrahedron Lett.* **1988**, *29*, 6417.

206. Du, X.-M.; Fan, H.; Goodman, J.L.; Kesselmayer, M.A.; Krogh-Jespersen, K.; LaVilla, J.A.; Moss, R.A.; Shen, S.; Sheridan, R.S. *J. Am. Chem. Soc.* **1990**, *112*, 1920.

207. (a) Ballinger, P.; Long, F. A. *J. Am. Chem. Soc.* **1960**, *82*, 795. (b) Dyatkin, B. L.; Mochalina, E. P.; Knunyants, I. L. *Tetrahedron* **1965**, *21*, 2991. (c) Takahashi, S.; Cohen, L. A.; Miller, H. K.; Peake, E. G. *J. Org. Chem.* **1971**, *36*, 1205.

208. The pKa values of various acids in acetonitrile have been compiled in "The IUPAC Chemical Data Series" No. 35. 1990. compiled by K. Izutsu.

209. Hammond, G. S. *J. Am. Chem. Soc. J. Am. Chem. Soc.* **1955**, *77*, 334.

210. Marcus, R. A. *J. Phys. Chem.* **1968**, *72*, 891.

211. For examples of the use of quadratic Brönsted correlations to solve for Marcus theory parameters see: (a) Pezacki, J. P., Wagner, B. D.; Lew, C. S. Q.; Warkentin, J.; Lusztyk, J. *J. Am. Chem. Soc.* **1997**, *119*, 1789. (b) Chiang, Y.; Grant, A. S.; Kresge, A. J.; Paine, S. W. *J. Am. Chem. Soc.* **1996**, *118*, 4366. (c) Albery, W. J.; Campbell-Crawford, A. J.; Curran, J. S. *J. Chem. Soc., Perkin Trans. 2* **1972**, 2206. (d) Kresge, A. J. *Chem. Soc. Rev.* **1973**, *4*, 475.

212. (a) Fischer,H.; DeCandis, F. X.; Ogden, S. D.; Jencks, W. P. *J. Am. Chem. Soc.* **1980**, *102*, 1340. (b) Gilbert, H. F.; Jencks, W. P. *J. Am. Chem. Soc.* **1977**, *99*, 7931. (c) Bednar, R. A.; Jencks, W. P. *J. Am. Chem. Soc.* **1985**, *107*, 7117.

213. Murdoch, J. R. *J. Am. Chem. Soc.* **1980**, *102*, 71.

214. (a) Elvidge, J. A.; Jones, J. R.; O'Brien, C.; Evans, E. A.; Sheppard, H. C. *Adv. Heterocyclic Chem.* **1974**, *16*, 1. (b) Ridd, J. H. *Phys. Methods Heterocyclic Chem.* **1971**, *4*, 55.

215. McClelland, R. A.; Kahley, M. J.; Davidse, P. A.; Hadzialic, G. *J. Am. Chem. Soc.* **1996**, *118*, 4794.

216. It has been shown that the slope of the Brönsted plot can be influenced by pre-equilibrium desolvation. Thus, the magnitude of the obtained coefficient alone may not exactly reflect the thermodynamics of the reaction. See: Murray. C. J.; Jencks, W. P. *J. Am. Chem. Soc.* **1990**, *112*, 1880.

217. Larson, J. W.; McMahon, T.B. *J. Am. Chem. Soc.* **1987**, *109*, 6230.

218. Kresge, A. J.; Powell, M. F. *J. Org. Chem.* **1986**, *51*, 819, and 822.

219. (a) Stivers, J. T.; Washabaugh, M. W. *Bioorg. Chem.* **1991**, *19*, 369. (b) Kluger, R.; Lam, J. F.; Pezacki, J. P.; Yang, C.-M. *J. Am. Chem. Soc.* **1995**, *117*, 11383.

220. Griess, P. *Justus Liebigs Ann. Chem.* **1861**, *120*, 125.

221. Lijinsky, W. In *Chemistry and Biology of N-nitroso Compounds*; Cambridge University Press: Cambridge, 1992.

222. (a) Druckrey, H.; Preussmann, R.; Ivankovic, S.; Schmahl, D. *Z. Krebsforsch.* **1967**, *69*, 103. (b) Druckrey, H. *Xenobiotica* **1973**, *3*, 271.

223. Lijinsky, W. *IARC Sci. Publ.* **1982**, *41*, 533.

224. (a) Mesic, M.; Revis, C.; Fishbein, J. C. *J. Am. Chem. Soc.* **1996**, *118*, 7412. (b) Chahoua, L.; Mesic, M.; Revis, C.; Vigroux, A.; Fishbein, J. C. *J. Org. Chem.* **1997**, *62*, 2500.

225. (a) Ukawa, S.; Tobita, C.; Mochizuki, M. *Mutat. Res.* **1988**, *203*, 391. (b) Ukawa, S.; Mochizuki, M. *Mutat. Res.* **1991**, *252*, 391.

226. (a) Finneman, J. I.; Fishbein, J. C. *J. Am. Chem. Soc.* **1996**, *118*, 7134. (b) Finneman, J. I.; Fishbein, J. C. *J. Am. Chem. Soc.* **1995**, *117*, 4228. (c) Ho, J.; Fishbein, J. C. *J. Am. Chem. Soc.* **1994**, *116*, 6611. (d) Finneman, J. I.; Ho, J.; Fishbein, J. C. *J. Am. Chem. Soc.* **1993**, *115*, 3016. (e) Hovinen, J.; Finneman, J. I.; Satapathy, S. N.; Ho, J.; Fishbein, J. C. *J. Am. Chem. Soc.* **1992**, *114*, 10321. (f) Gold, B.; Deshpande, A.; Linder, W.; Hines, L. *J. Am. Chem. Soc.* **1984**, *106*, 2072. (g) Moss, R. A. *Acc. Chem. Res.*, **1974**, *7*, 421.

227. (a) Leung, K. H.; Archer, M. C. *Chem. Biol. Interact.* **1984**, *48*, 169. (b) Lawson, T., Nagel, D. *Carcinogenesis* **1988**, *9*, 1007. (c) Liberato, D.; Saavedra, J. E.; Farnsworth, D.; Lijinski, W. *Chem. Res. in Toxicol.* **1989**, *2*, 307.

228. Antrub, H.; Stoner, G. D. *Cancer Res.* **1982**, *42*, 1307.

229. Wurdeman, R. L.; Church, K. M.; Gold, B. *J. Am. Chem. Soc.* **1989**, *111*, 6408.

230. (a) Singer, B. *Prog. Nucl. Acids Res. Molec. Biol.* **1975**, *15*, 219, and 330. (b) Singer, B. *Nature* **1976**, *264*, 333.

231. For reviews of aliphatic diazonium ion chemistry see: (a) Laali, K.; Olah, G. A. *Rev. Chem. Intermed.* **1986**, *6*, 237. (b) Kirmse, W. *Angew. Chem. Int. Ed. Engl.* **1976**, *15*, 251. (c) Collins, C. J. *Acc. Chem. Res.* **1971**, *4*, 315. (d) More O'Ferrall, R. A. *Adv. Phys. Org. Chem.* **1967**, *5*, 331. (e) Huisgen, R. *Angew. Chem.* **1955**, *67*, 273. (f) Zollinger, H. In *Diazo Chemistry*; VCH Publ.: New York, 1995; Vol. 1-2. (g) Whittaker, D. In *The Chemistry of Diazonium and Diazo Compounds*; Patai, S., Ed.; Wiley-Interscience: Chichester, 1978; pp. 617-639.

232. Jencks, W.P. *Chem. Soc. Rev.* **1981**, *10*, 345.

233. (a) Berner, D.; McGarrity, J. F. *J. Am. Chem. Soc.* **1979**, *101*, 3135. (b) McGarrity, J. F.; Cox, D. P. *J. Am. Chem. Soc.* **1983**, *105*, 3961.

234. Mohrig, J. R.; Keegstra, K. *J. Am. Chem. Soc.* **1967**, *89*, 5492.

235. McGarrity, J. F.; Smyth, T. *J. Am. Chem. Soc.* **1980**, *102*, 7303.

236. Foster, M. S. ; Beauchamp, J. L. *J. Am. Chem. Soc.* **1972**, *94*, 2425.

237. Rossini, F. D.; Montgomery, R. L. *J. Chem. Thermodyn.* **1978**, *10*, 465.

238. McMahon, T. B.; Heinis, T.; Nicol, G.; Hovey, J. K.; Kebarle, P. *J. Am. Chem. Soc.* **1988**, *110*, 7591.

239. Traeger, J. C.; McMoughlin, R. G. *J. Am. Chem. Soc.* **1981**, *103*, 3607.

240. Glaser, R.; Choy, G. S.-C.; Hall, M.K. *J. Am. Chem. Soc.* **1991**, *113*, 1109.

241. Glaser, R.; Choy, G. S.-C. *J. Am. Chem. Soc.* **1993**, *115*, 2340.

242. Brosch, D.; Kirmse, W. *J. Org. Chem.* **1991**, *56*, 907 and refs. therein.

243. Kirmse, W.; Schnurr, O.; Jendralla, H. *Chem. Ber.* **1979**, *112*, 2120.

244. (a) Southam, R. M.; Whiting, M. C. *J. Chem. Soc., Perkin Trans. 2* **1982**, 1228.

245. Mohrig, J. R.; Keegstra, K.; Maverick, A.; Roberts, R.; Wells, S. *J. Chem. Soc. Chem. Commun.* **1974**, 780.

246. Berner, D.; McGarrity, J. F. *J. Am. Chem. Soc.* **1979**, *101*, 3135.

247. Bunse, M.; Kirmse, W. *Chem. Ber.* **1993**, *126*, 1499.

248. McClelland, R. A. *Tetrahedron* **1996**, *52*, 6823 and references therein.

249. For examples see: (a) Hagen, G.; Mayr, H. *J. Am. Chem. Soc.* **1991**, *113*, 4954. (b) Irrgang, B.; Mayr, H. *Tetrahedron Lett.* **1991**, *47*, 219. (c) Mayr, H.; Schnieder, R.; Grabis, U. *J. Am. Chem. Soc.* **1990**, *112*, 4460. (d) Mayr, H.; Schnieder, R.; Irrgang, B.; Schade, C. *J. Am. Chem. Soc.* **1990**, *112*, 4454. (e) Mayr, H.; Schnieder, R.; Schade, C.; Bartl, J.; Bederke, R. *J. Am. Chem. Soc.* **1990**, *112*, 4446. (f) Mayr, H. *Angew. Chem., Int. Ed. Engl.* **1990**, *29*, 1371. (g) Bartl, J.; Steenken, S.; Mayr, H. *J. Am. Chem. Soc.* **1991**, *113*, 7710. (h) Roth, M.; Mayr, H. *Angew. Chem., Int. Ed.*

Engl. 1995, *34*, 2250. (i) Patz, M.; Mayr, H.; Bartl, J.; Steenken, S. *Angew. Chem., Int. Ed. Engl.* 1995, *34*, 490. (j) Mayr, H.; Gorath, G. *J. Am. Chem. Soc.* 1995, *117*, 7862. (k) Mayr, H.; Patz, M. *Angew. Chem., Int. Ed. Engl.* 1994, *33*, 938. (l) Mayr, H.; Rau, D. *Chem. Ber.* 1994, *127*, 2493. (m) Kuhn, O.; Rau, D.; Mayr, H. *J. Am. Chem. Soc.* 1998, *120*, 900. (n) Burfeindt, J; Patz, M.; Müller, M.; Mayr, H. *J. Am. Chem. Soc.* 1998, *120*, 3629.

250. For an example in radical chemistry see: Newcomb, M.; Tanaka, N.; Bouvier, A.; Tronche, C.; Horner, J. H.; Musa, O. M.; Martinez, F. N. *J. Am. Chem. Soc.* 1996, *118*, 8505.

251. It has been shown that the relative reactivity of cycloalkyl systems, toward nucleophilic addition, could result from a complex interplay of numerous factors. As an example, BH_4^- additions to cycloalkanones show the reactivity order $k_{butyl} > k_{hexyl} > k_{pentyl}$, see: (a) Brown, H. C.; Wheeler, O. H.; K. Ichikawa *Tetrahedron* 1957, *1*, 214. (b) Brown, H. C.; Ichikawa, K. *Tetrahedron* 1957, *1*, 221.

252. Young, J. C. *Can. J. Chem.* 1975, *53*, 2530.

253. Chiang, Y.; Kresge, A. J.; Popik, V. V. *J. Am. Chem. Soc.* 1995, *117*, 9165.

254. For comparison with phenyl and diphenyldiazomethanes see: Finneman, J. I.; Fishbein, J. C. *J. Org. Chem.* 1994, *59*, 6251 and refs. therein. For comparison with α-diazocarbonyl compounds see ref. 15b and refs. therein.

255. McClelland, R. A.; Chan, C.; Cozens, F.; Modro, A.; Steenken, S. *Angew. Chem. Int. Ed. Engl.* 1991, *30*, 1337.

256. (a) McClelland, R. A.; Cozens, F. L.; Li, J.; Steenken, S. *J. Chem. Soc. Perkin Trans. 2* 1996, 1531 (b) Cozens, F. L.; Mathivanan, N.; McClelland, R. A.; Steenken, S. *J. Chem. Soc. Perkin Trans. 2* 1992, 2083. (c) Cozens, F. L.; Li, J.; McClelland, R. A.; Steenken, S. *Angew. Chem. Int. Ed. Engl.* 1992, *31*, 743. (d) . McClelland, R. A.; Mathivanan, N.; Steenken, S. *J. Am. Chem. Soc.* 1990, *112*, 4857.

257. Mayr, H.; Patz, M. *Angew. Chem. Int. Ed. Engl.* 1994, *33*, 958.

258. (a) Steenken, S.; McClelland, R. A. *J. Am. Chem. Soc.* 1990, *112*, 9648. (b) Mathivanan, N.; Cozens, F.; McClelland, R. A.; Steenken, S. *J. Am. Chem. Soc.* 1992, *114*, 2198. (c) Lew, C. S. Q.; McClelland, R. A. *J. Am. Chem. Soc.* 1993, *115*, 11516.

259. Cozens, F.; Li, J.; McClelland, R. A.; Steenken, S. *Angew. Chem. Int. Ed. Engl.* 1992, *31*, 743.

260. Richard, J. P.; Rothenberg, M. E.; Jencks, W. P. *J. Am. Chem. Soc.* 1984, *106*, 1361.

261. Richard, J. P.; Jencks, W. P. *J. Am. Chem. Soc.* 1984, *106*, 1373.

262. Richard, J. P.; Jencks, W. P. *J. Am. Chem. Soc.* 1982, *104*, 4691.

263. McClelland, R. A.; Kanagasabapathy,V. M.; Banait, N. S.; Steenken, S. *J. Am. Chem. Soc.* 1991, *113*, 1009.

264. Mazur, R. H.; White, W.N.; Semenow, D. A.; Lee, C.-C.; Silver, M. S.; Roberts, J. D. *J. Am. Chem. Soc.* 1959, *81*, 4390.

265. Factors which govern competitive solvolytic elimination mechanisms have been actively studied recently and it has been shown that high acidity of the β-hydrogen is required for E2 elimination to compete. We have assumed that elimination products arise from the corresponding carbocations (E1). It is possible that elimination occurs *via* an E2 mechanism within the diazonium ion counterion pairs, however it would be difficult to distinguish betweeen the mechanistic possibilities because the transition state for the E2 reaction would most likely resemble that of the E1 reaction because of the leaving group ability of N_2. See: (a) Pirinccioglu, N.; Thibblin, A. *J. Am. Chem. Soc.* 1998, *120*, 6513. (b) Meng, Q.; Thibblin, A. *J. Chem. Soc. Perkin Trans. II* 1998, 583. (C) Meng, Q.; Thibblin, A. *J. Am. Chem. Soc.* 1997, *119*, 4834. (d) Meng, Q.; Thibblin, A. *J. Am. Chem. Soc.* 1997, *119*,1217. (e) Meng, Q.; Thibblin, A. *J. Am. Chem. Soc.* 1995, *117*, 9399. (f) Meng, Q.; Thibblin, A. *J. Am. Chem. Soc.* 1995, *117*. 1839. (g) Thibblin, A. *Chem. Soc. Rev.* 1993, *22*, 427.

266. It has been suggested that concerted (uncatalyzed) eliminations may occur in solvolysis reactions which would not occur with a neutral leaving group (Toteva, M. M.; Richard, J. P. *J. Am. Chem. Soc.* 1996, *118*, 11434.).

267. For analogous reactions see: (a) Gassman, P. G.; Talley, J. J. *J. Am. Chem. Soc.* 1980, *102*, 1214. (b) Gassman, P. G.; Talley, J. J. *J. Am. Chem. Soc.* 1980, *102*, 4138. (c) Gassman, P. G.; Saito, K; Talley, J. J. *J. Am. Chem. Soc.* 1980, *102*, 7613.

268. Walkimar, de M., Carneiro, J.; Schleyer, P. v. R.; Koch, W.; Raghavachari, K. *J. Am. Chem. Soc.* 1990, *112*, 4064.

269. Olah, G. A. *Acc. Chem. Res.* 1971, *4*, 420.

270. Ma, J. C.; Dougherty, D. A. *Chem. Rev.* 1997, *97*, 1303.

271. (a) Roberts, D. D. *J. Org. Chem.* **1984**, *49*, 2521. (b) Bentley, T. W.; Bowen, C. T.; Brown, H. C.; Chloupek, F. J. *J. Org. Chem.* **1981**, *46*, 38. (c) Peters, E. N. *J. Am. Chem. Soc.* **1976**, *98*, 5627. (d) Roberts, D. D. *J. Org. Chem.* **1971**, *37*, 1510. (e) Bentley, T. W.; Jurczyk, S.; Roberts, K. *J. Chem. Soc. Perkin Trans. II* **1987**, 293. (f) Gassman, P. G.; Saito, K. *Tetrahedron Lett.* **1981**, 1311. (g) Ando, T.; Tsukamoto, S. *Tetrahedron Lett.* **1977**, 2775. (h) Creary, X.; Geiger, C. C. *J. Am. Chem. Soc.* **1982**, *104*, 4151. (i) Fry, J. L.; Lancelot, C. J.; Lam, L. K. M.; Harris, J. M.; Bingham, R. C.; Raber, D. J.; Hall, R. E.; Schleyer, P. v. R. *J. Am. Chem. Soc.* **1970**, *92*, 2538. (j) Fry, J. L.; Harris, J. M.; Bingham, R. C.; Schleyer, P. v. R. *J. Am. Chem. Soc.* **1970**, *92*, 2540. (k) Schleyer, P. v. R.; Fry, J. L.; Lam, L. K. M.; Lancelot, C. J. *J. Am. Chem. Soc.* **1970**, *92*, 2542.

272. Raber, D. J.; Harris, J. M.; Hall, R. E.; Schleyer, P. v. R. *J. Am. Chem. Soc.* **1971**, *93*, 4821 and references therein.

273. (a) Olah, G. A.; Reddy, V. P.; Prakash, G. K. S. *Chem. Rev.* **1992**, *92*, 69. (b) Richey, H. G. Jr. In *Carbonium ions*; Vol. III, Olah, G. A.; Schleyer, P. v. R., Eds.; Wiley-Interscience: NY, 1972; p. 1201. (c) Wiberg, K. B.; Hess, A. Jr.; Ashe, A. J. III In *Carbonium ions*; Vol. III, Olah, G. A.; Schleyer, P. v. R., Eds.; Wiley-Interscience: NY, 1972; p. 1295.

274. Cyclopropyl groups adjacent to carbocations have been shown by X-ray crystallography to adopt bisecting conformations in several analogues. See: (a) Childs, R. F.; Kostyk, M. D.; Lock, C. J. L.; Mahendran, M. *J. Am. Chem. Soc.* **1990**, *112*, 8912. (b) Childs, R. F.; Faggiani, R.; Lock, C. J. L.; Mahendran, M. *J. Am. Chem. Soc.* **1986**, *108*, 3613. (c) Chadda, S. K.; Childs, R. F.; Faggiani, R.; Lock, C. J. L. *J. Am. Chem. Soc.* **1986**, *108*, 1694. (d) Childs, R. F.; Faggiani, R.; Lock, C. J. L.; Mahendran, M.; Zweep, S. D. *J. Am. Chem. Soc.* **1986**, *108*, 1692. (e) Childs, R. F.; Faggiani, R.; Lock, C. J. L.; Varadarajan, A. *Acta. Crystallogr.* **1984**, *C40*, 1291. (f) Childs, R. F.; Varadarajan, A.; Lock, C. J. L.; Faggiani, R.; Fyfe, C. A.; Wasylishen, R. E. *J. Am. Chem. Soc.* **1982**, *104*, 2452.

275. (a) Wolf, J. F.; Harch, P. G.; Taft, R. W.; Hehre, W. J. *J. Am. Chem. Soc.* **1975**, *97*, 2902. (b) Taft, R. W.; Martin, R. H.; Lampe, *J. Am. Chem. Soc.* **1965**, *87*, 2490. (c) Deno, N. C.; Richey, H. G. Jr.; Liu, J. S.; Lincoln, D. N.; Turner, J. D. *J. Am. Chem. Soc.* **1965**, *87*, 4533.

276. (a) Moss, R. A.; Shen, S.; Jespersen, K. K.; Potenza, J. A.; Schugar, H.-J.; Munjal, R. C. *J. Am. Chem. Soc.* **1986**, *108*, 134. (b) Kerber, R. C.; Hsu, C.-M. *J. Am. Chem. Soc.* **1973**, *95*, 3239.

277. For example, the carbon bearing the positive charge in *c-pr*C+(CH₃)₂ has a chemical shift of δ 279.9 ppm, whereas that for PhC+(CH₃)₂ is δ 254.2 ppm. See: (a) Olah, G. A.; Prakash, G. K. S.; Liang, G. *J. Org. Chem.* **1977**, *42*, 2666. (b) Olah, G. A.; White, A. M. *J. Am. Chem. Soc.* **1969**, *91*, 5801.

278. Amyes, T. L.; Richard, J. P.; Novak, M. *J. Am. Chem. Soc.* **1992**, *114*, 8032.

279. Okimoto, M.; Chiba, T. *J. Org. Chem.* **1990**, *55*, 1070.

280. Lambert, J. B.; Wang, G.; Finzel, R. B.; Teramura, D. H. *J. Am. Chem. Soc.* **1987**, *109*, 7838.

281. Arnal, E.; Elguero, J.; Jacquier, R.; Marzin, C.; Wylde, J. *Bull. Soc. Chim. France* **1964**, 878.

282. Roedig, A., Hörnig, L. *Liebigs Ann. Chem.* **1956**, *598*, 208.

Appendix I

X-Ray Crystallographic Data
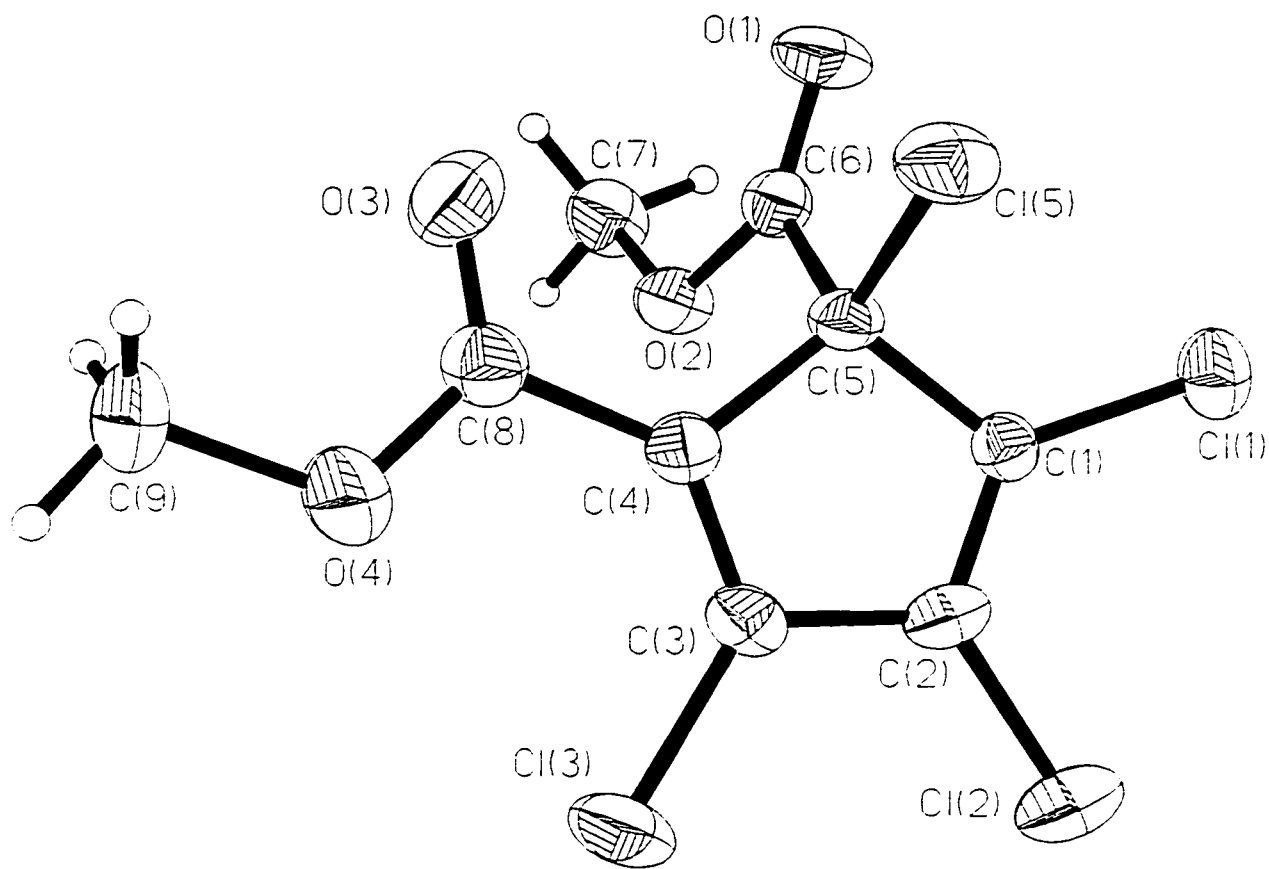
Atomic Numbering for 4,5-Dicarbomethoxy-1,2,3,5-tetrachlorocyclopentadiene (**III-14**).

Table S1. Crystal data and structure refinement for 4,5-dicarbomethoxy-1,2,3,5-tetrachlorocyclopentadiene, III-14.

	III-14
empirical formula	$C_9H_6Cl_4O_4$
M_r	319.94
T [K]	300(2)
λ [Å]	0.71073
description	colorless plate
crystal size [mm]	0.06 x 0.28 x 0.30
crystal system	Monoclinic
space group	P2$_1$/c
a [Å]	8.9176(3)
b [Å]	19.8980(9)
c [Å]	8.0463(4)
α [°]	90.0
β [°]	115.837(2)
γ [°]	90.0
V [Å^3]	1285.03(10)
Z	4
ρ_{calcd} [g cm^{-3}]	1.654
abs. Coeff. [mm^{-1}]	0.918
F(000)	640
θ range for collection [°]	2.05 to 27.51
limiting indices	$-11 < h < 11$
	$-25 < k < 25$
	$-10 < l < 10$
reflections collected	11297
independent reflections	2870
R(int)	0.0932
refinement method	Full-matrix least-squares on F^2
weighting scheme	$w=1/[\sigma^2F_o^2 + (0.0403((F_o^2+ 2F_c^2)/3))^2$ $+ 1.6544((F_o^2 +2F_c^2)/3))^2]$
data/restraints/parameters	2870/0/179
goodness-of-fit on F^2	1.043
final R indices [I>2σ(I)][a]	$R1 = 0.0647$, $wR2 = 0.1108$
R indices (all data)[a]	$R1 = 0.1550$, $wR2 = 0.1457$
rel. trans. (max., min.)	0.8646, 0.6680
Extinction coeff.	0.0029(10)
Largest diff. peak [eÅ^{-3}]	0.555
Largest diff hole [eÅ^{-3}]	-0.341

[a]$R1 = \Sigma (\| F_o | - | F_c \|)/ \Sigma | F_o |$; $wR2 =[\Sigma[w(F_o^2 - F_c^2)^2]/\Sigma[w(F_o^2)^2]]^{0.5}$

Table S2. Atomic coordinates [x 10⁴] and equivalent isotropic
displacement parameters [Å² x 10³] for **III-14**. U(eq) is defined as
one third of the trace of the orthogonalized Uij tensor.

	x	y	z	U(eq)
Cl(1)	4641(2)	5350(1)	6901(2)	65(1)
Cl(2)	1755(2)	4181(1)	4355(2)	77(1)
Cl(3)	-1446(2)	4942(1)	1065(2)	76(1)
Cl(5)	2056(2)	6698(1)	5939(2)	64(1)
O(1)	4440(5)	6922(2)	4413(5)	68(1)
O(2)	3260(4)	6217(2)	2010(4)	54(1)
O(3)	163(5)	7166(2)	1744(6)	90(1)
O(4)	-1907(5)	6445(2)	240(5)	77(1)
C(1)	2792(5)	5483(2)	5013(6)	42(1)
C(2)	1664(6)	5030(2)	4041(7)	47(1)
C(3)	250(5)	5380(3)	2582(6)	47(1)
C(4)	524(5)	6038(2)	2662(6)	44(1)
C(5)	2225(6)	6169(2)	4229(6)	42(1)
C(6)	3454(6)	6503(2)	3587(7)	46(1)
C(7)	4316(10)	6479(4)	1196(10)	69(2)
C(8)	-416(7)	6618(3)	1496(7)	57(1)
C(9)	-2825(11)	7000(4)	-998(11)	96(2)

Table S3. Bond lengths [Å] and angles [deg] for **III-14**.

C(1)-Cl(1)	1.706(5)	O(1)-C(6)-C(5)	125.1(4)
C(1)-C(2)	1.323(6)	O(2)-C(6)-C(5)	108.5(4)
C(1)-C(5)	1.496(6)	C(3)-C(4)-C(8)	133.7(5)
C(2)-Cl(2)	1.705(5)	C(3)-C(4)-C(5)	107.8(4)
C(2)-C(3)	1.470(6)	C(8)-C(4)-C(5)	118.3(4)
C(3)-Cl(3)	1.712(5)	C(4)-C(3)-C(2)	110.6(4)
C(3)-C(4)	1.329(6)	C(4)-C(3)-Cl(3)	128.5(4)
C(4)-C(5)	1.514(6)	C(2)-C(3)-Cl(3)	120.8(4)
C(4)-C(8)	1.493(7)	O(3)-C(8)-O(4)	126.1(5)
C(5)-C(6)	1.550(6)	O(3)-C(8)-C(4)	121.4(5)
C(5)-Cl(5)	1.790(4)	O(4)-C(8)-C(4)	112.5(5)
C(6)-O(2)	1.332(5)	C(1)-C(5)-C(4)	103.1(4)
C(6)-O(1)	1.184(5)	C(1)-C(5)-C(6)	111.9(4)
C(7)-O(2)	1.458(6)	C(4)-C(5)-C(6)	113.2(4)
C(8)-O(4)	1.318(6)	C(1)-C(5)-Cl(5)	109.8(3)
C(8)-O(3)	1.185(6)	C(4)-C(5)-Cl(5)	110.6(3)
C(9)-O(4)	1.474(7)	C(6)-C(5)-Cl(5)	108.2(3)
		C(1)-C(2)-C(3)	108.4(4)
C(6)-O(2)-C(7)	115.7(4)	C(1)-C(2)-Cl(2)	127.8(4)
C(2)-C(1)-C(5)	110.0(4)	C(3)-C(2)-Cl(2)	123.8(4)
C(2)-C(1)-Cl(1)	127.7(4)		
C(5)-C(1)-Cl(1)	122.3(3)		
C(8)-O(4)-C(9)	113.6(5)		
O(1)-C(6)-O(2)	126.3(4)		

Table S4.   Anisotropic displacement parameters [Å^2 x 10^3] for **III-14**. The anisotropic displacement factor exponent takes the form: -2p^2 [(ha*)^{2}U11 + ... + 2hka*b*U12].

	U11	U22	U33	U23	U13	U12
Cl(1)	51(1)	84(1)	52(1)	11(1)	15(1)	8(1)
Cl(2)	96(1)	46(1)	104(1)	3(1)	57(1)	-4(1)
Cl(3)	63(1)	88(1)	70(1)	-20(1)	23(1)	-34(1)
Cl(5)	78(1)	59(1)	65(1)	-16(1)	41(1)	-6(1)
O(1)	75(3)	67(3)	69(3)	-24(2)	38(2)	-36(2)
O(2)	61(2)	60(2)	48(2)	-6(2)	31(2)	-14(2)
O(3)	81(3)	72(3)	99(3)	28(3)	22(3)	-5(3)
O(4)	57(2)	84(3)	70(3)	6(2)	8(2)	7(2)
C(1)	43(3)	49(3)	35(3)	1(2)	17(2)	0(2)
C(2)	57(3)	37(3)	60(3)	-2(2)	36(3)	-3(3)
C(3)	40(3)	62(3)	44(3)	-6(3)	22(2)	-11(3)
C(4)	41(3)	49(3)	44(3)	3(2)	20(2)	-1(2)
C(5)	47(3)	38(3)	42(3)	-6(2)	20(2)	-4(2)
C(6)	47(3)	47(3)	45(3)	1(3)	21(2)	0(3)
C(7)	77(5)	86(5)	54(4)	-4(4)	38(4)	-16(4)
C(8)	47(3)	62(4)	60(3)	1(3)	22(3)	1(3)
C(9)	83(6)	86(6)	79(5)	23(5)	-1(4)	21(5)

Table S5.   Hydrogen coordinates (x 10^4) and isotropic displacement parameters (Å^2 x 10^3) for **III-14**.

	x	y	z	U(eq)
H(7A)	4030(67)	6259(28)	23(85)	87(19)
H(7B)	4201(94)	6987(40)	919(101)	147(32)
H(7C)	5431(69)	6409(26)	2057(74)	69(18)
H(9A)	-3697(93)	6731(37)	-2099(104)	137(28)
H(9B)	-1866(82)	7265(36)	-1143(88)	109(25)
H(9C)	-2620(102)	7457(48)	-106(111)	165(34)
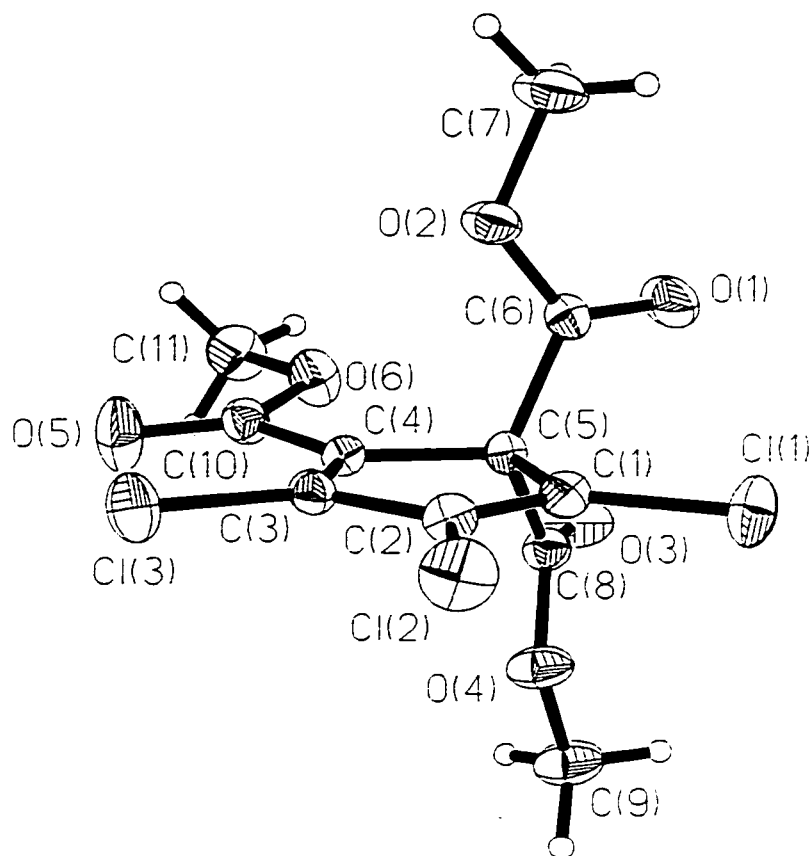
Atomic Numbering for 4,5,5-Tricarbomethoxy-1,2,3-trichlorocyclopentadiene (III-16).

Table S6. Crystal data and structure refinement for 4,5,5-tricarbomethoxy-1,2,3-trichlorocyclopentadiene, **III-16**.

	III-16
empirical formula	$C_{11}H_9Cl_3O_6$
M_r	343.53
T [K]	299(2) K
λ [Å]	0.71073
description	colorless plate
crystal size [mm]	0.10 x 0.18 x 0.30
crystal system	Triclinic
space group	P-1
a [Å]	8.4138(4)
b [Å]	12.0117(5)
c [Å]	14.2489(5)
α [°]	102.368(2)
β [°]	93.306(2)
γ [°]	90.050(2)
V [Å^3]	1404.16(10)
Z	4
ρ_{calcd} [g cm^{-3}]	1.625
abs. Coeff. [mm^{-1}]	0.673
F(000)	696
θ range for collection [°]	2.42 to 27.53
limiting indices	$-8 < h < 10$
	$-15 < k < 13$
	$-11 < l < 18$
reflections collected	10349
independent reflections	6326
R(int)	0.0240
refinement method	Full-matrix least-squares on F^2
weighting scheme	$w=1/[\sigma^2 F_o^2 + (0.0758P((F_o^2+ 2F_c^2)/3))^2$ $+ 1.7229((F_o^2 +2F_c^2)/3))^2]$
data/restraints/parameters	6326 / 0 / 362
goodness-of-fit on F^2	1.046
final R indices [I>2σ(I)][a]	$R1 = 0.0593$, $wR2 = 0.1631$
R indices (all data)[a]	$R1 = 0.0914$, $wR2 = 0.1780$
rel. trans. (max., min.)	0.8971, 0.7340
Extinction coeff.	0.010(2)
Largest diff. peak [eÅ^{-3}]	0.602
Largest diff hole [eÅ^{-3}]	-0.294

[a] $R1 = \Sigma (\| F_o | - | F_c \|)/ \Sigma | F_o |$; $wR2 =[\Sigma[w(F_o^2 - F_c^2)^2]/\Sigma[w(F_o^2)^2]]^{0.5}$

Table S7. Atomic coordinates [x 10⁴] and equivalent isotropic displacement parameters [Å² x 10³] for **III-16**. U(eq) is defined as one third of the trace of the orthogonalized Uij tensor.

	x	y	z	U(eq)
Cl(1)	16548(1)	8638(1)	5640(1)	57(1)
Cl(2)	15882(2)	6203(1)	6405(1)	61(1)
Cl(3)	14055(2)	6806(1)	8415(1)	58(1)
Cl(1A)	11861(1)	4132(1)	5593(1)	62(1)
Cl(2A)	11156(2)	6943(1)	6310(1)	67(1)
Cl(3A)	9163(2)	7390(1)	8257(1)	66(1)
O(1)	14029(4)	10846(3)	6406(2)	65(1)
O(2)	12388(3)	9543(2)	6719(2)	47(1)
O(3)	16290(4)	11369(2)	7980(3)	64(1)
O(4)	17683(3)	9802(2)	7953(2)	49(1)
O(5)	13201(4)	9171(3)	9596(2)	71(1)
O(6)	13375(4)	10663(2)	8902(2)	50(1)
O(1A)	11342(4)	2568(3)	7858(3)	66(1)
O(2A)	12718(3)	4173(2)	7948(2)	53(1)
O(3A)	9224(4)	2359(3)	6184(3)	74(1)
O(4A)	7471(3)	3713(2)	6664(2)	49(1)
O(5A)	8087(5)	5656(3)	9396(3)	86(1)
O(6A)	8570(4)	3821(2)	8839(2)	57(1)
C(1)	15651(4)	8507(3)	6644(2)	36(1)
C(2)	15395(4)	7549(3)	6944(3)	37(1)
C(3)	14609(4)	7832(3)	7843(2)	35(1)
C(4)	14377(4)	8963(3)	8107(2)	32(1)
C(5)	15032(4)	9516(3)	7339(2)	31(1)
C(6)	13764(4)	10083(3)	6780(2)	36(1)
C(7)	11148(5)	9875(4)	6090(4)	66(1)
C(8)	16388(4)	10372(3)	7789(3)	36(1)
C(9)	19056(5)	10473(4)	8404(4)	58(1)
C(10)	13583(4)	9585(3)	8952(3)	40(1)
C(11)	12705(6)	11399(4)	9725(3)	58(1)
C(1A)	10835(4)	4769(3)	6546(2)	37(1)
C(2A)	10555(4)	5877(3)	6841(3)	39(1)
C(3A)	9708(4)	6061(3)	7714(3)	39(1)
C(4A)	9442(4)	5074(3)	7966(3)	36(1)
C(5A)	10142(4)	4118(3)	7232(2)	33(1)
C(6A)	11450(4)	3498(3)	7713(3)	38(1)
C(7A)	14058(5)	3737(4)	8439(4)	61(1)
C(8A)	8902(4)	3261(3)	6644(3)	40(1)
C(9A)	6223(5)	3021(4)	6063(4)	64(1)
C(10A)	8622(5)	4900(3)	8803(3)	44(1)
C(11A)	7883(6)	3526(4)	9667(3)	65(1)

Table S8. Bond lengths [Å] and angles [deg] for **III-16**.

Cl(3)-C(3)	1.696(3)
Cl(2)-C(2)	1.696(4)
Cl(1)-C(1)	1.691(4)
Cl(3A)-C(3A)	1.694(4)
Cl(1A)-C(1A)	1.694(4)
Cl(2A)-C(2A)	1.711(4)
O(4)-C(8)	1.323(4)
O(4)-C(9)	1.445(5)
O(5)-C(10)	1.192(4)
O(4A)-C(8A)	1.320(4)
O(4A)-C(9A)	1.455(5)
C(1A)-C(2A)	1.332(5)
C(1A)-C(5A)	1.516(5)
O(5A)-C(10A)	1.207(5)
O(1A)-C(6A)	1.183(4)
O(3A)-C(8A)	1.180(5)
O(3)-C(8)	1.174(4)
C(10)-O(6)	1.323(4)
C(10)-C(4)	1.470(5)
C(3)-C(4)	1.347(5)
C(3)-C(2)	1.452(5)
O(6A)-C(10A)	1.309(5)
O(6A)-C(11A)	1.452(5)
C(8)-C(5)	1.549(5)
C(2)-C(1)	1.333(5)
C(6)-O(1)	1.181(4)
C(6)-O(2)	1.316(4)
C(6)-C(5)	1.540(5)
C(10A)-C(4A)	1.465(5)
C(6A)-O(2A)	1.323(4)
C(6A)-C(5A)	1.539(5)
C(1)-C(5)	1.507(5)
C(4)-C(5)	1.524(4)
C(8A)-C(5A)	1.543(5)
C(3A)-C(4A)	1.332(5)
C(3A)-C(2A)	1.445(5)
C(5A)-C(4A)	1.521(5)
O(2)-C(7)	1.448(5)
O(2A)-C(7A)	1.450(5)
O(6)-C(11)	1.452(5)
C(8)-O(4)-C(9)	116.6(3)
C(8A)-O(4A)-C(9A)	115.8(3)
C(2A)-C(1A)-C(5A)	109.4(3)
C(2A)-C(1A)-Cl(1A)	127.6(3)

C(5A)-C(1A)-Cl(1A)	122.9(3)
O(5)-C(10)-O(6)	125.1(4)
O(5)-C(10)-C(4)	124.3(4)
O(6)-C(10)-C(4)	110.7(3)
C(4)-C(3)-C(2)	111.1(3)
C(4)-C(3)-Cl(3)	127.6(3)
C(2)-C(3)-Cl(3)	121.2(3)
C(10A)-O(6A)-C(11A)	117.6(3)
O(3)-C(8)-O(4)	124.7(3)
O(3)-C(8)-C(5)	126.1(3)
O(4)-C(8)-C(5)	109.2(3)
C(1)-C(2)-C(3)	108.5(3)
C(1)-C(2)-Cl(2)	127.7(3)
C(3)-C(2)-Cl(2)	123.7(3)
O(1)-C(6)-O(2)	125.2(3)
O(1)-C(6)-C(5)	124.2(3)
O(2)-C(6)-C(5)	110.4(3)
O(5A)-C(10A)-O(6A)	124.2(4)
O(5A)-C(10A)-C(4A)	124.4(4)
O(6A)-C(10A)-C(4A)	111.4(3)
O(1A)-C(6A)-O(2A)	125.0(3)
O(1A)-C(6A)-C(5A)	125.7(3)
O(2A)-C(6A)-C(5A)	109.3(3)
C(2)-C(1)-C(5)	110.4(3)
C(2)-C(1)-Cl(1)	127.1(3)
C(5)-C(1)-Cl(1)	122.5(3)
C(3)-C(4)-C(10)	127.9(3)
C(3)-C(4)-C(5)	107.7(3)
C(10)-C(4)-C(5)	124.4(3)
O(3A)-C(8A)-O(4A)	125.2(4)
O(3A)-C(8A)-C(5A)	123.9(4)
O(4A)-C(8A)-C(5A)	110.7(3)
C(4A)-C(3A)-C(2A)	110.5(3)
C(4A)-C(3A)-Cl(3A)	128.9(3)
C(2A)-C(3A)-Cl(3A)	120.6(3)
C(1A)-C(5A)-C(4A)	101.8(3)
C(1A)-C(5A)-C(6A)	111.1(3)
C(4A)-C(5A)-C(6A)	110.9(3)
C(1A)-C(5A)-C(8A)	107.4(3)
C(4A)-C(5A)-C(8A)	114.5(3)
C(6A)-C(5A)-C(8A)	110.8(3)
C(3A)-C(4A)-C(10A)	127.2(3)
C(3A)-C(4A)-C(5A)	108.7(3)
C(10A)-C(4A)-C(5A)	124.1(3)
C(1)-C(5)-C(4)	102.3(3)
C(1)-C(5)-C(6)	107.3(3)
C(4)-C(5)-C(6)	114.4(3)

C(1)-C(5)-C(8)	111.5(3)
C(4)-C(5)-C(8)	110.1(3)
C(6)-C(5)-C(8)	111.0(3)
C(1A)-C(2A)-C(3A)	109.6(3)
C(1A)-C(2A)-Cl(2A)	126.2(3)
C(3A)-C(2A)-Cl(2A)	124.2(3)
C(6)-O(2)-C(7)	116.3(3)
C(6A)-O(2A)-C(7A)	116.8(3)
C(10)-O(6)-C(11)	116.5(3)

Table S9. Anisotropic displacement parameters [$\text{Å}^2 \times 10^3$] for **III-16**. The anisotropic displacement factor exponent takes the form: $-2p^2$ [$(ha^*)^2$ U11 + ... + 2hka*b* U12]

	U11	U22	U33	U23	U13	U12
Cl(1)	71(1)	59(1)	42(1)	5(1)	23(1)	-7(1)
Cl(2)	77(1)	33(1)	68(1)	-2(1)	12(1)	9(1)
Cl(3)	77(1)	43(1)	63(1)	28(1)	10(1)	-7(1)
Cl(1A)	59(1)	75(1)	48(1)	3(1)	17(1)	6(1)
Cl(2A)	75(1)	56(1)	77(1)	36(1)	-6(1)	-15(1)
Cl(3A)	82(1)	30(1)	81(1)	-3(1)	5(1)	13(1)
O(1)	60(2)	69(2)	81(2)	50(2)	-13(2)	-14(2)
O(2)	40(2)	44(2)	60(2)	22(1)	-11(1)	-2(1)
O(3)	56(2)	31(2)	98(3)	5(2)	-17(2)	-2(1)
O(4)	35(1)	38(1)	72(2)	8(1)	-8(1)	-3(1)
O(5)	102(3)	63(2)	58(2)	26(2)	41(2)	16(2)
O(6)	68(2)	43(2)	38(1)	5(1)	14(1)	15(1)
O(1A)	55(2)	43(2)	104(3)	32(2)	-13(2)	-3(1)
O(2A)	37(2)	42(2)	80(2)	19(1)	-14(1)	1(1)
O(3A)	59(2)	42(2)	102(3)	-21(2)	-15(2)	8(2)
O(4A)	35(1)	45(2)	63(2)	4(1)	-6(1)	-1(1)
O(5A)	117(3)	55(2)	85(3)	2(2)	63(2)	14(2)
O(6A)	84(2)	45(2)	44(2)	8(1)	20(2)	0(2)
C(1)	36(2)	35(2)	33(2)	4(1)	2(1)	-1(2)
C(2)	39(2)	30(2)	40(2)	5(2)	2(2)	0(2)
C(3)	35(2)	35(2)	37(2)	14(2)	-1(1)	-4(2)
C(4)	29(2)	36(2)	33(2)	9(1)	2(1)	-1(1)
C(5)	34(2)	30(2)	30(2)	8(1)	3(1)	-1(1)
C(6)	40(2)	35(2)	33(2)	10(1)	1(2)	0(2)
C(7)	49(3)	66(3)	86(3)	32(3)	-25(2)	-1(2)
C(8)	34(2)	33(2)	41(2)	9(2)	1(2)	-2(2)
C(9)	37(2)	55(3)	78(3)	8(2)	-10(2)	-8(2)

C(10)	42(2)	43(2)	34(2)	9(2)	4(2)	5(2)
C(11)	69(3)	57(3)	43(2)	-4(2)	11(2)	19(2)
C(1A)	36(2)	41(2)	34(2)	5(2)	1(1)	-1(2)
C(2A)	39(2)	35(2)	45(2)	14(2)	-6(2)	-4(2)
C(3A)	37(2)	29(2)	46(2)	0(2)	-7(2)	3(2)
C(4A)	33(2)	32(2)	40(2)	4(2)	-2(2)	4(1)
C(5A)	32(2)	25(2)	41(2)	5(1)	0(1)	2(1)
C(6A)	36(2)	31(2)	45(2)	6(2)	4(2)	5(2)
C(7A)	41(2)	58(3)	84(3)	19(2)	-18(2)	7(2)
C(8A)	39(2)	31(2)	47(2)	5(2)	-1(2)	-1(2)
C(9A)	46(3)	65(3)	77(3)	12(2)	-15(2)	-17(2)
C(10A)	43(2)	41(2)	44(2)	1(2)	8(2)	1(2)
C(11A)	87(4)	66(3)	47(2)	18(2)	10(2)	-10(3)

Table S10. Hydrogen coordinates (x 10^4) and isotropic displacement parameters (Å^2 x 10^3) for III-16.

	x	y	z	U(eq)
H(7A)	10201(5)	9431(4)	6098(4)	99
H(7B)	11495(5)	9744(4)	5446(4)	99
H(7C)	10926(5)	10669(4)	6308(4)	99
H(7AA)	14904(5)	4296(4)	8573(4)	92
H(7AB)	14425(5)	3050(4)	8037(4)	92
H(7AC)	13734(5)	3576(4)	9031(4)	92
H(9A)	19920(5)	9975(4)	8488(4)	87
H(9B)	18796(5)	10913(4)	9020(4)	87
H(9C)	19364(5)	10976(4)	8004(4)	87
H(9AA)	5234(5)	3421(4)	6127(4)	96
H(9AB)	6115(5)	2312(4)	6263(4)	96
H(9AC)	6496(5)	2873(4)	5403(4)	96
H(11A)	7914(6)	2716(4)	9608(3)	98
H(11B)	6799(6)	3773(4)	9697(3)	98
H(11C)	8482(6)	3896(4)	10244(3)	98
H(11D)	12607(6)	12156(4)	9612(3)	87
H(11E)	13393(6)	11415(4)	10290(3)	87
H(11F)	11674(6)	11112(4)	9818(3)	87
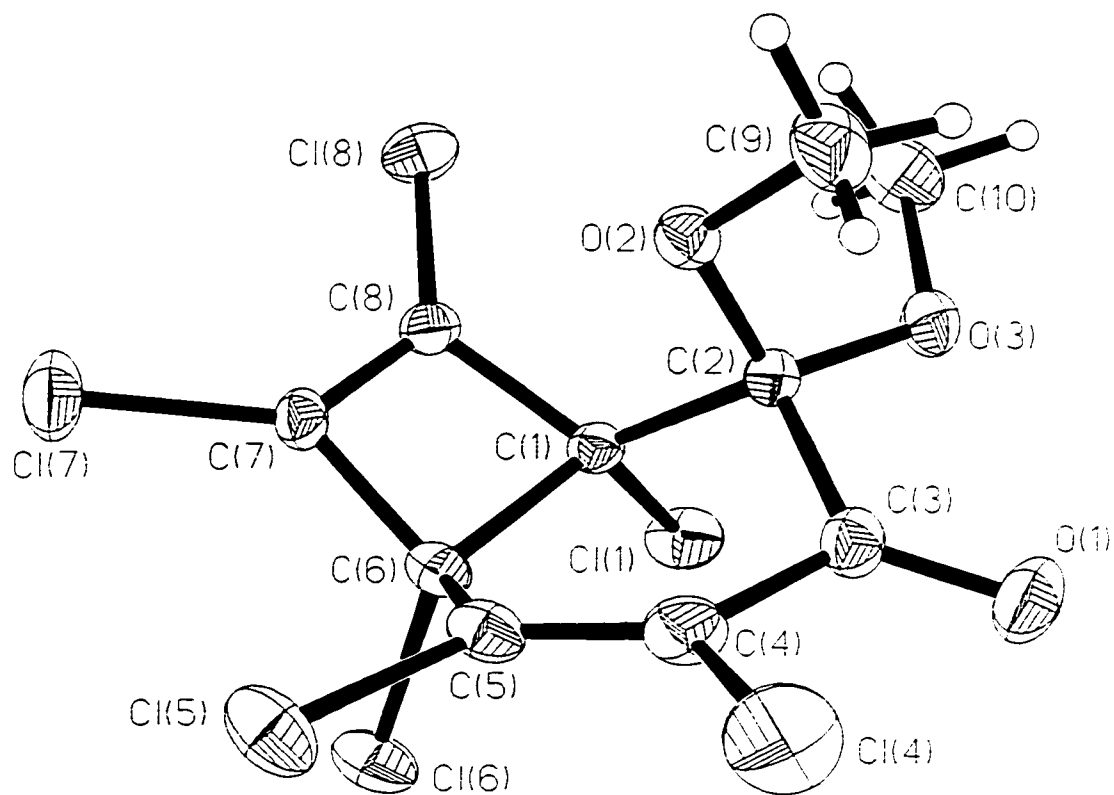
Atomic Numbering for 2,2-Dimethoxy-1,4,5,6,7,8-hexachlorobicyclo[4.2.0] octa-4,7-dien-3-one (III-28).

Table S11. Crystal data and structure refinement for 2,2-Dimethoxy-1,4,5,6,7,8-hexachlorobicyclo[4.2.0]octa-4,7-dien-3-one, **III-28**.

	III-28
empirical formula	$C_{10}H_6Cl_6O_3$
M_r	386.85
T [K]	300(2)
λ [Å]	0.71073
description	colorless plate
crystal size [mm]	0.04 x 0.20 x 0.24
crystal system	Monoclinic
space group	$P2_1/c$
a [Å]	16.073(4)
b [Å]	8.186(2)
c [Å]	11.952(3)
α [°]	90.0
β [°]	111.238(10)
γ [°]	90.0
V [Å^3]	1465.8(6)
Z	4
ρ_{calcd} [g cm^{-3}]	1.753
abs. Coeff. [mm^{-1}]	1.169
F(000)	768
θ range for collection [°]	1.36 to 27.50
limiting indices	$-20 < h < 20$
	$-10 < k < 10$
	$-12 < l < 15$
reflections collected	12752
independent reflections	3306
R(int)	0.0619
refinement method	Full-matrix least-squares on F^2
weighting scheme	$w=1/[\sigma^2 F_o^2 + (0.0295((F_o^2 + 2F_c^2)/3))^2$ $+ 1.1256((F_o^2 + 2F_c^2)/3))^2]$
data/restraints/parameters	3306 / 0 / 197
goodness-of-fit on F^2	1.049
final R indices [I>2σ(I)][a]	R1 = 0.0473, wR2 = 0.0847
R indices (all data)[a]	R1 = 0.0933, wR2 = 0.1014
rel. trans. (max., min.)	0.8748, 0.6368
Extinction coeff.	0.0044(7)
Largest diff. peak [eÅ^{-3}]	0.497
Largest diff hole [eÅ^{-3}]	-0.390

[a]$R1 = \Sigma (||F_o| - |F_c||)/ \Sigma |F_o|$; $wR2 = [\Sigma[w(F_o^2 - F_c^2)^2]/\Sigma[w(F_o^2)^2]]^{0.5}$

Table S12. Atomic coordinates [x 10^4] and equivalent isotropic displacement parameters [Å^2 x 10^3] for **III-28**. U(eq) is defined as one third of the trace of the orthogonalized Uij tensor.

	x	y	z	U(eq)
Cl(1)	1798(1)	6216(1)	9319(1)	45(1)
Cl(4)	4300(1)	2859(1)	13335(1)	76(1)
Cl(5)	2299(1)	2321(1)	13203(1)	59(1)
Cl(6)	1203(1)	3141(1)	10358(1)	53(1)
Cl(7)	521(1)	5258(1)	12558(1)	61(1)
Cl(8)	957(1)	8959(1)	11115(1)	50(1)
O(1)	4246(2)	5148(3)	11347(3)	62(1)
O(2)	3080(1)	7413(3)	12632(2)	37(1)
O(3)	3370(2)	7892(3)	10883(2)	42(1)
C(1)	2060(2)	6261(4)	10885(3)	28(1)
C(2)	3046(2)	6815(4)	11519(3)	32(1)
C(3)	3643(2)	5281(4)	11703(3)	39(1)
C(4)	3411(2)	3986(4)	12431(3)	42(1)
C(5)	2580(2)	3760(4)	12357(3)	37(1)
C(6)	1817(2)	4632(4)	11445(3)	33(1)
C(7)	1202(2)	5708(4)	11805(3)	34(1)
C(8)	1364(2)	7034(4)	11291(3)	31(1)
C(9)	3955(3)	7842(8)	13459(5)	61(1)
C(10)	2993(4)	9506(5)	10688(5)	64(1)

Table S13. Bond lengths [Å] and angles [deg] for III-28.

Cl(1)-C(1)	1.764(3)	C(3)-C(4)-Cl(4)	114.9(2)
Cl(4)-C(4)	1.715(3)	C(4)-C(5)-C(6)	121.7(3)
Cl(5)-C(5)	1.716(3)	C(4)-C(5)-Cl(5)	122.3(3)
Cl(6)-C(6)	1.794(3)	C(6)-C(5)-Cl(5)	115.8(2)
Cl(7)-C(7)	1.690(3)	C(5)-C(6)-C(7)	121.6(3)
Cl(8)-C(8)	1.690(3)	C(5)-C(6)-C(1)	116.2(2)
O(1)-C(3)	1.197(4)	C(7)-C(6)-C(1)	85.3(2)
O(2)-C(2)	1.400(4)	C(5)-C(6)-Cl(6)	107.1(2)
O(2)-C(9)	1.440(4)	C(7)-C(6)-Cl(6)	111.1(2)
O(3)-C(2)	1.383(4)	C(1)-C(6)-Cl(6)	114.6(2)
O(3)-C(10)	1.437(5)	C(8)-C(7)-C(6)	95.0(2)
C(1)-C(2)	1.555(4)	C(8)-C(7)-Cl(7)	134.6(3)
C(1)-C(6)	1.603(4)	C(6)-C(7)-Cl(7)	130.3(2)
C(1)-C(8)	1.511(4)	C(7)-C(8)-C(1)	95.7(3)
C(2)-C(3)	1.547(4)	C(7)-C(8)-Cl(8)	133.9(3)
C(3)-C(4)	1.501(5)	C(1)-C(8)-Cl(8)	130.4(2)
C(4)-C(5)	1.319(5)	C(8)-C(1)-C(2)	117.6(2)
C(5)-C(6)	1.495(4)	C(8)-C(1)-C(6)	83.8(2)
C(6)-C(7)	1.499(4)	C(2)-C(1)-C(6)	113.5(2)
C(7)-C(8)	1.319(4)	C(8)-C(1)-Cl(1)	115.4(2)
		C(2)-C(1)-Cl(1)	109.4(2)
		C(6)-C(1)-Cl(1)	115.2(2)
C(2)-O(3)-C(10)	117.0(3)	O(3)-C(2)-O(2)	114.0(2)
C(2)-O(2)-C(9)	115.5(3)	O(3)-C(2)-C(3)	104.9(2)
O(1)-C(3)-C(4)	123.0(3)	O(2)-C(2)-C(3)	109.9(3)
O(1)-C(3)-C(2)	124.3(3)	O(3)-C(2)-C(1)	116.0(3)
C(4)-C(3)-C(2)	112.6(3)	O(2)-C(2)-C(1)	104.3(2)
C(5)-C(4)-C(3)	121.2(3)	C(3)-C(2)-C(1)	107.6(2)
C(5)-C(4)-Cl(4)	123.9(3)		

Table S14. Anisotropic displacement parameters [$A^2 \times 10^3$] for III-28. The anisotropic displacement factor exponent takes the form: $-2p^2$ [$(ha^*)^2 U11 + ... + 2hka^*b^* U12$]

	U11	U22	U33	U23	U13	U12
Cl(4)	54(1)	69(1)	90(1)	31(1)	8(1)	24(1)
Cl(5)	72(1)	46(1)	56(1)	19(1)	22(1)	-10(1)
Cl(6)	61(1)	39(1)	49(1)	-9(1)	10(1)	-15(1)
Cl(7)	49(1)	78(1)	68(1)	1(1)	37(1)	-12(1)
Cl(8)	52(1)	38(1)	65(1)	-1(1)	25(1)	13(1)
Cl(1)	60(1)	44(1)	29(1)	1(1)	14(1)	1(1)
O(1)	48(2)	62(2)	91(2)	7(2)	42(2)	12(1)
O(3)	46(1)	39(1)	49(2)	6(1)	29(1)	-5(1)
O(2)	34(1)	43(1)	35(1)	-8(1)	14(1)	-9(1)
C(3)	29(2)	42(2)	45(2)	1(2)	13(2)	1(2)
C(4)	41(2)	35(2)	46(2)	6(2)	13(2)	7(2)
C(5)	45(2)	28(2)	35(2)	4(1)	12(2)	-3(2)
C(6)	37(2)	28(2)	31(2)	-2(1)	10(2)	-7(1)
C(7)	25(2)	41(2)	37(2)	-5(2)	13(2)	-6(1)
C(8)	28(2)	31(2)	33(2)	-4(1)	10(1)	0(1)
C(1)	33(2)	27(2)	26(2)	0(1)	12(1)	0(1)
C(2)	34(2)	31(2)	35(2)	-1(1)	19(2)	-2(1)
C(9)	43(2)	86(4)	49(3)	-21(3)	12(2)	-24(3)
C(10)	82(4)	37(2)	83(4)	16(2)	41(3)	-1(2)

Table S15. Hydrogen coordinates (x 10^4) and isotropic displacement parameters ($A^2 \times 10^3$) for III-28.

	x	y	z	U(eq)
H(9A)	3915(29)	8380(58)	14115(43)	85(16)
H(9B)	4293(38)	6885(72)	13763(49)	119(23)
H(9C)	4236(32)	8449(59)	13102(41)	87(17)
H(10A)	2918(30)	9957(58)	11416(42)	90(17)
H(10B)	2416(34)	9494(59)	10108(43)	94(18)
H(10C)	3393(30)	10186(60)	10492(39)	87(15)